

SAFETY FIRST IN REHABILITATION ROBOTS!

Investigating how
safety-related physical
human-robot interaction
can be assessed



Jule Bessler-Etten

SAFETY FIRST IN REHABILITATION ROBOTS!

INVESTIGATING HOW SAFETY-RELATED PHYSICAL
HUMAN-ROBOT INTERACTION CAN BE ASSESSED

Jule Bessler-Etten

The publication of this thesis was financially supported by:



**UNIVERSITY
OF TWENTE.**

Cover and chapter openers design: Jos Spoelstra

Printed by: Ipskamp Printing

Lay-out: Jule Bessler

ISBN: 978-90-365-5503-6

DOI: 10.3990/1.9789036555036

© 2022 Jule Bessler-Etten, The Netherlands. All rights reserved. No parts of this thesis may be reproduced, stored in a retrieval system or transmitted in any form or by any means without permission of the author. Alle rechten voorbehouden. Niets uit deze uitgave mag worden vermenigvuldigd, in enige vorm of op enige wijze, zonder voorafgaande schriftelijke toestemming van de auteur.

SAFETY FIRST IN REHABILITATION ROBOTS!

INVESTIGATING HOW SAFETY-RELATED PHYSICAL
HUMAN-ROBOT INTERACTION CAN BE ASSESSED

DISSERTATION

to obtain
the degree of doctor at the University of Twente,
on the authority of the rector magnificus,
prof.dr.ir A. Veldkamp,
on account of the decision of the Doctorate Board
to be publicly defended
on Thursday the 19th of January 2023 at 14.45 hours

by

Jule Bessler-Etten

born on the 11th of June, 1992
in Ibbenbüren, Germany

THIS DISSERTATION HAS BEEN APPROVED BY:

Supervisor:

prof.dr. J.H. Buurke

Co-supervisor:

dr. G.B. Prange-Lasonder

GRADUATION COMMITTEE:

Chair/secretary prof.dr. J.N. Kok | *University of Twente*

Supervisor prof.dr. J.H. Buurke | *University of Twente, Roessingh Research and Development*

Co-supervisor dr. G.B. Prange-Lasonder | *University of Twente, Roessingh Research and Development*

Members prof.dr. J.S. Rietman | *University of Twente, Roessingh Research and Development*
prof.dr.ir. G.D.S. Ludden | *University of Twente*
prof. L. O'Sullivan | *University of Limerick*
prof.dr.ir. D. Lefeber | *Vrije Universiteit Brussel*
dr.ing. R. Behrens | *Fraunhofer Institute for Factory Operation and Automation IFF*

CONTENTS

Chapter 1	General introduction	8
Chapter 2	Occurrence and type of adverse events during the use of stationary gait robots – A systematic literature review	16
Chapter 3	Safety assessment of rehabilitation robots: A review identifying safety skills and knowledge gaps	38
Chapter 4	Prototype measuring device for assessing interaction forces between Human Limbs and Rehabilitation Robots – A Proof of Concept Study	62
Chapter 5	Assessing effects of exoskeleton misalignment on knee joint load during swing using an instrumented leg simulator	74
Chapter 6	Soft tissue characteristics affect the relation between leg-exoskeleton misalignments and knee joint loads in a dummy leg	98
Chapter 7	Investigating change of discomfort during repetitive force exertion through an exoskeleton cuff	118
Chapter 8	General discussion	134
&	References, List of abbreviations, Summaries, Acknowledgements, About the author, Progress range	148

Chapter 1

General introduction



ROBOTICS IN REHABILITATION

Robotic devices are increasingly used for rehabilitation and assistance of patients. This development can be explained by the increasing technical possibilities on the one hand and the increasing need on the other hand. The proportion of elderly and chronically ill people is increasing, which increases the need for care. Since this trend is expected to intensify in the future, it will become more and more challenging to match this need with the available clinicians and specialists [1], [2]. Robotic devices have the potential to reduce the physical workload of the therapists and at the same time provide continuous assistance and prolonged repetitive training sessions. Traditional gait training for example is a physically demanding activity which often requires two or more therapists to be present. A robotic gait trainer has the advantage that only one therapist needs to be present, who can potentially supervise several patients at the same time. Research has shown that robotic devices can be a valuable addition to traditional physical therapy in terms of therapy outcomes [3]–[5].

A robot can be defined as a ‘programmed actuated mechanism with a degree of autonomy, moving within its environment, to perform intended tasks’ [6]. A rehabilitation, assessment, compensation and alleviation robot (RACA robot; in this thesis referred to as rehabilitation robot) is defined as a ‘medical robot intended by its manufacturer to perform rehabilitation, assessment, compensation or alleviation comprising an actuated applied part’ [6]. New technologies, devices and device types are rapidly emerging. This becomes evident when observing the market share, number of companies and publications related to rehabilitation robotics, which have all been increasing considerably over the past years [7]–[10]. A recent systematic literature review found 87 unique robotic devices in studies involving patients with neurological diseases of which many were still in research state and not yet on the market [11]. The website exoskeletonreport.com lists 48 powered exoskeletons on the market in the medical domain [12].

Rehabilitation robots can be classified based on a number of different characteristics, including the intended use (e.g. assistive or therapeutic), the body area (e.g. upper limb or lower limb), the type in terms of movability (e.g. stationary, mobile, ambulatory), or its appearance (e.g. end-effector or exoskeleton, spanning over one or multiple joints). One possible classification is shown in Figure 1.1. Due to new devices and device types emerging and the variety of characteristics and definitions, such a classification needs to be considered with care. It might not include every device and has to be revised regularly.

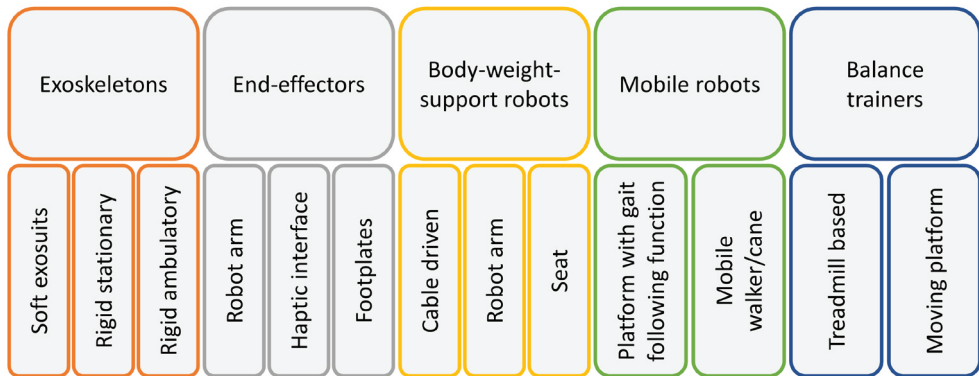


Figure 1.1| Rehabilitation robot types.

An increasing number of rehabilitation robots can be considered as established devices in clinical practice. They are used in rehabilitation centers and physiotherapy or occupational therapy practices. Some assistive devices are also available for home use. However, many devices that are developed and used in research are not (yet) on the market. This becomes evident in the above-mentioned systematic literature review [11] including 316 studies published between 2000 and 2021, more than half of which were randomized controlled trials (RCTs). Only 19 of the 87 rehabilitation robots represented in the literature review are CE-marked according to the authors. CE stands for *conformité européenne* and the CE mark is a requirement for selling goods in Europe. It is a sign of conformity with the European health, safety and environmental protection standards. The majority of investigated devices are therefore still in research state and not available on the market. Some of the barriers to implementation of rehabilitation robots in clinical practice are organizational issues such as integrating rehabilitation robot training in the therapy schedules or reimbursement, and others are technical [13], [14]. Besides developments in mechanical design and actuation, some practical barriers to rehabilitation robot development and implementation are the intention detection, intuitive control and finding the right balance between over-constrained exoskeletons and under-constrained end-effector-based devices [15]–[17]. Another barrier is safety. Rehabilitation robots interact closely with vulnerable patients which is why safety is pivotal. Ensuring safety in these physical interactions can however be difficult and an unsafe device will not be introduced to the market.

SAFETY AS AN IMPLEMENTATION BARRIER

Safety can be considered as one of the most important implementation barriers. Some of the reasons for that are:

- **Safety is often considered too late in the research and development process.** Although safety is pivotal for the success and feasibility of a device, the function is often more central in the development phase.

- **Safety certification is complex.** Before a rehabilitation robot can enter the European market, it needs to obtain a CE-mark. The Medical Device Regulation (MDR) [18] sets the quality and safety requirements that have to be met. The MDR has replaced the Medical Device Directive and with that change the focus on safety increased, introducing a life-cycle approach with connected processes of risk management, post-market surveillance and post-market clinical follow-up. In the case of rehabilitation robots (which can also be seen as machinery), the essential health and safety requirements of the Machinery Directive [19] need to be met as well. Standards can be used as an aid for demonstrating conformity to those regulations. However, finding out which standards are applicable for a particular device is often considered challenging by rehabilitation robot developers [20]–[22]. This is partly due to the diversity and rapid changes of the field encompassing a large and still growing list of device types. Moreover, medical standards include only few procedures for testing the mechanical safety of rehabilitation robots [23].
- **Rehabilitation robots have inherent risks.** By definition, rehabilitation robots are moving machines which are connected to a human through an actuated part. This means that they exert a potentially hazardous force to their user in order to fulfil their purpose. They can be used in different settings, ranging from relatively controlled rehabilitation settings to uncontrolled environments like a patient's home or public spaces. They are therefore prone to come in contact with not only trained therapists but also vulnerable patients, untrained individuals and even children and pets.

UNDERSTANDING REHABILITATION ROBOT SAFETY – LEARNING FROM OTHER DOMAINS

We have established that there are still a lot of gaps and challenges in rehabilitation robot safety. Some of those issues might be easier to solve through learning from other robot domains with more experience in safety assessment. Within the EU-funded project COVR, which served as a starting point for this research, this opportunity presented itself. Five partners, specialized in robots closely interacting with humans in different domains, teamed up to simplify safety assessment and certification and thereby contribute to more devices being introduced to the market. The domain of industrial robotics has the longest history and therefore the most experience with safety assessments of robots. Collaborative robots are robots that closely interact with humans, by sharing a joint workspace. The purpose of those robots is to combine the skills and experience of workers with the strength and accuracy of robots and they have been first introduced in the 1990s [24], [25]. Since then, workflows have been developed to ensure safety of collaborative robot systems. They are documented in standards and in the Machinery Directive [26]. These experiences and a number of similarities between robots in rehabilitation and collaborative robots enabled us to learn from the industrial domain when exploring solutions for rehabilitation robot safety assessments. For example, exoskeletons are used both to assist patients in movements and to support workers during physically demanding tasks. Furthermore, there are a number of rehabilitation robotic systems which are based on industrial collaborative robots [27], [28]. Other aspects are very different between the domains. This includes the controlled environment and the restricted group of users in industry (healthy workers). These aspects simplify how robot safety can be approached in industry when comparing it to the healthcare situation.

Although the dissimilarities in application and setting bring differences that have to be considered in safety assessments, a cross-fertilization between domains can simplify the development of new procedures for safety testing. This cross-fertilization was employed in the COVR project to facilitate and support safety assessment of collaborative robots across domains and thereby increase robot safety. The project developed the concept of safety skills [29]. Safety skills are abstract representations of the ability of a robot system to reduce a specific risk. They are independent of the way this is implemented and can be validated on a system level, instead of testing each safety function, which would be specific to how each safety measure is implemented and not usually generalizable to other devices. One example for a safety skill is *limit range of movement*. The skill avoids risks associated with exceeding the physical range of motion of the user or a pre-defined working range of the robot. It can be implemented in various ways but can be validated irrespective of the method of implementation by measuring the actual ranges of motion during certain situations. Through comparing those measured ranges with the pre-defined safe ranges, the safety skill can be validated. COVR developed a range of protocols, which are step-by-step testing procedures based on best practice. They are built around the safety skill approach and can be assessed through a website called the COVR Toolkit (www.safearoundrobots.com). The protocols can be filtered by robot type and safety skill and are independent of the domain of the application. The Toolkit includes additional information such as a tool for finding the relevant standards and directives or regulations for a robot system based on its application domain and robot type, information about risk assessment, legal background and relevant academic publications. Safety facilities at project partner sites were established as part of the project and information about relevant equipment and the availability at those facilities can be found in the Toolkit. The Toolkit also contains case stories presenting experiences from specific problems and insights of people working on collaborative robot safety.

THIS THESIS

During the development of new safety test protocols and guidelines for safety assessment of rehabilitation robots, it became evident that there are large knowledge gaps. It is not yet fully understood what should be tested to prove device safety and how. It is further not known which limit values can be considered as safe thresholds in the physical interaction of rehabilitation robots with humans. The main aim of the research presented in this thesis is **to gain more insight into safety challenges in rehabilitation robotics and to take first steps towards addressing those challenges**. This was approached by investigating the following research questions:

1. **What are the most pressing risks and safety issues in rehabilitation robotics?**
2. **How can those safety issues be avoided or managed?**
3. **What are suitable methods to quantify metrics relevant for the identified safety issues?**
4. **What are acceptable limit values to guarantee the safety of rehabilitation robot use?**

A systematic literature review on the occurrence and type of adverse events during the use of stationary robotic gait trainers builds the starting point for the research (**Chapter 2**). The results of this helped to identify the most pressing issues in rehabilitation robot safety. In a second review (**Chapter 3**), those

results were abstracted to identify the hazards relating to the identified adverse events and compare this to known risks in other rehabilitation robot device types. Based on this, we defined safety skills applicable to rehabilitation robotics, which can help avoiding safety issues through safety validation. This work further identifies knowledge gaps which need to be filled in order to simplify the safety assessment of rehabilitation robots. The identified safety issues included soft tissue injuries and musculoskeletal injuries caused by interaction forces and torques. The assessment of those safety issues and potential influencing factors such as misalignments between the human anatomy and the device, or patient characteristics, were further investigated in the following chapters.

The safety issue of physical interaction at soft tissue level is addressed in **Chapter 4**, where a prototype measuring device for assessing net forces and the pressure distribution at the interface between a human limb and a rehabilitation robot is presented and critically assessed.

To increase the understanding of misalignments which can be considered a common safety concern in exoskeleton use, the two following chapters present the results of research investigating the effects of misalignment on joint load. In both chapters, an instrumented leg simulator and a manually flexed passive knee brace were used to measure the changes in knee joint load in different misalignment scenarios. The research in **Chapter 5** includes an analysis of knee joint forces and torques during swing with several directions of translational and rotational misalignments. In **Chapter 6**, those misalignment experiments are repeated with a modified instrumented leg simulator to investigate the effect of using different artificial soft tissues on the outcomes.

Next to a lack of measurement methods and procedures for safety assessments of rehabilitation robots, we identified a lack of knowledge regarding acceptable limit values for the close and prolonged physical interaction between rehabilitation robots and humans. Therefore, **Chapter 7** presents research on comfort thresholds for repetitive forces applied to the human thigh for prolonged durations mimicking the use of an exoskeleton.

Finally, in **Chapter 8**, the results of these studies are integrated and discussed. This chapter also includes suggestions for future work to address remaining challenges and further improve the understanding of rehabilitation robot safety and how to assess it.

Robot-assisted gait training (RAGT) devices are used in rehabilitation to improve patients' walking function. While there are some reports on adverse events (AEs) and associated risks in overground exoskeletons, the risks of stationary gait trainers cannot be accurately assessed. We therefore aimed to collect information on AEs occurring during use of stationary gait robots and identify associated risks as well as gaps and needs for safe use of these devices.

We searched both bibliographic and full-text literature databases for peer-reviewed articles describing outcomes of stationary RAGT and specifically mentioning AEs. We then compiled information on occurrence and types of AEs and on the quality of adverse event reporting. Based on this, we analyzed risks of RAGT in stationary gait robots.

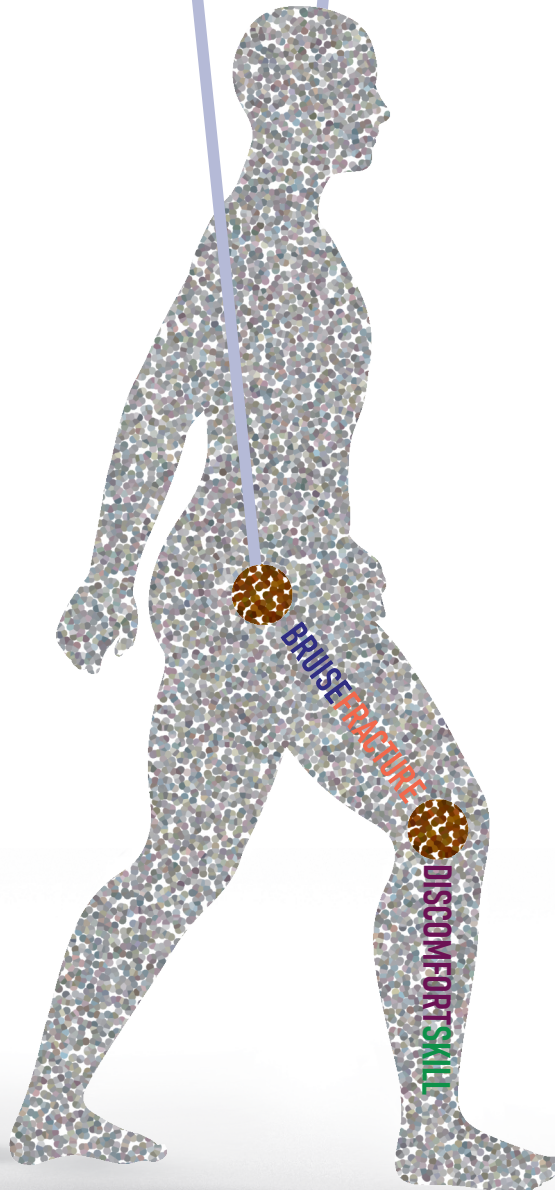
We included 50 studies involving 985 subjects and found reports of AEs in 18 of those studies. Many of the adverse event reports were incomplete or did not include sufficient detail on aspects like severity or patient characteristics, which hinders precise counts of adverse event related information. Over 169 device-related AEs experienced by between 79 and 124 patients were reported. Soft tissue-related AEs occurred most frequently and were mostly reported in end-effector-type devices. Musculoskeletal AEs had the second highest prevalence and occurred mainly in exoskeleton-type devices. We further identified physiological AEs including blood pressure changes which occurred in both exoskeleton-type and end-effector-type devices.

Training in stationary gait robots can cause injuries or discomfort to skin, underlying tissue and the musculoskeletal system as well as unwanted blood pressure changes. The underlying risks for the most prevalent injury types include excessive pressure and shear at the interface between robot and human (cuffs/harness), as well as increased moments and forces applied to the musculoskeletal system likely caused by misalignments (between joint axes of robot and human). There is a need for more structured and complete recording and dissemination of AEs related to robotic gait training to increase knowledge on risks. With this information, appropriate mitigation strategies can and should be developed and implemented in RAGT devices, to increase their safety.

Chapter 2

Occurrence and type of adverse events during the use of stationary gait robots

A systematic literature review



INTRODUCTION

Robot-assisted gait training (RAGT) is frequently used in rehabilitation to promote walking function in individuals with various disabilities such as stroke, spinal cord injury or cerebral palsy. The rates of disability, e.g. as a result of chronic stroke, are rising due to population ageing. According to the World Health Organization, the proportion of the world's population aged over 60 years will increase drastically from 12% in 2015 to 22% in 2050 [2]. This leads to an increasing amount of persons with chronic walking disabilities which will in turn lead to a lack of skilled physical therapists.

Robotic gait trainers can be used for various patient groups to provide them with high-intensity gait training. While traditional gait training on a treadmill is associated with high physical strain on the therapists and a need for two to three therapists per patient, robotic gait trainers have the advantage of reducing the time and effort required from the therapist. As a result, they potentially allow for longer or more frequent sessions of high intensity gait training for the patient [30].

There are different types of robotic gait trainers. Overground gait trainers include ambulatory exoskeletons such as the ReWalk (Argo Medical Technologies Ltd, Israel), Ekso GT (Ekso Bionics, USA), HAL (Cyberdyne, Japan), Rex (Rex Bionics, New Zealand) and Indego (Parker Hannifin Corp., USA). Stationary gait trainers can be divided into two subcategories: exoskeleton-type devices and end-effector-type devices. Exoskeleton type devices usually consist of a treadmill, an overhead harness for body-weight support and a lower limb exoskeleton fixed to a frame. Examples of exoskeleton-type devices are the Lokomat (Hocoma, Switzerland), AutoAmbulator (Motorika, USA), RoboGait (Bama Technology, Turkey), Walkbot (P&S Mechanics, South Korea) and the NX-A3 (Guangzhou YiKing Medical Equipment Industrial, China). End-effector type devices such as the GEO system (Reha-Technology Switzerland), LokoHelp (Woodway, Germany), Gait Trainer GTII (Reha Stim Medtec, Germany) and THERATrainer Lyra (medica Medizintechnik, Germany) consist of an overhead body-weight support and robotic end-effectors which are attached to the patient's feet and are moved along reference trajectories of normal walking.

The advantages of RAGT with regard to time and physical effort required by the therapist are obvious [31]. However, the mechanical power of the robots in combination with the close physical connection with the patient inevitably introduces safety issues. The robot is attached to the patient's limbs, which can lead to dangerous interaction forces. Safe ranges of normal and shear forces that can be applied to a patient during training with a robot are yet to be defined. While recent research has focused on safe limit values in collision situations of physical human-robot-interaction (pHRI) [32], [33], situations of continuous contact are challenging to assess. This is mostly due to a lack of reliable measurement methods, especially concerning shear forces. Much effort has recently been put into the development of those measurement methods [34]–[42]. A method that can be considered as gold standard for measuring normal and tangential forces is the load cell. However, these sensors are rather bulky and expensive, which are possible reasons why many studies implement force sensitive resistors to assess the interaction between a human and a robotic, orthotic or load-carrying device [38], [40], [42]. Drawbacks of force sensitive resistors include a typically non-linear transfer function as well as sensitivity to changes of humidity and surface curvature [38], [43], which are highly relevant during measurement of prolonged human-robot interaction (HRI) between skin and cuff. A number of studies

have focused on developing and implementing alternative sensing devices such as optical sensors [35]–[37], vision-based tactile sensors [39] and pneumatic padding [34], [41], however, these methods are still in research state.

Besides the much needed safe limit values for continuous HRI, simplifying the safety evaluation process is another contributor to improving safety in collaborative and rehabilitation robotics. This is for example done in the COVR project (www.safearoundrobots.com) by providing various structured tools for robot developers, including establishing best practices for safety-related measurements and promoting the development and application of unified safety testing procedures. As a first step in this, specifically regarding rehabilitation robots, risks and needs covering all aspects of continuous patient-robot interaction should be assessed in a structured way, which in turn should inform the development of relevant measurement methods. Therefore, adverse events (AEs) of existing rehabilitation robots need to be taken into account and associated risks need to be identified. A recent review assessed aspects of risk management and occurrence of AEs in overground exoskeletons [44]. Both the FDA (Food and Drug Administration of the United States) database MAUDE (Manufacturer and User Facility Device Experience) and peer-reviewed publications including any of the overground exoskeleton device names mentioned above were searched for AEs during usage of exoskeletons. The review found, among other AEs, a number of device malfunctions, skin and tissue damages and two incidences of bone fractures. Both incidences of bone fractures were attributed to misalignment of the device causing a discrepancy between human joint axis and robot joint axis. This is an indication for the need for extensive post-market surveillance and appropriate testing methods for safety of robotic gait rehabilitation devices.

A recent Cochrane review assessing clinical effects of electromechanical-assisted training for walking after stroke [31] also collected information on any AEs reported in those studies. The most frequently documented adverse effects and reasons for dropout were pain and skin breakdown. In the light of obvious differences between stationary RAGT and overground exoskeletons, such as use of body-weight support (BWS) in stationary RAGT compared to crutches in overground exoskeletons to decrease the risk of falls, and professional supervision compared to oversight by a trained family member, it seems straightforward to assume that AEs in stationary RAGT are less frequent and less severe than in overground exoskeletons due to its controlled environment. However, there is insufficient structured information available on occurrence of AEs in stationary RAGT. Moreover, there currently is no European equivalent to the US MAUDE database in operation and other parts of the world have in turn different processes [20], which makes it difficult to find reliable worldwide information on the frequency and severity of AEs.

Therefore, this paper presents a systematic literature review of AEs that occurred during training with stationary robotic gait trainers. We hypothesized that there are incidences of skin breakdown and bone fractures in RAGT and further expected that the reporting of these events is lacking detail. We searched both bibliographic and full-text literature databases for peer-reviewed articles describing outcomes of RAGT and specifically mentioning AEs. From this, we extracted information about AEs and their reporting, with the objective to get an overview of the occurrence and type of AEs in stationary robotic gait trainers and identify particular risks involved.

METHODS

Search strategy and data sources

We conducted an electronic database search in relevant bibliographic (PubMed, Scopus, Web of Science) and full-text databases (IEEE Xplore Digital Library, SpringerLink, ScienceDirect, SAGE Publications, AHA Journals) from inception to June 2019. We used the following search terms for all data bases:

- Robotics, robot-assisted, robotics-assisted, electromechanical, electro-mechanical
- Exercise therapy, rehabilitation, training
- Gait, walk, walking, step, stepping, locomotor, locomotion
- Bodyweight-supported treadmill training, locomotor training, Lokomat, Gangtrainer (GT), GEO, WALKBOT, LokoHelp
- Adverse, skin breakdown, skin lesion, skin sore, pressure sore, discomfort, abrasion

The complete search strategy used in PubMed can be found in the Annex. This search was adapted to suit the other databases and we searched full text (where available), title abstract and keywords. Reference lists of included articles were scanned for potentially relevant additions.

Study selection

The criteria that were applied for study selection can be found in Table 2.1. We did not apply criteria in terms of study design, population or comparators as we aimed to find all available information on AEs in stationary robotic gait training with humans. After exclusion of duplicate entries, the titles were screened by two reviewers independently (GP and JB). Following that, the abstracts of the remaining studies were screened by EP and JB and in a third step the full texts were screened by RS and JB. A third reviewer could be consulted in case of a disagreement between the two respective reviewers (EP for title screening and GP for abstract and full text screening). Title and abstract screening were performed using a web-based tool [45].

Data extraction and analysis

As this systematic review's main aim was to collect and analyze AEs in RAGT, we did not perform a methodological quality judgement. We employed the PRISMA reporting guidelines [46] as far as they were applicable to this review. Restrictions of their applicability were due to the fact that this review does not focus on clinical effects of an intervention. For collecting relevant data from all included studies, we developed a structured table. The data categories that the studies were screened for are:

1. Subject characteristics
2. Training device
3. Study design
4. Description of AEs and dropouts

Table 2.1 | Inclusion and exclusion criteria.

Criteria	Inclusion criteria	Exclusion criteria
1	Articles must be peer-reviewed (full) papers	Conference abstracts and other non-peer-reviewed articles were excluded
2	Articles must be trials with human subjects	All articles that were not trials including human subjects (e.g. Literature reviews, study protocols, animal studies) were excluded
3	Articles must address robotic-assisted stationary gait training <ul style="list-style-type: none"> • Either exoskeleton-type or end-effector-type • Person standing upright, doing stepping movements • Being attached to the lower extremity • Stationary 	Articles addressing other technologies (e.g. surgical robots, overground exoskeletons, upper-limb robots) were excluded
4	Articles must include a specific statement about AEs (this can also be a statement saying that no AEs occurred)	Articles not including any statement about AEs related to the robotic gait training were excluded
5	Articles must be available in English language	Articles written in other languages were excluded

We collected information on number of subjects performing gait training, age, diagnoses, time since onset and severity. Since the diagnoses varied strongly, no overarching measure for disease severity or disease stage could be defined to describe functional level or chronicity. The study design type as well as number and duration of sessions were noted. Device types (exoskeleton-type, end-effector-type, soft exosuit) and names were collected. Moreover, we screened for information on amount of BWS and type of HRI. Types of HRI such as active, passive and assistive were based on a review by Basteris et al. [47].

Regarding AEs, we collected the number of studies reporting the presence of AEs, number of affected study participants, methods used to detect AEs as well as numbers and types of AEs. Where it became apparent that several studies reported on the same trial (same intervention and same patients), we excluded any double reports to avoid bias. The description of AEs was assessed for completeness. An AE description was considered as complete whenever it included (1) a description of the AE itself including number of occurrence, (2) the number of subjects affected and (3) the intervention during which the AE occurred. A statement that no AE occurred was rated as incomplete if it contained contradictory information or was lacking information (e.g. only part of the intervention considered, only referring to serious adverse events (SAE)). We only collected AEs that were related to RAGT. When an event was described by the authors as unrelated to the intervention, it was not included in the data for this review. We did however include events with unspecified causes.

For better comparison between studies, AE type and severity were categorized as follows. For the type of AEs, we used the categories soft tissue-related (e.g. skin reddening, lesions, bruises, discomfort from harness), musculoskeletal (e.g. joint pain, muscle pain, bone fractures) and physiological (e.g.

blood pressure changes). Events that matched neither of these categories (e.g. headache, fear) were classified as other. Severity of AEs was classified as mild, moderate or severe (adapted from [48], [49]):

- Mild: Event is noticeable but easily tolerable. No medical intervention needed and treatment does not have to be interrupted or only for a short rest (e.g. minor discomfort, reddening)
- Moderate: Event interferes with activities or treatment but can be managed by simple measures. No long term effects (e.g. skin lesions without complications)
- Severe: Event is incapacitating, requires medical attention / treatment, normal treatment cannot be continued (e.g. bone fractures, skin lesions with complications)

If there was no description of an interruption of training or any other indication of a more severe event, the AE was assumed to be mild. Where there was no description of the AE that allowed us to conclude the severity, it was counted as unknown. Note that a severe AE as classified in this study does not automatically constitute an SAE according to the definition of the Medical Device Regulation [18]. However, any SAE would be counted as severe in this review. To compare the severity of different AE types and between different devices or device types, we rated mild AEs with a severity of 1, moderate AEs with a severity of 4 and severe AEs with a severity of 10 and calculated the overall severity per device and per AE type as follows:

$$severity_{overall} = \frac{1n_{mild} + 4n_{moderate} + 10n_{severe}}{n_{total} - n_{unknown}}$$

where n_{mild} is the number of mild adverse events, $n_{moderate}$ is the number of moderate adverse events, n_{severe} is the number of severe adverse events, n_{total} is the total number of reported adverse events and $n_{unknown}$ is the number of adverse events with unknown severity level.

The classes of AE severity and their ratings (1 for mild, 4 for moderate and 10 for severe) are chosen arbitrarily, based on the authors' experience and judgement. They are not validated and are used solely to get a rough estimate of severities for comparisons between device types or AE types.

We performed Pearson's chi-squared tests of independence (MATLAB®, version 2019b, Mathworks, Natick, Massachusetts, USA) to investigate whether there are any relationships between devices or device types, AE types and AE severities. We employed a significance level of 5%.

RESULTS

Study selection

We identified 1081 unique records through database searching and one addition through reference searching (Figure 2.1). Of those, 139 records remained after title and abstract screening, of which 50 met the inclusion criteria and were analyzed [49]–[98]. We identified some studies with overlap in patients ([50], [90]; [71], [72]; [73], [74]; [92], [93]) and excluded double reports in the analysis of subject numbers and AE numbers.

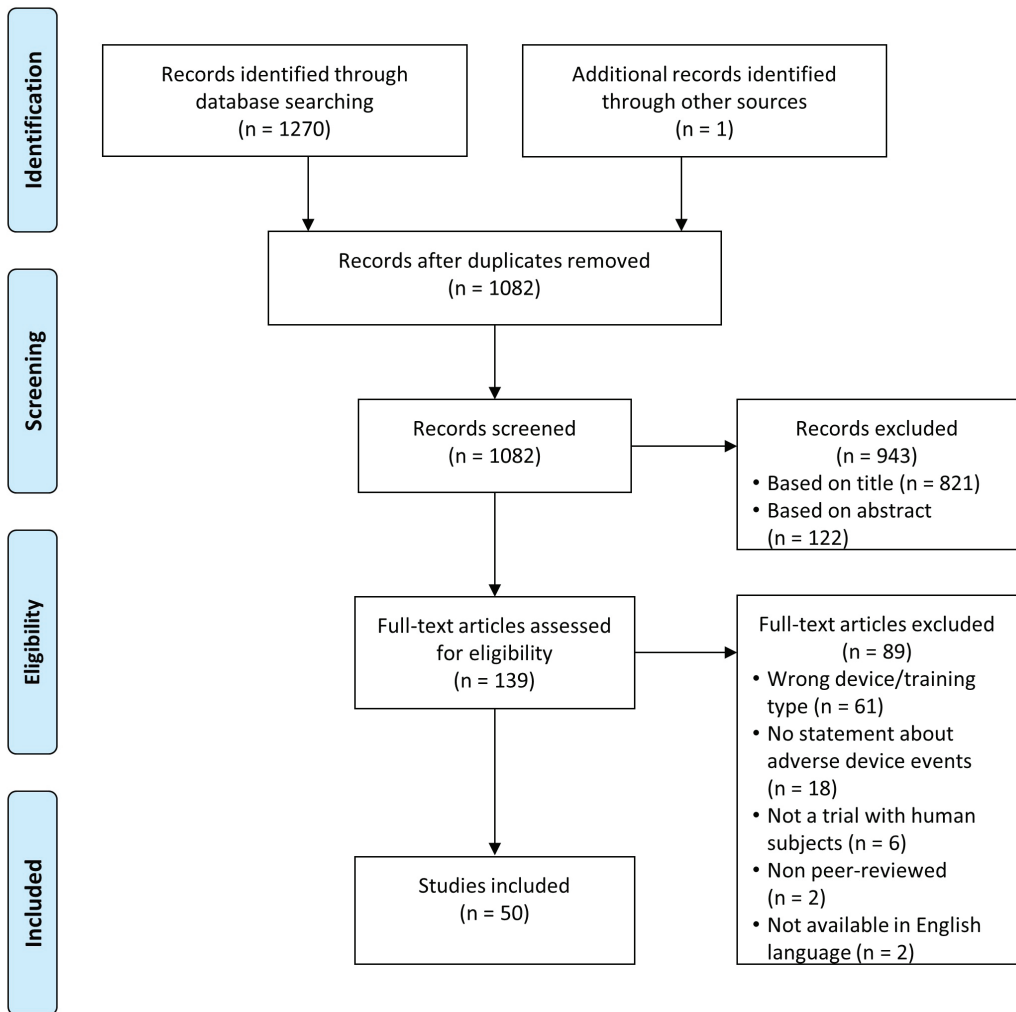


Figure 2.1 | Flow diagram study identification based on [46].

Patients and devices

The included studies described RAGT in 985 subjects of which 14 were healthy individuals, 341 SCI patients, 326 stroke patients, 42 traumatic brain injury patients, 67 cerebral palsy patients, 74 Parkinson's disease patients, 76 multiple sclerosis patients, 15 cardiac patients and 30 patients with other diagnoses. The identified studies reported on gait training in 10 different devices: Lokomat (489 subjects in 27 studies), Gait Trainer GT (301 subjects in 8 studies; 244 subjects trained in GT II, 24 in GT I and for 33 subjects the model was not specified), HAL (108 subjects in 9 studies), MorningWalk (25 subjects in 1 study), LokoHelp (22 subjects in 2 studies), Anklebot (14 subjects in 1 study), Gait-Assistance Robot GAR (13 subjects in 1 study), G-EO (7 subjects in 1 study), a soft exosuit (5 subjects in 1 study) and PH-EXOS (1 subject in 1 study). One study reported the use of both Lokomat and G-EO and one study reported the use of both Lokomat and GT.

Table 2.2 Overview of studies with adverse events (AEs) vs. studies without adverse events.

	Studies that reported AEs	Studies that reported no AEs
Number of studies	18	32
Completeness of AE description (complete/incomplete)	14/4	28/4
Number of subjects performing RAGT	291	694
Dropouts	19 dropouts in 6 studies, 0 lost to follow-up, 1 not stated	47 dropouts in 8 studies, 6 lost to follow-up in 4 studies, 3 not stated
Diagnosis	SCI, TBI, CP, stroke, PD, MS, other	SCI, TBI, CP, stroke, PD, MS, cardiac, other, healthy
Age (mean (SD of means))	42 (19)	53 (12)
Months since onset (range)	[0;276]	[1;420]
Level of severity	mild to severe (FAC 0-4, ASIA A-D)	mild to severe (FAC 0-5, ASIA A-D)
Study design type	7 RCT (2 pilot), 3 longitudinal uncontrolled, 2 longitudinal repeated measure (1 randomized, 1 controlled), 1 retrospective review of data, 4 case reports, 1 case series	16 RCT (2 pilot, 3 repeated measures), 9 longitudinal uncontrolled (2 pilot), 4 cross-sectional repeated measure (1 pilot), 2 longitudinal controlled, 1 longitudinal repeated measure series
Number of studies per device	12 Lokomat ^A , 3 HAL ^B , 2 LokoHelp ^C , 1 GT ^D , 1 G-EO ^E	15 Lokomat ^F , 6 HAL ^G , 7 GT ^H , 1 soft exosuit ^I , 1 Anklebot ^J , 1 Morning Walk ^K , 1 GAR ^L , 1 PHEXOS ^M
Number of sessions per participant (range)	[4;60]	[1;179]
Training duration per session (range) [min]	[6;60]	[0.5;45]
Total duration of training period (range) [days]	[8;84]	[1;365]
BWS (range)	[0% body weight; 100% body weight]	[0% body weight; 50% body weight]
Device types	15 exoskeleton, 4 end-effector	24 exoskeleton, 8 end-effector, 1 exosuit
Types of HRI	assistive, active, passive	assistive, active, passive, path guidance, resistive

SCI: spinal cord injury; TBI: traumatic brain injury; CP: cerebral palsy; PD: Parkinson's disease; MS: multiple sclerosis; SD: standard deviation; FAC: functional ambulation category; ASIA: American Spinal Injury Association; RCT: randomized controlled trial

^A[49], [55], [56], [59], [60], [64], [69], [73], [74], [92], [93], [98]; ^B[70], [71], [84]; ^C[62], [63]; ^D[82]; ^E[59]; ^F[52]–[54], [57], [66], [76]–[81], [88], [89], [94], [96]; ^G[50], [67], [72], [90], [91], [95]; ^H[54], [58], [65], [68], [83], [86], [87]; ^I[51]; ^J[61]; ^K[75]; ^L[85]; ^M[97]

Adverse events

Of the 50 included studies, 18 reported AEs and 32 reported that there were no AEs (Table 2.2). The information on AEs was rated as incomplete in 8 (16%) of the 50 studies. In the studies with reported AEs, 78% of the AE descriptions were complete while in the studies without reported AEs, 88% of the descriptions were complete. The dropout rate was 7% of the participants in both groups. Studies with AEs had 16 participants on average and studies without AEs had 22 participants on average. Apart from the fact that none of the studies with healthy participants reported AEs, there were no striking differences in subject characteristics. Both age and diagnoses were comparable. Studies with AEs were less frequently randomized controlled trials (39% compared to 50% of studies without AEs) and were more likely to be case reports or case series, some of which were focused on reporting AEs [60], [64], [74]. Concerning devices involved, 44% of the Lokomat studies, 33% of the HAL studies and 13% of the GT studies reported AEs. There were no AEs reported for MorningWalk, Anklebot, Gait-Assistance Robot GAR, the soft exosuit or PH-EXOS. The range of BWS in studies reporting AEs was between 0 and 100% of body weight, while it was between 0 and 50% of body weight in the studies reporting no AEs.

The AE descriptions from the 18 studies that did report AEs are collected in Table 2.3. The most frequently reported AEs were changes to skin or soft tissue (more than 47 occurrences in 40 subjects) including skin reddening, skin lesions, skin abrasions, a blood blister, chafing, skin irritation due to EMG electrodes and bruises [49], [59], [69], [71], [73], [74], [84], [93], [98]. The most severe AE reported was one bone fracture in the context of Lokomat training [60]. The fracture to the proximal anterior and medial part of the tibia occurred in a patient with T12 incomplete paraplegia. The authors did not report any unusual event causing the injury. The patient had trained 18 sessions in the Lokomat (30 min per session, 5 times per week, 50% BWS, guiding force between 75 and 100%) and complained of pain in the anterior region of the knee at the beginning of session 19. Bone densitometry performed after the event revealed low bone mineral density. The result of this did not classify as severe osteoporosis, which would have constituted a contraindication for Lokomat training. The two other severe AEs were an open skin lesion and a tendinopathy during Lokomat training [49]. Mild or moderate joint pain was reported 21 times and occurred mostly in the knee [49], [62]–[64], [82], [84]. Other musculoskeletal AEs included muscle pain, tendinopathy and lower back pain [49], [62], totaling 40 occurrences. There were 21 physiological AEs in 7 subjects including giddiness (mild) [56] and blood pressure changes (both hypotension and hypertension) [64], [70], [82], [93] which were all classified as moderate (Figure 2.2). Another frequent AE (more than 17 occurrences) was discomfort related to the harness (e.g. to the groin, armpit or shoulders) which was mostly classified as mild [55], [56], [62]–[64], [84], [93]. Other AEs identified in this review with 7 occurrences were pain (not specified) [59], fear of the gait robot [56], headache, menstrual cramps [62], the feeling of being trapped and the sense of the gait robot being heavy over the lower back [84].

Table 2.3 Adverse events (AE) detailed.

Reference	Device	AE description	AE occurrence	Severity	Category AE	Caused by	Caused dropouts
Borggraefe et al., 2010 [49]	Lokomat	muscle pain	16	mild	musculoskeletal	not stated	no
		joint pain	14	mild (12), moderate (2)	musculoskeletal	not stated	yes (2)
		skin erythema	12	mild	soft tissue-related	cuffs	no
		open skin lesions	4	mild (2), moderate (1), severe (1)	soft tissue-related	cuffs	yes (2)
		tendinopathy	1	severe	musculoskeletal	not stated	yes
Carda et al., 2012 [55]	Lokomat	mild discomfort	3	mild	soft tissue-related	harness	no
Chin et al., 2010 [56]	Lokomat	discomfort and redness in groin area	a few	mild	soft tissue-related	harness	no
		skin abrasions	3	moderate	soft tissue-related	cuffs	no
		giddiness	1	mild	physiological	not stated	no
		lower limb bruises	1	moderate	soft tissue-related	cuffs	yes
		fear of gait trainer	1	moderate	other	not stated	yes
Esquenazi et al., 2017 [59]	not stated (Lokomat or G-EO)	skin irritation and pain	4	unknown	soft tissue-related/other	not stated	no
Filippo et al., 2015 [60]	Lokomat	proximal tibia fracture	1	severe	musculoskeletal	not stated	not applicable
Freivogel et al., 2008 [62]	LokoHelp	discomfort in groin or armpit	11	mild	soft tissue-related	harness	no
		discomfort in right hip	1	mild	musculoskeletal	not stated	no
		lower back pain	1	mild	musculoskeletal	not stated	no
		headache	3 (1) ^A	mild	other	not stated	no
		menstrual cramps	1	mild	other	not stated	no
		knee pain	1	moderate	musculoskeletal	not stated	no
		not described	5	unknown	unknown	not stated	no
Freivogel et al., 2009 [63]	LokoHelp	discomfort	33	unknown	soft tissue-related	mostly harness	no
		knee pain	1	unknown	musculoskeletal	not stated	no

Geigle et al., 2013 [64]	Lokomat	atypical autonomic dysreflexia	4 (1) ^A	moderate	physiological	exercise (did not occur during pure suspension)	yes (dropped out due to elevated BP)
		knee pain	1	minor	musculoskeletal	not stated	
		discomfort	1	minor	soft tissue-related	harness	
Husemann et al., 2007 [69]	Lokomat	skin lesions	2	moderate	soft tissue-related	not stated	yes
Ikumi et al., 2016 [70]	HAL	transient blood pressure change	6 (1) ^A	moderate	physiological	not stated	no
Jansen et al., 2018 [71]	HAL	skin reddening	4	mild	soft tissue-related	EMG electrodes, leg cuffs, shoes	no
Kelley et al., 2013 [73], [74]	Lokomat	skin changes (redness or broken skin)	12 (5) ^A	moderate	soft tissue-related	straps/cuffs	no
Morone et al., 2011 [82]	GT	severe symptomatic hypotension	8 (3) ^A	moderate	physiological	not stated	not stated
		knee pain	1	moderate	musculoskeletal	not stated	not stated
Nilsson et al., 2014 [84]	HAL	knee / malleolus pain	2	moderate	musculoskeletal	cuff pressure	no
		discomfort (feeling of being trapped)	1	moderate	other	straps	no
		discomfort (shoulders)	2	mild	soft tissue-related	straps	no
		sense of suit being heavy over lower back	1	mild	other	weight of suit	no
		skin irritation	1	mild	soft tissue-related	EMG electrodes	no
		groin pain, chafing	1	moderate	soft tissue-related	harness	no
Stoller et al., 2014 [92], [93]	Lokomat	tibia skin lesion	1	moderate	soft tissue-related	cuffs padding)	yes
		groin pain	1	moderate	soft tissue-related	harness	yes
		high blood pressure	2 (1) ^A	moderate	physiological	not stated	no
Vaney et al., 2012 [98]	Lokomat	minor bruising	some	mild	soft tissue-related	straps	no

^AWhen AE occurrence is presented as X (Y), X is the number of events and Y the number of subjects.

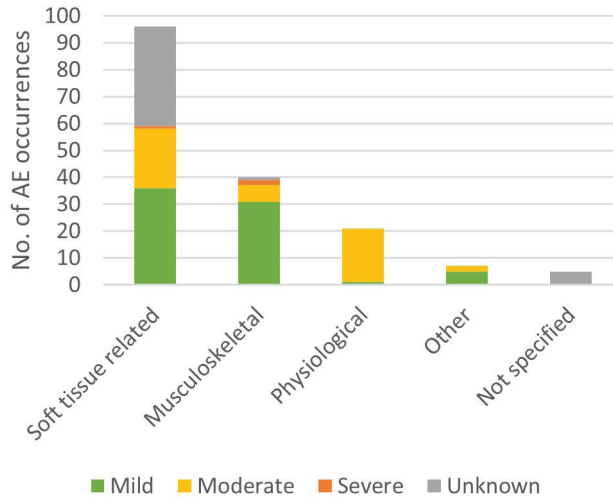


Figure 2.2| Occurrence of adverse event severities per adverse event types.

There was limited information available on duration of gait training before an AE occurred. Chin et al. [56] stated that the dropouts due to bruises and fear of the Lokomat system occurred after 2 to 5 training sessions of 15-45 minutes each and the tibia fracture [60] occurred after 18 sessions of 30 minutes each. Knee pain in LokoHelp [62] occurred after 4 sessions of 30 minutes. Autonomic dysreflexia during Lokomat training [64] occurred 20 minutes into the 10th training session after having completed 9 40-minute-sessions, and transient blood pressure change in HAL training [70] was observed 6 times in 10 sessions of 60 minutes including preparation time. In a case report on the management of skin injuries during Lokomat training [74], it is reported that the subject walked a total of 2 hours in 5 sessions in the Lokomat before the first injury was observed. Borggraefe et al [49] found no correlation between AE incidence and age, duration of RAGT, number of sessions or total distance walked. They did however report that both obese children included in the study developed soft tissue-related AEs (skin erythema, open skin lesion) and that in two cases skin lesions developed next to skin areas covered by diapers.

Methods used to detect AEs included documentation of patient feedback or complaints [49], [60], [62]–[64], [84], [92], [93], patient questionnaires [49], MRI for the detection of a fracture [60], blood pressure monitoring [64], [70], [92], [93], and medical screening before, after and when needed during each training session [73], [74].

Table 2.4 summarizes the frequencies of injury types, severities and causes in the different devices. More than 169 AEs were reported in more than 79 subjects. Exact numbers cannot be stated as the description of AEs was incomplete in 4 studies [56], [59], [63], [98]. Therefore, the occurrences are displayed as ranges in this table. In graphical representations and further analysis of this data, the minimum numbers will be used and presented. In total, between 8 and 13% of the participants experienced AEs. For the Lokomat users, this was between 12 and 18%, for the LokoHelp users between 18 and 90%, for the HAL users 9%, for the GT users 1% and for the G-EO users between 0 and 57%.

Table 2.4 Adverse events classified per device.

	Total	Lokomat	LokoHelp	HAL	GT	G-EO
Event types						
Soft tissue-related	>96 ^{A, B, C, D}	>40 ^{A, B, D}	44 ^C	8	-	≤4 ^B
Musculoskeletal	40	33	4	2	1	-
Physiological	21	7	-	6	8	-
Other	7	1	4	2	-	-
Not specified	5	-	5	-	-	-
Event severity						
Mild	>73 ^{A, D}	>48 ^{A, B, D}	17	8	-	-
Moderate	50	30	1	10	9	-
Severe	3	3	-	-	-	-
Unknown	43 ^C	≤4 ^B	39 ^C	-	-	≤4 ^B
Part of device causing AE						
Cuffs / straps	>42 ^D	>33 ^D	-	9	-	-
Harness	>50 ^A	>5 ^A	≤44 ^C	1	-	-
Total no. of events	>169 ^{A, D}	>81 ^{A, B, D}	57	18	9	≤4 ^B
Total no. of subjects	79<n≤124 ^{A, B, D}	57<n≤90 ^{A, B, D}	4<n≤20 ^D	10	4	≤4 ^B

^A"A few patients experienced discomfort and developed redness in their groin area"; unknown how many patients/events [56].

^B"4 reported adverse events that were study related due to skin irritation and pain"; unknown whether adverse events occurred in Lokomat or G-EO training and how many subjects were affected [59].

^C34 complaints, unclear by how many of the 16 subjects; "mostly" related to the harness (soft tissue) [63].

^E"Some minor bruising from the straps"; number of affected subjects/events not stated [98].

The chi-squared tests indicated that there is no independence of variables in all tested combinations: devices and reported AE types ($X^2 = 88.05$, $p < 0.01$), device types and reported AE types ($X^2 = 15.88$, $p < 0.01$), AE types and severity level ($X^2 = 75.70$, $p < 0.01$), devices and severity level ($X^2 = 115.05$, $p < 0.01$) and device types and severity level ($X^2 = 70.80$, $p < 0.01$). We can therefore conclude that there are relationships between devices, device types, AE types and severity levels of AEs. In other words: The occurrence of AE types differs between device types and between devices, as does the severity between devices, device types and AE types. Articles that did not state absolute numbers [56], [59], [98] were excluded from this analysis.

Relations of AE severity and AE types with device types and devices are detailed in Figure 2.3. Relative to the total number of subjects that trained in each of the devices, on average 16.6 AE occurrences per 100 subjects were reported for Lokomat training, 259 occurrences per 100 subjects for LokoHelp training, 16.7 occurrences per 100 subjects for HAL training, and 3 occurrences in 100 subjects for GT training. While there were no physiological AEs reported in LokoHelp and only physiological AEs in GT, subjects training in the two exoskeleton-type devices Lokomat and HAL were reported to have experienced soft tissue-related, musculoskeletal and physiological AEs (Figure 2.3 (A)). The overall severity of AEs in GT was highest (4.00) with all AEs being moderate, followed by HAL (2.67), Lokomat (2.44) and LokoHelp (1.17) with the majority of AEs being mild (Figure 2.3 (B)). Regarding AE types,

physiological AEs had the highest overall severity (3.86), followed by soft tissue-related AEs (2.27) and other AEs (1.86). Musculoskeletal AEs had the lowest overall severity of 1.92.

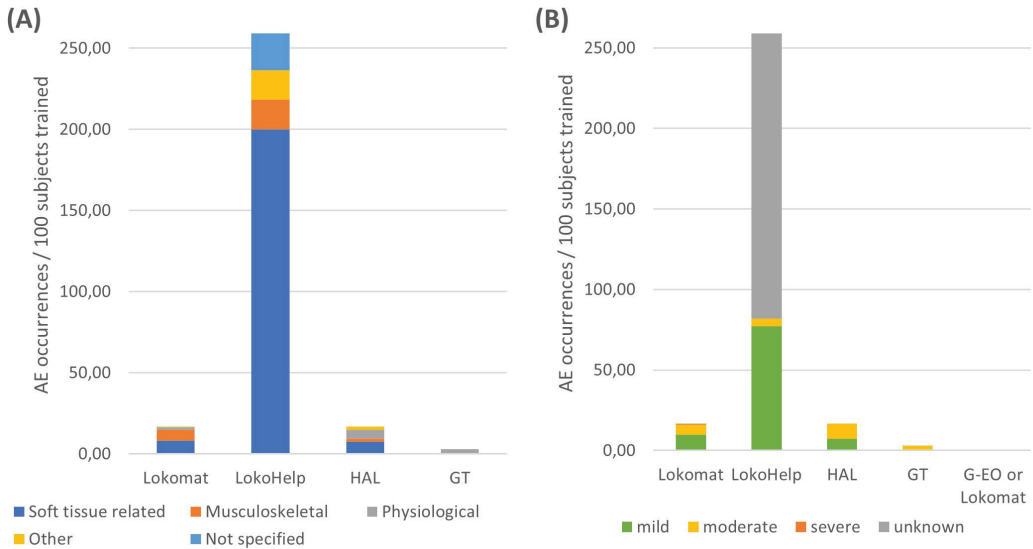


Figure 2.3| Distributions of adverse event types and severities per devices. (A) Occurrences of adverse event types relative to the total number of subjects trained in each device. (B) Occurrences of adverse event severities relative to the total number of subjects trained in each device.

DISCUSSION

In this systematic literature review, we extracted and analyzed information on AEs in RAGT from 50 included studies, involving 985 subjects in total. AEs occurred in 36% of the included studies and in 8 to 13% of the subjects. The findings show that skin injuries and a bone fracture occurred in RAGT, supporting our hypothesis. Moreover, a substantial amount of reports of joint pain, blood pressure change and discomfort caused by the harness indicates that injuries associated with RAGT are broader than skin damage and bone fractures.

The most frequently reported AEs (>96 occurrences, constituting more than half of all AEs) were injuries or discomfort to skin or underlying tissue [49], [59], [69], [71], [73], [74], [84], [92], [93], [98], joint pain (21 occurrences) [49], [62]–[64], [82], [84], blood pressure change (20 occurrences) [64], [70], [82], [92], [93] and discomfort related to the harness (more than 20 occurrences) [55], [56], [62]–[64], [84], [92], [93]. Next to a tendinopathy and an open skin lesion [49] classifying as severe AEs, the most severe AE (and only SAE) was a tibia fracture [60].

Occurrence and severity of adverse events

The overall severity of physiological AEs was highest (3.86), which is related to the fact that training is usually interrupted when a sudden blood pressure change occurs. While one might expect that

musculoskeletal AEs are generally more severe than soft tissue-related AEs, the overall severity of musculoskeletal AEs (1.92) was slightly lower than that of soft tissue-related AEs (2.27). Mild musculoskeletal AEs were minor pain or discomfort to joints or muscles. There were 22 moderate and 1 severe soft tissue-related AEs which included open skin lesions (one of which was severe), bruises and groin pain. For 37 soft tissue-related events no severity could be inferred from the reported information which might have an influence on the overall severity. It can however be concluded that not only physiological and musculoskeletal but also soft tissue-related AEs can require interrupting the RAGT or even medical attention. Specifically in subjects with restricted blood flow or reduced sensation, complications can arise from smaller skin or soft tissue injuries and healing can be impaired [99], which can explain the relatively high overall severity of soft tissue-related AEs. Remarkably, in studies that included healthy subjects, no AEs were experienced, which supports the notion that disturbed physiological and/or sensory function in patients could be a relevant factor. This implies that risks for soft tissue-related AEs should be taken just as seriously as risks for musculoskeletal AEs.

Regarding the devices, the largest absolute number of AEs was reported for training in Lokomat (more than 81 events in 57 to 90 subjects). However, one has to keep in mind that the 50 included articles included 27 Lokomat studies with 489 subjects. So, per 100 subjects, an average of 16.6 AEs were reported in Lokomat training. This is comparable with 18 AEs in 108 subjects performing RAGT with HAL resulting in an average of 16.7 AEs per 100 subjects. For GT, an average of 3.0 AEs per 100 subjects was reported (9 AEs in 301 subjects) and for G-EO between 0 and 57.1 events per 100 subjects. By far the highest relative AE occurrence was reported for LokoHelp training, where the reports (57 AEs in 22 subjects) result in an average of 259 AEs per 100 subjects. Interestingly, while LokoHelp training resulted in the highest relative number of AEs, it also resulted in the lowest overall severity (1.17). Lokomat and HAL are comparable not only in occurrence but also in overall severity of AEs (2.44 and 2.67 respectively). All AEs reported in relation with GT training were moderate (overall severity 4).

Risk factors

The results of the analyses suggest that AEs do occur in RAGT, independent of subjects' age and diagnosis. There were no striking differences in level of severity or time since onset of the disease. We did however observe that there were no reports of AEs in healthy participants. This could be due to a number of reasons: Firstly, only 14 out of 985 subjects (1.4%) were healthy individuals. Secondly, RAGT with healthy individuals was only performed during one day in each of the studies [51], [66], [97], as they are not the targeted population for a training program to improve walking. Both of these aspects decrease the chance of suffering an injury. Thirdly, the characteristics of certain patient groups such as restricted blood flow, reduced sensation, uncontrolled muscle activities or reduced bone mineral density might increase the risk of sustaining injuries in RAGT, in contrast to healthy individuals. The current findings allow us to identify which risk factors are most likely involved in the various AEs reported during stationary RAGT in patients.

Soft tissue-related adverse events

According to the results, skin and other soft tissue injuries are the most frequent AEs related to RAGT. They are mostly caused by either the cuffs/straps [49], [56], [71], [73], [74], [84], [92], [93], [98] or by the harness [55], [56], [62]–[64], [84], [92], [93] and occurred in both device types, although slightly more frequently in end-effector-type devices (13.5 occurrences per 100 subjects) than in exoskeleton-type

devices (7.7 occurrences per 100 subjects on average). Both the cuffs/straps and the harness are mentioned as causes for soft tissue injuries in 7 unique studies respectively. In addition to that, one article mentions diapers as well as obesity as possible risk factors for skin injuries [49]. Remarkably, issues related specifically to cuffs or straps have only been reported in exoskeleton-type devices (Lokomat and HAL). End-effector type devices are only attached to the foot and sometimes to the shank which decreases the number of contact interfaces between human (skin) and robot, reducing the chances for skin irritation at the cuffs and straps in end-effector-type devices. In contrast, exoskeletons have a risk of misalignment between joint axes, which can lead to displacements of the cuff relative to the human limb, resulting in increased shear and pressure in the interface between cuff or strap and skin, which can contribute to soft tissue injuries [100]–[102].

The harness has been stated to be the cause of AEs in Lokomat (>5 AEs) [55], [56], HAL (1 AE) [84] and LokoHelp (44 AEs) [62], [63] with 88% of the events related to the end-effector-type device LokoHelp. Affected body regions included the groin area [56], [62], [84], [93] and armpits [62]. One might assume that higher percentages of BWS lead to a higher risk of discomfort or injuries related to the harness because the pressure in the interface harness-skin is increased. The range of documented BWS in end-effector-type devices was between 0 and 50% and in exoskeleton-type devices between 0 and 100%. It is striking that all studies with BWS above 50% of body weight reported AEs. In the studies reporting discomfort due to the harness, the maximum BWS ranged between 30 and 100% of body weight. All studies reporting BWS above 55% also reported discomfort related to the harness, with the exception of one case report [74] where only the first session was started at 100% BWS but as of the end of session 1, BWS was always <50%. Nevertheless, the large number of harness-related AEs in LokoHelp training was reported in two studies with BWS under 30% [62], [63]. Therefore, lower BWS might decrease but not completely avoid the risk of discomfort related to the harness. Other possible factors might be the design, fitting or material of the harness as well as the clothes worn by the subjects [74], [101].

Overall, the susceptibility to soft tissue-related AEs could be influenced by harness or cuff design and fit, subject characteristics and materials involved in the cuff-skin interface. One study analyzed this aspect and reported that there was no correlation between the incidence of AEs and age [49], but that both obese children included in the study developed a soft tissue-related AE. Moreover, they observed two open skin lesions adjacent to the area where diapers were worn. Another study reported that wrapping the legs of a subject presenting with thin and flaky skin with viscoelastic polymer sheets and elastic bandages helped manage soft tissue-related AEs [74]. Therefore, in addition to the fit of cuffs and harness, both the subjects' weight and/or body composition and materials present in the interface between skin and robot cuffs or the harness might alter the risk for soft tissue-related AEs.

Musculoskeletal adverse events

The findings of this review show that RAGT can lead to musculoskeletal injuries, such as a bone fracture and joint pain. Musculoskeletal AEs were reported in relation to training in Lokomat, LokoHelp, GT and HAL and therefore in both exoskeleton-type devices and end-effector-type devices. However, 88% of the reported musculoskeletal AEs occurred in an exoskeleton-type device (on average 5.6 musculoskeletal AEs per 100 subjects in exoskeleton-type devices compared to 1.4 musculoskeletal AEs per 100 subjects in end-effector-type devices). This leads to the assumption that the risk of sustaining a musculoskeletal injury is higher during exoskeleton-type RAGT. However, it is possible this is influenced

by a single study reporting many occurrences of musculoskeletal AEs (31) in one exoskeleton-type device [49]. The only SAE (bone fracture) reported in the included articles occurred in an exoskeleton-type device. To the best of our knowledge, there are no reports of bone fractures in end-effector-type devices. While this was the only occurrence of a bone fracture in RAGT found through this review, there are several reports of bone fractures in overground exoskeletons [44], [103]. Misalignment is frequently mentioned as assumed cause for bone fractures in overground exoskeleton devices [44], [103], but this has not been discussed as a possible cause in the case report of the tibia fracture sustained during Lokomat training [60]. The authors of this case report discussed low bone mineral density as a possible influencing factor but did not report any details of the relevant training session or discussed other possible reasons. Due to the oversimplification of exoskeleton joints compared to anatomical joints, misalignments are unavoidable [101], [104]. This might lead to the assumption that end-effector-type devices are inherently safer than exoskeleton-type devices. However, end-effector-type devices provide less guidance of the movements and could therefore create movements in arbitrary directions and excessive moments which can cause considerable harm [101]. In end-effector-type gait trainers, this risk could be mitigated by providing appropriate BWS. However, in all end-effector-type gait trainer studies included in this review, BWS was reported to be 50% or lower while exoskeleton-type studies reported BWS up to 100%. This is not related to less severely affected subjects being involved in end-effector-type RAGT studies. The subjects in studies with both types of gait trainers varied strongly in disease severity and walking ability.

Physiological adverse events

Giddiness and changes in blood pressure were reported in relation to Lokomat, HAL and GT training [56], [64], [70], [82], [92], [93]. There were 13 occurrences in 4 subjects reported in exoskeleton-type devices and 8 occurrences in 3 subjects reported in end-effector-type devices. It is striking that all reported blood pressure changes occurred in more severely affected subjects with SCI (ASIA A and C) or subacute stroke (FAC < 3). This indicates that the risk for blood pressure changes in RAGT might be increased in subjects that do not ambulate independently. It is also worth noting that hypertension in SCI as a result of autonomic dysreflexia seems to be linked to the stepping movements in combination with the upright position and did not occur during pure suspension in the harness [64]. A close blood pressure monitoring of patients with a history of blood pressure changes or high risks of orthostatic hypotension or autonomic dysreflexia could help mitigate the risk of physiological AEs.

Documentation of adverse events

The documentation of AEs lacks detail in most studies. A significant amount of included articles (36%) did not provide a complete description of AEs, even though the requirements for regarding AE documentation as complete were relatively low: description of events, the number of affected subjects and the associated device. The assumed cause of the event was only stated in about half of the reports. Moreover, there is a need for documentation on how different types of AEs can be managed or avoided [74].

Although we did not consider this as critical for documenting AEs, it is striking that most reports did not include any information on duration of training before the AEs occurred or characteristics of the affected subjects. Training time before occurrence of an AE was often not stated. Based on literature, one could assume that skin related AEs are more likely to occur in the first training sessions as the skin

can habituate to the stress [105], [106]. In the two studies stating durations of training before the soft tissue-related AEs, they occurred between session 2 and 5 [56], [74]. A more detailed analysis of this aspect is not possible as there is not enough information available on whether the complaints occurred in the beginning or end of the sessions and due to the fact that most studies did not report on training time before AE onset. Subject characteristics related to AEs were only analyzed in detail in one of the included studies [49]. In order to establish more generalizable relations between subject or training characteristics and risk factors, more detailed reports of those aspects in relation to AEs are needed.

Structural documentation of AEs related to RAGT (or any medical device for that matter) is currently not optimally supported or facilitated by regulatory bodies. In other words, AE reporting is not sufficiently obligatory and public. Although some information on safety is shared through the reporting system of the FDA in the US, reporting is only mandatory if it is an SAE and only for manufacturers and healthcare institutions, but not for individual healthcare professionals and consumers [107]. In the EU, there is currently no central reporting system. There are obligations for the manufacturers to report AEs to the competent authorities on a national level but this information is currently not shared with the public. In relation to the current transition from the EU Medical Device Directive to Medical Device Regulation, the reporting system EUDAMED is expected to be (re-)launched in May 2022, with more firm rules for reporting. Information on SAE, device deficiencies, vigilance and post-market surveillance is intended to be submitted through this platform, which will be partly open to the public. Dissemination will include information on device safety and issued certificates, vigilance and post-market surveillance [108], although the exact extent to which information will be accessible to whom is currently unknown. Based on the outcomes of the current review, such facilities are needed to allow and stimulate a more structural reporting of and access to AEs (and not only SAEs). This cannot only inform the end user of risks associated with a certain device but also encourage new, safety-related, developments and ultimately improve safety of RAGT.

Limitations

The findings of this systematic literature review need to be interpreted with care, for several reasons. The primary outcome of the study are AEs reported in RAGT which is why terms related to AEs and injuries were included in the search query. However, most bibliographic databases search for the entered search terms in titles, keywords and abstracts of articles. During this process, we found that information on AEs is frequently not contained in those elements but in the body of text, complicating the search for relevant articles. Therefore we also searched full-text databases, but we cannot be sure that we identified all relevant articles with that method.

Another limitation of this review is a potential overlap of studies. We excluded double reports as much as possible, but we cannot rule out that some articles contained information on the same participants in the same experiment without stating this (e.g., data from a case report on a specific AE might be part of a clinical trial too). Furthermore, some of the relationships between AE occurrence and device type could be biased by few studies stating a lot of AEs for one specific device [49], [62], [63] or including vague statements such as only reporting on (the absence of) SAE or not specifying AE occurrence for each of the interventions involved [56], [59], [97].

Other limitations are related to an expected underrepresentation and incomplete documentation of AEs. It is possible that many other studies where no AEs occurred were published but not included in this article, if they did not contain a statement about AE occurrence. Moreover, we noticed strong variations in the level of detail in which AEs are recorded during a study and reported in articles: while some articles only include more obvious or severe AEs, others may mention all cases of slight discomfort and have asked participants specifically about their experience. The high relative occurrence of AEs in LokoHelp, but with lowest overall severity, is a likely example of this. This hampered a reliable comparison of AE occurrence and severities between device types or devices. More detailed descriptions of AEs and their effects with regard to interruption of training or needed medical attention would allow for a more accurate and detailed severity rating, thereby enabling more valid comparisons. We therefore suggest that editors focus on a correct and complete statement on AEs in scientific reports on medical devices. A statement saying that there were no AEs is just as important as a detailed description on occurred AEs to learn about risks associated with a device. The extension to the CONSORT statement [109] for reporting of harms in randomized controlled trials [110] could serve as a guideline for this. While the CONSORT statement is specifically designed for improving reporting in randomized controlled trials, we suggest that the checklist for reporting of harms is also relevant for other study types. Based on the experiences collected in the process of this systematic literature review we would like to encourage a focus on the following aspects when reporting on AEs in medical device trials:

- Collection of AE information: How were numbers of AEs obtained? Who reported them and were any questionnaires or procedures involved?
- Documentation of AE information: Are all AEs reported or only a specific subset? Report both number of affected subjects and number of occurrences per subject. If no AE occurred, this should be stated clearly.
- AE descriptions: Describe the observed AE concisely including the location. Describe unusual events or subject characteristics that might be related to the AE and discuss possible reasons.
- AE consequences: Did the intervention have to be interrupted? For how long? Was medical attention required? Did the AE cause a dropout and who made that decision? Preferably use standardized definitions of severity levels.

Implications for the use of rehabilitation robots

The aim of this review is to raise awareness of the safety of rehabilitation robots, and while it focuses on risks and needs of rehabilitation robots, it is not intended to discourage their use. Although AEs do occur in RAGT, it has positive effects on gait and has potential to decrease the burden on healthcare professionals [31], [63], [68]. Therefore, a proper balancing of risks and benefits is needed, but in order to do this, proper information about AEs is needed as part of ethical and regulatory decisions to allow use of rehabilitation robots in clinical practice. In order to do this well, correct and sufficient information about AEs is needed. Moreover, AEs should not only be documented but also disseminated to raise awareness of risks. The need for information flow goes both ways: Manufacturers should make their risk/benefit weighting more transparent to allow for healthcare professionals ideally to make an informed decision on the use of robotic devices in therapy, in-/exclusion criteria, associated risks and possible measures. In return, healthcare professionals and researchers should report on AEs and their management, where applicable, in a structured and systematic way to inform developers of rehabilitation robots about ways to improve safety of their devices.

Conclusions

In the present systematic literature review on AEs during the use of stationary robotic gait trainers, including 50 studies and 985 subjects, we found that a total of 169 AEs occurred in 36% of the studies, affecting between 8 and 13% of the subjects. The most frequent types of AEs were soft tissue-related AEs and musculoskeletal AEs, while physiological AEs had the highest overall severity followed by soft tissue-related AEs. Soft tissue-related AEs occurred slightly more frequently in end-effector-type devices than in exoskeleton-type devices and were often associated with the cuffs or straps (only mentioned in relation to exoskeleton-type devices) or with the harness (mostly mentioned in relation to end-effector-type devices). Musculoskeletal AEs were reported more frequently in exoskeleton-type devices than in end-effector-type devices. We have identified two main risk factors: forces in the skin-robot-interface causing skin injuries and forces on the musculoskeletal level causing pain or injuries to the musculoskeletal system. On a more detailed level, hazards are most likely related to an incorrect model fit, insufficient compliance at the points of force transmission from robot to human, materials present at the human-robot interface, misalignments of rotation axes, or subject characteristics like uncontrolled muscle activities or susceptibility to injuries due to overall health status. We additionally identified a lack of completeness of AE reporting in RAGT studies and would like to stress the need for accurate and complete documentation and dissemination of AEs for the identification of hazards and possible mitigation measures. Therefore, AE documentation should receive more attention and researchers, relevant authorities, as well as journal editors should ensure appropriate documentation and dissemination of RAGT related AEs.

The present findings suggest that future developments in RAGT should focus on the subjects' safety, especially mitigating risks associated with pressure and shear applied to the subject's skin, as well as forces applied to the musculoskeletal system that can be harmful due to misalignments. To further investigate effects of these hazards, appropriate measurement methods and experiments are needed. Further, the investigation of forces present in the human-robot interface as well as investigations on acceptable limit values for comfort and safety could help to establish best practices for safe use of rehabilitation robots.

ANNEX

Search Strategy PubMed

- #1 robotics [MeSH] OR robot-assisted OR robotics-assisted OR electromechanical OR electro-mechanical
- #2 exercise therapy [MeSH] OR rehabilitation OR training
- #3 gait OR walk OR walking OR step OR stepping OR locomotor OR locomotion
- #4 #1 AND #2 AND #3
- #5 "body weight support" OR "body weight supported"
- #6 #5 AND "treadmill training"
- #7 #4 OR #6 OR "locomotor training" OR Lokomat OR Gangtrainer OR G-EO OR WALKBOT OR LokoHelp
- #8 adverse OR "skin breakdown" OR "skin lesion" OR "skin sore" OR "pressure sore" or discomfort OR abrasion
- #9 #7 AND #8

The assessment of rehabilitation robot safety is a vital aspect of the development process, which is often experienced as difficult. There are gaps in best practices and knowledge to ensure safe usage of rehabilitation robots. Currently, safety is commonly assessed by monitoring adverse events occurrence. The aim of this article is to explore how safety of rehabilitation robots can be assessed early in the development phase, before they are used with patients.

We are suggesting a uniform approach for safety validation of robots closely interacting with humans, based on safety skills and validation protocols. Safety skills are an abstract representation of the ability of a robot to reduce a specific risk or deal with a specific hazard. They can be implemented in various ways, depending on the application requirements, which enables the use of a single safety skill across a wide range of applications and domains. Safety validation protocols have been developed that correspond to these skills and consider domain-specific conditions. This gives robot users and developers concise testing procedures to prove the mechanical safety of their robotic system, even when the applications are in domains with a lack of standards and best practices such as the healthcare domain.

Based on knowledge about adverse events occurring in rehabilitation robot use, we identified multi-directional excessive forces on the soft tissue level and musculoskeletal level as most relevant hazards for rehabilitation robots and related them to four safety skills, providing a concrete starting point for safety assessment of rehabilitation robots. We further identified a number of gaps which need to be addressed in the future to pave the way for more comprehensive guidelines for rehabilitation robot safety assessments. Predominantly, besides new developments of safety by design features, there is a strong need for reliable measurement methods as well as acceptable limit values for human-robot interaction forces both on skin and joint level.

Chapter 3

Safety assessment of rehabilitation robots

A review identifying safety skills and knowledge gaps



INTRODUCTION

Rehabilitation robots have become increasingly relevant in the past years as new technologies are becoming available and with an increasing need for physical rehabilitation. With the world population ageing and chronic disabilities becoming more frequent as a consequence [1], [2], a lack of skilled clinicians is expected to develop.

In this article, we are using the term rehabilitation robotics as an overarching term that refers to a "medical robot intended by its manufacturer to perform rehabilitation, assessment, compensation or alleviation comprising an actuated applied part" [6]. The actuated applied part is an important feature of a rehabilitation robot. It means that there is a part of the robot which is in contact with the human and intended to provide physical interaction, driven by an actuation system and controlled by the robot alone or in a shared control of robot and patient. There is a wide range of device types that fall under this description and that can be classified in various ways. One way to classify them is by their intended use (i.e. rehabilitation, assessment or assistive), which however can be ambiguous as many devices can be used both in a rehabilitation or training situation and in a home environment as an assistive device [111]. They can be further classified according to their mobility (i.e. fixed or stationary devices versus mobile/ambulatory/wearable devices), the targeted body part (upper limb versus lower limb) and the mechanical setup of each device (e.g. exoskeletons, end-effectors, soft exosuits). Due to considerable research efforts in the field, there are constantly new devices developed and new device types evolving. Therefore, one might need to refine and/or extend the classification of rehabilitation robots in the future [112]. Nonetheless, the most common device types will be introduced in the following sections.

Types of rehabilitation robots

Exoskeletons are rigid anthropomorphic structures that are attached to a human's body segments by the means of cuffs or straps. The exoskeleton's rigid segments are usually attached to the lateral sides of the patient's limbs. The actuation is often either achieved through servo or DC motors at the joints or through cable driven systems [113]. They can be used for different body parts including hand, arms and legs and can be either part of a stationary system, e.g. ArmeoPower for upper extremity and Lokomat for lower extremity (both Hocoma, Volketswil, Switzerland) or wearable and mobile, e.g. MyoPro arm exoskeleton (Myomp, Cambridge, MA, USA) and ReWalk lower limb exoskeleton (ReWalk Bionics, Marlborough, MA, USA).

Exosuits are soft robots that act in a similar way as exoskeletons. However, instead of being built out of rigid structures, they are largely made from soft materials like fabric. Common actuation systems include variable stiffness actuators, series elastic actuators and pneumatic actuators [113], [114]. Exosuits can be used for the upper limb, often as a glove like the Carbonhand (Bioservo Technologies, Kista, Sweden) or for the lower limb like the Myosuit (MyoSwiss, Zurich, Switzerland).

Rehabilitation robot systems based on an end-effector are usually attached to a distal segment of the patient and can, similarly to exoskeletons, be used for upper or lower limbs. While this rehabilitation robot type to some extent is comparable with (collaborative) robot arms in the industrial domain, the shapes and forms of end-effector-type devices in healthcare can be much more diverse. There are devices which make use of an industrial robot arm as the basis. Robot arm type devices for upper

limb rehabilitation can for example be used for assessing or training the range of motion of a patient sitting in a chair, such as Burt (Barrett Technology, Newton, MA, USA), and those for lower limbs can be used for mobilization of patients' legs, such as ROBERT (Life Science Robotics, Aalborg, Denmark). There are other end-effector-type devices which do not have the shape of a robot arm and are often based on a haptic interface, such as the InMotion ARM, (Bionik Laboratories, Toronto, Canada). End-effector based gait trainers such as the G-EO (Reha Technology, Olten, Switzerland), are usually used in combination with a body-weight support system.

Robots for body-weight support are oftentimes used for gait rehabilitation. They can be used as an independent system which is connected to the ceiling via a railing system such as the ZeroG, (Aretech, Ashburg, VA, USA) or FLOAT (Reha-Stim Medtec, Schlieren, Switzerland), in combination with a mobile robot (see below) or as part of a stationary gait trainer (exoskeleton or end-effector). However, body-weight support systems which are built-in subsystems of a stationary or mobile gait trainer robot are not necessarily robots. They can also be dynamic weight lifters without any sensing function or autonomy. There are also robotic arm support systems like the ExoArm (Focal Meditech, Tilburg, Netherlands), which provide an active weight support for the patient's arm and can for example be attached to a wheelchair.

Mobile platform robots are used for gait rehabilitation. They can be combined with a body-weight support to bridge the gap between stationary gait trainers and overground gait training like the Andago (Hocoma, Volketswil, Switzerland). Another type of mobile rehabilitation robot is a robotic walker or cane.

Balance trainers are robots that can be used for balance training and often include a platform (fixed, mobile or in the form of a treadmill) and a weight support system which are programmed to disturb the patient's balance. Examples are the Balance Training Assist (Toyota Motor Corporation, Toyota, Japan) and the Balance Tutor (MediTouch, Netanya, Israel).

Rehabilitation robots as collaborative robots

By definition, a collaborative robot is a robot that works in close interaction with a human. Oftentimes, the task of the collaborative robot is to take over the heavy lifting or repetitive tasks from the workers. Therefore, a rehabilitation robot, which takes over physically demanding or repetitive tasks from the therapist, can be seen as one type of collaborative robot. However, while collaborative robots in industry work together with factory workers, robots in rehabilitation have two very different main types of users: patients and therapists. The therapist can be seen as the equivalent to the factory worker in this comparison as the rehabilitation robot is performing tasks like supporting the patient in repetitive movements or supporting the patient's body weight. The patient has a different role as he or she is usually physically attached to the robot in contrast to the therapist who is standing in close proximity or at most touching the robot with the hands. Safety is an inherent challenge of rehabilitation robots, which does not only include the occupational safety of the therapist but also the safety of the patient who is strapped to the powerful machine that is the robot. In addition to the close interaction, the individual characteristics of each patient are an issue. Pathologies can change pain perception or cause sudden or prolonged movement restrictions, all of which are aspects that can introduce risks. Moreover, rehabilitation robots like wearable exoskeletons can be used in an uncontrolled environment,

as for example a patient's home or a park, which introduces additional hazards that are not present in a controlled environment such as a factory floor.

Implementation barriers

There has been a lot of development of new technologies for rehabilitation robotics in the recent years. However, a number of implementation barriers remain. In addition to ongoing developments in the fields of actuation and mechanical design [16], [115], there are still limited solutions available for recognizing the user's intent for movement and using it as a control input [15], [16]. Moreover, rehabilitation robots are not able to perfectly mimic the movements of the human body. Joints of exoskeletons are often simplified approaches to mimic the movement of the human joints which makes the exoskeleton over-constrained and leads to limitations in degrees of freedom. End-effector-type devices on the other hand are under-constrained which is why they might not offer enough support for more severely affected patients [16].

Beyond those practical barriers, there are some barriers regarding safety. To achieve a comfortable and effective interaction between robot and patient, the mechanical interface needs to be designed in a way that it is compliant enough to ensure comfort and avoid injuries and at the same time stiff enough to transfer the forces to the patient's musculoskeletal system to achieve the intended effect of the robot [15], [16]. Moreover, the mismatch between robot and human joints as addressed above is also an aspect that needs to be considered when discussing safety. A misalignment between the joints of the patient and the robot can lead to unwanted interaction forces, which can potentially be unsafe [101]. Another type of misalignment is unavoidable and related to the oversimplification of the exoskeleton joints. While the flexion axis of the human knee joint for example is displaced during knee flexion, an exoskeleton's knee joint is typically realized by a simple hinge. Therefore, there is a misalignment building during each step [104]. End-effector-type rehabilitation robots offer more degrees of freedom and are under-constrained. Therefore, misalignment as it occurs in exoskeleton devices is avoided in end-effector-type devices. However, due to the under-constrained nature of end-effector-type devices, they can impose unnatural movements on the wearer which might also lead to excessive forces on the musculoskeletal system [101]. Recent studies investigating potential effects of interaction between humans and robots [32], [116], do not focus on rehabilitation robots. Interaction with rehabilitation robots, as opposed to other collaborative robots, is characterized by prolonged physical contact with cyclic loading and unloading and vulnerable users. This underlines the need for carefully considering potential negative effects of the human-robot interaction in the rehabilitation domain and investigating how to avoid or minimize them.

Before rehabilitation robots can be made commercially available in the European Union (EU), they need CE certification. To achieve that, the manufacturer needs to demonstrate that their device is safe. However, safety validation of rehabilitation robots is complex. This is partly due to the fact that the field of rehabilitation robots is a rather new field, which reduces the availability of best practices and applicable safety standards. Especially when it comes to explicit testing procedures that can be used during robot development, information in regulations and standards is rare, or scattered across multiple standards. The familiarization with applicable regulations and standards and the process of safety validation takes a lot of time, which can be a burden, especially for small to medium enterprises and start-ups.

The assessment of rehabilitation robot safety is a vital aspect of the development process, which is often experienced as difficult. Safety of rehabilitation robot use in clinical trials, including the monitoring and reporting of adverse events [3], [31], is one important aspect. However, this has been covered elsewhere [117] and will therefore not be addressed in this article. This article is instead focusing on guidance for validating mechanical safety of rehabilitation robots in the development phase, as required for the risk management process [118], [119].

To provide directions for developers as a guideline to evaluate rehabilitation robot safety, this article first gives an overview of the state of the art in rehabilitation robot safety validation. Key information on the regulatory background and safety certification process is summarized and a new concept for a cross-domain knowledge platform on safety validation is introduced. Then, we will identify the most relevant hazards when using rehabilitation robots based on a recent systematic literature review and additional literature. Next, we explain how those hazards are translated to so-called safety skills. These are abstract representations of safe target behaviors of a robot that can be validated by executing structured testing protocols. This article concludes by identifying the most pressing gaps and needs that have to be overcome and recommending ways to achieve this.

REHABILITATION ROBOT SAFETY AND VALIDATION – STATE OF THE ART

Regulatory background

In the EU the legislation for medical devices applies for rehabilitation robots. In 2017, EU regulation 2017/745 [18], also known as the Medical Device Regulation (MDR), was accepted by the European Parliament. The MDR is replacing council directives 90/385/EEC and 93/42/EEC, also known respectively as the Active Implantable Medical Devices Directive (AIMDD) and the Medical Device Directive (MDD), where the MDD was the relevant legislation for rehabilitation robots. On May 26, 2017, a transition period started to enable companies, developers and Notified Bodies to take the appropriate measures to comply with the MDR, which will become fully operational May 26, 2021 [120].

Where the MDD appeared to focus mainly on safety of a medical device during the design process [20], the MDR emphasizes safety and performance during its entire lifetime. This is apparent in a number of articles focusing on post-market surveillance, including required periodic post-market safety reports. The level of detail needed for this post-market evaluation depends on the risk classification of the medical device and the methodology has to be adequately defined by the manufacturer before the device can receive CE marking. So, where for a class I device a post-market surveillance strategy consisting of user surveys could suffice, class III devices could also require a more elaborate post-market strategy that involves the collection of data related to performance and safety of the device in use. The MDR also adds a strong focus on the performance of the medical device, being more prescriptive than the MDD on how medical claims of the device can be proven, how to conduct clinical investigation in the pre-market phase, and extending it to post-market surveillance as well (e.g. post market clinical follow-up, PMCF). The goal for this is that all claims with respect to clinical performance as stated by the manufacturer have to be supported by clinical data but also to evaluate and improve the initial risk analysis, thus providing additional information for the risk/benefit analysis. These processes should

be properly described for the risk management process, as described in ISO 14971 *Medical devices – Application of risk management to medical devices* [119]. The clinical data to support the clinical performance claims can be collected during clinical studies. In essence, the requirements in the MDR for conducting clinical studies follow the Good Clinical Practice (GCP) guidelines for medical devices [121]. The MDR also contains a clear definition for clinical data to support the clinical performance claims, which is also more prescriptive than in the MDD.

As an aid for demonstrating conformity, standards are often used. For active medical devices, usually the standard IEC 60601-1 *Medical electrical equipment - Part 1: General requirements for basic safety and essential performance* is the standard to use, including the additional standards from the IEC 60601-1 series, like the EN-IEC 60601-1-2, IEC 60601-1-10, etc. Over the past years many different domain-specific standards (IEC 60601-2-xx and IEC 80601-2-xx series) have been developed in addition to IEC 60601-1, which translate the general safety and performance requirements from the IEC 60601-1 into more domain specific safety and performance requirements. In 2019 a new domain-specific standard has been published for the rehabilitation robots domain. This standard (IEC 80601-2-78 *Medical electrical equipment – Part 2-78: Particular requirements for basic safety and essential performance of medical robots for rehabilitation, assessment, compensation or alleviation*) is a domain-specific standard that clarifies a number of items specific to rehabilitation robots, that are not clearly addressed in the IEC 60601-1 or for which interpretation of the IEC 60601-1 can be complicated, e.g. for active applied parts, the definition of support systems etc.

When a device complies with relevant so called harmonized standards, the developer can assume that the device is in agreement with the EU legislation. However, for medical devices the current relevant harmonized standards are harmonized for the MDD. At the time of writing this paper, no standards that have been harmonized under the MDR have been published yet in the Official Journal of the European Union. The EU has published a timeline for harmonization of standards according to the MDR. The harmonization deadline for process related standards (e.g. ISO 13485, ISO 14971, ISO 14155) and for labelling requirements (ISO 15223-1 and EN 15986) is May 26, 2020, while the timeline for harmonization of more technical standards ranges between September 2021 and May 2024 [122]. This means that for the period between May 2021 and May 2024 there probably will be no or just a limited number of harmonized standards that can officially be used to demonstrate conformity with the MDR. Manufacturers therefore should discuss with their notified body at an early stage the methods to demonstrate conformity with the MDR to avoid additional costs during the CE process.

Manufacturers of rehabilitation robots should also be aware that article 1.6 of the MDR in essence states that devices that can also be seen as machinery (such as a robot) should also meet essential health and safety requirements as set out in Annex I of the Machinery Directive [18]. This is particularly relevant for demonstrating conformity for CE, since some of the safety aspects relevant for rehabilitation robots can be more explicitly described in the Machinery Directive. Similarly to the applicability of the Machinery Directive, there might be standards from other domains which are more specific than the general safety and performance requirements listed in the MDR and can therefore be relevant for rehabilitation robots. As rehabilitation robots can have similarities with personal care robots as well as with collaborative robots, some of the relevant standards for these domains, like the ISO 13482 or ISO/TS15066, could be used for demonstrating specific essential health and safety aspects of the device

related to the machine aspects of the device. Although robots as medical devices are out of scope for those standards, some methods as well as essential health and safety requirements might be relevant. However, the user has to consider any restrictions or differences between the domains and be aware that the respective standard is not directly applicable.

State of the art for ensuring safety of collaborative robots

Using the Machinery Directive [19] and the related harmonized standard ISO 12100:2010 *Safety of machinery – General principles for design – Risk assessment and risk reduction* [118], there is a typical workflow that any engineer focusing on safety of a collaborative robot system will follow. This workflow is described in [26] together with useful examples, and includes the description of the system and the task (i.e. the robot, the environment, the users), the identification of hazards, an assessment of the resulting risk, and the identification of risk mitigation strategies. In addition to the documentation of the system and the risks involved, a validation of the risk mitigation strategies is also required. This validation is defined as a set of actions to evaluate with evidence that a set of safety functions meet a set of target conditions [29], and is essentially a measurement to prove that a specific system complies with designated operating conditions characterized by a chosen level of risk. Currently there is no guidance from standards on how validation measurements should be executed.

The current cross-domain nature of robotics raises another dilemma for roboticists that many other users of the Machinery Directive and related harmonized standards do not encounter. This arises from the fact that the standards focusing on safety of collaborative robotics are domain-specific, i.e. for manufacturing or medical applications, and it is not always clear to a roboticist which standards are applicable to their system. Currently these standards covering different domains are not synchronized and can have conflicting requirements. This can lead to uncertainty, especially when robots are used in new domains (such as agriculture) or for multiple domains (i.e. an exoskeleton used for medical purposes or to support workers in manufacturing).

Concept safety skills

One proposed method to overcome these current challenges is based around the concept of safety skills. These have been proposed in [29] and address the specific nature of human-robot collaboration by defining a set of abstract safety skills as the ability of a robot system to reduce risk. There can be different actual methods for implementation, depending on the specifics of the application, and these skills can be validated based on those application specifications at a system level.

The EU-funded project COVR (www.safearoundrobots.com) has developed this safety skills concept and the corresponding guidance for validation of these safety skills (in the form of so-called “protocols”) as a means for simplifying the process of ensuring safety for collaborative robots across all domains. While some safety skills would be familiar to engineers well-versed in the manufacturing domain, such as *maintain separation distance* (compare to Safety-Rated Monitored Stop (SRMS) or Speed and Separation Monitoring (SSM) from the ISO/TS 15066) and *limit interaction energy* (compare to Power and Force Limiting (PFL) from the ISO/TS 15066), others might not be known within that domain. The safety skills were identified through a combination of a top-down and bottom-up approach, taken from safeguarding methods suggested in available robotics safety standards from different domains, as well as through an exhaustive analysis of hazards for known, possible robotics types for various

domains.

The most important contribution of the concept of skills is that they offer engineers planning applications featuring collaborative robots a strong conceptual framework for considering risk mitigation strategies. Together with the associated protocols they offer clear guidance for how to execute the validation measurement, regardless of the domain. Since the skills and protocols reference and adhere to the currently available directives and safety standards, engineers are working within the current legal framework. The COVR project has developed a toolkit (toolkit.safearoundrobots.com) which users can use to identify relevant European Directives and Regulations, harmonized standards, and protocols based on their robotic application and safety skill used.

Concept validation protocols

As previously mentioned, the COVR protocols have been developed to support robotics application designers in the process of validating the completed systems. There are currently nineteen validation protocols available through the COVR Toolkit, with at least 12 more planned for the near future. These protocols are structured such that the required validation measurement (as part of the CE process) can be executed, and they are specific for valid combinations of robot devices and safety skills. The main sections of a protocol include:

- Introduction, including definitions and a specification of the scope and limitations of the protocol
- Description of the target behavior and metrics of the safety skill to be validated
- Description of the conditions (including the system description, eventual sub-systems, the environment, and other relevant aspects to consider for the validation measurement)
- Description of the measurement set-up including measurement devices, test arrangement, best practices for data acquisition
- Procedure (including eventual preparation, the test plan, test execution, data analysis practices, and suggestions for reporting and documentation)
- Eventual annexes with further information

These protocols can be considered to be an industry-wide best practice, providing guidance that goes beyond what is currently available in robotics safety standards on how to execute the validation measurement. They only look at system level behavior (not individual sensor functionality) and are closely related to the concept of safety skills. The protocols are testing procedures for safety validation and not to be confused with protocols used to evaluate safety during robot use, e.g. by monitoring adverse events in clinical trials [49], [123], [124]. While addressing comfort and safety during use of rehabilitation robots is important [117], we are aiming to develop procedures for validating mechanical safety in the development phase, usually without a human in the loop. Ultimately, this aims to advance safety of a rehabilitation robot as much as possible before testing it clinically with (impaired) persons, potentially reducing the number or severity of adverse events occurring.

IDENTIFIED HAZARDS

Before safety skills and accompanying protocols can be applied to validate risk mitigation measures, risks need to be assessed based on the hazards associated with a cobot. Knowing which hazards need to be considered is therefore important to account for safety early in the design process of a rehabilitation robot and monitor it throughout its lifetime. This section provides an overview of frequent adverse effects of rehabilitation robot use and relates them to the underlying hazards.

In a recent systematic literature review [117], we collected information on occurrence and type of adverse events reported in connection with training in stationary robotic gait trainers. We counted approximately 17 adverse events per 100 subjects trained in a stationary robotic gait trainer. The adverse events were categorized with the most frequent types being soft tissue-related adverse events and musculoskeletal adverse events (Figure 3.1). The third category, physiological adverse events (e.g. sudden blood pressure changes), is regarded as unrelated to the mechanical setup of the robotic device in most cases, but to the being engaged in activity in general, and is therefore not analyzed in this article. Soft tissue-related adverse events in stationary gait trainers included skin irritation, skin reddening, skin abrasions, open skin lesions and bruising as well as discomfort and pain to soft tissue areas. Musculoskeletal adverse effects extracted from the systematic review were a tendinopathy, a tibia fracture, muscle pain, lower back pain, malleolus pain and discomfort and pain to joints.

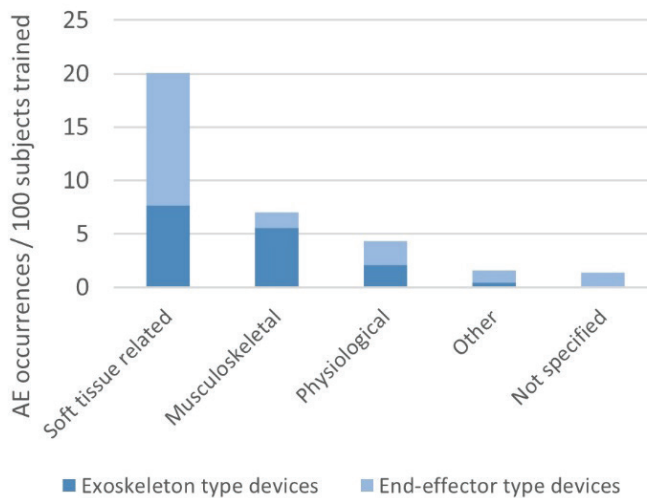


Figure 3.1| Types and occurrence of adverse events (AE) in stationary robotic gait training.

In addition to general risk factors of the particular target population(s) for sustaining an injury, which include patient characteristics such as restricted blood flow, reduced sensation, uncontrolled muscle activities and low bone mineral density, there are risk factors which are connected to the design of the device. The soft tissue-related and musculoskeletal adverse events are all regarded to be attributable to forces exceeding safe limits.

In order to fulfill their function of supporting a certain movement in a patient, rehabilitation robots need to apply forces to the patient's musculoskeletal system. Those forces are applied through contact points such as cuffs, straps, foot plates or harnesses and travel through soft tissues to the musculoskeletal system of the user. Excessively high forces can cause injuries both in soft tissue and in the musculoskeletal system. The nature and causes of those forces can however vary per event. As this principle of applying forces through contact points is the same for all rehabilitation robots, the following sections refer to not only stationary gait trainers, but rehabilitation robotics in general. Although the hazards identified through our recent review [117] are based on incidents with stationary lower limb robots, comparable hazards have been reported in upper limb and mobile devices [44], [101], [103], [125]. Although the interface mechanics between human and robot are often comparable, there are some obvious differences, such as lower weight bearing in upper limb rehabilitation robots and different location and surface area of device-skin interface. The device type and its design therefore have an influence on hazards to be considered. Nonetheless, the authors expect the identified categories of hazards to be relevant for all common rehabilitation robot types.

Hazardous forces at the device-skin interface

Taking a closer look at hazardous forces that occur at the device-skin interface, we see that there is a need for further classification, based on the direction of the force in relation to the skin. Typically, there are normal forces and pressures, as well as shear forces and/or friction. In the following sections, these forces will be investigated in greater detail.

Normal forces and pressure

Normal forces and pressures are unavoidable, and even intended, at human-robot interfaces like the contact area between the patient's skin and a cuff or harness. Circumferential pressures develop where a strap is tightened around a body part and local pressure areas are present where forces applied by the robot are transmitted through soft tissues and where gravity acts on the patient's body weight that is supported by the robot. Too high pressures at the physical human-robot interface can obstruct blood flow or compress tissue, which can lead to injuries like bruises. Pressure injuries usually develop over bony prominences, where local pressure peaks arise [105]. Prolonged exposure to pressure, or pressure in combination with shear, can lead to pressure ulcers [126], [127]. Direction, distribution and duration of pressure are important factors for comfort and safety [115], [128]. Pressure magnitudes and distribution are influenced by the forces acting on the human-robot link, the surface area and shape of the interface, the compliance of the interface material and the characteristics of the body part to which the robot is attached [99], [101], [105], [129], [130]. Moreover, external factors such as moisture, age, and preexisting conditions can have an effect on the soft tissue's response to pressure [105].

Shear forces and friction

Shear forces are forces in tangential directions which are oftentimes present at the interface between skin and robotic device in addition to pressures. Especially in dynamic situations, the robot's movement is applying multidirectional forces to the human which are transmitted through the soft tissue. Moreover, shear forces and slipping at the connection points between human and robot can occur when the robot kinematics are different from the human kinematics (see section *Misalignment* below for a more detailed explanation) and the exoskeleton segments are therefore too long or too short in

certain joint positions [101], [104]. A part of this mismatch can be compensated by the compliance of soft tissue and cuff [131], but the shear forces, torques and slipping of cuff material on skin can nevertheless lead to soft tissue injuries or discomfort [132], [133].

The shear stress developing in soft tissues is influenced by the amount of pressure, the contact area between skin and attachment surface of the robot as well as by the friction coefficient that the robot surface material has with the human skin [134]. This interaction can be influenced by clothes worn underneath the robot cuff which add another layer of different friction coefficients between the cuff material and the skin. The coefficient of friction can in turn be influenced not only by the material but also by skin conditions such as humidity and surface topography [135]. Damp skin (i.e. small amount of water at interface) has a higher friction coefficient than dry skin, and wet skin (i.e. large amount of water at interface) has a lower friction coefficient than dry skin [105]. The material used at the human-robot interface therefore has an impact on the interaction between the robot attachment and the human soft tissue: While materials that have a low coefficient of friction with human skin might slip easily, materials with a higher coefficient of friction adhere to the skin and the shear acts in deeper layers of the soft tissue. Skin can react to shear and friction in various ways. When the friction is low and the movement repeated over a long period of time, the skin can adapt to the mechanical stress and get thicker by forming calluses [105], [136]. Larger amounts of friction can lead to the formation of blisters where the friction force is transmitted through the surface layers of the skin (stratum corneum and stratum granulosum) and degenerates the deeper layer stratum spinosum. Clefts are produced which fill with fluid from the deeper dermis layer and the blister can rupture upon maintained mechanical stress leaving an open skin lesion [136]. This type of skin response mostly occurs in areas with firm attachment of the skin to underlying tissues and a superficial layer thick and tough enough to form a roof on the blister. In areas with a thin superficial skin layer, shear forces and friction are more likely to cause an abrasion rather than a blister [105]. When skin slides over a rough contact material, chafing or abrasions of the surface layer(s) of the skin can occur.

Soft tissue injuries such as abrasions, skin lesions and discomfort to soft tissue are likely to be caused by interaction forces at the physical interface between human and robot. Due to the increased number and surface area of contact points in exoskeleton-type devices opposed to end-effector-type devices, one might expect that the risk of sustaining such an injury is higher when using exoskeleton-type devices. However, the above-mentioned systematic literature review [117] showed that that was not the case in stationary gait trainers (see also Figure 3.1). Many events of discomfort or injuries to soft tissue which were reported in end-effector-type device studies were attributed to the safety harness worn by the patient and the amount of body-weight support seemed to have an influence on the risk of soft tissue-related adverse events caused by the harness in exoskeleton-type devices but not in end-effector-type devices. All soft-tissue related adverse events related to straps or cuffs were however reported in exoskeleton-type devices.

Hazardous forces on the musculoskeletal system

When the force exerted by the robot has travelled through the soft tissue and reaches the musculoskeletal system of the user, it can support or initiate movement of the human body. Too high forces can however cause harm to musculoskeletal structures such as ligaments, cartilage, muscles and bones. Not only the magnitude but also the direction and speed of applied forces play an important

role in determining the injury risk.

Misalignment

When an exoskeleton is not perfectly aligned to the human skeleton, the exoskeleton joint axes will not be congruent with the human joint axes. Such resulting misalignments create undesired interaction forces which can reduce comfort and safety [101]. Misalignments can either be caused by a kinematic mismatch between the exoskeleton joint and the human joint or by poor fitting of the exoskeleton. An exoskeleton joint is always a simplified representation of the human joint which leads to unavoidable misalignments during movements. In addition to that, robotic devices for rehabilitation are usually one-size-fits-all solutions which, in contrast to customized medical devices such as orthoses and prostheses, can be worn by users of a range of body shapes and heights. Straps and segment lengths can be adjustable but the device is not custom-made for one patient and in rehabilitation settings usually used by several patients per day. Appropriate adjusting and fitting before each training session is therefore crucial to minimize the risk of injuries sustained due to misalignments. Besides causing excessive forces on the human musculoskeletal system [44], at the same time misalignment will cause high pressure and/or shear forces through slipping at the cuffs or straps [101], [104], see previous section. Forces that are not compensated for in the design of the robot or its interface will be transmitted to the musculoskeletal systems. If torques and forces are very high or acting in arbitrary directions on the musculoskeletal system, they can cause overloading and thereby pain and injuries to bones, joints and muscles [44], [137].

Exceeding normal range of motion

Exceeding the physiological range of motion can lead to traumatic joint injuries such as ligament tears or capsule injuries [138], [139]. Besides those obvious and traumatic injuries, repeated overstretching and mechanical stress can lead to microscopic injuries which, when the mechanical stress remains, can in sum cause serious issues [138].

While misalignments only occur in exoskeleton-type devices, the risk of exceeding the normal range of motion is relatively easily avoidable in exoskeletons where the movements of the segments of the patient's limb can be derived from and controlled by the movements of the exoskeleton segments. However, one has to consider that the range of motion of the user can vary according to patient-specific conditions or training aims and therefore has to be configurable to the patient. This can be achieved by adding an additional layer of safety features which is adaptable, for example using a software feature to reduce the range of motion. Further, force controls can be implemented which prevent for the human joints to be extended beyond safe limits. End-effector-type devices can only provide limited guidance for the movement to be executed. Arbitrary movements which apply excessive forces to the patient and lead to a joint exceeding the normal range of motion are a serious hazard associated with end-effector based rehabilitation robots [101].

Other hazards arising from usage of rehabilitation robotics

Many of the injuries reported in literature that have been associated to the use of rehabilitation robotics can be attributed to the hazards above. However, additional events and failures can occur which can also lead to injuries sustained by rehabilitation robot users. For gait rehabilitation robots, falls present an important hazard. In stationary gait rehabilitation robots, body-weight support systems with a harness

are often used to prevent falls. Falls of patients in lower limb exoskeletons or exosuits can be caused by a loss of balance, actuator failure or power failure [44]. In contrast to healthy individuals, patients using lower limb exoskeletons already have a gait impairment and therefore have limited ability to recover from balance disturbances [140], [141]. Moreover, the robotic device disturbing the patient's interaction with the ground and adding additional weight to the patient's limbs are complicating factors. A common measure to avoid falls and maintain balance is the use of crutches. Features such as a "graceful collapse" can reduce the injury risk in the event of power failure. Some exoskeletons can detect falls and perform certain actions to reduce the injury risk [44].




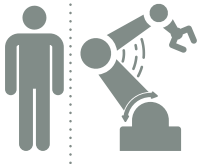
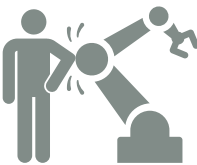
In addition to the risks for the patient using a rehabilitation robot, one has to consider risks for bystanders and other types of users such as the physical therapist. The therapist is specially trained for working with the respective rehabilitation robot. Nevertheless, hazardous situations can occur when the therapist is supervising the training in close proximity to the robot. For example, a collision can occur where the therapist can sustain an injury due to an impact or due to being clamped between two robot segments or between a rigid object such as a wall and the robot. Wearable robots used for assistive purposes might be used in a home environment or other uncontrolled environments such as a park or shopping mall. In those situations, bystanders including children and pets are not trained in dealing with robotic devices and might behave in an unexpected way like moving into the robot's trajectory or pushing a finger into an opening of the robot. Rehabilitation robot developers need to take those hazardous situations into account and avoid injuries e.g. by power and force limiting functions.

TRANSLATING HAZARDS TO SAFETY SKILLS AND VALIDATION PROTOCOLS

The hazards detailed in the previous section have proven to be relevant in rehabilitation robotics based on reports of adverse events in literature. To achieve the goal of a safe physical interaction between rehabilitation robots and their users, the risks connected to those hazards need to be addressed in the safety validation process. The authors propose to evaluate the mechanical safety of rehabilitation robots by validating safety skills (see section *Concept safety skills*). This way, the same approach can be used independent of how the safety function is technically implemented as long as the same safety skill is addressed.

As a first step, safety skills were identified based on the hazards described in previous sections (Table 3.1). By analyzing the hazards extracted from the reported adverse events, and methods to mitigate the related risks, the most relevant safety skills for rehabilitation robots were identified and linked to the corresponding hazard(s). Subsequently, for each of the identified safety skills, testing protocols are defined that describe how a particular safety skill should be assessed. In the following sections, each safety skill is described in more detail and the basic concepts for validating those safety skills are explained (detailed validation protocols can be found on the publicly available online COVR Toolkit which is currently under development (toolkit.safearoundrobots.com)). In the future, additional safety skills relevant for rehabilitation robots might be identified and new protocols developed. We highly recommend performing all safety tests with dummies and simulators instead of a human to avoid dangerous situations during safety testing [142].

Table 3.1| Overview of identified hazards, influencing factors, potential injuries and related safety skills. Note that this list is not extensive and additional relevant hazards and safety skills might be identified in the future.

Hazard	Influencing factors	Device part (device type)	Potential injuries	Safety skill
Continuous or repetitive pressure exceeding safe limits	- Design and fit of mechanical interface (pressure distribution/peaks, high circumferential pressure)	- Cuffs/straps (mostly exoskeleton devices) - Harness (stationary devices)	Soft tissue-related (e.g. bruises, pressure ulcers)	 Limit restraining energy
Shear forces exceeding safe limits	- Direction, speed, pressure, duration - Material at human-robot interface (friction, microclimate) - Sliding of mechanical human-robot interfaces (improper fit, misalignment)	- Cuffs/straps (mostly exoskeleton devices) - Harness (stationary devices)	Soft tissue-related (e.g. skin abrasions, blisters, skin lesions)	 Limit restraining energy
Misalignment	- Direction and amount of misalignment (translational vs. rotational misalignment, micro vs. macro misalignment)	- Exoskeleton joints (only exoskeleton devices)	Musculoskeletal (e.g. joint pain/injuries, bone fractures); Soft tissue-related (e.g. skin abrasions, bruises)	 Maintain proper alignment
Exceeding physiological range of motion	- Direction, force, speed	- Exoskeleton joints or end-effectors (mostly end-effector devices)	Musculoskeletal (e.g. joint pain/injuries, muscle strain)	 Limit range of movement
Collision with bystander	- Impact/clamping force, speed, weight - Environment (walls that can cause clamping), surface material and shape	- Moving parts (all device types)	Various (e.g. bruises)	 Limit physical interaction energy

Limit restraining energy

Many rehabilitation robots are strapped to the patient during use, which means that they exert a restraining energy on the user, for example at the site of a cuff (see also the definition of restraint type physical assistant robot, ISO 13482 [143]). In order to ensure a safe interaction between the restraining parts of the robot and the human skin and soft tissue, the safety skill *limit restraining energy* needs to be validated. The safety tests will need to assess whether the interaction forces at the physical interfaces between human and robot stay within safe limit values. The forces present are repetitive and/or continuous forces and are exerted in different directions, which can have various negative effects on the skin and soft tissue of the user as explained above. It is expected that the stress concentration at the edge of a robot cuff is highest [144] which is why special attention should be given to the forces present at those locations. Moreover, the presence of pressure peaks over bony prominences is a known phenomenon [99]. Therefore, it is advised to assess the distribution of interaction forces over the whole interface or at least at the locations with the expected highest stress concentrations.

Pressures and their distributions can be assessed with thin and preferably flexible sensors mounted to the robot's connection surface or to a dummy limb's artificial skin. During testing, the robot is performing movements which lead to force application to the dummy at the site of the robot's restraining part representative for normal use. In some cases, it might not be possible to perform the test with the complete robot setup as it is used in practice. Wearable (i.e. non-stationary) exoskeletons might have to be fixed to a rigid frame or the execution of the forces might have to be performed by a separate robotic manipulator equipped with the cuff to be tested and programmed to execute the same forces as the rehabilitation robot would. Where there are different training situations with varying pressure levels, the worst-case scenario as identified in the risk management process is used for testing. The robot passes the safety skill validation test if the pressures remain within the safe levels at all times. The concept of performing a safety validation test for shear forces is similar. Thin and flexible shear sensors are used instead of pressure sensors. Alternatively, a piece of porcine skin can be attached to the dummy surface and analyzed for any damages after applying the shear force that is applied by the rehabilitation robot surface during normal use. When there is no damage to the porcine skin and no recorded shear forces higher than the defined safe limit values, the validation test is passed.

Maintain proper alignment

Strategies to avoid negative effects of misalignment to the user's musculoskeletal system must be considered, especially in exoskeletons. The validation of the corresponding safety skill *maintain proper alignment* includes measuring the forces applied to a user's joint and checking whether they exceed a safe limit value or not. As mentioned above, those validation tests cannot be performed on a human user for safety reasons. Therefore, a dummy limb is needed to enable measuring of internal joint forces. The instrumented dummy used for this validation test consists of two rigid tubes connected by a joint mimicking the human bones and joint, and a compliant material mimicking the soft tissue. One of the tubes is equipped with a six degrees of freedom force and torque sensor. During the experiment, the instrumented dummy limb is fastened to the exoskeleton to represent the user's limb in a normal use situation. The exoskeleton joint is then moved through its usual range of motion with different misalignment settings. A misalignment can either be a translation of the exoskeleton flexion axis relative to the flexion axis of the human (dummy) joint or a rotation of the robotic flexion axis relative to the joint flexion axis of the human. The exoskeleton passes the validation test if the maximum torques

and forces acting on the dummy joint at no point in time exceeded the safe limit values.

As explained in previous sections, a misalignment can not only lead to injuries to the musculoskeletal system but can also lead to soft tissue injuries as the cuffs or straps might shift or exert a higher pressure than during well-aligned situations. It is therefore advised to perform the validation protocols of the safety skill *limit restraining energy* under the condition of different misalignments to test for the effects of misalignments on the human-robot interaction on soft tissue level.

Limit range of movement

The range of movement for a rehabilitation robot has to be restricted in such a way that the physiological range of motion of the patient inside the robot is not exceeded. The safety skill *limit range of movement* can be relevant for a number of device types where the robot initiates or supports movement of limbs. For the validation of single degree of freedom joint range of movement (usually in exoskeletons), a simple test setup using an angle measurement device such as an electro-goniometer can be used. A dummy payload is attached to the exoskeleton which is then programmed to move back and forth over the specified angular range of motion at maximum angular velocity. The exoskeleton joint angles are measured over time and compared with the safe range of movement. If the safe range of movement is exceeded at no point in time, the validation test is passed.

For more complex joints and end-effector devices, the spatial range of movement can be assessed using a marker-based motion analysis system. Markers are attached to a reference point, based on which the safe spatial range of movement is defined, and to an endpoint that relates to the simulated human body part attached to the robot. The robot is then programmed to move the endpoint through the safe range of motion, along the borders of the safe range of motion and also to coordinates outside of the safe range of motion that are within the robot's reach. The robot passes the validation test if the endpoint exceeds the safe range of motion at no point in time.

Limit physical interaction energy

To account for the safety of therapists working with a rehabilitation robot as well as bystanders, the hazard of accidental contacts such as collisions with a rehabilitation robot or a part thereof has to be considered. The skill *limit physical interaction energy* protects bystanders from injuries caused by collision with a rehabilitation robot. The concept of the validation process of this safety skill is to simulate an accidental contact of the rehabilitation robot with the human by evoking a contact of the robot with a bio-fidelic measurement instrument that mimics the biomechanical characteristics of the human body. The bio-fidelic measurement instrument consists of a load cell connected to an impactor via an interchangeable spring [145]. On the other side, the load cell is connected to a rigid housing and the impactor is covered by a soft damping material. The combination of the spring and the damping material are chosen in such a way that it has the same biomechanical characteristics as the human body or the body part with which the collision can occur. A foil sensor for pressure measurement is mounted on top of the measurement instrument. To execute the validation test, the measurement instrument is fixed in a position in which the accidental contact with the robot can occur. The robot or exoskeleton is then instructed to move along a set trajectory with a pre-defined speed reflecting normal use or the worst-case situation. The impact forces and pressures are analyzed based on safe limit values for transient contacts in which the human segment that gets into contact with the robot can

move freely and/or clamping contacts in which the robot clamps the human against a rigid object such as a wall or the rigid support structure of a robot. If the safe limit values for forces and pressures are not exceeded in any of the test repetitions and conditions, the validation of the safety skill is passed.

DISCUSSION

By combining existing knowledge about reported injuries of gait robots with potential underlying mechanisms in relation to physical human-robot interaction, we have identified five main hazards relevant to physical safety of humans interacting with rehabilitation robots. These five hazards were related to four different safety skills. These were used as a framework for describing safety validation protocols for each of those skills that are broad enough to be used for a range of rehabilitation robot types. Some of those protocols are publicly available in detail, in draft version or currently under development. Nevertheless, this analysis also highlighted particular knowledge gaps that are yet to be closed to achieve a sufficient set of clear guidelines for rehabilitation robot developers. These gaps and associated needs for simplifying safety validation of rehabilitation robots are discussed below.

The potential and limitations of cross-fertilization among domains

Since rehabilitation robotics is a relatively young and highly dynamic field, availability of specific standards, validated testing procedures and safe limit values is limited. It can therefore be beneficial to consult standards or best practices from other domains that deal with similar safety issues. For example, testing procedures are more specific in standards and technical reports or technical specifications for collaborative robots in industry, some of which are also relevant to rehabilitation robots. For the safety skill *limit interaction energy*, best practices and methodologies from ISO/TS 15066 [146] can be adapted for use with rehabilitation robotics. Further, even though EN-ISO 13482 and the corresponding test methods [143], [147] are limited to personal care robots, excluding medical applications per definition, some of the methods can be taken into consideration when developing safety validation methods for rehabilitation robotics. However, the applicability of non-medical standards to medical devices is limited. One has to consider differences in use and most importantly the vulnerability of patients using rehabilitation robots. Therefore, one cannot use thresholds or limit values stated in non-medical standards. Moreover, the cognitive and/or physical abilities of rehabilitation robot users are most likely restricted compared to factory workers which has to be taken into consideration during risk assessment.

Gaps and needs in research for producing and executing protocols

Measurement techniques and devices

There is a pressing need for reliable and accessible measurement methods to assess the physical interaction between humans and rehabilitation robots. Regarding the assessment of normal forces present at the interface between human skin and robot contact surface, a means to measure pressures or normal forces and their distribution over the contact area would be most beneficial. Pressures and shear forces at the interface between cuffs and human soft tissue are distributed unequally with peaks at the sites of bony prominences and along the edges of the cuff [99], [105], [144]. Load cells measuring the net force exchange between the human and robot are therefore deemed insufficient to assess forces that might harm the rehabilitation robot user on soft tissue level.

Pressure mats have been used for analyzing contact surfaces in e.g. backpacks [148], wheelchairs [149]–[151], beds [152]–[154] and prosthetics [155], [156], and also in previous experiments to measure interface pressures in exoskeletons [157], [158] or soft exosuits [159]. For this purpose, pressure mats must be flexible and compliant as the contact surface of a rehabilitation robot is usually curved and a stiff sensor would change the physical human-robot interaction. While those pressure mats are available in a variety of sizes, pressure ranges and sensitivities, they are not easily adjustable for use in many differently shaped devices. One needs a pressure mat that fits in the respective cuff or other contact surface without overlapping and that has an appropriate measurement range and sensitivity for the contact situation under consideration. Weight bearing interfaces such as footplates or harness straps will yield much higher contact pressures than for example a forearm splint.

An affordable alternative for commercial pressure mats are thin film polymer sensors called Force Sensitive Resistors (FSRs). FSRs are often used in commercial pressure mats, where they are arranged in a matrix, but can also be purchased as single sensors which can be arranged in groups or used individually. Advantages of FSRs are their thinness, low cost, sensitivity and sensing range. They are commercially available in different shapes and sizes and can be assembled in grids, which makes them suitable for many biomechanical applications including interface pressure measurements in rehabilitation robotics [40], [158], [160]. However, FSRs also have limitations, including sensor drift and hysteresis [161]. In addition to that, surface characteristics such as curvature and compliance as well as temperature can have an impact on the measurement outcomes [162]. When single FSRs are used at a human-robot interface, a portion of the applied force is getting lost as it is distributed over not only the sensing area of the FSRs but also the edges of the sensors and the space in between FSRs [163]. A method to avoid this problem is to glue “pucks” or semi-spheres to the sensing area of the FSRs to apply the force to that area only [38], [158]. However, these added structures will change the pressure distribution by introducing an additional, uneven layer to the human-robot interface. Recent experiments have shown that the thin FSRs left indentations on the skin, leading to the assumption that an added layer of “pucks” or semi-spheres will introduce pressure peaks at the edges of those structures [163].

The continuous or repetitive shear force present at the interface between a rehabilitation robot and the user’s soft tissue is expected to have a larger effect on the soft tissue injury risk than the pressure [164], [165]. It is therefore of utmost importance to have reliable measurement methods available. A lot of research has gone into the development of thin sensors for interface stress measurements, especially in prosthetic sockets and shoes [155], [166]. A concept that has received much attention and seems promising is a sensor that works based on capacitance changes due to deformation of a polymer pillar structure [167]–[170]. Those thin and flexible sensors have been used for different application areas, including prosthetic socket interfaces and fingertip contact forces [171]–[173], and might also be suitable for assessing the interface pressure and shear at contact areas between rehabilitation robots and their users. Georganakis et al. [174] suggested a setup where a force sensor with three degrees of freedom is built into a cuff. As opposed to the reliability and robustness of load cells, capacitance sensors can be more prone to errors. A general drawback of using sensors for assessing the effects of shear forces is that the sensor material adds another layer to the interface between human and robot which, based on the changes in surface topography and friction, can alter the physical human-robot interaction.

A different approach for assessing safety of shear forces applied to the human soft tissue is to apply the same forces to a surrogate skin and analyze it for any damage. Porcine skin is widely accepted as surrogate for human skin as the macroscopic morphology, cutaneous blood supply and wound healing characteristics are similar [125]. The proposed method to test restrained-type physical assistance robots is to fix a piece of porcine skin to a dummy of a shape and compliance comparable to the human body part [175] and apply the forces that would be applied by the rehabilitation robot during normal use [100], [133] using a manipulator. After that, the porcine skin sample is analyzed under the microscope to check for signs of skin damage [116], [147]. This method is a way to validate the skill *limit restraining energy* by showing that normal use of the rehabilitation robot does not lead to skin injuries. It does however have some limitations as it requires the use of porcine skin specimens and the availability of special equipment such as a cryostat and microscope. Moreover, porcine skin does have a morphology comparable to the one of human skin but it is considerably thicker [125] and might therefore differ in its reaction to physical stress. To avoid using porcine skin for safety testing, Mao et al. [176] have developed an artificial dummy skin for abrasion tests. However, its comparability in abrasion damage onset with human skin has not yet been validated.

Measuring the effect of rehabilitation robot use on internal body structures remains another challenge. In addition to ethical considerations about safety testing with humans, it is also technically impossible to directly measure the stress on bones and joints *in vivo*. Instrumented dummies therefore appear to be the only reasonable option for assessing the safety skill *maintain proper alignment* and other safety skills for limiting the forces applied to the musculoskeletal system. While crash test dummies are a gold standard for assessing the impact of collisions on the human body in the car industry, those dummies are very costly and not optimized for assessing physical human-robot interaction in continuous contacts. Akiyama et al. [104] proposed a dummy leg setup to measure the effects of misalignment at the cuff locations. However, the skeletal system will be reached by a part of the applied force only as the soft tissue has a dampening function. It might therefore be more beneficial to use a setup with force and torque sensors included in the 'skeletal' structure of the dummy limb to investigate the effects of misalignment on the skeletal system. Complex systems are needed to replicate the physical interaction between humans and robots. A simplification of joints used for dummy limbs can resolve the kinematic mismatch that would be present between a human joint and the simplified rehabilitation robot joint. Therefore, complex, potentially actuated joints that can replicate the rehabilitation robot user's behavior are needed. There is no validated measurement system or best practice available yet for developers to use for safety testing of their device.

Safe limit values

To perform safety validation of a rehabilitation robot, the developer not only needs information on how to test the respective safety skill, but also on the safe limit values that can be used as a pass/fail criterium for the test. While much research has been performed on safe limit values for accidental contacts such as collisions between a factory worker and a collaborative robot, little is known about acceptable force magnitudes for continuous contacts with patients.

Pain onset thresholds have been investigated for pressures and forces applied during accidental contacts such as collisions or clamping situations with a collaborative robot [32], [177], [178]. Those limit values for many different locations on the human body have been adopted for ISO/TS 15066

[146]. They might also serve as guideline for accidental contacts between rehabilitation robots and bystanders. However, one has to keep in mind that the underlying pain onset experiments were performed with healthy adults. Therefore, while the biomechanical limit values might be applicable for physical therapists, they are not for certain other types of bystanders such as children, elderly persons or patients. In addition, contacts in collaborative robots are typically the result of foreseeable misuse or technical failure [177], while they are intended in rehabilitation robots. Therefore, those limit values are explicitly applicable to accidental contacts only (i.e. safety skill *limit interaction energy*), which means that they cannot be used for those continuous contacts usually present between a rehabilitation robot and patient (i.e. safety skill *limit restraining energy*). In fact, it has been reported that after two or three repeated measurements at the same location, effects on the skin such as bruises, reddening and skin abrasions were observed [179]. Moreover, sustained pressure at a level of half the magnitude of the pain onset threshold becomes painful after a few minutes [180]. In rehabilitation robot use, the human body is exposed to sustained pressure, often including cyclic loading and unloading phases. Such intermittent pressure at low frequencies can be perceived as very uncomfortable as it leads to summation of pain [115], [128].

Depending on the rehabilitation robot type, the pressure can for example be exerted through cuffs, harnesses, straps or splints. Comfort and pain onset thresholds should therefore not be assessed with indenters which have a relatively small contact surface but with algometers that mimic the interface of the rehabilitation robot. Previous research has therefore focused on circumferential tissue compression. Acceptable levels of circumferential pressures are expected to be about 20 times lower than single point pressure pain onset thresholds such as the ones indicated in ISO/TS 15066 [128]. More specifically, a systematic review found pain detection thresholds in healthy persons (i.e. pain onset thresholds; perceived discomfort) for circumferential pressure of between 16 and 34 kPa and pain tolerance thresholds (i.e. the pain becomes unbearable) of 42-91 kPa [128]. Another systematic review states that circumferential pressure limit values for chronic pain patients are significantly lower, with pain onset thresholds of about 10-18 kPa and pain tolerance thresholds of below 25 kPa [181].

Further, the increase of pain with time was higher and the adaptation to pain lower in patients with chronic pain compared to healthy subjects. Recent studies have investigated the relationship between perceived comfort and circumferential pressure applied using pneumatic cuffs of different widths to participants' thighs and shanks during standing and walking [182], [183]. They discovered that the discomfort and pain thresholds were lower during walking than during standing still and that narrower cuffs as well as anatomical sites with smaller volumes of soft tissue (shank as compared to thigh) lead to higher thresholds. These findings are bringing us an important step closer to comprehensive guidelines for safe limit values for pressure in rehabilitation robot use. However, the pressures were only applied for a relatively short duration of 60 s, which does not represent normal use of most rehabilitation robots. Therefore, more research is needed to identify acceptable limit values of sustained and cyclic pressure including the relationship between pressure magnitude and exposure time.

An additional challenge with regard to safe limit values for pressures are the varying patient characteristics. Most studies investigating pain pressure thresholds have been performed with healthy individuals. However, the systematic review mentioned above [181] identified that pain perception differs significantly between healthy individuals and patients with chronic pain. Moreover, the reaction

to contact pressure is highly dependent on factors such as the anatomical structure, tissue composition and stiffness, blood flow, lymphatic flow as well as the individual health status and diseases affecting inflammation and repair capacities [99]. As all these factors can be influenced by the condition of the common rehabilitation robot user, it remains very challenging to define clear thresholds.

Regarding acceptable limit values for shear forces applied by rehabilitation robots, the lack of reliable methods for assessing interface shear as explained above is a major limiting factor for research on comfortable and safe levels of shear forces at the interface between human soft tissue and robot contact surfaces. Based on research on the development of friction blisters with human participants [136], [184] as well as porcine skin [116], a relationship of tangential traction and time resulting in a threshold curve of inherently safe shear force (reaching from about 40-45 kPa at 3 min to about 25-30 kPa at 23 min) has been identified. As these experiments have been performed with a stainless steel plate which clearly has different characteristics than a cuff used in rehabilitation or physical assistant robots, the results were validated using a cuff mounted on a manipulator [116]. The results have been adopted in ISO/TR 23482-1 [147]. However, one has to consider that these limit values have been obtained from experiments with porcine skin and the reaction of human skin might be different. The reaction of human skin to friction has been investigated in the past [136], but the forces were only applied for a few minutes which does not represent normal rehabilitation robot use. The validation experiment using a cuff was based on net tangential forces applied by the rehabilitation robot over the whole cuff. Therefore, there is no information on the local magnitudes of applied shear which can be influenced by the cuff material and skin humidity and might not be evenly distributed over the contact surface of skin and cuff.

Furthermore, the limit values have been developed for exposure times of up to 23 minutes and rehabilitation robots might be used for durations longer than that. It is important to realize that the levels acceptable for shear stresses in rehabilitation robots should be clearly lower than the available limit values as development of friction blisters during rehabilitation robot use is unacceptable and depending on the patient's health status, blisters can lead to complications. Moreover, it has been shown that stresses on the skin increase with an increasing coefficient of friction present at the interface. The friction coefficient of skin and cuff depends, among other factors, on the curvature, the material used and the humidity at the interface [32], [99], [185]. The individual mechanisms behind a soft tissue injury can be difficult to identify as many factors can play a role. While the microclimate and skin condition clearly have an influence on susceptibility for skin injuries, the influence of hair is unclear [185]. More research is therefore needed on the influence of different environmental conditions and cuff materials on injury mechanisms. In addition to that, the increase in shear stress with an increasing coefficient of friction is higher in stiffer skin tissue, which occurs with aging and in certain conditions such as diabetes [186]. This is an indication that the same applies regarding the influence of patient characteristics on the injury risk, as for pressure limit values. These factors present a major challenge, and a pressing need, for defining clear limit values applicable for different patient groups and under normal use conditions of rehabilitation robots.

Normal physiological ranges of motion have been documented in literature and are common knowledge in clinical practice [187]. However, rehabilitation robot developers have to consider that their target group might have limitations regarding their passive range of motion, for instance due to contractures.

For rehabilitation robots used in a clinical setting, the range of motion could be individually set by the patient's therapist.

Regarding forces and torques applied to musculoskeletal structures, it is difficult to define acceptable limit values. They could be based on voluntary joint torques that can be applied by healthy individuals [188], [189] or on torques applied by therapists during conventional gait training [190], [191]. Moreover, knowledge on bone fracture occurrence in accidents can be taken into consideration [147], [192]–[194], although it has to be considered that rehabilitation robot users are exposed to continuous and cyclic forces which is a situation very different from impacts during accidents. Moreover, similar to all other categories above, the tolerance for forces and torques applied by a rehabilitation robot, for example due to misalignments, can be lower for patients than for healthy individuals. One reason for that can be a reduced bone mineral density which is common, for example, in spinal cord injury patients and can lead to an increased risk for bone fractures [195].

Safety by design

Through inherent safety, or safety by design, hazards can be addressed and minimized early in the design process. Safety features therefore should not only be added to existing devices, but the relevant hazards should already be mitigated by design features. To enable this, more research is needed on best suited materials and technologies. For example, the knowledge about optimal material choice for the physical human-robot interface is limited. Even in more established domains like orthotics and prosthetics, soft tissue injuries are a recurring problem and there is no gold standard or perfect solution [99].

To mitigate the hazard of misalignments by design, much research went into compensation mechanisms such as passive joints [101], [196]. These can work well for stationary devices, but make the device heavier and bulkier, which makes them unsuitable for truly wearable exoskeletons [101], unless the robot inertia is actively compensated [131]. Research suggests that misalignment in lower limb exoskeletons lead to increased forces mainly at the thigh cuff which could be compensated by compliant cuffs [131], however, the suitability and effectiveness of such a compensation strategy would have to be validated.

CONCLUSION

In the present review on safety assessment of rehabilitation robots, we pointed out the state of the art and needs regarding guidelines for evaluating rehabilitation robot safety, to provide directions for developers to design safe rehabilitation robots. Rehabilitation robotics is a very diverse and dynamic field which contributes to the complexity of its safety validation. In addition to that, the nature of physical contacts between rehabilitation robots and patients, which introduce intended continuous and cyclic interaction forces, poses a challenge. There is a lack of clear recommendations for safety testing in rehabilitation robot specific legislation and standardization. While the transition from MDD to MDR increases the focus on safety, developers and manufacturers need more precise and practical guidelines. The experience with collaborative robots in domains like manufacturing can potentially help to reach this goal as there are more best practices available than in the healthcare domain. The

concept of safety skills described in this paper makes use of cross-fertilization by defining domain-unspecific abilities of collaborative robots to reduce a risk, which can be validated according to structured validation protocols (www.safearoundrobots.com). Those protocols reflect industry-wide best practices and can be considered as guidelines for safety validation of collaborative and rehabilitation robots on a system level.

Based on knowledge about adverse events occurring in rehabilitation robot use, we identified excessive forces on the soft tissue level and on the musculoskeletal level in different directions as most relevant hazards for rehabilitation robots and related them to four safety skills, providing a concrete starting point for safety assessment of rehabilitation robots. We further identified a number of gaps and research needs which need to be addressed in the future to pave the way for more comprehensive guidelines for rehabilitation robot safety assessments. Predominantly, besides new developments of safety by design features, there is a strong need for reliable measurement methods as well as acceptable limit values for human-robot interaction forces both on skin and joint level.

Rehabilitation robots can provide high intensity and dosage training or assist patients in activities of daily living and decrease physical strain on clinicians. However, the physical human robot interaction poses a major safety issue, as the close physical contact between user and robot can lead to injuries. Moreover, the magnitude of forces as well as best practices for measuring them, are widely unknown. Therefore, a measurement setup was developed to assess normal and tangential forces that occur in the contact area between an arm and a splint. Force sensitive resistors and a force/torque sensor were combined with two different splint shapes. Initial experiments indicated that the setup gives some insight into magnitudes and distribution of normal forces on the splint-forearm-interface. Experiment results show a dependency of force distributions on the splint shape and sensor locations. Based on these outcomes, we proposed an improved setup for subsequent investigations.

Chapter 4

Prototype measuring device for
assessing interaction forces between
human limbs and rehabilitation robots

A proof of concept study



INTRODUCTION

Collaborative robots (cobots) are robots designed to work in a shared space with humans, which is in contrast to conventional robots working autonomously or with limited guidance and separated from the human through physical barriers. In times of aging populations and a high need for workforce, a cobot can be seen as a much-needed robotic coworker. A step towards the deployment of cobots has been made in many domains such as industry, agriculture and logistics but also in the healthcare domain. Rehabilitation robotics is a promising field as robots can help compensate for a shortage of skilled clinicians with an increase in elderly due to an ageing population, by facilitating high intensity training with a large number of repetitions. Robotic training devices can for example be used for repetitive and load carrying tasks. However, the deployment of rehabilitation robotics in clinical practice also yields a number of challenges - first and foremost the physical human-robot interaction. While the rehabilitation robot can be interpreted as a robotic coworker for the physical therapist (comparable to a cobot in an industrial setting), it is usually physically attached to body parts of the patient. This inevitably raises safety issues as the mechanisms present in the human-robot-interface are poorly understood and patients (as opposed to workers) can be particularly vulnerable and can have limited perception of pressure and pain.

The physical interaction between patients and rehabilitation robotics has been associated with a number of adverse events, mainly including skin-related adverse events such as skin breakdown, blisters, ulcers, etc. [49], [74], [197], but even some serious adverse events such as bone fractures have been reported [44], [60]. In order to avoid these (serious) adverse events and promote a safe deployment of collaborative and rehabilitation robots, methods are needed to assess the physical human-robot-interaction.

The Horizon 2020 project COVR (*Being safe around collaborative and versatile robots in shared spaces*; www.safearoundrobots.com) will contribute to increased safety in collaborative robotics by providing tools to simplify the safety evaluation process. The project driven by five research and technology organizations from five EU countries is aiming to decrease the complexity in safety testing and thereby increase deployment of cobots. The means to achieve these goals are a toolkit to help identify relevant standards and regulations as well as specific requirements; a series of testing protocols giving clear instructions on how to prove that a cobot fulfils all necessary requirements; shared safety facilities providing a room, equipment and expertise to perform the tests; and finally realistic trials offering funding to third parties to stress-test and improve the COVR services.

The COVR Toolkit will be an open-access web-based service, which can help identify relevant standards, regulations and testing protocols for physical human-robot interaction scenarios. In many cases, safety standards do not describe the safety-related validation procedures in sufficient detail. To fill those gaps, COVR will use experience on best practice and cross-fertilization among domains. Wherever this information on best practice is not available yet, the project will push for the development of new methodologies for testing and proving the safety of devices.

One of the most pressing issues in rehabilitation robotics is the physical interaction between a splint with straps or a cuff and the patient's soft tissue. Safe ranges of shear forces and normal forces that

can be applied to a patient during training or assistance through a robot are yet to be defined. In addition to that, there is a strong need for reliable measuring methods to determine forces developing at the interface between a rehabilitation robot and a human (limb). The continuous contact in combination with the autonomous movements of the robot forms a high risk for skin-related adverse events. Shear forces have been found to have a larger influence on e.g. pressure ulcers than normal forces [198], however, the methodological possibilities for measuring such shear forces are widely unknown. A method that can be considered as gold standard for measuring normal and tangential forces is the load cell, frequently using piezoresistors. However, these sensors are rather bulky and cost-intensive, which are possible reasons why many studies implement force sensitive resistors (FSRs) to assess the interaction between a human and a robotic, orthotic or load-carrying device [38], [40], [42], [148], [199]. A number of studies have focused on the development and implementation of alternative sensing devices such as optical sensors [35]–[37], vision-based tactile sensors [39] and pneumatic padding [34], [41], however, these methods are still in research state.

Physical human-robot interaction can compromise the safety of patients using rehabilitation robotics. Appropriate methodologies for measuring the interaction forces are not available which can hamper the development and deployment of safe rehabilitation robotics. Therefore, the aim of the current paper is to explore possibilities for those needed methodologies by designing and testing a prototype measuring device for assessing interaction forces between a splint with straps and a human forearm.

MATERIAL AND METHODS

To explore the feasibility of various sensor types for measuring the human robot interaction at the physical interface between a cuff or splint and a human limb, a measurement setup has been designed and tested. The interaction between the forearm and a one-size-fits-all splint with two straps was chosen as example case for the sake of simplicity. The requirements for the prototype measuring device were the support and fixation of the forearm as well as measurements of normal and tangential forces.

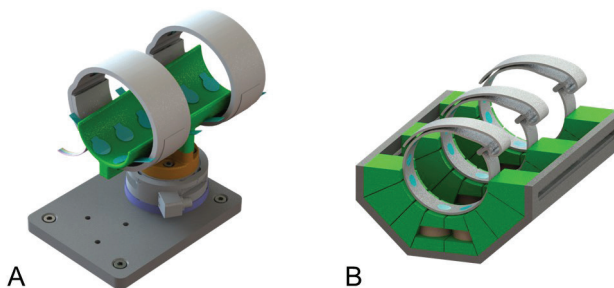


Figure 4.1 | Example concepts for prototype measuring device. The straps are depicted in light gray and force sensitive resistors in blue. Concept A has one 6 degrees of freedom (DOF) force and torque sensor underneath the splint and concept B includes several 3-DOF load cells implemented in the splint segments (both gray).

Load cells and FSRs were considered for force measurements in the setup. Load cells using strain gauges are very accurate and have a linear behavior. They are available in various sizes and with

various specifications, ranging from simple one degree of freedom (1-DOF) load cells to 6-DOF force and torque sensors. FSRs can only be used for measuring normal forces. FSRs measure changes in resistance, which can later be related to exerted normal force. Disadvantages of FSRs are a non-linear behavior and varying transfer functions, which increase the need for good calibration [38]. Figure 4.1 shows two of the concepts that were analyzed. Due to the small 3-DOF load cells included in concept B being very cost intensive, concept A was chosen. The advantages of the FSRs are that they are low cost and thin.

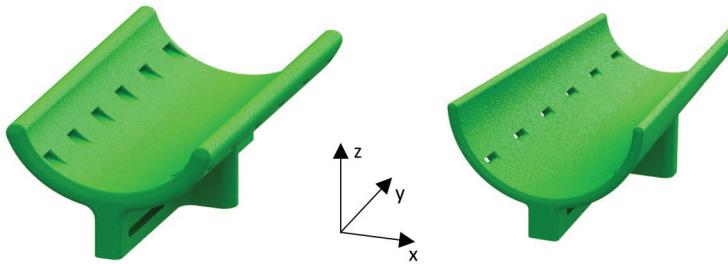


Figure 4.2| Variations in arc-shaped splint: parallel (left) and conical (right).

Two different variations of the arc-shaped splint were designed and 3D-printed to assess the influence of the fit of the splint on the interaction forces. Due to the approximately conical shape of the forearm, a parallel and a conical arc-shaped splint were used (Figure 4.2). To assess the pressure distribution underneath the forearm as well as on the sides of the forearm, the experiments were performed with two different arrangements of FSRs: with a center distance of 30-35 mm versus 50-55 mm (Figure 4.3).

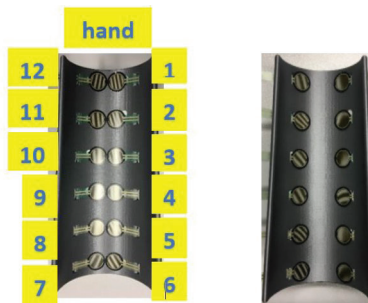


Figure 4.3| Variations of force sensitive resistor positioning. Left: FSR center distance 30-35 mm, right: center distance 50-55 mm.

All combinations of splint shape and FSR (Interlink Electronics, CA, USA and Tekscan, MA, USA) positions were used in pilot measurements to assess the feasibility and gather preliminary data for the interaction forces. One test subject's right arm was attached to the splint using the Velcro straps (see Figure 4.4) and the subject was instructed to follow a target line presented on a screen by exerting a predefined force or torque respectively. The measurement setup including the splint was mounted to a table. Thus, the subject did not move the splint but exerted forces and torques to the fixed splint. The force or torque exerted by the subject as measured by the 6-DOF force/torque sensor (SI-660-60 Delta, ATI, NC, USA) was also displayed on the screen. During the entire procedure, the data obtained by the

force/torque sensor and the FSRs was logged and subsequently synchronized using a trigger signal. Data retrieval was done with an Arduino microcontroller (FSRs; Arduino Mega 2560, software V.1.8.7, Arduino, MA, USA) and a DAQ device (6-DOF force/torque sensor; NI MAX, National Instruments, TX, USA). Data calibration was done in LabView (18.0, National Instruments, TX, USA) and synchronization as well as further processing in MATLAB (R2018A, MathWorks, MA, USA).

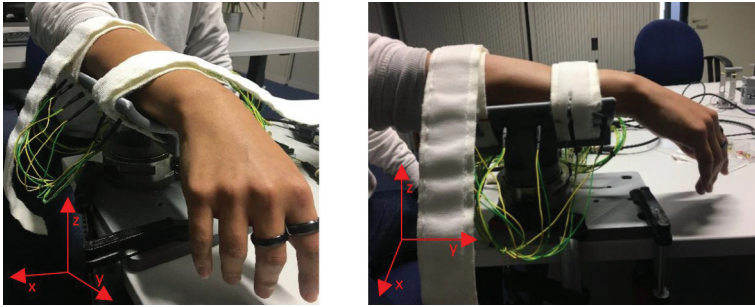


Figure 4.4| Experimental setup and orientation of coordinate system with respect to subject arm and splint.

The procedure was repeated for exerting forces in x-, y- and z-direction as well as torques around the x-, y- and z-axis (coordinate system as defined in Figure 4.2 and Figure 4.4). The results for forces exerted in x-direction (i.e. the subject pushing laterally (positive force) or medially (negative force) with respect to his body), torques around the x-axis (i.e. the subject pushing the wrist up and the elbow down (positive torque) or the wrist down and the elbow up (negative torque)) and to a limited extent forces exerted in z-direction (i.e. pushing the forearm up (positive force) and down (negative force)) will be discussed in this article. The expected normal forces on the human-splint interface were very clear for these scenarios and thus the results for these scenarios can give a first indication for the validity of the measurements performed with the current setup.

RESULTS

The 6-DOF force-torque sensor delivered reliable data, which was suitable for displaying to the subject how the target line was followed (Figure 4.5). It can be seen that the subject exerts forces and torques not only in the targeted direction and based on the weight of the arm but the actual movement is a combination of the target force and other forces and torques in lower magnitudes. The measured forces however cannot be related to shear forces on the interface between soft tissue and splint because they represent the net forces applied on the splint and not local forces acting on the subject's soft tissue.

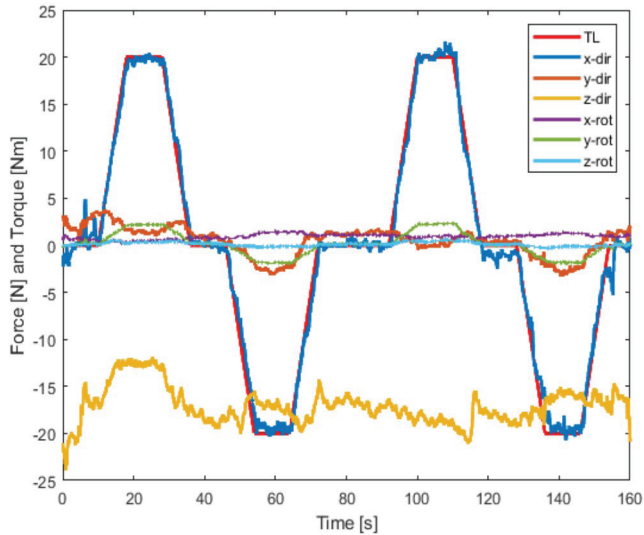


Figure 4.5] Example output of the 6-DOF sensor for target forces exerted in the x-direction (TL: target line; x-dir: force exerted in x-direction; y-dir: force exerted in y-direction; z-dir: force exerted in z-direction; x-rot: torque exerted around the x-axis; y-rot: torque exerted around the y-axis; z-rot: torque exerted around the z-axis).

The results of the FSR outputs are somewhat more questionable. For an alternating force applied in positive and negative x-direction, we expected to see a clear alternating pattern of sensor output of the right and left row of sensors. As shown in Figure 4.6, this could only be seen to a limited extent. While a similar pattern of sensor outputs can be observed during exertion of force in positive x-direction, the outputs connected to force exertion in negative x-direction are very low. A comparison of FSR data in parallel and conical arc-shaped splint shows that there are less and lower outputs in the conical splint. Figure 4.6 also shows clearly that there is a difference in output depending on the location of the sensors with the sensors placed on the side of the splint (50-55 mm) leading to generally higher outputs. It can further be observed that only the FSRs in the back of the splint (proximal part of the forearm) returned an output.

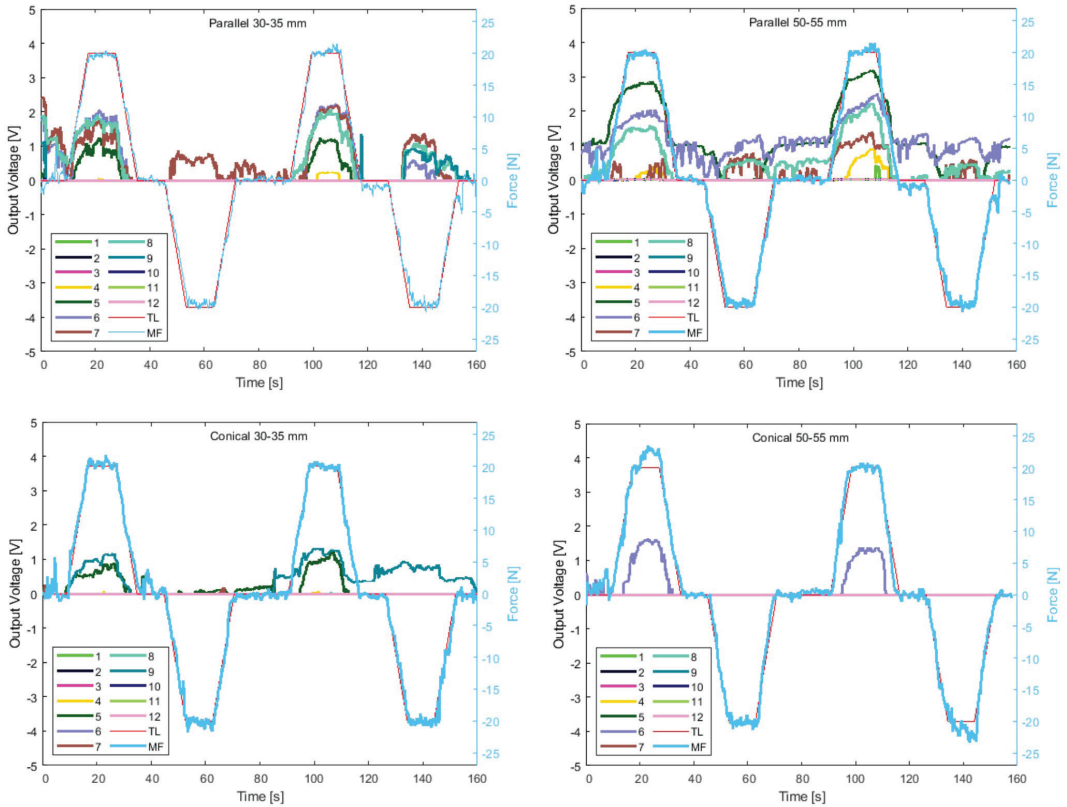


Figure 4.6) Outputs of FSRs for forces exerted in x-direction. Top: parallel arc-shaped splint, bottom: conical arc-shaped splint. Left: 30-35 mm distance of sensors, right: 50-55 mm distance of sensors (1-12: force sensitive resistors organized as shown in Figure 4.3; TL: target line; MF: force exerted in x-direction measured with 6-DOF force/torque sensor).

For the rotation around the x-axis (Figure 4.7), we observed interaction forces in the proximal part of the forearm and splint for positive target torques and interaction forces in the distal part for negative torques, which met our expectations. It can be observed that the output of sensor FSR 5 in the condition parallel arc-shaped splint and 50-55 mm sensor distance stays above a level of about 0.7 V while other sensors usually show no output in phases without torque exertion. Similar to the translation in x-direction, the data of the rotation presents with differences between the different conditions (marker location and splint shape).

For a force exerted in z-direction, the FSR data showed very low to no (conical, 30-35 mm) outputs which is contrary to the expectations of clear peaks whenever a force in negative z-direction is exerted. The outputs were in the magnitude of 0-2 V and primarily sensors in the elbow region of the splint showed outputs. It can further be observed that in all conditions, only a part of the FSRs is returning an output voltage. No situation was measured in which all FSR sensors are returning an output. In particular, sensor 2 never returned any visible outputs.

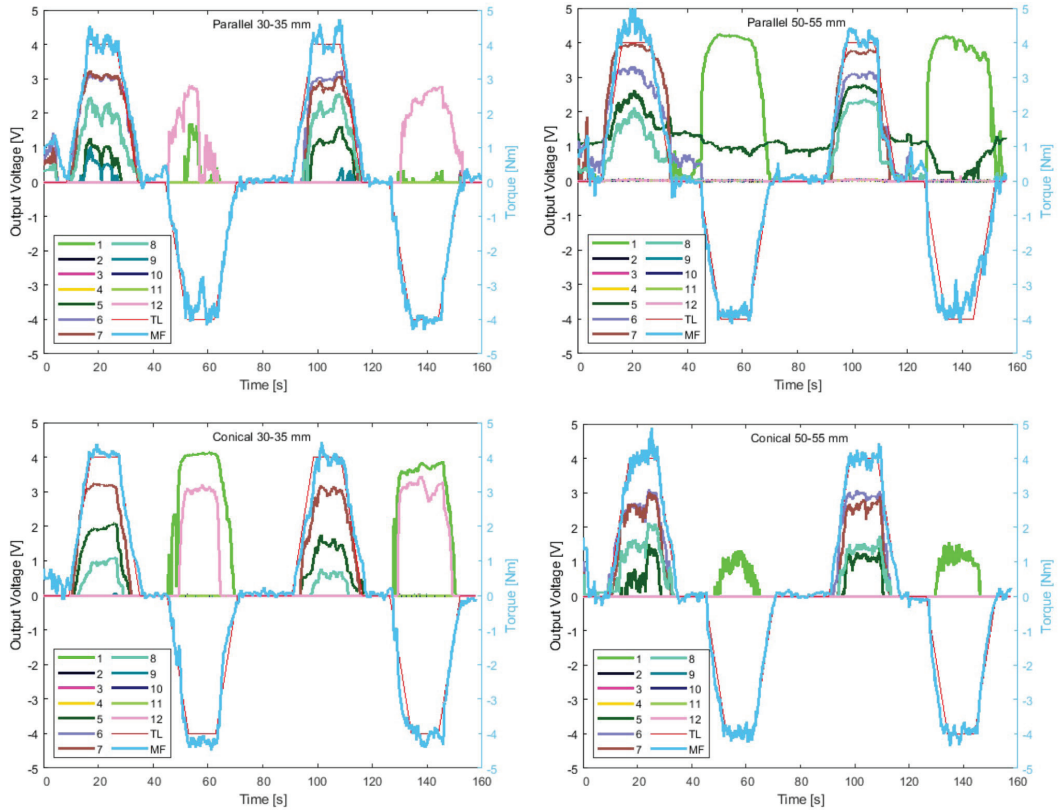


Figure 4.7] Outputs of FSRs for torques exerted around the x-axis. Top: parallel arc-shaped splint, bottom: conical arc-shaped splint. Left: 30-35 mm distance of sensors, right: 50-55 mm distance of sensors (1-12: force sensitive resistors organized as shown in Figure 4.3; TL: target line; MF: force exerted in x-direction measured with 6-DOF force/torque sensor).

DISCUSSION

The analysis of the experiments with the prototype measurement setup revealed that expectations for the interaction forces were partly met by the output of the FSRs. The fact that only the FSRs on the elbow region gave an output for force exertion in x-direction can be related to the fit of especially the parallel splint. The splint is too wide in the wrist region, which is why the force is exerted through the contact area between the splint and the proximal portion of the forearm. This part of the forearm is wider and thus closer to the splint edges. Outputs of sensors on the left side of the splint while the subject is exerting force to the right can be due to a contraction of the forearm musculature and the muscle bellies pressing on the FSRs, while the distal portion of the forearm is not or barely in contact with the splint. The low outputs that were observed during a force exertion in negative x-direction could also be explained by the anatomy of the forearm. The ulna is forming a relatively straight and equally distributed bony prominence on the lateral side of the right forearm placed in the splint and therefore an almost rigid body pressing against the side of the splint (for translations in positive x-direction). In

contrast, the medial side of the forearm is covered with a larger portion of soft tissue and the radial tuberosity forms a small bony prominence. This bony prominence might exert the major part of the force on the splint and if this prominence is not pressing on the center of one of the FSR sensors, the lack of output can be explained. This explanation would lead to an assumption that pressure exerted by bony prominences or muscle bellies is better detected by the FSRs than pressure exerted over a large area of soft tissue. However, this depends highly on the position of the bony prominence or muscle belly with respect to the FSR sensors, because the FSRs are only sensitive in the center of the sensor. This assumption could also explain the lack of FSR output observed during force exertion in negative z-direction; the compliance of the tissue prevents an activation of the FSRs and at the same time, the number of FSRs does not cover a big enough portion of the splint surface. The compliance of the tissue underneath the arm also led to an indentation of the skin through the FRS foils. The absence of outputs in single sensors can be either due to a malfunction or due to the sensor being positioned directly next to a bony prominence avoiding any contact with the sensor.

We have observed that the output varies with varying splint shapes. The conically shaped splint resulted in clearly lower FSR outputs with force exertion in x-direction. This could be due to the bony prominences or muscle bellies of the forearm not being aligned with the sensor locations or to a better fit leading to a more even distribution of interaction forces over a larger contact area. This indicates that the fit of the splint is crucial for avoiding injuries triggered by high normal forces. A snug fit is expected to spread the pressure better over the whole contact area while pressure peaks in the areas of bony prominences should be avoided through padding or indentations.

Moreover, the FSR output depends on the sensor location which underlines the need for a setup with a larger coverage of the splint surface with sensors, so that a mapping of the pressure or force distribution in the arm-splint contact area can be performed. To further avoid missing data due to force exertion on the non-sensitive edges of the FSRs, one could extend the setup by a matrix of semi-spheres. A layer of semi-spheres placed along the arm between the arm and the splint and arranged in a way that the tip of each semi-sphere is touching the center of a FSR, could translate the force exerted on the intersection area of each sphere to the sensitive center of one FSR. This method for concentrating force has been described and tested by Castellini and Ravindra [38].

One major limitation of the current experiment is that it was only performed with one subject. Therefore, no assessment of the reproducibility of the data and observations can be performed. Moreover, the forearm had to be repositioned several times to realize the different conditions (splint shape and sensor positions), which might have led to a displacement of e.g. bony prominences and pressure peaks. In addition to that, no onset forces exerted by the straps were measured and therefore differences in the initial conditions cannot be ruled out. However, the fact that the majority of FSRs gives a zero output at times that no target force is present, leads to the assumption that there was no significant onset force. The increased output of sensor FSR 5 in the condition parallel arc-shaped splint and 50-55 mm sensor distance can be due to a malfunction of the sensor or an increased onset pressure as the same can be observed for all measurements in this condition. An additional limitation of the FSRs is the non-linearity of its outputs. A calibration of the FSRs for a translation of the voltage output to forces would be necessary to gain insight in the magnitude of forces.

Since the curvature underneath the sensors can have an influence on the resistor output, the calibration would have to be performed after placing the sensors on the splint surface. As mentioned above, the reliability of the FSR data might be increased by adding a layer of semi-spheres along the arm between the sensors and the human subject. Moreover, the indentation of the skin observed in the experiments calls for an additional layer in the contact area. This layer would have to be added on top of the layer of semi-spheres to provide a smooth surface on which the forearm can rest, which does however not influence the outputs.

As discussed above, there are some drawbacks of FSRs restricting the reliability of the outputs. While the above-mentioned adjustments to the setups could increase the reliability, the use of load cells as an addition or replacement has to be considered. Load cells deliver reliable data and can measure tangential forces, which are an essential aspect in human-robot interaction. The data of the 6-DOF force sensor used in this study has a restricted relevance for the assessment of interaction forces because it was used as feedback for the subject to follow the target line. Furthermore, it was mounted underneath the splint, which gives us an indication of the net forces exerted by the subject but not of local phenomena on soft tissue level. To get some more insight in the amount of forces and torques exerted in directions other than the target direction and the influence on the FSR output, the relationship between both sensor data should be examined in more detail. A number of 3-DOF load cells implemented in a segmented splint similar to the setup proposed in Figure 4.1 B could give an indication of the interaction forces in several different areas of the splint. This approach could be combined with a mapping of forces or pressures at the contact area between subject and splint, either using an increased number of FSRs and a layer of semi spheres or using a pressure sensor matrix with sufficient resolution and sensitivity. These mapped forces or pressures should be validated with respect to the net forces measured by the 6-DOF force sensor. Larger FSRs are not recommended as a mounting of the FSRs to a curved surface can reduce measurement range and cause resistance drift. The smaller the active area, the less deformation takes place. Furthermore, the onset force of the straps should be measured to achieve comparable results between measurements, e.g. using tensile force sensors. This approach for an improved measurement setup could increase the validity of the results and lead to a more detailed assessment for human-robot interactions. To cover some additional factors relevant for skin injuries, assessments of humidity, temperature [198], skin movement [133] and blood flow [200] could be included.

CONCLUSION

Initial experiments using FSRs and a 6-DOF force and torque sensor showed a dependency of human-robot interaction forces between splint and forearm of the splint shape, type of movement and location of sensors. Additional measurements with an increased number of subjects and an improved measurement setup are proposed to increase the knowledge about physical human-robot interaction and gain new insights into shear forces acting on the human body.

In addition to valid measurement methodologies, there is a need for research exploring safe ranges of human-robot interaction forces.

Background: Exoskeletons are working in parallel to the human body and can support human movement by exerting forces through cuffs or straps. They are prone to misalignments caused by simplified joint mechanics and incorrect fit or positioning. Those misalignments are a common safety concern as they can cause undesired interaction forces. However, the exact mechanisms and effects of misalignments on the joint load are not yet known. The aim of this study was therefore to investigate the influence of different directions and magnitudes of exoskeleton misalignment on the internal knee joint forces and torques of an artificial leg.

Methods: An instrumented leg simulator was used to quantify the changes in knee joint load during the swing phase caused by misalignments of a passive knee brace being manually flexed. This was achieved by an experimenter pulling on a rope attached to the distal end of the knee brace to create a flexion torque. The extension was not actuated but achieved through the weight of the instrumented leg simulator. The investigated types of misalignments are a rotation of the brace around the vertical axis and a translation in anteroposterior as well as proximal/distal direction.

Results: The amount of misalignment had a significant effect on several directions of knee joint load in the instrumented leg simulator. In general, load on the knee joint increased with increasing misalignment. Specifically, stronger rotational misalignment led to higher forces in mediolateral direction in the knee joint as well as higher ab-/adduction, flexion and internal/external rotation torques. Stronger anteroposterior translational misalignment led to higher mediolateral knee forces as well as higher abduction and flexion/extension torques. Stronger proximal/distal translational misalignment led to higher posterior and tension/compression forces.

Conclusions: Misalignments of a lower leg exoskeleton can increase internal knee forces and torques during swing to a multiple of those experienced in a well-aligned situation. Despite only taking swing into account, this is supporting the need for carefully considering hazards associated with not only translational but also rotational misalignments during wearable robot development and use. Also, this warrants investigation of misalignment effects in stance, as a target of many exoskeleton applications.

Chapter 5

Assessing effects of
exoskeleton misalignment on knee
joint load during swing using an
instrumented leg simulator



BACKGROUND

Wearable robots for physical assistance and rehabilitation are playing an increasingly relevant role in our societies. The ageing population increases the need for technologies supporting people with chronic disability as well as the ageing workforce. Technical advancements enabling the use of robots in close interaction with humans across domains can help address this need [201]. Many different types of exoskeletons exist, along with a variety of application areas and use cases.

Especially in the field of rehabilitation robotics, misalignments are a common safety concern in exoskeleton use [117], [202]. A mismatch between the user's anatomical joint and the exoskeleton joint can cause undesired interaction forces, which in turn can reduce comfort and safety [101], [203]. One can distinguish between two main causes of misalignments: a kinematic mismatch between the exoskeleton joint and the anatomical joint and wrong positioning or fitting of the exoskeleton. A kinematic mismatch between the exoskeleton joint and the anatomical joint is unavoidable as anatomical joints are too complex in their mechanics and kinematics to be perfectly mimicked by exoskeleton joints [137]. Limited degrees of freedom (DOF) in an exoskeleton can lead to misalignments during movement. To take the knee joint (as one of the less complex joints in the human body) as an example, its kinematics are characterized by a translation of the axis of rotation with increasing knee flexion [104]. This behavior is not replicated by the hinge joints that are typically used as an exoskeleton knee joint [203]. The micro-misalignments that are created in the course of a knee flexion (or the movement of any other joint supported by an exoskeleton) are therefore an inherent hazard. Wrong positioning or poor fit of an exoskeleton can lead to larger misalignments as the exoskeleton joint axis might be considerably translated or rotated with respect to the anatomical joint axis. As contemporary robotic exoskeleton systems, unlike many orthotic devices, are usually one-size-fits-all solutions, they can only be adjusted to the user to a certain degree by e.g. changing the segment length and adjusting straps that are used to attach the device to the user's limbs. Careful utilization of those adjustment options by trained experts is vital to minimize misalignments. Inaccurate setting of the exoskeleton segment lengths can cause a proximal/distal translation of the exoskeleton joint axis with respect to the anatomical joint. Another source of poor positioning can be (potentially unsupervised) donning of the system by its user. The exoskeleton joint might be positioned in a way that its rotation axis is rotated with respect to the anatomical joint rotation axis. Moreover, deviations in soft tissue, clothing worn under the exoskeleton, cushion thickness or strap length could lead to the exoskeleton joint axis being translated (in anteroposterior direction) with respect to the anatomical joint axis. Misalignments can not only lead to undesired forces and torques on the musculoskeletal system but also to increased pressure and shear at the fixation points of the exoskeleton (e.g. cuffs), where a relatively too long or too short exoskeleton segment will push or pull on the user's soft tissue [101], [104], [131]. Misalignments have previously been discussed as potential cause for bone fractures in lower limb exoskeleton use [44], [103].

Recent research efforts have focused on the development of misalignment compensation mechanisms [114], [137], [203]. Common strategies for misalignment compensation include manual alignment, the use of compliant elements, and the addition of kinematic redundancy. Manual alignment can reach good results but requires a trained person and can be time-consuming and is only a valid option if the exoskeleton joint's mechanics are very similar to those of the anatomic joint. Compliant elements

either at the frame and brace level or at the joint level can allow for small compensatory movements and thereby reduce the effects of small misalignments. Another option is to add kinematic redundancy, i.e. to add more DOF. This however often makes the device heavier and bulkier and can introduce additional inertia to the system [203]. Literature on the effects of misalignments is scarce. Some studies investigated the effects of compensation mechanisms on forces at the skin-cuff interface [204], [205] and one study introduced a misalignment to a lower limb exoskeleton to study the effects on gait [131]. Due to the limited amount of studies, there is an overall lack of knowledge regarding misalignments in wearable robots. This includes missing information on the occurrence of adverse events caused by misalignments, effects of misalignments on comfort and safety of exoskeleton users, and acceptable levels of misalignment. Assuming that misalignments cannot be prevented completely, knowledge on acceptable levels of misalignment not causing significant harm to the exoskeleton user is required. As a first step towards this knowledge, the mechanisms behind misalignments and its influences on forces acting on the body need to be better understood.

The aim of this study is to investigate the influence of different directions and magnitudes of misalignments on the forces and torques in the musculoskeletal system using a dummy limb. The approach of using a dummy limb with simple mechanics and readily available components was chosen with the exoskeleton developer in mind who is regularly confronted with the challenge of testing and validating device safety. In addition to the use in the present study, it can be a first step into developing a system that can be replicated by others that want to assess effects of misalignments in their device. We hypothesized that the forces and torques applied to the knee joint during exoskeleton use are higher when a misalignment is introduced compared with the well-aligned situation. We investigated the effects of different directions of misalignment between the knee joint of a passive leg simulator and the joint of a passive knee brace being manually flexed. The investigated directions of misalignment include a rotation around the vertical axis and a translation in anteroposterior as well as proximal/distal direction.

METHODS

A series of experiments was executed using an instrumented leg simulator (ILS) and a passive knee brace in different alignment settings, which was manually flexed by the experimenter. The apparatus and procedures are explained in detail in the following sections.

Apparatus

The ILS has been specifically developed and built for this study. It consists of two rigid segments which are connected through a simple hinge joint and covered with a compliant material to mimic soft tissue (Figure 5.1). The rigid part of the leg segments mimicking the bones consists of two aluminum tubes of 22 mm diameter and 2 mm wall thickness. The upper and lower segment are connected through a simple hinge joint with a centered rotation axis (Beukenholdt zeilmakerij, Leiderdorp, the Netherlands). To measure the effects of misalignments with regard to forces and torques on the musculoskeletal system, the ILS is instrumented using a 6 DOF force and torque (FT) sensor (ATI FT-Delta DI60-660, ATI Industrial Automation, Apex, North Carolina, USA), which is connected to the bottom of the upper rod and the top of the joint using custom 3D-printed parts. The soft tissue is mimicked by a hollow

polyether foam rubber cylinder with a specific gravity (SG) of 40, an inner diameter of 25 mm and an outer diameter of 130 mm (Joan's Comfortschuim BV, IJmuiden, the Netherlands). A circular weight is attached to the distal end of the lower leg segment. The total weight of the ILS is 4.2 kg and the lower leg weight is 3.3 kg.

To mimic leg exoskeleton use in a simple way, we used a passive semi-rigid knee brace (A. C. lite by DonJoy, DJO, LLC, Lewisville, Texas, USA) with a polycentric joint and straps above and below the knee, which is commonly used to support knee ligament instabilities. The brace can be attached to the ILS and then moved by the experimenter by pulling on a string attached to the distal posterior strap of the orthosis (see Figure 5.1). To quantify the pulling force that generates the flexion torque at the orthosis joint, a tensile force sensor (Model No. 615, Tedeo-Huntleigh, Chatsworth, California, USA) was attached to the string. The ILS is symmetrical and therefore does not have specific characteristics of a left or right leg. However, the used knee brace is designed for the left leg and therefore the ILS will be considered as a left leg simulator in this article. The upper orthosis segment was mounted in a steel frame to keep it in place. To avoid slipping of the ILS due to its weight, its upper end was also fixed to the same frame.

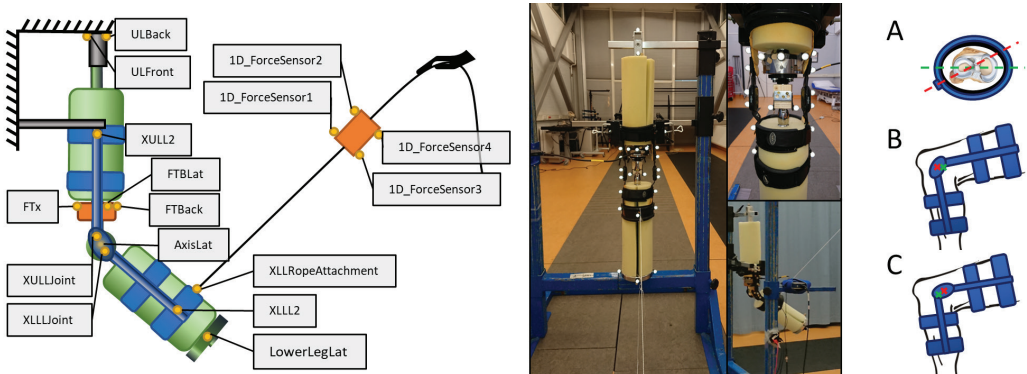


Figure 5.1 | Overview of the setup. Left: Schematic representation of the setup and marker placement, lateral view. The ILS is shown in green, the orthosis in blue, the frame in grey/black, the sensors in orange and the markers in yellow. Markers XULM2, FTFM, AxisMed, XULMJoint, XLLMJoint, XLLM2 and LowerLegMed are not shown as they are placed on the medial side. Detailed information about marker placement can be found in the Annex. Middle: Photos of the setup. Right: Visualization of internal rotational misalignment (A), posterior translational misalignment (B) and distal translational misalignment (C) of a leg with respect to a knee brace, where the red dashed line and crosses represent the orthosis center of rotation and the green dashed line and crosses represent the leg center of rotation.

Procedure

At the start of the experiment, the ILS and brace were aligned as good as possible by an experienced researcher based on visual assessment. They were positioned inside the measuring volume of an 8 camera marker-based optoelectronic tracking system (Vicon Nexus with 4 Vero and 4 Vantage cameras, VICON, Oxford UK). The apparatus was equipped with 33 markers (Figure 5.1; details about marker placement can be found in the Annex) to define its segments and track their movement. The tensile force sensor was connected to an analog input channel of the optoelectronic measurement

system and the 6 DOF FT sensor was connected to a separate PC to record the data via in-house developed software. A synchronization signal was captured by both measurement systems to enable offline synchronization.

The alignment settings were achieved by manually moving the ILS with respect to the orthosis or rotating its joint in the setup. We attempted to reach different amounts of misalignment by visual inspection. The alignments were modified independently such that when one direction of misalignment was modified, the other two directions were kept at perfect alignment as far as that was possible based on visual inspection. The exact alignment parameters were later calculated using the marker data, to be used for analysis. For each of the alignment settings, at least two trials were recorded with each trial containing at least 10 knee flexions. The 10 knee flexions were exerted by the experimenter pulling on the string attached to the distal end of the orthosis. The extensions were not actuated but achieved through the weight of the distal ILS segment. The three directions of misalignment were:

- Rotational misalignment: A rotation of the knee flexion axis with respect to the orthosis flexion axis around the vertical (z-) axis. An alignment angle of zero represents a perfect rotational alignment of the two flexion axes, negative values correspond to an internal rotation of the ILS knee joint with respect to the knee brace joint and positive values correspond to an external rotation of the ILS knee joint with respect to the knee brace joint. We aimed for misalignments in a range of ± 20 deg in steps of about 5 deg. From the ILS/patient perspective, negative rotational misalignment values would correspond to an external rotation and positive values to an internal rotation of the brace.
- Translational misalignment in anteroposterior direction: A horizontal displacement of the ILS joint (in x-direction). A negative alignment distance represents a posterior translation of the ILS joint with respect to the knee brace joint and a positive alignment distance represents an anterior translation of the ILS joint axis with respect to the knee brace axis. We aimed for misalignments in a range of ± 10 mm in steps of 10 mm. From the ILS/patient perspective, negative anteroposterior misalignment values would correspond to anterior and positive values to a posterior translation of the brace.
- Translational misalignment in proximal/distal direction: A vertical displacement of the ILS (in z-direction). Negative values correspond to the ILS joint being translated distally with respect to the knee brace axis and positive values correspond to the ILS joint being translated proximally with respect to the knee brace axis. We aimed for misalignments in a range of ± 20 mm in steps of 10 mm. From the ILS/patient perspective, negative proximal/distal misalignment values would correspond to proximal and positive values to a distal translation of the brace.

For consistency, from this point onward, when using the terms internal/external rotation, anterior/posterior translation and proximal/distal translation, we refer to the device perspective. Thus, an internal rotation means that the ILS knee is rotated inwards with respect to the brace joint, an anterior translation means that the ILS knee is forward translated with respect to the brace joint, and a proximal translation means that the ILS knee is located higher than the brace joint.

We repeated the rotational misalignment trials in two brace strap pressure settings to investigate whether this has an effect on the outcomes in measured forces and torques. As we were not able

to measure strap pressure in the current setup, we could only group by “tight straps” and “loosened straps”. In the “tight straps” setting, the straps of the lower orthosis segment were pulled tight so that the foam was compressed while in the “loosened straps” setting the straps were closed without visibly compressing the foam with fully extended ILS. This additional condition was only tested in the rotational misalignment experiments since contrary to translational misalignments, an adjustment of the rotational misalignment did not require a re-attachment of the straps. Therefore, the two distinct settings were only applicable in the rotational misalignment session. The upper orthosis straps remained at approximately the same strap pressure during the entire experiment. For calibration, two static trials were recorded in which the lower leg of the ILS was hanging freely without the orthosis attached and without any movements being executed.

Data processing and analysis

The marker data were processed and labelled in Vicon Nexus 2.9.2 using a custom kinematic model and then exported for further analysis in Python 3.7.4. All data (marker data, FT sensor data, tensile force sensor data) were filtered using a low-pass bidirectional Butterworth filter of 4th order with a cutoff frequency of 6 Hz. We used the segment orientations to calculate the ILS and orthosis flexion angles as well as the rotational alignment as defined above. We did this by computing the rotation matrices of the lower segments in the local coordinate systems of the upper segments and the rotation matrices of the ILS segments in the local coordinate systems of the orthosis segments respectively and computing the Euler angles. The translational alignment in x- and z-direction (i.e. anteroposterior and proximal/distal alignment) was calculated as the distance of the ILS knee joint center (midpoint of markers AxisMed and AxisLat) from the orthosis joint center (midpoint of markers XULMJoint, XULLJoint, XLLMJoint and XLLLJoint). To extract one single alignment value per trial and misalignment type, we took the mean of the considered alignment parameter in the static situation before the first knee flexion (i.e. from the beginning of the trial to the point where the ILS flexion angle increases to more than 120% of the initial ILS flexion angle).

FT sensor data were corrected by subtracting the offset values obtained from the calibration recordings. The offset values were achieved by calculating the means of the FT sensor recordings from one of the calibration trials and then subtracting the lower leg weight from the Fz value. The offset values were subtracted from the FT sensor data for the entire time series of each trial before any further processing. The forces and torques at the ILS joint location were calculated from the recorded forces and torques at FT sensor location and the distance between the FT sensor reference frame origin and the ILS joint sensor. With the assumption that the part of the setup between the ILS joint and the FT sensor is rigid, we used the mean of the vertical distance (z-direction) in the static situation before the first flexion, similarly to the alignment calculations. We further assumed that the distance in x and y direction was zero due to the ILS design. This resulted in the following formulas:

$$\begin{aligned}
Fx_{joint} &= Fx_{sensor} + \frac{My_{sensor}}{Dz} \\
Fy_{joint} &= Fy_{sensor} - \frac{Mx_{sensor}}{Dz} \\
Fz_{joint} &= Fz_{sensor} \\
Mx_{joint} &= Mx_{sensor} + DzFy_{sensor} \\
My_{joint} &= My_{sensor} - DzFx_{sensor} \\
Mz_{joint} &= Mz_{sensor}
\end{aligned}$$

Where Fx_{sensor} , Fy_{sensor} and Fz_{sensor} are the forces measured by the FT sensor, Mx_{sensor} , My_{sensor} and Mz_{sensor} are the torques measured by the FT sensor and Dz is the vertical distance between the ILS joint center and FT sensor reference frame origin. Dz is negative as the ILS joint center is located below the FT sensor (Figure 5.2). For readability, Fx_{joint} , Fy_{joint} and Fz_{joint} will be referred to as Fx , Fy and Fz and Mx_{joint} , My_{joint} and Mz_{joint} will be referred to as Mx , My and Mz .

The flexion torque at the orthosis joint applied by the experimenter pulling on the string was calculated as follows:

$$\tau = r \cos \phi F$$

Where r is the distance between the orthosis joint center (midpoint of markers XULLJoint, XULMJoint, XLLLJoint and XLLMJoint) and the origin of the lower orthosis segment (midpoint of markers XLLL2 and XLLM2), F is the force measured by the tensile force sensor and ϕ is the angle between the actual tensile force vector and the force vector F' acting perpendicularly to the lower orthosis segment. It is calculated as the angle between the z-axis vector of the lower orthosis segment and the force vector of the tensile force (i.e. vector from XLLRopeAttachment marker to midpoint between all four 1D_ForceSensor markers) projected onto the x-z-plane, minus 90 degrees (Figure 5.2).

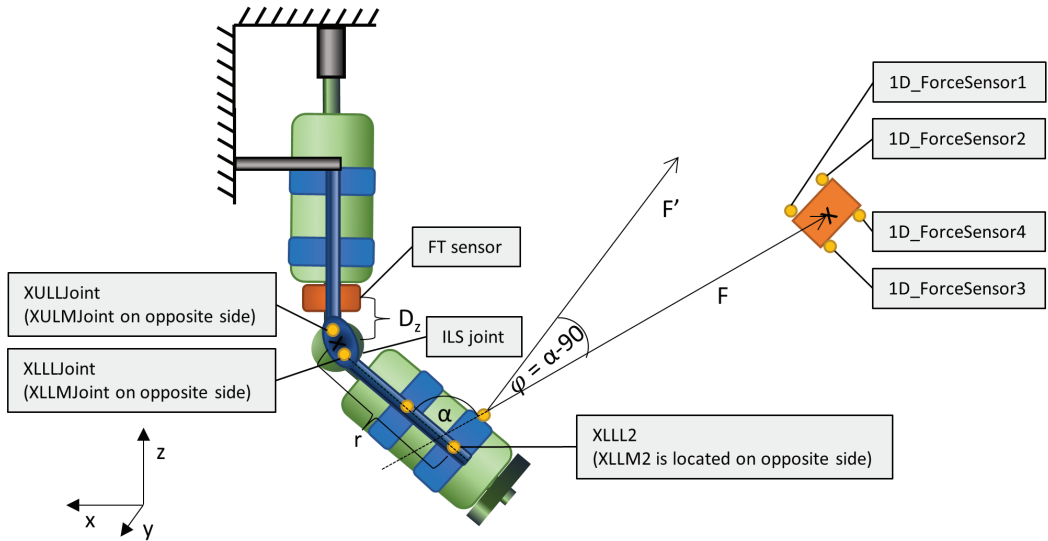


Figure 5.2| Schematic representation of the setup and measures used for calculating the forces and torques at the joint location as well as the actuation torque created by the pulling force.

For comparison between trials, we extracted peak forces ($F_{x_{peak}}$, $F_{y_{peak}}$, $F_{z_{peak}}$) and torques ($M_{x_{peak}}$, $M_{y_{peak}}$, $M_{z_{peak}}$) per repetition of the flexion/extension cycle for each of the trials. This was achieved by detecting the peaks in flexion torque, then slicing the data halfway between those peaks and finding the index of maximum absolute deviation from the starting value per force/torque component and slice. The ILS joint forces and torques at those indices were then extracted as peak forces/torques per repetition and trial. The means and standard deviations of all peaks per trial were later calculated to provide a better overview. Furthermore, peak flexion torques at the orthosis joint and peak ILS flexion angles per repetition were extracted.

The relationships between the following parameters were analyzed statistically employing a regression analysis:

- Misalignments and peak forces/torques at the ILS joint
- peak ILS flexion angle and misalignments
- Misalignments and peak manually applied flexion torque

For the analysis of misalignments and peak forces/torques at the ILS joint, we performed both a regression analysis of only absolute values to assess relationships between absolute misalignment and absolute joint load, and a regression analysis of the original values to also take the direction of misalignment as well as forces/torques into consideration. Regression lines with R-squared values larger than 0.7 are reported and considered as strong relationships. If no linear regression reaching this target was found, a 2nd degree polynomial regression analysis was performed with the same target R-squared. We employed a significance level of 0.05 for the probability of the F-statistic.

RESULTS

We recorded and analyzed 22 rotational misalignment trials ranging from 13 deg internal rotation to 19 deg external rotation, 6 anteroposterior translational misalignment trials ranging from 4 mm posterior to 14 mm anterior translation of the ILS joint center and 12 proximal/distal translational misalignment trials ranging from 23 mm distal translation to 12 mm proximal translation of the ILS joint center. Please note that two aligned trials were used in both the rotational misalignment and anteroposterior translational misalignment analysis (marked in Table 5.2 and Table 5.4).

Figure 5.3 shows a typical trial in an aligned setting, in which the ten repetitions of flexion and extension are clearly visible from the flexion torque and ILS joint angle data. As expected, while all torques as well as the forces in y- and z-direction stay close to zero throughout the trial, there is a clear increase of force in negative x-direction (i.e. the direction of the pulling force) with each ILS flexion.

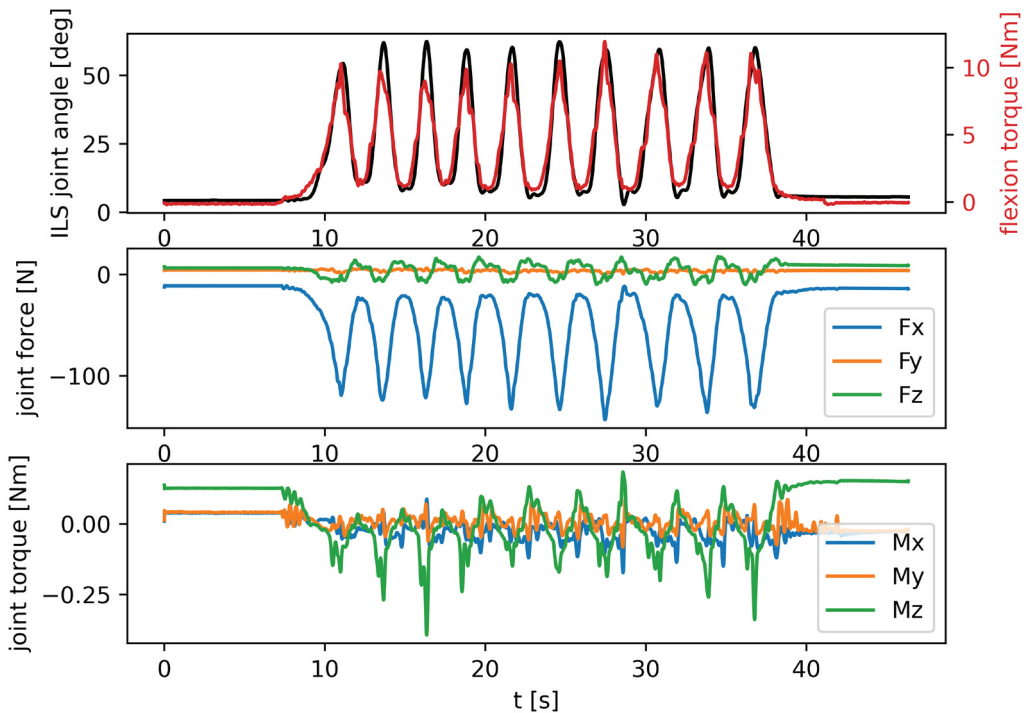


Figure 5.3| ILS joint angle, flexion torque and joint forces and torques over the course of a typical trial in aligned setup. The top graph shows the flexion angle of the ILS where 0 deg is full extension (black) and the flexion torque generated through the pulling force applied to the orthosis (red). The middle graph shows the forces in the ILS joint where positive Fx is forward directed force, positive Fy is pointing from medial to lateral, and positive Fz is compressive force. The bottom graph shows the torques in the ILS joint where positive Mx is abduction torque, positive My is flexion torque, and positive Mz is external rotation torque. See also Figure 5.2 for axis orientation.

Effects of misalignments on joint forces and torques

The results of the effects of all three investigated directions of misalignments are presented in the following sections.

Rotational misalignment

With a larger degree of rotational misalignment, higher absolute peak forces and torques were observed for F_y , M_x , M_y and M_z , when only looking at amount of misalignment, regardless of the direction of misalignment (Table 5.1). When considering a more detailed picture including direction of misalignment, we can also see that rotational misalignment clearly has an effect on joint forces in x- and y-direction (Figure 5.4). The peaks in negative x-direction around maximum flexion increase in magnitude with increasing rotational misalignments in both directions. A hysteresis is visible with a close to linear buildup of the force which is then released quickly with a large part of the force reduction happening before ILS joint extension. Joint force in y-direction is increasing with increasing joint angle when there is an external rotation misalignment and decreasing with increasing joint angle when there is an internal rotation misalignment. As mentioned above, the absolute peaks increase with increasing amount of misalignment in both directions. The pattern of joint force in z-direction varies per trial and the peaks do not show a clear relation with misalignment.

Table 5.1 | Results of regression analysis for absolute values of misalignment and joint forces/torques.

Misalignment	$ F_{x_{peak}} $	$ F_{y_{peak}} $	$ F_{z_{peak}} $	$ M_{x_{peak}} $	$ M_{y_{peak}} $	$ M_{z_{peak}} $
rotational	-	$y=2.20x+3.82$; $R^2=0.84$	-	$y=0.23x+0.08$; $R^2=0.92$	$y=0.20x-0.17$; $R^2=0.86$	$y=0.16x+0.12$; $R^2=0.89$
Translational anteroposterior	$y=-0.19x^2+6.46x+97.52$; $R^2=0.70$	-	-	$y=0.06x+0.08$; $R^2=0.94$	-	-
Translational proximal/distal	-	-	-	-	-	-

In the regression equations, x is the absolute amount of misalignment (in degrees for rotational misalignment and in mm for translational misalignments) and y is the outcome measure as indicated in the top row in N or Nm respectively. A dash indicates that first and second degree polynomial fits did not meet the criterium of $R^2 > 0.7$. All p-values were $p < 0.01$.

Joint torques around the x-axis are increasing in positive direction with increasing joint angle when there is an external rotation misalignment and increasing in negative direction with increasing joint angle when there is an internal rotation misalignment. Joint torques around the z-axis show a similar pattern in the opposite direction. Torques around the y-axis have peaks at around maximum flexion that strongly increase with increasing amount of misalignment in both directions. Trials with larger misalignments show a steeper increase in joint forces (except in z-direction) and torques with increasing flexion angle. Especially the trials with large misalignments show a very strong hysteresis; after a steady buildup of force or torque, there is a sudden drop at maximum flexion.

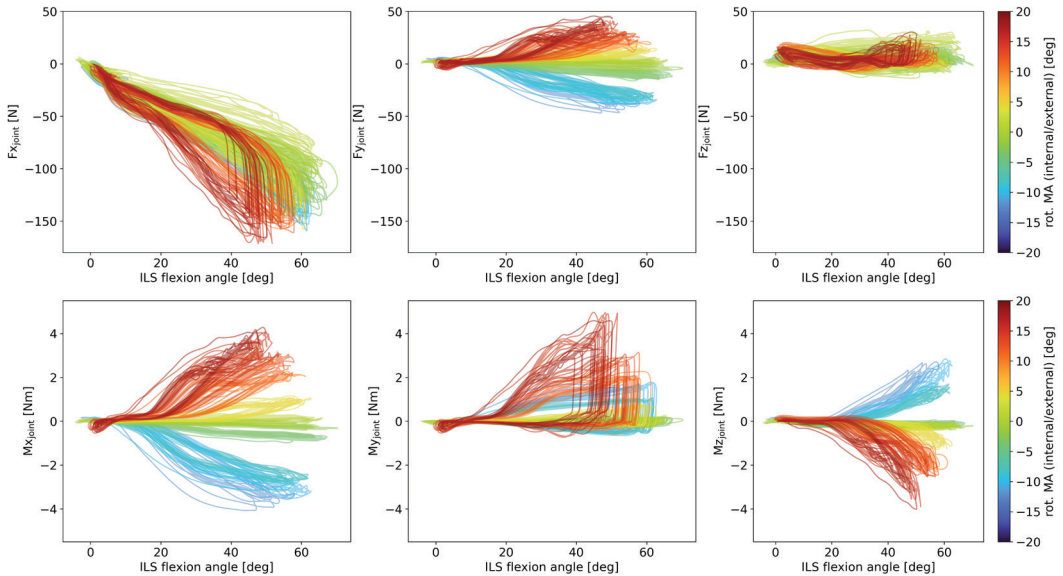


Figure 5.4| Hysteresis plots of ILS joint forces and torques over the ILS flexion angle. The amounts of rotational misalignment (rot. MA) are represented by the graph colors with darker blue shades representing stronger internal rotation and darker red shades representing stronger external rotation.

The means and standard deviations of the peak forces and torques per flexion/extension cycle and the amount of rotational misalignment per trial are shown in Table 5.2. Similar to the outcomes regarding the absolute misalignment values, the analysis concerning directions of misalignment revealed a positive linear regression between the amount of rotational misalignment and peak F_y ($F_{y_{peak}} = 2.61 \text{ Alignment}_{rot} - 3.63$; $R^2 = 0.95$; $p < 0.01$) as well as peak M_x ($M_{x_{peak}} = 0.24 \text{ Alignment}_{rot} - 0.26$; $R^2 = 0.98$; $p < 0.01$). For the relationship between the amount of rotational misalignment and peak M_y , we found a 2nd degree polynomial fit ($M_{y_{peak}} = 0.01 \text{ Alignment}_{rot}^2 + 0.02 \text{ Alignment}_{rot}$; $R^2 = 0.90$; $p < 0.01$) and for the relationship between the amount of rotational misalignment and peak M_z , we found a negative linear regression ($M_{z_{peak}} = -0.16 \text{ Alignment}_{rot} - 0.18$; $R^2 = 0.92$; $p < 0.01$).

Effects of strap pressure

In the present data, the different levels of strap pressure did not have an effect on the ILS joint peak forces and torques. The regression for the pooled data (tight and loose straps) explained at least the same proportion of the variance as the least performing regression of the two data subsets (Table 5.3)

Table 5.2 Peak forces and torques presented as M (SD) per rotational misalignment trial.

Rotational alignment [deg]	F _{x_{peak}} [N]	F _{y_{peak}} [N]	F _{z_{peak}} [N]	M _{x_{peak}} [Nm]	M _{y_{peak}} [Nm]	M _{z_{peak}} [Nm]
-12.9	-127.3 (8.2)	-41.6 (3.0)	6.5 (8.5)	-3.63 (0.21)	1.58 (0.09)	2.37 (0.22)
-10.7	-143.5 (7.5)	-36.9 (1.9)	14.0 (1.8)	-3.32 (0.12)	1.61 (0.13)	2.48 (0.24)
-9.0*	-140.1 (6.7)	-34.4 (2.4)	-3.1 (2.2)	-2.83 (0.15)	1.01 (0.03)	1.51 (0.16)
-8.1*	-140.9 (9.2)	-33.1 (1.8)	1.2 (6.9)	-2.68 (0.06)	0.97 (0.04)	1.47 (0.13)
-3.5*	-127.2 (9.2)	-12.3 (2.1)	-1.2 (1.0)	-0.83 (0.07)	-0.29 (0.02)	-0.23 (0.02)
-3.1*	-126.7 (6.0)	-12.7 (1.5)	4.0 (8.5)	-0.74 (0.02)	-0.27 (0.01)	-0.23 (0.03)
-1.8~	-119.6 (5.2)	-7.7 (0.7)	6.5 (6.7)	-0.34 (0.03)	-0.21 (0.01)	-0.26 (0.02)
-1.6~	-113.4 (7.6)	-5.9 (0.6)	10.8 (0.7)	-0.32 (0.04)	-0.20 (0.01)	-0.27 (0.04)
-1.0	-108.7 (4.7)	-2.9 (1.3)	9.2 (1.5)	-0.20 (0.02)	-0.19 (0.01)	-0.30 (0.04)
-0.5*	-129.8 (6.8)	1.5 (1.7)	-8.5 (1.2)	-0.11 (0.03)	-0.06 (0.01)	-0.24 (0.08)
-0.1	-98.7 (3.7)	-1.9 (0.7)	12.8 (1.5)	-0.22 (0.02)	-0.17 (0.02)	-0.36 (0.05)
-0.1*	-96.7 (5.5)	0.1 (0.8)	19.5 (1.6)	-0.01 (0.06)	-0.10 (0.14)	-0.24 (0.03)
0.3*	-120.9 (22.8)	2.9 (3.2)	-3.5 (11.6)	-0.09 (0.07)	0.06 (0.05)	-0.21 (0.15)
1.8*	-77.1 (12.1)	7.0 (1.0)	27.5 (3.1)	0.20 (0.12)	0.29 (0.03)	-0.29 (0.05)
4.3*	-127.8 (5.7)	14.8 (2.2)	-6.1 (1.4)	1.00 (0.08)	0.64 (0.07)	-1.00 (0.17)
4.8*	-129.9 (12.3)	13.7 (1.4)	-5.3 (0.9)	0.97 (0.06)	0.66 (0.08)	-1.00 (0.17)
10.2*	-148.6 (4.9)	21.4 (1.2)	-5.2 (2.2)	2.17 (0.05)	2.01 (0.11)	-2.08 (0.16)
12.6*	-147.6 (4.1)	27.5 (3.3)	-4.4 (1.2)	2.41 (0.22)	2.00 (0.07)	-2.24 (0.22)
13.2	-149.9 (5.5)	27.0 (1.7)	17.5 (1.7)	2.95 (0.11)	2.77 (0.16)	-2.22 (0.19)
16.1*	-167.5 (4.5)	38.5 (2.5)	22.4 (3.5)	3.78 (0.22)	4.54 (0.41)	-3.24 (0.32)
16.2	-148.6 (4.5)	32.8 (2.9)	14.3 (1.9)	3.21 (0.16)	2.94 (0.17)	-2.22 (0.20)
18.6*	-143.3 (12.8)	38.4 (3.3)	6.7 (13.5)	3.77 (0.27)	3.67 (0.51)	-2.68 (0.56)

Trials marked with * in the first column were the trials with increased strap pressure. Trials marked with ~ in the first column were also used in the anteroposterior translational misalignment analysis.

Table 5.3 Results of regression analysis for tight straps, loosened straps and both conditions pooled.

Condition	F _{y_{peak}}	M _{x_{peak}}	M _{y_{peak}}	M _{z_{peak}}
tight straps	$y=2.61x-2.99$; R ² =0.94	$y=0.24x-0.25$; R ² =0.98	$y=0.01x^2+0.03x+0.12$; R ² =0.89	$y=-0.16x-0.26$; R ² =0.92
loosened straps	$y=2.56x-5.03$; R ² =0.97	$y=0.24x-0.27$; R ² =0.98	$y=0.01x^2+0.01x-0.11$; R ² =0.94	$y=-0.17x-0.07$; R ² =0.91
pooled (both)	$y=2.61x-3.73$; R ² =0.95	$y=0.24x-0.26$; R ² =0.98	$y=0.01x^2+0.02x+0.05$; R ² =0.90	$y=-0.16x-0.18$; R ² =0.92

In the regression equations, x is the amount of rotational misalignment in degrees and y is the outcome measure as indicated in the top row in N or Nm respectively. All p-values were p<0.01.

Translational misalignment in anteroposterior direction

As the current setup does not allow for easy translation of the orthosis in anteroposterior direction, only three different levels of anteroposterior alignment could be achieved (see Table 5.4, note that each misalignment setting was measured twice and there are slight variations in measured amount of misalignment in those two repetitions per setting). With a larger degree of anteroposterior misalignment, higher absolute peak forces and torques were observed for F_x (2nd degree polynomial fit) and M_x (linear fit), when only looking at amount of misalignment, regardless of the direction of misalignment (Table 5.1). When considering a more detailed picture including direction of misalignment, this pattern is confirmed in F_x , showing a higher absolute peak force and stronger hysteresis with larger misalignment (Figure 5.5). F_y is low overall, stays almost constant across the flexion/extension circle and varies slightly in starting values in the different conditions. The starting values of F_z are influenced by the misalignment in an opposite manner than those of F_y . The shapes of the curves clearly differ in the different alignment settings showing a positive peak at maximum flexion in the posterior translation setting and a positive peak at maximum extension and a negative peak at around half of the maximum flexion in the anterior translation setting. M_x shows only little variation in the aligned and posterior translation settings and a decrease with increasing flexion in the anterior translation setting. A tendency for positive peaks in posterior translation misalignment and negative peaks in anterior translation misalignment is visible. M_y and M_z show comparable behavior in all settings covering a small torque range.

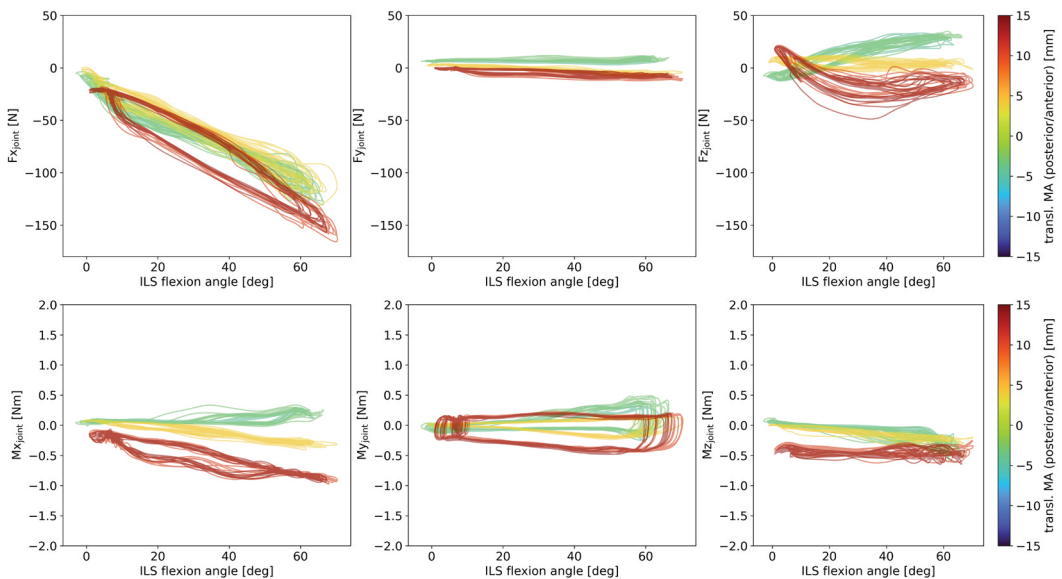


Figure 5.5 Hysteresis plots of ILS joint forces and torques over the ILS flexion angle. The amounts of anteroposterior translational misalignment (transl. MA) are represented by the graph colors with green-blue shades representing posterior translation and orange-red shades representing anterior translation.

Regression analysis of the peak forces and torques (Table 5.4) resulted in a negative linear relationship between anteroposterior translation and peak Fy ($Fy_{peak} = -1.07 \text{ Alignment}_{transAP} + 2.27$; $R^2 = 0.75$; $p < 0.01$), peak Mx ($Mx_{peak} = -0.07 \text{ Alignment}_{transAP} + 0.01$; $R^2 = 0.97$; $p < 0.01$) as well as peak My ($My_{peak} = -0.05 \text{ Alignment}_{transAP} + 0.13$; $R^2 = 0.88$; $p < 0.01$).

Table 5.4 Peak forces and torques presented as M (SD) per anteroposterior translational misalignment trial.

Translational alignment anteroposterior [mm]	Fx _{peak} [N]	Fy _{peak} [N]	Fz _{peak} [N]	Mx _{peak} [Nm]	My _{peak} [Nm]	Mz _{peak} [Nm]
-4.0	-113.5 (4.9)	7.1 (3.0)	31.1 (1.2)	0.27 (0.02)	0.33 (0.04)	-0.33 (0.09)
-2.5	-123.8 (4.3)	10.2 (1.1)	32.4 (1.1)	0.27 (0.04)	0.43 (0.04)	-0.45 (0.07)
3.9~	-113.4 (7.6)	-5.9 (0.6)	10.8 (0.7)	-0.32 (0.04)	-0.20 (0.01)	-0.27 (0.04)
4.3~	-119.6 (5.2)	-7.7 (0.7)	6.5 (6.7)	-0.34 (0.03)	-0.21 (0.01)	-0.26 (0.02)
11.5	-155.2 (6.2)	-10.5 (1.1)	-27.6 (2.7)	-0.91 (0.03)	-0.44 (0.01)	-0.41 (0.15)
14.4	-145.4 (6.4)	-9.0 (0.9)	6.4 (24.9)	-0.90 (0.04)	-0.44 (0.03)	-0.38 (0.09)

Trials marked with ~ in the first column were also used in the rotational misalignment analysis.

Translational misalignment in proximal/distal direction

For proximal/distal translational misalignment, there were no relationships (with $R^2 > 0.7$) between amount of misalignment and absolute peak joint forces or torques, when only looking at amount of misalignment, regardless of the direction of misalignment (Table 5.1). When looking at the ILS joint forces and torques over the flexion/extension cycle in all proximal/distal translational misalignment settings (Figure 5.6), a more nuanced picture is observed. Fx shows an increase of absolute peak force and hysteresis with larger misalignments, while Fy shows little change over the flexion/extension cycle but a slight variance in starting values. The starting values and shapes of Fz curves vary per trial with a tendency of more pronounced negative peaks and hysteresis in the proximal translation trials. Joint torques show little variance among the trials, except for the two trials at approximately 12 mm distal translation showing higher positive peaks in all directions, in y-direction together with the trials in strongest distal translation (approximately 22 mm).

Despite the lack of a relation between absolute amount of misalignment and peak forces/torques, when taking the direction of misalignment into account a relation did become evident. Regression analysis of the peak forces and torques (Table 5.5) revealed regression with R-squared larger than 0.7 in Fx ($Fx_{peak} = -0.04 \text{ Alignment}_{transPD}^2 + 0.81 \text{ Alignment}_{transPD} - 98.83$; $R^2 = 0.75$; $p < 0.01$) and Fz ($Fz_{peak} = -1.71 \text{ Alignment}_{transPD} - 10.8$; $R^2 = 0.76$; $p < 0.01$).

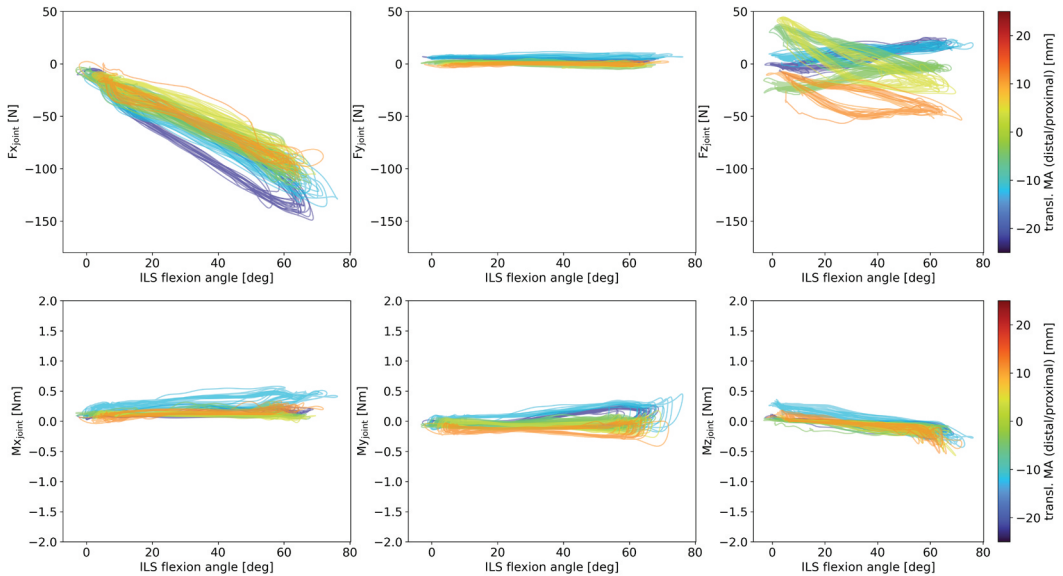


Figure 5.6] Hysteresis plots of ILS joint forces and torques over the ILS flexion angle. The amounts of proximal/distal translational misalignment (transl. MA) are represented by the graph colors with green-blue shades representing distal translation and orange-red shades representing proximal translation.

Table 5.5] Peak forces and torques presented as M (SD) per proximal/distal translational misalignment trial.

Translational alignment						
proximal/distal [mm]	$F_{x_{peak}}$ [N]	$F_{y_{peak}}$ [N]	$F_{z_{peak}}$ [N]	$M_{x_{peak}}$ [Nm]	$M_{y_{peak}}$ [Nm]	$M_{z_{peak}}$ [Nm]
-22.6	-136.5 (7.3)	2.3 (1.0)	21.6 (2.2)	0.24 (0.01)	0.24 (0.03)	-0.2 (0.04)
-22.1	-138.1 (4.5)	2.1 (0.8)	20.9 (2.1)	0.06 (0.02)	0.22 (0.02)	-0.18 (0.02)
-11.8	-122.7 (10.2)	5.4 (1.8)	19.4 (2.2)	0.44 (0.12)	0.35 (0.05)	-0.28 (0.07)
-11.7	-116.6 (7.1)	8.7 (2.4)	20.0 (2.1)	0.51 (0.03)	0.3 (0.02)	-0.29 (0.06)
-4.6	-103.1 (5.6)	-1.4 (1.0)	-5.4 (2.1)	0.08 (0.01)	-0.09 (0.06)	-0.15 (0.05)
-4.0	-102.6 (4.9)	-1.0 (0.6)	-7.2 (0.9)	0.06 (0.02)	-0.11 (0.07)	-0.2 (0.05)
-3.6	-105.4 (8.3)	-3.5 (1.2)	-2.3 (1.2)	0.11 (0.05)	0.04 (0.03)	-0.12 (0.06)
-3.2	-97.3 (15.8)	-1.2 (3.8)	0.5 (1.9)	0.23 (0.07)	0.07 (0.03)	-0.16 (0.08)
3.6	-92.9 (4.7)	-2.4 (0.6)	-22.2 (2.1)	0.03 (0.02)	-0.19 (0.01)	-0.32 (0.09)
4.8	-89.8 (7.3)	-2.3 (1.0)	-25.1 (1.9)	0.05 (0.02)	-0.02 (0.13)	-0.26 (0.12)
11.1	-95.7 (3.6)	2.4 (0.5)	-50.2 (2.0)	0.28 (0.03)	-0.29 (0.04)	-0.39 (0.07)
12.1	-100.7 (5.8)	2.0 (0.8)	-11.0 (1.8)	0.28 (0.02)	-0.19 (0.14)	-0.36 (0.09)

Change of misalignment during flexion

To assess whether and how the amount of misalignment changes in the dynamic situation during flexion and extension of the ILS and orthosis setup, this behavior is shown in Figure 5.7 for all three types of misalignment. The amount of misalignment is lower at maximum flexion than at maximum extension. In proximal/distal translational misalignment, there is little change among the repetitions of

the flexion/extension cycle and some trials show a more distal position of the ILS joint at maximum flexion. In addition to that, especially in the stronger rotational misalignment settings and in the strongest anterior translational misalignment setting, a reduction of the misalignment in the first flexion/extension cycle can be observed.

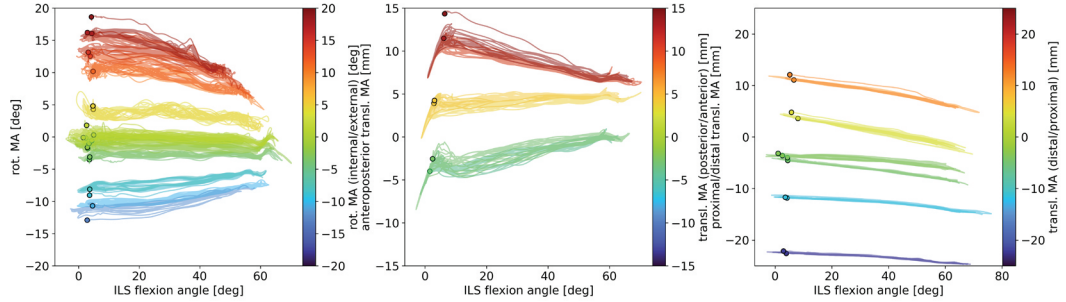


Figure 5.7| Behavior of misalignment over flexion/extension cycles of each trial. The amounts of misalignment (rot./transl. MA) are represented by the graph colors and the starting value of each misalignment setting is marked with a circle. Green to blue shades represent internal rotation, posterior translation and distal translation respectively (left to right), while orange to red shades represent external rotation, anterior translation and proximal translation respectively.

Effects of misalignment on manually applied flexion torque and maximum flexion angle

The administered flexion torque at the orthosis joint over the ILS flexion angle in all misalignment settings is shown in Figure 5.8. In the translational misalignment settings, there is no visible effect of misalignment on the required flexion torque. The rotational misalignment plot shows a tendency for increased maximum torque and/or a decreased maximum flexion angle in settings with larger misalignments. Regression analysis revealed no relationship between amount of misalignment and peak torque, but did reveal a relation of decreased maximum flexion angle with increased rotational misalignment, which however does not meet the criterium of $R^2 > 0.7$ for strong relationships set for this study ($\text{LegFlexionAngle}_{\text{peak}} = -0.04 \text{ Alignment}_{\text{rot}}^2 - 0.07 \text{ Alignment}_{\text{rot}} + 60.68$; $R^2 = 0.62$; $p < 0.01$).

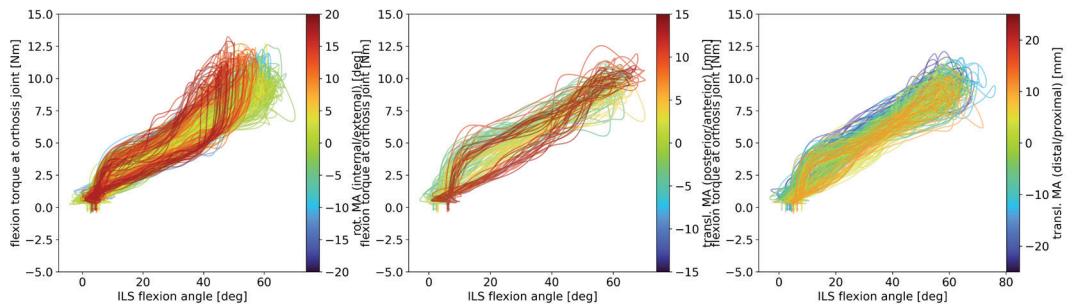


Figure 5.8| Behavior of flexion torque over flexion/extension cycles of each trial. The amounts of misalignment (rot. / transl. MA) are represented by the graph colors. Green to blue shades represent internal rotation, posterior translation and distal translation respectively (left to right), while orange to red shades represent external rotation, anterior translation and proximal translation respectively.

DISCUSSION

In this article, we mimicked the use of an exoskeleton and analyzed effects of different amounts and directions of misalignment using an ILS and a passive knee brace that was manually actuated, revealing an increasing load on the joint with increasing misalignment, supporting our hypothesis. More specifically, an increase in rotational misalignment around the vertical axis resulted in higher absolute forces in mediolateral (y-)direction as well as higher absolute torques around all three axes. The statistical analysis of translational misalignments and resulting joint forces and torques gave different results when testing only absolute values than the analysis of values considering the directions of misalignment and load. This is an indication that the effects on joint forces and loads are not symmetrical in translational misalignments, as opposed to rotational misalignments where both analyses resulted in the same relationships. Considering only absolute values, increased anteroposterior translational misalignment leads to increased absolute peak forces in anteroposterior direction and increased absolute peak ab-/adduction torques. Considering the directions of misalignment and load, an increase in translational misalignment in anteroposterior direction resulted in higher absolute peak forces in mediolateral direction as well as higher ab-/adduction and flexion/extension torques. An increase in translational misalignment in proximal/distal direction resulted in higher absolute forces in anteroposterior and vertical direction when considering directions of misalignment and forces/torques, even though no relationships were present regarding only the absolute values.

To the best of our knowledge, this is the first study showing the relative effect of different directions and amounts of misalignment on joint loads. Previous research using similar knee braces found increased forces in the brace hinge [206] but no significant differences in kinematics [207] with translational misalignment. In those studies, the braces were worn by human subjects and not actuated through any external force application. A cadaver study found that while the well-aligned brace reduced the strain on the anterior cruciate ligament, the misaligned situation showed an increased strain compared to the unbraced knee [208]. Despite the difference in research question and approach, with the present study using this passive knee brace to simulate a powered exoskeleton, the findings of the cadaver study are along similar lines as our outcome of an increasing joint load with increasing misalignment.

Among the rotational misalignment trials, the mean absolute peak force in anteroposterior (x-) direction was highest in a trial with 16.1 deg external rotation of the ILS joint and was 0.7 times or 90.5 N higher than the mean absolute peak forces at close to optimal alignment (0.1 deg internal rotation). The same trial resulted in the highest mean absolute peak torques in all three directions with peak Mx (ab-/adduction) being 3.8 Nm or 377 times higher, peak My (flexion/extension) being 4.44 Nm or 44 times higher and peak Mz (in-/external rotation) being 3 Nm or 12.5 times higher than in the aligned trial. The mean absolute peak force in mediolateral (y-) direction was highest in a trial with the strongest internal rotation (12.9 deg) and was 415 times or 41.5 N higher than in the aligned setting. None of the highest peak forces or torques recorded were associated with the trial with strongest external rotation (18.6 deg). While this is counterintuitive, it might be related to the reduction of misalignment within the first flexion of that trial leading to a lower effective misalignment comparable to the following trial which was the trial with the highest peak values in Fx, Mx, My and Mz. Remarkably, the lowest mean absolute peak force in anteroposterior (x-)direction was observed in a trial with 1.8 deg external rotation and not at the most accurately aligned trial (M (SD) of 77.1 N (12.1 N), which was approximately

20 N higher than at best rotational alignment). This might be due to the fact that the string used for applying flexion torque to the orthosis ripped at the end of the previous trial, which in turn led to a change in anteroposterior alignment (0.7 mm posterior translation while the mean across all rotational misalignment trials was 3.5 mm (SD 1.3 mm) anterior translation). Moreover, the maximum absolute mean peak forces and torques were not observed at the trials with the strongest misalignments, which might indicate that there is a saturation of maximum forces and torques at very large misalignments. This could be confirmed by testing a larger range of misalignments.

Concerning anteroposterior translational misalignment, the ranges of observed mean peak forces and torques were considerably lower than those observed in rotational misalignment. Similarly, the observed differences in mean absolute peak forces in the transversal plane (x- and y-direction) were lower than those observed in rotational misalignment. Both peak absolute F_x and peak absolute F_y were highest in a trial with 11.5 mm anterior translation of the ILS joint and lowest at 3.92 mm anterior translation with a difference of 41.8 N and 4.6 N respectively (being 0.4 times and 0.8 times respectively higher than the lowest observed mean absolute peak forces). The maximum and minimum mean absolute peak ab-/adduction and flexion/extension torques only varied by 0.64 Nm and 0.24 Nm respectively.

In the proximal/distal translational misalignment, the ranges of forces and torques were comparable to those in anteroposterior translational misalignment. The observed differences in maximum and minimum mean absolute peak forces in anteroposterior (x-) direction were also comparable to those observed in the anteroposterior translational misalignment trials with 48.3 N (0.5 times higher at 22.1 mm distal translation than the lowest values, observed at 4.8 mm proximal translation). Mean absolute peak forces in z-direction varied by 49.7 N, the result at 11.1 mm proximal translation being 111 times higher than that at 3.1 mm distal translation.

Overall, we observed much higher peak forces in mediolateral direction, as well as torques in all three planes in the rotational misalignment settings than in the translational misalignment settings. Although it is impossible to relate a certain amount of rotational misalignment to translational misalignment, we observed that rotational misalignments of approximately 10 deg resulted in much higher peak forces in mediolateral direction and peak torques in all planes than translational misalignments of 10 mm in any direction. Peak forces in anteroposterior direction showed similar increases in all types of misalignments. Further, the R^2 -values, specifically in regression of rotational misalignment versus joint forces and torques were very high with values equal to or larger than 0.9, indicating that a large portion of the variation in ILS joint force and torque results can be explained by differences in misalignment. While clinicians anecdotally report proximal/distal translational misalignment as being the biggest problem in practice when using lower limb exoskeletons, the results of this study show that rotational misalignments can also cause a substantial increase in forces and torques and that those effects should not be neglected. As such rotational misalignments can be caused in practice by unprecise positioning of the exoskeleton, limited DOF compared to human motion, or in patients with rotational deformities, their effects should be considered in the risk management process during exoskeleton development, in addition to the perhaps more obvious translational misalignments. The impact of both translational and rotational misalignments depends on the mechanics of the exoskeleton under consideration as compliant parts can alleviate effects of misalignments [203].

We found a reduction in maximum flexion with unchanged flexion torque in stronger rotational misalignments. Furthermore, the amount of misalignment showed a tendency to reduce with increasing flexion during the movement in rotational and anteroposterior misalignments. Since the applied flexion torque as well as forces and torques in the ILS joint increased with increasing flexion, it is indicated that the setup of ILS and orthosis was forced into a more aligned position. This can be attributed to (1) the compliance of orthosis frame and cuffs; (2) the compliance of the soft tissue; and/or (3) slipping of the orthosis cuffs. While this reduction of misalignment was reversed for the most part during extension, a small amount of misalignment reduction occurring in the first flexion/extension cycle was irreversible, specifically with large misalignments. This indicates that at least some of the misalignment reduction can be attributed to slipping or unreversed deformation of soft tissue, which can cause soft tissue injuries upon prolonged or repeated use. In future research, the behavior of the amount of misalignment over time could be further analyzed as it might be an additional indicator for increased load caused by increased misalignment. The exact effects of misalignments at a soft tissue level were not the focus of this study. They should however be investigated in future studies to increase the understanding of misalignments as a hazard in exoskeleton use. Furthermore, the observed levels of forces and torques should be related to comfort and safety of the user, providing robot developers with important knowledge on risks and potential mitigation strategies.

There are some limitations to the setup used in this study. The weight of the ILS (4.2 kg) is clearly lower than a human leg's weight, which is approximately 16% of the total body weight [209]. However, for the force and torque measurements during swing, only the weight of the lower leg segment is of relevance which, due to the circular weight at its distal end, accounts for most of the ILS weight with 3.3 kg. This would approximately correspond to the weight of the shank and foot of a person weighing 57 kg, although the weight distribution is not realistic as the major part of the weight is placed at the distal end of the ILS [209]. The weight in connection to the procedure used for adjusting the alignment might have caused additional limitations. Force in proximal/distal direction did not show clear trends linked to rotational or anteroposterior translational misalignments and showed a remarkable variation in starting values of each trial. Those starting values might have been influenced by a pre-tensioning effect caused by the amount of force with which the lower leg was pushed upwards by the experimenter during performing misalignment adjustments. A higher or lower starting value might further influence the analyzed peak values of F_z . These effects could be reduced in future experiments by trying to support the lower ILS weight in the same way during each adjustment. Moreover, the upper end of the upper leg rod and the upper orthosis segment were fixed to mimic a situation in which both the subject's hip joint and the upper orthosis segment remain in one position and to avoid slipping down of the ILS. In a realistic situation however, the exoskeleton and its wearer would either move through the room or the exoskeleton would be fixed at hip level, such as in a stationary robotic gait trainer, which would enable the human leg segments and the knee joint to move in the room. Weight effects are therefore not accurately reconstructed. In addition to that, we are simulating the situation during swing and are not considering a weight bearing situation, which would increase the forces on the musculoskeletal system considerably, especially during sit-to-stand movements [210]. This is supported by a report of a tibia fracture in exoskeleton use which occurred during sit-to-stand motion after an unexpected shutdown that likely caused a misalignment [103]. Those limitations however had to be accepted for the sake of practical feasibility of the setup.

Another aspect of the ILS, which is only a very limited and simple simulation of a real leg, is the soft tissue. We used a polyether foam rubber cylinder SG 40 which mimics the softness and friction of human tissue to some extent but we did not perform any tests to assess how well the real situation can be approached using this material. Also the cylindrical shape is a very simplistic approach of recreating the shape of a human leg, however often used as a representation of human body segments, including in technical standards [147]. The effect of the soft tissue characteristics on the outcomes is unknown. However, the reduction of misalignment magnitude during ILS flexion suggests some soft tissue compliance effects and the hysteresis observed in loads might be a sign for soft tissue compression [211]. It would therefore be interesting to explore other approaches for mimicking soft tissue, such as those suggested in literature and standardization [52], [71], [176], to better understand the effect of different soft tissue characteristics. In addition to that, the joint that was used for simulating the human knee is a simple hinge with a centered axis of rotation, which does not reproduce the translation of the axis of rotation or the tibiofemoral rotation characterizing an anatomical knee joint [104], [212]. Micro-misalignments caused by the kinematic mismatch between anatomical joint and exoskeleton joint can therefore not be assessed using the current setup. For example, the external rotation of the tibia with respect to the femur accompanying the final 20 degrees of extension in a human knee [212] would lead to a more pronounced misalignment with an external rotational misalignment and thereby to stronger effects on the load. In the present study, the load increase within the first 20 degrees of flexion was low. However, in a weight bearing situation those effects might be more pronounced. Furthermore, the current setup does not allow quantifying the strap pressure which might in theory have an effect on the behavior and resulting forces and torques. Specifically in translational misalignment trials, where the straps had to be re-attached after each adjustment, the varying and non-standardized strap pressures could be a concern. However, a comparison of rotational misalignment effects with very tight and loosened straps resulted in no clear differences. Assuming that the effect of varying strap pressures would also be negligible in other misalignment conditions, we can have increased confidence that the required re-attachment of straps did not affect the results in the translational misalignment trials. Therefore, despite the discussed limitations of the set-up itself, these factors should not affect analysis of the differences between different misalignments. They do, however, hinder generalization of the results to real-life situations in terms of absolute forces/torques.

Other limitations are connected to the use of a passive orthosis instead of an active exoskeleton. The orthosis used in this study is a passive knee brace commonly used for providing stability after knee joint ligament injuries. Its exact kinematics and stiffness might differ from the behavior of exoskeletons which affects the generalizability of the results. The same amounts and directions of misalignments might lead to different changes in joint load when other devices are considered, due to variations in joint kinematics and compliance [203]. As each exoskeleton design and mechanical properties vary per device, a degree of uncertainty will remain. We replaced the actuation of an exoskeleton with a pulling force exerted on the lower orthosis segment by an experimenter. This is a simple and effective method of mimicking exoskeleton actuation but it underlies some uncertainties and variations. We observed a reduced maximum flexion with increased rotational misalignment against unchanged maximum flexion torque at the orthosis joint. The same flexion torque was therefore reached at lower flexion angles with higher misalignments. The experimenter likely felt the resistance and did not pull harder to reach the same flexion angle but instead kept the maximum pulling force relatively constant. Forcing the same flexion angle in all conditions would better mimic the behavior of an exoskeleton with trajectory

control and might have led to higher absolute peak forces and torques. A standardization of the peak flexion angle using an electro-goniometer or a static indicator for the desired lower leg position could be considered for future research. However, such an approach might cause breakage of certain setup parts and the current approach, while more subjective and prone to variation, might mimic the torque control of an actuated exoskeleton. Another limitation is connected to the calculation of misalignment magnitudes. As the resting state before the first flexion was used to obtain the misalignment values per trial and misalignment was often irreversibly reduced during the first flexion/extension cycle, the amount of misalignment might better be calculated based on the situation after a few flexions or at the end of a trial. It is however relevant to note that this reduction in misalignment takes place, suggesting that injuries might occur in the very first step as either the biological structures are forced to move in unnatural directions or the cuffs of the exoskeleton slip on the skin. In addition to that, we noticed slight misalignments in the directions not targeted for misalignment. For example, when the anteroposterior position of the ILS joint was not supposed to be misaligned and was intended to be kept at 0 mm, it did show an anterior translation of 4.8 mm on average with a standard deviation of 2.6 mm. Those small misalignments in other directions than the direction analyzed in the respective trials can affect the outcomes. They were however small compared to the target misalignments and a perfect alignment is unlikely to be achieved in any exoskeleton use situation.

Those limitations in the setup and procedure might reduce the reliability of the absolute values of joint forces and torques measured in this setup, as an anatomical leg might behave differently and damping of forces and torques through soft tissue might not be perfectly mimicked. A potential solution is to improve the ILS setup by adding a different type of soft tissue, which has documented characteristics resembling human soft tissue [147], [175]. However, despite these limitations, the current study does show the relative effect of different amounts of misalignment on joint forces and torques, supporting the hypothesis that translational and rotational misalignments increase the load on the knee joint.

Despite these limitations, present findings are a first step towards understanding the effects of misalignments on the musculoskeletal system. We showed that misalignments of a lower leg exoskeleton can lead to a manifold increase of internal knee forces and torques compared to those experienced in a well-aligned situation. This is supporting the need for carefully considering hazards associated with not only translational but also rotational misalignments during wearable robot development and use. To support robot developers in validation of this and other safety aspects, the European project COVR provides procedures for validation tests in an online Toolkit (www.safearoundrobots.com) [213], [214]. Future research can increase this knowledge by investigating more conditions and exploring options to develop improved limb simulators. A setup that can measure effects of misalignments in a weight bearing situation would increase the impact of the results. Furthermore, the knowledge base should be extended by investigating effects of misalignment on soft tissue level and by relating the observed effects to comfort and safety in real human subjects.

CONCLUSION

The present work assessed the effects of different amounts of rotational and translational misalignments during exoskeleton use on musculoskeletal forces using a novel ILS and a manually actuated orthosis. To our knowledge this is the first study showing the relative effect of different amounts and directions of misalignment on joint forces and torques. We found that knee joint forces and torques increase in various directions when a misalignment is introduced. In general, we saw an increasing load on the knee joint with increasing misalignment. Specifically, larger internal rotation of the ILS knee joint with respect to the orthosis joint led to higher forces in medial direction in the knee joint as well as higher adduction, flexion and external rotation torques. Stronger external rotation of the ILS knee joint with respect to the orthosis joint led in turn to higher lateral joint forces as well as higher abduction, flexion and internal rotation torques. Stronger posterior translation of the ILS joint with respect to the orthosis joint led to higher lateral knee forces as well as higher abduction and flexion torques while stronger anterior translation of the ILS joint with respect to the orthosis joint led to higher medial knee forces as well as higher abduction and extension torques. Stronger distal translation of the ILS joint with respect to the orthosis joint led to higher posterior and compression forces while proximal translation of the ILS joint tended to lead to increased posterior and tensile forces. These findings show that all types of misalignment, including rotational misalignment, should be considered specifically when designing and applying exoskeletons for rehabilitation, assistance or augmentation of human functioning. Future research should focus on improved dummy limbs, testing with actuated exoskeletons and testing the weight bearing situation, as well as on the potential effects of increased loads, to create a knowledge base on the effects of exoskeleton misalignments.

ANNEX

See Table 5.6.

Table 5.6 | Description of used marker set.

Marker name	Placement description
FTx	FT sensor on top rim front (marks positive x-direction)
FTConn*	FT sensor on top of connector block
FTBlat	FT sensor on top rim lateral-back side (relative to orthosis lateral/medial definition)
FTBack	FT sensor on top rim mid back
FTFL*	FT sensor on top rim front lateral (relative to orthosis lateral/medial definition)
FTFM	FT sensor on top rim front medial (relative to orthosis lateral/medial definition)
AxisLat	Lateral point physical axis leg joint
AxisMed	Medial point physical axis leg joint
ULTop*	Top marker on upper leg - frame mounting connector
ULFront	Front marker on upper leg - frame mounting connector
ULBack	Back marker on upper leg - frame mounting connector
LowerLegBack*	Marker at mid back of circular weight
LowerLegLat	Marker at most lateral position of circular weight
LowerLegMed	Marker at most medial position of circular weight
XULLFrame	Orthosis UpperLeg lateral location on frame fixation point
XULMFrame	Orthosis UpperLeg medial location on frame fixation point
XULM1*	Upper marker placed on medial upper orthosis frame
XULM2	Middle marker placed on medial upper orthosis frame
XULMJoint	Marker at the upper part of the medial joint plate of the orthosis
XULL1*	Upper marker placed on lateral orthosis frame
XULL2	Middle marker placed on lateral orthosis frame
XULLJoint	Marker at the upper part of the lateral joint plate of the orthosis
XLLMJoint	Marker at the lower part of the medial joint plate of the orthosis
XLLM1*	Middle marker placed on medial lower orthosis frame
XLLM2	Lower marker placed on medial lower orthosis frame
XLLLJoint	Marker at the lower part of the lateral joint plate of the orthosis
XLLL1*	Middle marker placed on lateral lower orthosis frame
XLLL2	Lower marker placed on lateral lower orthosis frame
XLLRopeAttachment	Mid back marker on lower strap of lower leg part orthosis, where rope is attached
1D_ForceSensor1	Proximal (to leg) top point on sensor
1D_ForceSensor2	Distal top point on sensor
1D_ForceSensor3	Proximal bottom point on sensor
1D_ForceSensor4	Distal bottom point on sensor

Markers marked with an asterisk were not used for the calculations in this article but were placed for potential reconstruction of missing markers and further analysis. Markers FTFM, FTBack, FTBlat and FTx define the FT sensor segment, AxisMed, AxisLat, ULFront and ULBack define the upper ILS segment, AxisMed, AxisLat, LowerLegMed and LowerLegLat define the lower ILS segment, XULMJoint, XULLJoint, XULM2 and XULL2 define the upper orthosis segment, XULMJoint, XULLJoint, XLLM2 and XLLL2 define the lower orthosis segment, and XLLRopeAttachment, 1D_ForceSensor1, 1D_ForceSensor2, 1D_ForceSensor3 and 1D_ForceSensor4 define the tensile force sensor segment.

Background: Misalignments are a common safety concern in exoskeletons. The mismatch between exoskeleton joint axis and human joint axis can potentially lead to hazardous forces applied to the musculoskeletal system. It is not yet known to which extent soft tissue characteristics affect the joint load in misalignment situations. The aim of this study was to investigate the influence of different artificial soft tissues on the effects of misalignments on the joint load.

Methods: We measured knee joint load during swing in different misalignment situations, using an instrumented leg simulator. Rotational misalignments around the vertical axis and translational misalignments in proximal/distal direction were applied between the instrumented leg simulator and a passive knee brace being manually flexed to simulate exoskeleton use. The experiments were repeated with four different artificial soft tissues of varying hardness attached to the rigid skeleton of the instrumented leg simulator.

Results: Knee joint forces and torques in several directions increased significantly with increasing misalignments in each of the materials. The change of peak joint load over amount of misalignment differed significantly between artificial soft tissues. Overall, we found a tendency for stronger increase of peak joint load with increasing misalignments in harder artificial soft tissues, specifically in mediolateral force, ab-/adduction torque and flexion torque.

Conclusions: Increasing rotational and translational misalignments lead to increasing joint loads during swing. Changes in joint load induced by misalignments are significantly affected by the characteristics of soft tissue. In harder soft tissues, the increase in joint load is stronger than in softer artificial soft tissues.

Chapter 6

Soft tissue characteristics affect the relation between leg-exoskeleton misalignments and knee joint loads in a dummy leg



INTRODUCTION

Exoskeletons are wearable devices acting in parallel with the human body to support movement. They usually consist of rigid or semi-rigid segments connected through joints and are attached to the human limbs using cuffs and straps. Exoskeletons can be used as training devices in rehabilitation, compensate for impairments in activities of daily living, or support humans in physically demanding tasks, for instance in industrial environments [50], [115], [133], [215]. Ensuring safety in exoskeleton use is crucial as they are closely interacting with humans, and often with particularly vulnerable patients. It is therefore very important to understand hazards in order to improve exoskeleton technologies and deploy them safely [202].

One of the aspects relevant for safe use of exoskeletons is misalignment [101], [131], [137], [203]. A misalignment is a kinematic mismatch between the exoskeleton and the human anatomy. The center or axis of rotation of the exoskeleton is not in the same position as the center or axis of rotation of the anatomical joint. In a misaligned situation, the forces and torques applied to the human body are not applied as intended as the exoskeleton is forcing a movement around an axis which is not congruent with the anatomical joint axis of the wearer. Therefore, misalignments can cause excessive joint loads. Moreover, misalignments can lead to excessive forces at the cuff-skin interface when a translation or rotation of the exoskeleton joint axis leads to the system pushing and pulling at the cuff site. Potential causes for misalignments include limited degrees of freedom (DOF), improper fit and wrong positioning of the exoskeleton. The DOF in exoskeletons are commonly limited compared to the human anatomy. This can include exoskeleton joints that do not allow for hip ab-/adduction or for the rolling motion of a human knee joint. This is often unavoidable as anatomic joints are complex and their mechanics are not perfectly replicated by exoskeleton joints. Self-aligning mechanisms can be a solution for this, however, they can lead to a limitation in joint mobility and increased robot inertia [131], [204], [205], [216]. Misalignments resulting of a limitation in DOF are often small and might only be present in certain ranges of motion. Misalignments resulting of improper fit, such as incorrect segment lengths, can occur when the exoskeleton is not correctly adjusted or not sufficiently adjustable to the wearer. Incorrect positioning can be a problem when users don the exoskeleton without proper training or supervision. Unexpected movements can also cause the exoskeleton to change its position [103].

Some studies state that misalignments can lead to excessive interaction forces and cause discomfort [101], [203]. Although this seems obvious, literature confirming this assumption and generating knowledge on the exact effects of misalignments on physical human-robot interaction (pHRI) is scarce. As it is almost impossible to assess those effects *in vivo* for ethical as well as practical reasons, dummies mimicking the behavior of humans can be a useful tool for research as well as safety tests. There are however limitations in their ability to simulate real human limb behavior. One study measured the forces at the lower leg cuff site of an exoskeleton using a dummy leg and found a change in forces when there was a misalignment as well as a compensatory twist of the cuff in the case of rotational misalignments [104]. Similarly, a study investigating the optimal position for the rotation axis of an ankle stretching device found the lowest forces at the interface between the device and the forefoot of the participants in the best aligned setting [217]. Another study investigated the effects of knee joint misalignments on exoskeleton gait in transparent mode and found that misalignment had no significant effect on gait in healthy participants, the participants did not report discomfort but the net

forces and torques at the thigh cuff were higher in the misaligned scenario. They further stated that an excessively long exoskeleton thigh has less negative effect than an excessively short exoskeleton thigh [131]. Those studies confirm that misalignments cause increased forces at the interface between cuffs and exoskeleton. However, little is known about the effects of misalignments on the joint load. As a first step to generate knowledge on these effects, we assessed them in a previous study using an instrumented leg simulator (ILS), or dummy leg, and found that the amount of misalignment had a significant effect on several directions of knee joint load in the ILS [218]. The ILS used for those experiments consisted of a rigid 'skeleton' composed of two aluminum rods, a hinge joint and a 6 DOF force and torque (FT) sensor, and a layer of artificial soft tissue. For the artificial soft tissue, we had chosen a hollow polyether foam rubber cylinder. This was a first approximation for mimicking soft tissue as said material was readily available, could easily be fit around the aluminum tubes, and its softness mimicked the behavior of soft tissue to some extent. We discussed that other materials can be used to generate more comprehensive knowledge on misalignment effects, since it is not yet known to which extent the choice of artificial soft tissue influences the measured joint load. Such knowledge can not only help understand how variations in soft tissue characteristics between exoskeleton users affect the risk of misalignment-related injuries, but also advance the development of suitable test methods for performing safety validation tests related to exoskeleton misalignment. Scientific literature and standardization documents suggest the use of Hitohada gel in combination with adhesive tape and wound dressing material for mimicking human soft tissue, since it has shown to have a viscoelasticity and friction comparable to that of skin [77], [191], [219], [220]. Manufacturing this artificial soft tissue requires some time and effort as the gel has to be prepared by mixing the resin and pouring it into a mold for hardening. The resulting material is quite sticky and squishy and has to be wrapped around the rigid parts of the dummy after adding an outer layer of double-sided tape and wound dressing. If other, less cumbersome, materials yield the same results, those might be preferred by exoskeleton developers and manufacturers wishing to test the safety of their device. Furthermore, it is not yet known to which extent the hardness of the (artificial) soft tissue influences the effects of misalignments on joint loads. It is important to investigate those effects, since amount and composition of soft tissue can vary significantly between individuals and also between body parts which means that the risk connected to misalignments might also vary between individuals and body parts if the soft tissue affects the joint load. Previous research has shown that the artificial soft tissue based on Hitohada gel is harder than human soft tissues at the anterior and posterior thigh and softer than the those at the lateral thigh [175].

The aim of this study is to investigate the influence of four different artificial soft tissues on the effects of misalignments on the joint load. This can help understand how inter- and intraindividual differences in amount and softness of soft tissue can affect the risk connected to exoskeleton misalignments. In addition to this, we can find out whether the choice of artificial soft tissue in a dummy affects the outcomes in safety testing misalignment effects. If this is not the case, simple and readily available materials might be used instead of complex dummy tissues. We hypothesized that the joint forces and torques increase more with increasing misalignment when using a harder artificial soft tissue, and increase less with increasing misalignment when using a softer artificial soft tissue. We investigated those effects using four different artificial soft tissues in a range of misalignment scenarios: Two readily available foams varying in hardness and two complex dummy skins based on gel materials, one of which was the suggested Hitohada gel. The foams were softer than the Hitohada gel and the second

gel material was harder than the Hitohada gel, to cover a wide yet realistic hardness range [221].

METHODS

A series of experiments has been executed with an ILS and a passive knee brace in a range of (mis-)alignments and using four different materials as artificial soft tissue. The apparatus and procedures are described in more detail in the following sections. A subset of the data (hard foam) has already been analyzed for a previous publication [218].

Apparatus

The apparatus (Figure 6.1) has been described in detail in [218]. It consists of two aluminum rods connected through a hinge joint mimicking the skeleton of the upper and lower leg, and a layer of artificial soft tissue. It is instrumented using a 6 DOF FT sensor positioned between the distal end of the upper leg rod and the proximal end of the knee hinge. A circular weight of 2 kg attached to the distal end is used to realize a weight close to a human lower leg weight.

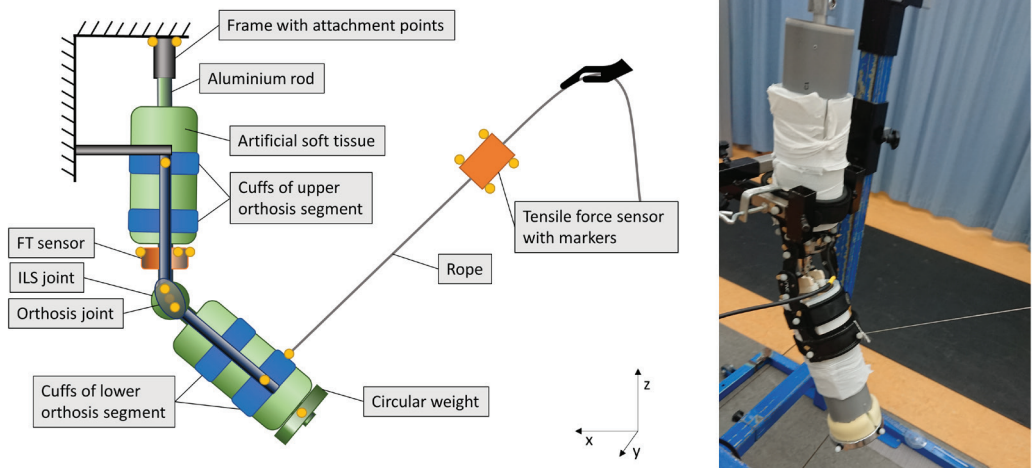


Figure 6.1| Schematic drawing and photo of the setup. In the schematic drawing, the ILS is shown in green, the orthosis in blue, the frame in black, the sensors in orange and the reflective markers for motion tracking in yellow.

The rigid part of the ILS was used in combination with four different types of artificial soft tissues (Figure 6.2) to compare their effects on the joint load in different misalignment scenarios:

- Soft foam: A hollow foam rubber cylinder SG 25 with an inner diameter of 25 mm and an outer diameter of 130 mm (Joan's Comfortschuim BV, IJmuiden, the Netherlands), directly attached to the aluminum rods using hook & loop fasteners.
- Hard foam: A hollow foam rubber cylinder SG 40 with an inner diameter of 25 mm and an outer diameter of 130 mm (Joan's Comfortschuim BV, IJmuiden, the Netherlands), directly attached to the aluminum rods using hook & loop fasteners.

- Hitohada: A urethane gel material with Asker C hardness of 0 (EXSEAL Co. Ltd., Gifu, Japan) molded into rectangular sheets of about 10 mm thickness wrapped around a PVC drain pipe of 130 mm diameter which is fit around the aluminum rod. The outside of the Hitohada gel was covered by double-sided adhesive tape which was then covered using gauze bandage.
- Ecoflex: A silicone material with Shore 00 hardness of 30 (Smooth-On, Inc., Macungie, PA, USA) molded into rectangular sheets of about 10 mm thickness wrapped around a PVC drain pipe of 130 mm diameter which is fit around the aluminum rod. The outside of the Ecoflex silicone was covered by double-sided adhesive tape which was then covered using gauze bandage.

Since hardness information was not available on a unified scale and the available measures of SG, Asker C hardness and Shore 00 hardness cannot be compared, we compared the hardness of each foam through measurements. We applied pre-defined normal forces through a surface of 36 cm² and measured the displacement of the compression. The total ILS weight was between 4.2 and 7.0 kg depending on the artificial soft tissue with 3.0 kg (soft foam), 3.3 kg (hard foam), 3.9 kg (Hitohada) and 3.7 kg (Ecoflex) accounting for the lower ILS segment.

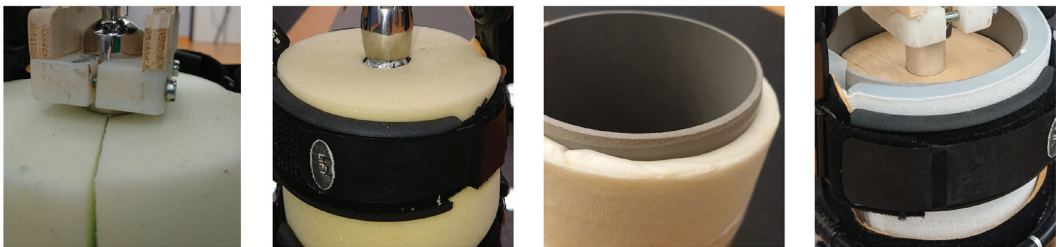


Figure 6.2| The four types of artificial soft tissue. From left to right: soft foam, hard foam, Hitohada, Ecoflex.

As documented in [218], we used a passive knee brace (A. C. lite by DonJoy, DJO, LLC, Lewisville, Texas, USA) to mimic exoskeleton use in a simple way. It was manually actuated through a string attached to the distal posterior end of the orthosis and the pulling force was recorded using a tensile force sensor. Both the proximal end of the ILS and the upper orthosis segment were mounted in a steel frame to keep them in place and support the weight. As the ILS is symmetrical and the orthosis used is designed for the left leg, we are considering the ILS to be representing a left leg.

Procedure

We measured the ILS joint load during flexion/extension cycles mimicking the swing phase. An experimenter pulled on the string attached to the distal end of the orthosis to generate a flexion torque. The extension was achieved through the weight of the ILS. Each trial consisted of at least ten flexion/extension cycles. We used a marker-based optoelectronic tracking system (Vicon, Oxford, UK) to record the kinematics of the apparatus. The detailed information about marker placement can be found in [218]. Based on the experience from those previous experiments, the misalignment settings were again achieved through manual adjustments of the ILS position within the orthosis or through a rotation of the ILS joint based on visual assessment. The two investigated directions of misalignment (Figure 6.3) in the present set of experiments were:

- Rotational misalignment: A rotation of the knee flexion axis with respect to the orthosis flexion axis around the vertical (z-) axis. An alignment angle of zero represents a perfect rotational alignment of the two flexion axes, negative values correspond to an internal rotation of the ILS knee joint with respect to the knee brace joint and positive values correspond to an external rotation of the ILS knee joint with respect to the knee brace joint. We aimed for misalignments in a range of +/- 20 deg in steps of about 5 deg. From the user perspective, negative rotational misalignment values would correspond to an external rotation and positive values to an internal rotation of the brace.
- Translational misalignment: A vertical displacement of the ILS (in z-direction). Negative values correspond to the ILS joint being translated distally with respect to the knee brace axis and positive values correspond to the ILS joint being translated proximally with respect to the knee brace axis. We aimed for misalignments in a range of +/- 20 mm in steps of 5 mm. From the user perspective, negative translational misalignment values would correspond to proximal and positive values to a distal translation of the brace.

For consistency, the alignments will be referred to from the device perspective in the remainder of this article. Therefore, the terms internal/external rotation and proximal/distal translation can be interpreted as internal/external rotation of the ILS joint with respect to the orthosis joint axis and proximal/distal translation of the ILS joint with respect to the orthosis joint axis respectively.

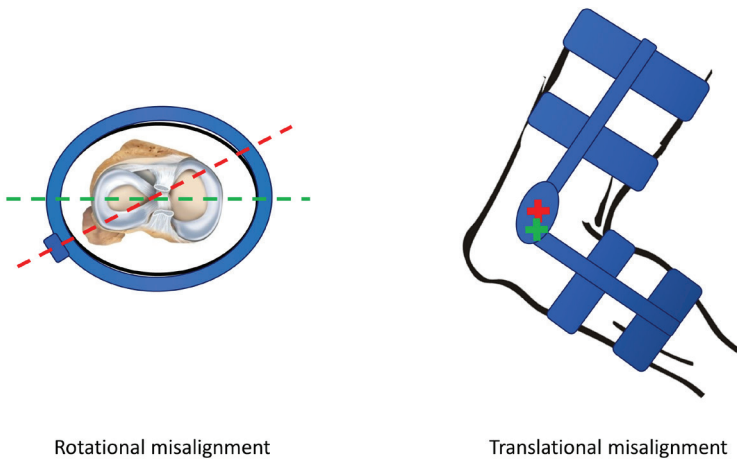


Figure 6.3| Visualization of the two investigated directions of misalignment, where the red dashed line and cross represent the orthosis center of rotation and the green dashed line and cross represent the leg center of rotation. The left sketch shows an internal rotational misalignment of the leg with respect to the orthosis and the right sketch shows a distal translational misalignment of the leg with respect to the orthosis.

Data processing and analysis

The marker data was used to calculate ILS joint angle and amount of misalignment. The joint load in the knee was calculated based on the FT sensor data and the distance between ILS joint and sensor location as described in [218]. Overall, the processing and analysis of data per soft tissue configuration was achieved in the same way as described in [218] with a few exceptions. The misalignment value for

each trial was extracted using the mean of the last second (last 100 frames) instead of the beginning of the trial. This was due to our observation in previous experiments that the misalignment can change considerably during the first flexion. For the same reason, more than ten repetitions per trial were recorded in trials with strong misalignments and only means of the last ten repetitions were used for statistical analysis of peak joint load. The perpendicular pulling force and actuation torque were calculated using the pulling force measured by the tensile force sensor, the angle between the force vector and the lower ILS segment and the distance between the rope attachment point and the brace joint as explained in [218]. The peak joint load per flexion-extension cycle was extracted by first finding the peaks of the actuation torque and then extracting the forces and torques in all directions at those indices (Figure 6.4). To correct for variations in pulling force applied to the system by the experimenter, the peak joint forces were then normalized to the peak perpendicular pulling force and the peak joint torques were normalized to the peak actuation torque. The normalization was achieved by dividing the joint forces and torques at peak actuation torque by the perpendicular pulling force and actuation torque respectively. To obtain an indication of the actual variation in pulling force and resulting actuation torque as well as the magnitudes of non-normalized joint forces and torques, the means and standard deviations of the actuation torque per artificial soft tissue and type of misalignment were calculated.

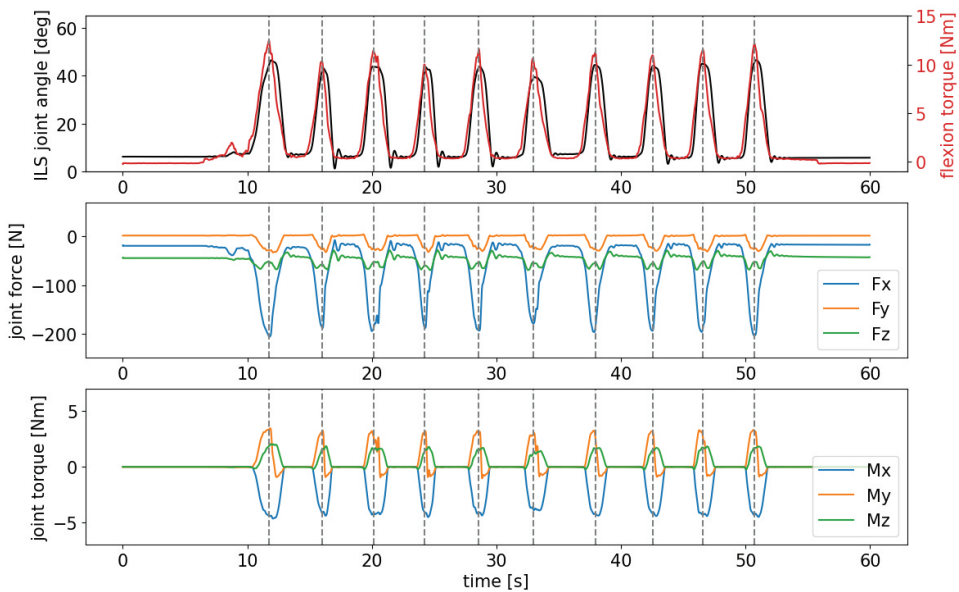


Figure 6.4 ILS joint angle, actuation torque and joint loads in an example trial (Hitohada, -10 deg rotational misalignment). The top graph shows the flexion angle of the ILS joint where 0 deg is full extension (black) and the actuation torque, i.e. flexion torque generated through the pulling force applied to the orthosis (red). The middle graph shows the forces in the ILS joint where positive Fx is forward directed force, positive Fy is medial to lateral directed force and positive Fz is compressive force. The bottom graph shows the torques in the ILS joint where positive Mx is abduction torque, positive My is flexion torque and positive Mz is external rotation torque. The vertical dashed lines indicate the indices of peak actuation torque which were used to extract peak joint forces and torques for statistical analyses. Note that these graphs show the original joint forces and torques in N and Nm respectively before normalization.

Multiple linear regression models were estimated for the means of normalized peak joint forces and torques (outcome variables) in all directions of those ten repetitions using ordinary least squares. The artificial soft tissue type was used as categorical predictor and amount of misalignment was used as continuous predictor. We analyzed the main effects of tissue type and the interaction effects between misalignment and tissue type. The presence of a main effect of tissue type means that the peak joint load in a particular tissue type at perfect alignment is different from zero. Significant differences of main effects between tissue types mean that the peak joint load at perfect alignment is different between tissue types, i.e., the intercepts of the regression lines differ. The presence of an interaction effect means that, for a particular tissue type, the peak joint load changes with increasing misalignments. Significant differences between interaction effects comparing different tissue types mean that the change in peak joint load with increasing misalignments is different between those tissue types, i.e., the slopes of the regression lines differ. A significance level of 0.05 was employed for detecting significant main effects of the tissue as well as interaction effects between the tissue and amount of misalignment. Where the relationship between amount of misalignment and joint load was non-linear based on visual inspection, we chose a second order polynomial for the model fit. Otherwise, linear fits were chosen. If one of the predictors did not have a significant effect on the model, the respective predictor was removed from the regression analysis.

RESULTS

The results of the hardness measurements are shown in Figure 6.5. Soft foam compressed fastest over the range of normal stress, followed by hard foam. Hitohada and Ecoflex showed a slower increase in compression and lower compressions overall.

We recorded and analyzed a total of 125 rotational misalignment trials and 107 translational misalignment trials across the four different artificial soft tissue conditions. Table 6.1 shows the means and standard deviations of the actuation torque to which the joint torques were normalized. The joint forces were normalized to the orthogonal pulling force which can be calculated from the torques by dividing them by the lever arm of 0.14 m. The results of the analyses of joint loads are presented in the following sections. Note that $F_{x_{peak}}$, $F_{y_{peak}}$ and $F_{z_{peak}}$ refer to the peaks of the unitless normalized joint forces and $M_{x_{peak}}$, $M_{y_{peak}}$ and $M_{z_{peak}}$ refer to the mean peaks per trial of the unitless normalized joint torques.

Table 6.1| Mean and standard deviation of flexion torque applied by the experimenter to the knee brace in each of the artificial soft tissue conditions in rotational misalignment (rot. MA) and translational misalignment (transl. MA) trials.

Artificial soft tissue	Mean and standard deviation (M (SD)) of actuation torque in rot. MA (Nm)	Mean and standard deviation (M (SD)) of actuation torque in transl. MA (Nm)
Soft foam	9.69 (0.77)	10.07 (0.37)
Hard foam	10.63 (0.81)	10.06 (0.50)
Hitohada	10.73 (0.63)	10.64 (0.54)
Ecoflex	12.34 (0.95)	12.03 (0.49)

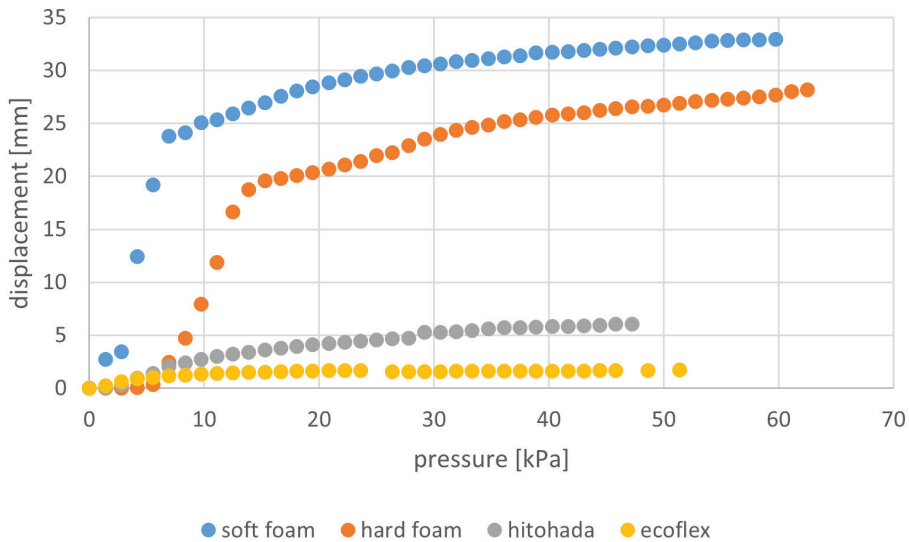


Figure 6.5| Results of hardness measurements for artificial soft tissue materials, presented as displacement over normal stress.

Effects of rotational misalignment on peak joint forces and torques

We found a fit for each of the directions of forces and torques in the rotational misalignment data with all adjusted $R^2 > 0.9$ and all p-values of the F-statistic < 0.01 . (Table 6.2, Figure 6.6). For $F_{x_{peak}}$ a second degree regression equation with significant main effects and significant interaction effects for all tissues was found. Increased amount of misalignment in both directions led to increased negative $F_{x_{peak}}$, i.e. stronger backwards directed joint force. The main effects were significantly different between each of the tissues while the interaction effect did not differ significantly between tissues. At perfect alignment, $F_{x_{peak}}$ is significantly lower than zero in all tissues and the absolute force is affected by the tissue such that it can be ordered from lowest to highest (soft foam, hard foam, Hitohada, Ecoflex). The regression analysis for $F_{y_{peak}}$ resulted in a linear relationship with generally speaking increasing negative (lateral to medial) $F_{y_{peak}}$ with increasing negative rotational misalignments and increasing positive (medial to lateral) $F_{y_{peak}}$ with increasing positive rotational misalignments. For the main effects of the soft tissues we found significant effects for all tissues and significant differences between all tissues except for soft foam vs. Hitohada. The interaction effect was also significant for all soft tissues and the slope for soft foam was significantly lower than all other tissues' slopes. The model for $F_{z_{peak}}$ consists of regression lines with significant main effects being significantly different between tissues and significant positive interaction effects for soft foam, Hitohada and Ecoflex. There are significant differences between all slopes except for the comparison of hard foam and Hitohada.

The scatter plot for $M_{x_{peak}}$ shows negative (adduction) torques in trials with internal rotational misalignment and positive (abduction) torques in trials with external rotational misalignments. The corresponding model revealed significant main and interaction effects for all tissues as well as a significant difference in main effects in all comparisons except for soft foam vs. hard foam and a significant difference in interaction effects in all comparisons except for Hitohada vs. Ecoflex. The increase of absolute peak torques with increasing misalignments is stronger in Hitohada and Ecoflex

than it is in hard foam which in turn shows a stronger increase than soft foam. The regression analysis for My_{peak} resulted in second degree polynomial regression equations with no main effects. The interaction effects were all significant and all significantly different from each other with Ecoflex showing the steepest curve, followed by Hitohada, hard foam and soft foam, in that order. Increasing amount of rotational misalignment led to increased peak flexion torques, irrespective of the direction of rotational misalignment. The model for Mz_{peak} describes linear relationships between rotational misalignment and Mz_{peak} with stronger internal rotation leading to increased positive Mz_{peak} (external rotation torque) and stronger external rotation leading to increased negative Mz_{peak} (internal rotation torque).

Table 6.2| Results of the regression analyses for rotational misalignment. P-values <0.05 are printed in bold. Note that there are no p-values for the main effect in My_{peak} since there were no significant main effects and the intercept was therefore removed from the model.

	Fx_{peak}	Fy_{peak}	Fz_{peak}	Mx_{peak}	My_{peak}	Mz_{peak}
Adj. R-squared	0.907	0.959	0.920	0.983	0.905	0.922
Df Model	7	7	7	7	4	7
Df Residuals	117	117	117	117	121	117
F-statistic	173.7	412.4	206.0	1004.0	300.4	210.7
P (F-statistic)	<0.001	<0.001	<0.001	<0.001	<0.001	<0.001
p-values main effect						
Soft foam	<0.001	<0.001	<0.001	0.019	n/a	0.772
Hard foam	<0.001	<0.001	<0.001	<0.001	n/a	0.036
Hitohada	<0.001	<0.001	<0.001	<0.001	n/a	0.880
Ecoflex	<0.001	<0.001	<0.001	<0.001	n/a	<0.001
Soft foam vs. hard foam	<0.001	<0.001	<0.001	0.067	n/a	0.067
Soft foam vs. Hitohada	<0.001	0.071	<0.001	<0.001	n/a	0.932
Soft foam vs. Ecoflex	<0.001	<0.001	<0.001	<0.001	n/a	<0.001
Hard foam vs. Hitohada	<0.001	<0.001	<0.001	0.001	n/a	0.089
Hard foam vs. Ecoflex	<0.001	<0.001	<0.001	<0.001	n/a	<0.001
Hitohada vs. Ecoflex	0.038	<0.001	<0.001	<0.001	n/a	<0.001
p-values interaction effect (for Fx_{peak} and My_{peak} this refers to the interaction effect between MA^2 and tissue)						
MA x soft foam	<0.001	<0.001	0.015	<0.001	<0.001	<0.001
MA x hard foam	<0.001	<0.001	0.321	<0.001	<0.001	<0.001
MA x Hitohada	<0.001	<0.001	0.007	<0.001	<0.001	<0.001
MA x Ecoflex	0.003	<0.001	<0.001	<0.001	<0.001	<0.001
Soft foam vs. hard foam	0.592	<0.001	0.026	<0.001	<0.001	<0.001
Soft foam vs. Hitohada	0.450	<0.001	<0.001	<0.001	<0.001	0.060
Soft foam vs. Ecoflex	0.465	<0.001	<0.001	<0.001	<0.001	0.341
Hard foam vs. Hitohada	0.260	0.085	0.396	<0.001	0.005	<0.001
Hard foam vs. Ecoflex	0.752	0.470	0.026	<0.001	<0.001	0.001
Hitohada vs. Ecoflex	0.241	0.345	<0.001	0.266	<0.001	0.012

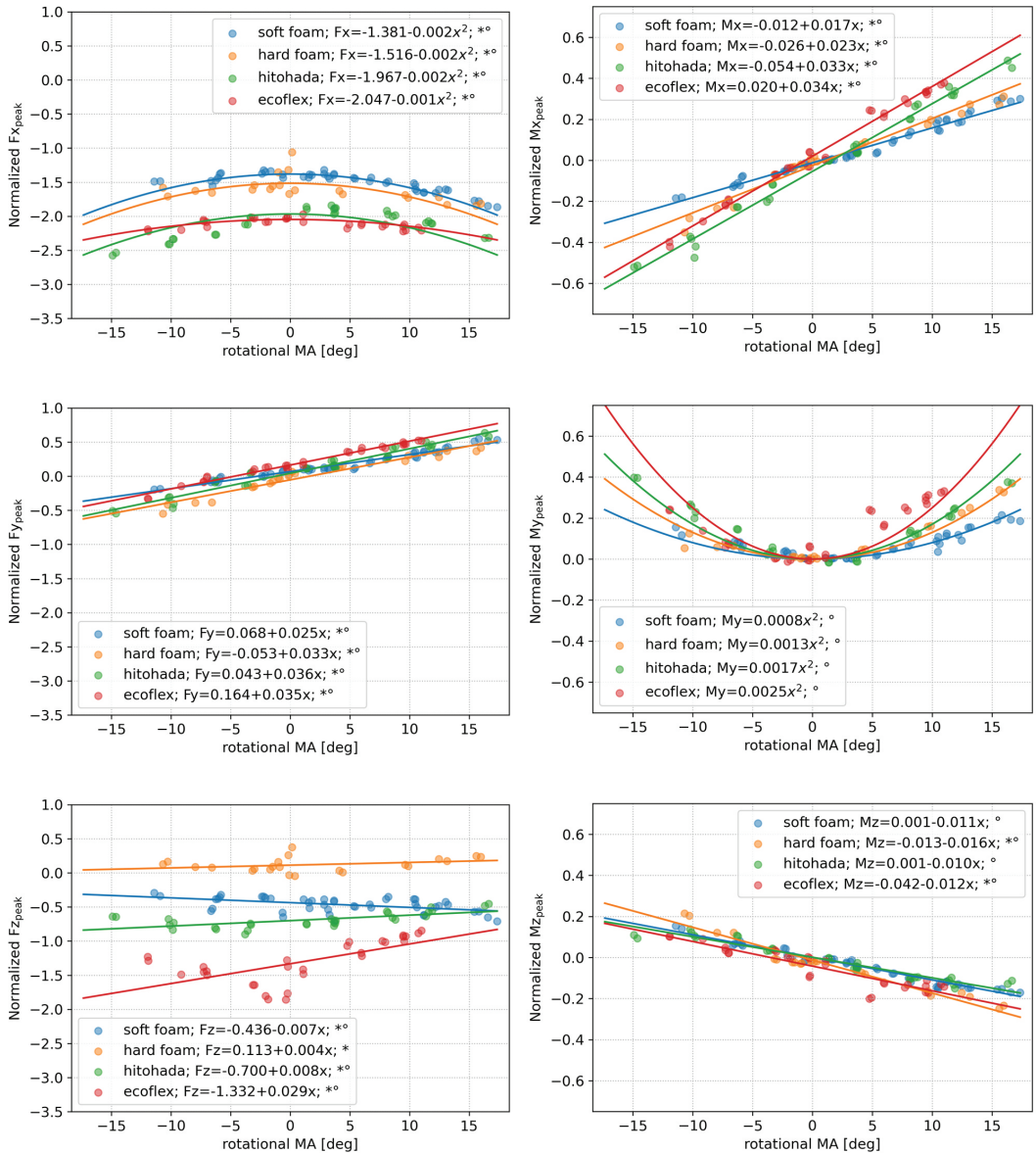


Figure 6.6) Scatter plots of the peak normalized joint forces and torques over the amount of rotational misalignment. The solid lines show the regression lines per artificial soft tissue of which the equations are shown in the legends. In the equations, x stands for the rotational misalignment in degrees, asterisks mark a significant main effect of the artificial soft tissue and circles mark a significant interaction effect of artificial soft tissue and amount of misalignment. Negative values of rotational misalignment are an internal rotation and positive values are an external rotation of the ILS joint with respect to the brace joint. Positive F_x is forward directed force, positive F_y is from medial to lateral directed force and positive F_z is compressive force. Positive M_x is abduction torque, positive M_y is flexion torque and positive M_z is external rotation torque.

Effects of translational misalignment on peak joint forces and torques

The regression analyses of translational misalignment data resulted in linear fits for all directions of forces and torques (all p-values of the F-statistic <0.01) with R^2 -values ranging from 0.727 to 0.965 (Table 6.3, Figure 6.7). For $F_{x_{peak}}$, a linear fit was found with increasing negative (backwards directed) force with increasing distal translational misalignment. The main effect was significant for each of the tissues and also significantly different between all tissues. The interaction effect between misalignment and tissue type was also significant for all tissues and significantly different in all combinations except for soft foam vs. hard foam. The peaks in F_y showed little variation with significant main effects of the linear models in soft foam, Hitohada and Ecoflex and a significant interaction effect in Hitohada. The main effects were significantly different in all combinations while the interaction effects differed significantly in Hitohada and soft foam, Hitohada and Ecoflex, as well as hard foam and Ecoflex. The linear model fits for $F_{z_{peak}}$ have significant main effects and interaction effects for all tissues. All combinations except for Hitohada vs. Ecoflex resulted in significant differences in the main effect. The interaction effect is significantly higher (i.e. smaller negative slope) for soft foam compared to all other tissues. In addition to that, the slope of Hitohada is significantly steeper than that of Ecoflex.

The linear model fits for $M_{x_{peak}}$ have significant main effects in soft foam, Hitohada and Ecoflex and small interaction effects, with Hitohada showing the only statistically significant interaction effect. All main effects are statistically different from one another while the only significant difference in interaction effects was found in the combination soft foam vs. Hitohada. In the model for $M_{y_{peak}}$, there were significant main effects for soft foam and Ecoflex and a significant interaction effect for hard foam. There were significant differences in main effects between soft foam and all other tissues as well as between Ecoflex and all other tissues. Interaction effects showed significant differences between soft foam and hard foam, between hard foam and Hitohada as well as between Hitohada and Ecoflex. For $M_{z_{peak}}$, the main effects were significant for each of the tissues, with peak torques being different in each pair of tissues. Significant interaction effects were found for soft foam, Hitohada and Ecoflex with significant differences in the comparisons soft foam vs. hard foam, soft foam vs. Ecoflex and Hitohada vs. Ecoflex.

Table 6.3 Results of the regression analyses for translational misalignment. P-values <0.05 are printed in bold.

	$F_{x_{peak}}$	$F_{y_{peak}}$	$F_{z_{peak}}$	$M_{x_{peak}}$	$M_{y_{peak}}$	$M_{z_{peak}}$
Adj. R-squared	0.902	0.777	0.965	0.727	0.757	0.809
Df Model	7	7	7	7	7	7
Df Residuals	99	99	99	99	99	99
F-statistic	140.8	53.64	414.9	41.41	48.06	64.97
P (F-statistic)	<0.001	<0.001	<0.001	<0.001	<0.001	<0.001
<i>p-values main effect</i>						
Soft foam	<0.001	<0.001	<0.001	<0.001	<0.001	<0.001
Hard foam	<0.001	0.793	<0.001	0.091	0.619	0.006
Hitohada	<0.001	<0.001	<0.001	<0.001	0.183	<0.001
Ecoflex	<0.001	<0.001	<0.001	<0.001	<0.001	<0.001
Soft foam vs. hard foam	<0.001	<0.001	<0.001	<0.001	<0.001	<0.001
Soft foam vs. Hitohada	<0.001	<0.001	<0.001	<0.001	<0.001	<0.001
Soft foam vs. Ecoflex	<0.001	<0.001	<0.001	<0.001	<0.001	<0.001
Hard foam vs. Hitohada	<0.001	<0.001	<0.001	<0.001	0.780	0.003
Hard foam vs. Ecoflex	<0.001	<0.001	<0.001	<0.001	<0.001	<0.001
Hitohada vs. Ecoflex	<0.001	0.001	0.220	<0.001	<0.001	<0.001
<i>p-values interaction effect</i>						
MA x soft foam	0.018	0.386	0.004	0.878	0.450	<0.001
MA x hard foam	0.002	0.096	<0.001	0.699	0.032	0.879
MA x Hitohada	<0.001	0.042	<0.001	0.017	0.066	0.008
MA x Ecoflex	<0.001	0.073	<0.001	0.764	0.262	0.025
Soft foam vs. hard foam	0.068	0.061	<0.001	0.678	0.024	0.015
Soft foam vs. Hitohada	<0.001	0.031	<0.001	0.040	0.276	0.236
Soft foam vs. Ecoflex	<0.001	0.520	<0.001	0.749	0.186	<0.001
Hard foam vs. Hitohada	<0.001	0.842	0.523	0.288	0.005	0.157
Hard foam vs. Ecoflex	<0.001	0.024	0.309	0.825	0.142	0.268
Hitohada vs. Ecoflex	0.044	0.008	0.026	0.070	0.032	0.001

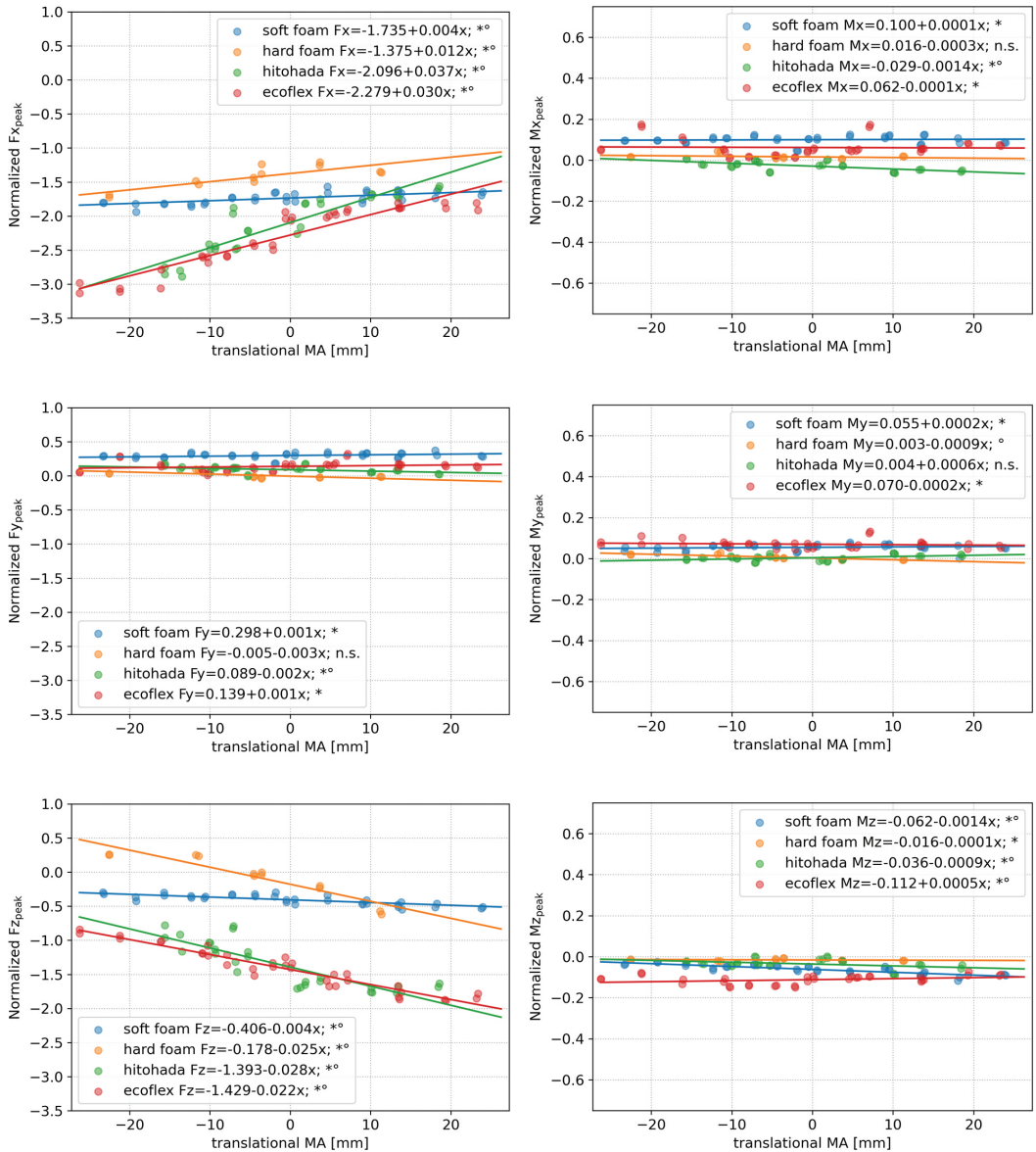


Figure 6.7 Scatter plots of the peak normalized joint forces and torques over the amount of translational misalignment. The solid lines show the regression lines per artificial soft tissue of which the equations are shown in the legends. In the equations, x stands for the translational misalignment in mm, asterisks mark a significant main effect of the artificial soft tissue and circles mark a significant interaction effect of artificial soft tissue and amount of misalignment. Negative values of translational misalignment are a distal translation and positive values are a proximal translation of the ILS joint with respect to the brace joint. Positive F_x is forward directed force, positive F_y is from medial to lateral directed force and positive F_z is compressive force. Positive M_x is abduction torque, positive M_y is flexion torque and positive M_z is external rotation torque.

DISCUSSION

To our knowledge, this is the first study investigating the effects of differences in soft tissue characteristics and rotational and translational misalignments of an exoskeleton on joint load by mimicking the situation with an instrumented leg simulator using four different materials as artificial soft tissue and a passive knee brace that was manually flexed. The analyses revealed significant differences of the effects between artificial soft tissues. The materials used varied in hardness with soft foam being the softest material, followed by hard foam, Hitohada and finally Ecoflex. The hardness measurements showed that the foams behave differently than the gel materials when compressed, showing a steep increase in displacement at low pressures and then saturating. Hitohada and Ecoflex compressed slower over increasing pressures and showed lower total displacements which can be partly attributed to the smaller thickness of those materials. However, previous research performed hardness measurements with thicker layers of Hitohada gel (45 and 55 mm compared to 10 mm in our study) and found similar ranges of displacement, albeit with a more linear trend [175]. For each of the materials, we found a significant increase of forces and torques in several directions with increasing rotational as well as translational misalignment. Overall, there is a tendency for stronger increase of peak joint load with increasing misalignments in harder artificial soft tissues, specifically in mediolateral force (F_y), ab-/adduction torque (M_x) and flexion torque (M_y).

In the rotational misalignment data, a very large portion of the variation could be explained by the models with adjusted R^2 values ranging from 0.905 to 0.983. We found that in most cases the main effects of the tissue type were relatively small although in many cases statistically significant. The load usually increased with increasing misalignments and we were mainly interested in whether different artificial soft tissue materials behave differently in misaligned situations. Therefore, the main effects, which only refer to the perfectly aligned situation, are of less relevance. There were however striking variations in main effects in peak F_x and F_z . The gel materials Hitohada and Ecoflex showed clearly larger backward directed forces in the well-aligned situation than the foams did. This might hint at differences in the behavior of those materials even in a situation without misalignments. This could have to do with differences in viscoelasticity, hardness, or with the fact that the foam materials were full foam cylinders and the gel materials were attached to a rigid cylinder which reduces their compressibility. The pre-loads might also be related to the strap pressure with which the brace was fixed to the ILS. We aimed to apply comparable strap pressure between tissues but did not quantify it. In peak F_z , a clear increase of tensile force in the well aligned trials could be observed between tissues in the order hard foam, soft foam, Hitohada, Ecoflex. While this was discussed in previous work as potentially being related to the amount of force with which the experimenter supports the ILS weight when adjusting the amount of misalignment [218], it is striking that, with the exception of hard foam, harder tissues showed stronger tensile forces in this experiment. It is possible that the softer the material, the more freedom there is for the ILS joint to move within the setup and reduce the forces, also in a well-aligned situation. The analysis further revealed significant interaction effects between the artificial soft tissue material and amount of misalignment on the joint load in all directions, except for the effects on peak F_z in the hard foam condition. This shows that, especially in peak F_x , F_y , M_x , M_y and M_z , the loads increased significantly when the rotational misalignment was increased, in each of the artificial soft tissues. But there were also differences in the extent to which the loads increased based on the artificial soft tissues. The peak mediolateral forces were significantly higher with increasing

misalignments in hard foam, Hitohada and Ecoflex than in soft foam. The slope in tensile/compressive force was significantly smaller in soft tissue and significantly larger in Ecoflex than in the other artificial soft tissues, although the absolute change was smallest in hard foam since Fz in soft foam had a negative linear relationship with the amount of misalignment. The effects of amount of rotational misalignment on peak ab-/adduction torque (Mx) were significantly larger in Hitohada and Ecoflex than in the foam materials, and in turn significantly larger in hard foam than in soft foam. We thus observed that harder tissue types intensify the effects of misalignments on the peak ab-/adduction torque. A similar effect was present in peak My where the increase in flexion torque with increasing misalignment was strongest in Ecoflex followed by Hitohada, hard foam and then soft foam. All of those differences in interaction effects were significant. The effects on internal/external rotation torques were stronger in hard foam than in all other artificial soft tissue conditions and stronger in Ecoflex than in Hitohada while the differences between other interaction effects were not significant.

For the translational misalignment data we could also find significant model fits for each direction of load. The R²-values, although still high, were slightly lower than those of the rotational misalignment models, ranging from 0.727 to 0.965. Similarly to the rotational misalignment models, the differences in main effects were strongest in peak Fx and peak Fz. The overall variation in those directions of forces (mediolateral and compressive/tensile) is larger than in other directions of load. Especially in the conditions Hitohada and Ecoflex, the data shows a strong increase in backward directed forces with increasing distal misalignment and a strong increase in tensile force in proximal misalignment of the ILS with respect to the orthosis. It is striking that the backwards directed peak forces (Fx) increase clearly with increasing distal misalignment, while they are relatively constant in the proximal misalignment settings, especially in Hitohada and Ecoflex. For those data points, an s-shaped curve could have been a better fit than the linear model. The distal translation of the ILS joint with respect to the orthosis joint has a stronger negative effect on anteroposterior joint load than proximal translation. For peak mediolateral forces (Fy), only the model for hard foam had a significant interaction effect, albeit small. The significant differences of interaction effects between artificial soft tissue conditions might have limited relevance as all normalized peak forces are within a range of [-0.04; 0.37] which is in the order of magnitude of 30 N. Similarly, the torques around all three axes show a comparably small variation across misalignment settings and artificial soft tissue conditions. Although some of the interaction effects are statistically significant, their relevance is questionable as the slopes are very small (all smaller than 0.0015 which corresponds to an approximate increase in torque of less than 0.2 Nm per 10 mm of misalignment). Previous research [131] found no changes in gait timing and kinematics in healthy individuals walking in an exoskeleton with translational knee joint misalignments of 20 mm. The interaction forces at the cuffs however were significantly increased in the misaligned situation and the authors concluded that a too short exoskeleton thigh segment is more disadvantageous than a too long exoskeleton thigh segment when considering interaction forces at the cuffs. This is in line with the distal translation of the ILS joint with respect to the orthosis joint having a stronger negative effect on anteroposterior joint load than proximal translation in the present study.

Overall, we found a number of significant differences in joint load between artificial soft tissues. No two materials behaved the same way. In several directions of load we could observe that peak forces and torques increased more strongly with increasing misalignments when a harder material was used as artificial soft tissue, which confirms our hypothesis. For the investigated ranges of rotational

misalignment and translational misalignment, we found slightly larger maximum peak forces in forward/backward direction in connection with translational misalignments. While the ranges of tensile/compressive force were comparable between the two directions of misalignments, the maximum peak loads in all other directions were larger in the rotational misalignment trials. As discussed previously [218], we can however not directly compare a certain amount of translational misalignment in mm with an amount of rotational misalignment in deg. The occurrence and magnitude of misalignments in actual use of exoskeletons needs more research in order to find out which directions of misalignments occur and which ranges of translations and/or rotations have to be considered.

There are some limitations to the setup and approach of this study that should be considered when interpreting the results. The ILS is a simple approximation for mimicking a human leg and cannot perfectly replicate a human leg's shape, joint kinematics, weight distribution, and viscoelasticity. The upper and lower leg segment shapes are simplified to cylinders in the ILS, as is suggested in literature [147]. The simple monocentric hinge joint that was used for the ILS knee does not replicate the translation of the knee joint center of rotation or the tibiofemoral rotation characterizing an anatomical knee [104], [212]. Micro-misalignments that are caused by an incongruity between the human knee joint and the exoskeleton joint can therefore not be investigated with the current setup. The outcomes of this study are thus limited to assessing the effects of larger misalignments, which can be caused by incorrect positioning or fitting of an exoskeleton. An ILS with complex joint mechanics replicating the human joint kinematics and an actuated joint to mimic the human in co-control and/or a resistance of the human to the movements initiated by the exoskeleton (e.g., caused by spasticity) would be very valuable for future research, to explore the mechanisms behind exoskeleton misalignments and other safety aspects in more detail. The total ILS weight is too low to realistically mimic a human leg, although the upper segment was fixed which is why only the lower ILS segment's weight is of relevance. The weight at the circular end increased the lower ILS segment weight to values between 3 and 3.9 kg, which is in the same order of magnitude as a human lower leg. Nevertheless, the weight distribution is not realistic, as the major part of the weight is at the distal end [209]. In addition to that, the differences in weight distributions caused by differences in artificial soft tissue weight might have had an influence on the results. To minimize this influence, the weight was subtracted from the force sensor data. The hardness and viscoelasticity of the artificial soft tissues cannot perfectly replicate the behavior of human soft tissue. The tissue in a human leg is not equally distributed across the leg and there are large intra- as well as inter-individual differences, depending on factors such as body composition and muscle activation. However, using the artificial soft tissue based on Hitohada gel can be considered as the gold standard at this point in time as it has shown to be resembling human thigh tissue in viscoelasticity and friction to some extent [175], [176], which is why it is suggested to be used for safety testing of personal care robots [147]. We used a range of artificial soft tissues to investigate how their properties affect joint load in misalignment scenarios and whether simple and readily available materials can be used instead of the suggested Hitohada gel. The results of this study have shown that the choice of artificial soft tissue has significant effects on how the misalignment affects joint loads. The gel materials led to clearly stronger increases in joint loads than the softer foam materials. Comparing our hardness measurements with existing literature [175], we confirmed that Hitohada corresponds best to the hardness of body areas with little soft tissue, such as the lateral thigh. For areas with larger amounts of soft tissue, such as the anterior and posterior thigh, a material softer than Hitohada and harder than the hard foam used in this study should be found.

However, the research comparing Hitohada with human tissue was only based on experiments with a single, healthy, participant. The reported differences of hardness between body sites stress the need for finding the most appropriate materials for artificial soft tissues and also for considering different body compositions of potential users in the risk assessment of wearable robots such as exoskeletons. Therefore, future research should investigate the suitability of different materials for manufacturing artificial soft tissues, based on experiments with large groups of human subjects with varying body compositions covering subjects of different age and with different medical conditions. Moreover, the hardness and behavior of soft tissue differs depending on exact body location and muscle activation [50], [175]. These factors should therefore also be considered in future research. Another limitation of the setup is connected to the choice of applying a pulling force to a passive brace to replicate actuated exoskeleton use. While this simplified the setup considerably, the manual flexion of the brace is not as standardized as the trajectory control or torque control of an actuated exoskeleton would be. To correct for any variations in the manually applied flexion torque, we normalized the resulting joint loads to perpendicular pulling force and actuation torque respectively. This way we correct for the random error introduced by manual pulling, but also compare unitless values rather than absolute forces and torques (in N or Nm respectively). Due to the other limitations of the setup however, the absolute values are deemed less relevant than the relative changes over amount of misalignment and between artificial soft tissue types. Moreover, the reported actuation torques and pulling forces allow for an indication of the absolute values of joint load. The choice of orthosis might also influence the results as different orthotic or exoskeleton devices can have different mechanics, which can considerably influence joint kinematics and compliance [203]. An additional aspect to consider is the fixation of both the orthosis and the upper end of the ILS in a frame. This was required to avoid slipping of the ILS and orthosis and to guarantee a high amount of reproducibility across trials, but does not exactly recreate the situation of walking with an exoskeleton. A limitation that probably has a larger effect on the outcomes, is the inability of the setup to recreate a weight bearing situation. We can only observe the effects during swing, while misalignments probably create a much larger risk during the stance phase, in which the knee load – and therefore presumably the effect of misalignment – is substantially increased. Especially during sit-to-stand, the load on the knee is high and misalignments are assumed to be causing high risks [103], [210]. For reasons of practical feasibility, these limitations had to be accepted. More research is needed to further investigate effects of exoskeleton misalignments on joint loads, specifically considering weightbearing situations.

Despite the discussed limitations, this study's findings increase the understanding of how exoskeleton misalignments can affect joint loads, and specifically shed light on the influence of the soft tissue. We showed that the choice of artificial soft tissue in a dummy leg significantly affects the outcomes of joint load changes caused by misalignments. We further supported previous findings showing that both rotational and translational exoskeleton misalignments can lead to considerable increase of joint loads. These findings bring us one step closer to understanding how hazards related to exoskeleton misalignments can be assessed using dummy limbs. Future research can increase this knowledge by using improved measurement setups to enable testing of weightbearing situations. This might allow conclusions on which magnitudes and directions of misalignments create potentially hazardous joint loads. In addition to that, the best choice of materials for creating artificial soft tissues should be investigated further, along with research towards acceptable limit values for physical human-robot interaction on a musculoskeletal level. Such research on safety and comfort limits for human-robot

interaction is not only needed for acceptable levels of forces exerted onto the musculoskeletal system, but also for the interaction at the soft tissue and skin level which can also be affected by misalignments [104], [137], [204], [205], [217].

CONCLUSION

In this study, we investigated the effects of misalignments using a manually flexed knee brace and an ILS with four different artificial soft tissues. We found that the changes in joint load induced by misalignments are significantly affected by the artificial soft tissue material. We saw a tendency for stronger increases in load with harder materials and found out that none of the investigated materials behaved the same way as another one. We further confirmed that increasing rotational and translational misalignments lead to increasing joint loads during swing. The differences between tissues were most pronounced in tensile force, ab-/adduction torque and extension/flexion torques when considering rotational misalignments. In the translational misalignment experiments, the effects were strongest on backwards directed and tensile force, where the maximum loads were considerably higher in the gel materials (Hitohada and Ecoflex) than in the foam materials. Future research should focus on improving the dummy to better mimic the characteristics of human joint kinematics and kinetics as well as human soft tissue. In addition to that, safe limit values should be defined based on research with healthy humans and patients.

This article investigates discomfort development for forces exerted repetitively and for extended durations through a rigid cuff.

Three force patterns, chosen to mimic exoskeleton use, were applied to the thigh of 15 healthy participants for 30 minutes. Changes in perceived comfort and skin effects were recorded.

Discomfort was detected at normal forces ranging from 40 to >230 N. Repetitive force application triggered discomfort after a median of 4.1 minutes (normal force only) and 5.4 minutes (normal and shear force) respectively. Discomfort increased over time but the repetitive force applications did generally not result in pain and there were no significant differences between repetitive loading patterns.

Exoskeleton design and use should be informed by comfort thresholds specific to prolonged repetitive loading. Large interindividual differences in perception of discomfort limit the possibilities for generally applicable comfort thresholds. Further research is needed to investigate how patient groups perceive such repetitive loading.

Chapter 7

Investigating change of discomfort during repetitive force exertion through an exoskeleton cuff



INTRODUCTION

Rehabilitation robots are an increasingly widely used tool for training or assistance of patients. In addition to that, wearable robotic devices like exoskeletons are being used to support workers during heavy lifting or other strenuous activities. Wearable robots for physical assistance or rehabilitation exert forces onto the user's body to fulfil their purpose. Those forces are transmitted at a physical human-robot interface, often in the form of cuffs, splints or straps, which can cause discomfort or injuries. Recent literature reviews have shown that those issues are the most frequently reported type of adverse events in stationary robotic gait training and wearable exoskeletons [44], [117]. Literature further states that discomfort can cause disuse of otherwise well-performing devices [203]. Another important factor to consider is the safety of the user. Discomfort and pain are a warning sign and prolonged exertion of excessive forces to the skin can cause injuries like blisters, skin abrasion, pressure injuries or bruises [105], [116], [126], [132], [133], [136].

There is limited knowledge about the acceptable levels of prolonged force exertion onto the skin through cuffs or straps. Some of the available information (Table 7.1) on pain pressure thresholds [32], [177], [178] has been included in a standardization document for collaborative robots (ISO/TS 15066) [146]. Those limit values are intended for accidental impact or clamping contacts between an industrial collaborative robot and a healthy worker. Those limit values, subdivided into the different parts of the human body, are strictly only applicable for healthy workers and for accidental contacts that occur incidentally and with a short duration. The experimenters observed some bruises and skin abrasions after only a few repetitions of the contact which is why those limit values are no suitable guideline for continuous contacts [179]. Moreover, the limit values were obtained based on experiments with small indenters. Those indenters have a different effect on the force distribution than cuffs, splints or straps used in rehabilitation and physical assistant robots, which are characterized by a larger contact area and often include some kind of cushioning. Therefore, discomfort detection thresholds (DDT) and pain detection thresholds (PDT) in physical assistance and rehabilitation robots should be investigated using algometers that mimic the contact with a wearable robot. Two recent systematic reviews found pain detection and pain tolerance thresholds for circumferential pressures in healthy individuals that were about 20 times lower than those used in ISO/TS 15066. Thresholds in chronic pain patients were even lower than those in healthy participants [128], [181]. Studies using pneumatic cuffs discovered that the discomfort and pain thresholds were lower during walking than during standing and that narrower cuffs (compared to a wider cuff exerting the same amount of pressure) as well as anatomical sites with smaller volumes of soft tissue (shank as compared to thigh) led to higher thresholds [182], [183]. In another study, cyclic loading of circumferential pressure at the knee was applied during treadmill walking and the number of compressions at a range of pressure levels until discomfort detection and pain detection were recorded. The researchers found that only in the two highest inflation pressure levels of 30 and 40 kPa, and only in 13% and 17% respectively of the participants, the PDT was reached within the maximum trial duration of 180 s. The results give a valuable insight into tolerance of circumferential pressure at the leg in static and dynamic conditions. However, in these studies, the pressure was applied for (1) a duration of 60 s in static conditions and (2) a maximum duration of 3 minutes in cyclic loading during walking. Those durations are not representative of normal use of wearable robots. As pressure at a level of 50% of the PDT applied continuously becomes painful after a few minutes [180] and intermittent pressure at low frequencies leads to summation of pain [115],

it is crucial to investigate the comfort levels during prolonged repetitive force exertion. In addition to that, the above-mentioned studies investigating discomfort and pain in standing and walking applied pressure using a pneumatic inflatable cuff to mimic soft exoskeleton or exosuit use. Due to the use of (semi-)rigid orthoses in exoskeletons, the interaction is different from that in exosuit use.

Table 7.1 | Contact pressures and pressure thresholds in literature

Pressure [kPa]	Description	Reference
≤ 5	Tolerable even on atrophied skin	[222]
5	Average pressure sitting	[223]
15-30	Peak pressure sitting	[223]
11-24	Peak pressure in front thigh pad during walking in LOPES gait trainer	[224]
12	Discomfort detection threshold for ramp inflation of pneumatic cuff	[183]
32	Discomfort detection threshold for staircase inflation of pneumatic cuff	[183]
38	Averaged thigh pressure during walking with REX exoskeleton	[40]
36	Pain detection threshold for ramp inflation of pneumatic cuff	[183]
61	Pain detection threshold for staircase inflation of pneumatic cuff	[183]
133	Sit-to-stand peak pressure in REX exoskeleton	[40]
480	Pain pressure threshold thigh	[180]
700-2500	Pain/safety threshold quasi-static impact thigh muscle	[146], [225]

Some research has been performed on safe limit values for continuous sliding contacts. The relationship of shear stress and rubbing time beyond which blisters are generated has been described for durations of up to about 30 minutes [102], [184] and was adopted in a standardization document for physical assistant robots [147]. Those limit values provide a valuable guideline for continuous sliding of a cuff on the skin. However, it is important to realize that the levels acceptable for shear stresses in rehabilitation robots should be clearly lower than those documented in literature as the generation of friction blisters during rehabilitation robot use is unacceptable and depending on the patients' health status, blisters can lead to complications. In addition to that, the shear stress in a wearable robot is expected to be characterized by cyclic loading and not continuous rubbing. Depending on the cuff design and applied pressure, there might not be a sliding contact but a shear stress acting on the lower layers of the soft tissue.

The aim of this study was to gain new knowledge on safety and comfort connected to prolonged exertion of repetitive shear and normal forces through a cuff, mimicking rehabilitation robot / exoskeleton use. This knowledge can inform wearable robot developers and thereby improve the safety of the devices. We hypothesized that (1) discomfort increases over time when cyclic loading is applied, (2) discomfort increases faster when normal forces are combined with shear forces compared to normal force only. We applied forces similar to those exerted by exoskeletons to healthy participants' thighs and evaluated a continuous comfort rating. We further assessed the occurrence of injuries or skin changes (referred to as negative signs in this article) and the influence of subject characteristics on the comfort thresholds to explore how perceived comfort relates to changes to the skin and whether it is affected by subject characteristics such as age or body mass index (BMI). The experiment was executed with two groups of healthy participants; younger adults and older adults. Those two groups were chosen

to allow for comparability with previous studies, which tested mostly with young healthy participants [106], [182], and to investigate whether older adults, which are usually included in the target population for rehabilitation robots or exoskeletons, experience different levels of discomfort when repetitive forces are applied to their soft tissue for long durations.

METHODS

Study design

In this cross-sectional intervention study, pre-defined force patterns were applied to healthy participants' anterior thighs through a custom-made test setup. Changes in perceived comfort were recorded continuously. A baseline measurement at the beginning of the measurement session was used for determining the DDT (only normal force). This was followed by two measurements with repetitive loading (normal force and combination of normal and shear force) in which the force magnitudes were based on the DDT. More specifically, the peak normal force was set to DDT and the peak shear force was set to 10% DDT. The repetitive loading force patterns were designed to resemble forces exerted by lower limb exoskeletons and were applied for 30 minutes each to mimic the duration of a regular training session.

Test setup

A custom assessment device has been developed for this study to exert normal and shear forces in a controlled manner. It consisted of an adjustable chair and mounting platform (Biodex Medical Systems Inc., Shirley, New York, USA), an actuator unit with actuators for normal force and shear force and a 3 DOF force sensor, and a thigh cuff with straps (Figure 7.1). The device was controlled by the experimenter via a PC using a custom graphical user interface to set the desired force profiles and record measured forces as a function of time. In addition to that, a physical slider with a visual analog scale (VAS) of 100 mm ranging from 'no discomfort at all' to 'worst imaginable discomfort' was used to continuously record changes in perceived comfort.

Force application

The actuator unit (Figure 7.2) was designed in such a way that it can be mounted to the movable platform of the Biodex System. The actuator for normal force (model DSZY1-12-20-A-025-IP65, Drive-System Europe Ltd. / MSW Motion Control GmbH, Werther, Germany) can deliver dynamic forces in the vertical direction. The actuation for shear force was realized using a spindle module (model KR2001A-0130-0-10A0, LM systems BV, Veenendaal, the Netherlands) and acted along the longitudinal axis of the participant's thigh. These actuators were used to exert continuous and repetitive normal and shear forces and were limited to a maximum of 230 N normal force and 50 N shear force through software. The force sensor (model K3D60a ± 200 N/VA, ME-Meßsysteme GmbH, Henningsdorf, Germany) was mounted between the actuators and the cuff and measured the forces in all three directions.



Figure 7.1 | Photos of the setup. The close-up on the top right shows the comfort slider with VAS and the close-up on the bottom right shows the thigh cuff with straps. The actuator unit is located inside the black cover between the comfort slider and the cuff (circled in blue).

The physical interface for applying the forces to the thigh was designed as a cuff with straps. The cuff consisted of a stainless steel clamp with a contact area of 6657 mm² and covered with a urethane cushioning material. Based on the contact area, the maximum net pressure and shear stress that could be applied were 34.6 kPa and 7.5 kPa respectively. It was mounted to the actuator unit and fixed to the participant's leg using straps. Two sizes of the clamp with the same contact area but varying bending radii were available to accommodate for different thigh shapes and diameters. The smaller sized cuff was used unless the entire area of the clamp would not make contact with the thigh, in which case the wider cuff was used. This decision was taken by the same researcher for each participant. It was fixed to the thigh, about 10 cm proximal to the knee. Its design, shape, closing mechanism and location on the thigh were based on common lower limb exoskeleton designs.

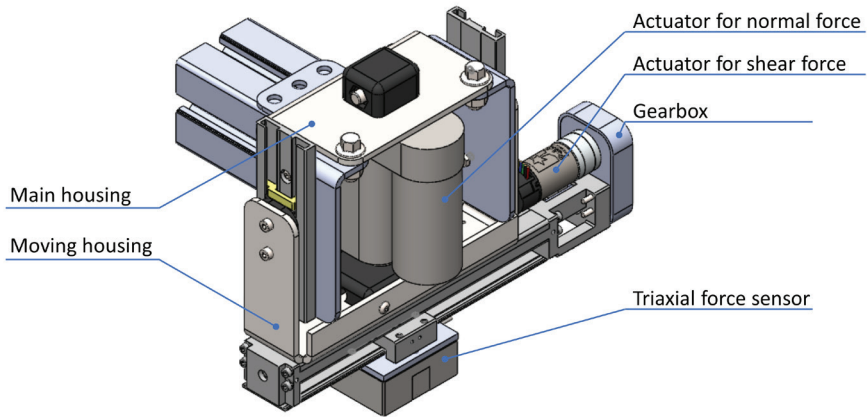


Figure 7.2| Actuator unit.

Discomfort

The participant's user interface for comfort rating was a physical slider (PTB0143-2010BPB103 linear slide potentiometer, Bourns, Inc., Riverside, CA, USA) with a slider knob (MP3190, Multicomp Pro, Premier Farnell Ltd., Utrecht, the Netherlands). Its casing showed the 10 mm ranging from no discomfort to worst imaginable discomfort. The comfort rating was recorded continuously and synchronized with the force recordings. In addition to the slider, a stop button was mounted on top of the actuator unit. The participants were instructed to push this button as soon as they experienced pain. Activation of the stop button resulted in an immediate release of the forces. In addition to ensuring participant safety, the data of this switch was used to identify the PDT.

Participants

We included healthy volunteers of two distinct age groups: between 18 and 35 years old or between 55 and 85 years old. Those two groups were chosen to allow for an investigation of age effects in perceived comfort and negative signs. Moreover, previous studies on comfort thresholds mostly tested with healthy young participants although older persons are more likely to use wearable robots. Volunteers were excluded from the study if they had skin lesions at the thigh, sensory impairments, an increased bleeding tendency or severe blood pressure fluctuations. The study was approved by the Medical Ethical Committee of the East-Netherlands (METC Oost-Nederland) under trial registration number NL.80800.091.22 and registered at clinicaltrials.gov under NCT05347810.

Procedure

Each participant attended a single measurement session. Before the experiment was executed, written informed consent was obtained and it was confirmed that the participant did not have any medical conditions that would preclude them from participating. We then noted the participant's age, gender, height, weight and skin characteristics at the cuff site. Ambient temperature and humidity were also documented. Next, the chair and footrest were adjusted to the participant's leg length so that the thigh was oriented horizontally and the knee was at approximately 90 deg. Participants were wearing cut off leggings legs (95% cotton, 5% elastane) at the cuff site and the cuff was positioned in such a way that

there was a preloading of approximately 10 N to ensure good contact.

Three different force patterns were applied to the participants' thighs: the staircase pattern (baseline), the repetitive normal force pattern (repN) and the repetitive normal and shear force pattern (repNS). After one pattern was completed, we switched to the other leg. The starting leg was randomized. As a baseline measurement, a staircase pattern of normal forces was applied (Figure 7.3, top). Each 10 s long iteration consisted of loading and unloading of the cuff pressure and the normal force was increased by 10 N with each iteration until the maximum force of 230 N was reached or the participant pushed the stop button, whichever occurred first. After applying this pattern one time without recording data, to allow for the participant to experience the sensation and for the experimenter to ensure appropriate positioning of the participant and actuator, the same pattern was applied once more. This time, the trial was recorded and the participant was instructed to start moving the slider of the VAS as soon as they experienced discomfort and then continuously indicate their perceived (dis-)comfort on the VAS. The DDT as measured during this baseline trial (i.e. the amount of force at which the participant started moving the slider), was used as the maximum amount of normal force in the two following repetitive loading force patterns repN and repNS (Figure 7.3, center and bottom). Since the baseline trial consisted of only normal forces, we used 10% of the DDT in normal force as peak shear force in repNS. If the DDT was not reached, 230 N was set as the maximum normal force and 23 N as the maximum shear force. The two repetitive force patterns were each applied for 30 minutes (unless the stop button was pressed before completion) and their order was randomized. The duration per loading cycle was 5 s, a full trial thus consisted of 360 loading cycles. During repetitive force application trials, all participants watched the same nature documentary to stay engaged but not too distracted. They were instructed to continuously indicate their perceived comfort on the VAS by moving the slider away from 0 as soon as they started experiencing discomfort. They were encouraged to change the slider position every time they experienced a change in the perceived (dis-)comfort, whether it was an increase or decrease in discomfort. After each trial, the participant's skin at the cuff site was inspected for reddening or injuries and any skin changes or other negative signs such as muscle soreness or other discomfort or pain which persisted after the trial end were recorded using a custom form.

To follow up on the development of those negative signs, each participant was contacted again 2-4 days after participation for a short semi-structured interview.

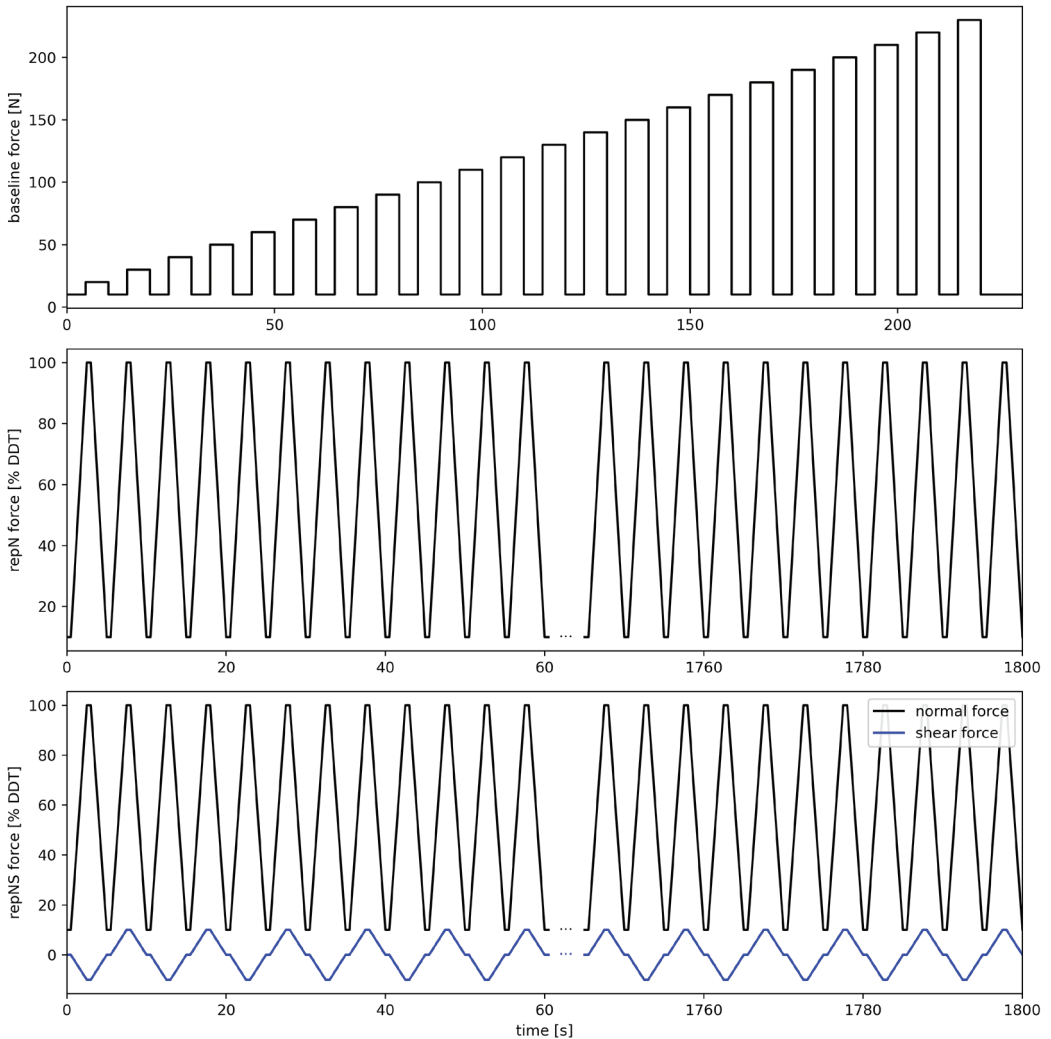


Figure 7.3 Applied force patterns in the conditions baseline (top), repetitive normal force (repN; center) and repetitive normal and shear force (repNS; bottom). The repetitive force patterns are relative to the discomfort detection threshold (DDT) as determined in the baseline trial.

Data analysis

Data processing and analysis was done using Python 3.7. VAS data (sampled at 1000 Hz) was filtered using a 4th order bi-directional low-pass filter with cutoff frequency of 2 Hz to remove high-frequency noise. We extracted VAS at the end of each trial (endVAS) and also after 10 and 20 minutes of the repetitive force trials (VAS10 and VAS20 respectively). For repetitive force trials we also extracted time to DDT (tDDT), defined as the first instance with $VAS \geq 1$ mm.

The following rules were employed for missing data: Where PDT was reached during a repetitive force trial, endVAS (and VAS10 or VAS20 where applicable) was set to the last recorded VAS value. One

repNS trial was incomplete due to an actuator failure and was therefore excluded from analysis. In case DDT was not reached during a repetitive force trial, tDDT was set to the maximum trial duration (30 min) and endVAS was 0.

Linear regression of VAS over time was analyzed per participant with the assumption that $VAS_{t=0}$ was 0, i.e. there was no intercept. Multiple linear regression was executed using ordinary least squares. The resulting slopes (VASslope) were statistically analyzed to investigate whether the change of discomfort over time differed between age groups and between force patterns. To explore any other relationships between subject characteristics (age, BMI), environmental conditions (temperature, humidity) and comfort parameters (DDT, endVAS, tDDT), Pearson correlation of those parameters was calculated. A relationship was considered moderate if the absolute value of the correlation coefficient was >0.5 and strong if it was >0.7 .

Due to the small sample sizes, we used Kruskal-Wallis tests to test for differences between participant groups and Wilcoxon signed rank tests to test for differences between the two repetitive force patterns, with significance set to $p < 0.05$. Where applicable, medians are presented together with interquartile ranges (IQR), calculated as the difference between the 75th and the 25th quartiles.

RESULTS

Participants and environmental conditions

This study included 15 participants, 10 of which formed the younger group (7 female, 3 male) and 5 of which formed the older group (3 female, 2 male). One participant in the older group was familiar with pain complaints in the lower back and sometimes involving the leg, but did not meet the exclusion criteria. The anthropometric data is summarized in Table 7.2. Ambient temperature and humidity during testing were 23.1 ± 0.4 °C and 44.7 ± 6.0 % respectively.

Table 7.2 Anthropometric data of participant groups.

	Younger				Older			
	Age (years)	Height (cm)	Weight (kg)	BMI (kg/m ³)	Age (years)	Height (cm)	Weight (kg)	BMI (kg/m ³)
Mean	26.5	170.8	73.0	25.1	61.2	175.6	80.9	26.0
SD	1.4	9.6	11.4	3.8	2.4	4.8	18.6	4.6
Median	27.0	169.5	73.5	24.2	60.0	176.0	81.8	26.1
IQR	0.8	6.9	16.3	6.0	4.0	3.0	21.5	5.3

Discomfort and pain

DDT was reached in 13 participants in each of the applied force patterns. This corresponded to 9 participants in the younger group and 4 participants in the older group in each of the force patterns. Note that the repNS data of one participant in the younger group could not be analyzed due to an actuator malfunction. Each of the participants reached DDT in at least one of the force patterns. PDT was reached in one participant of the younger group during the staircase pattern (190 N) and in one participant of the older group during the repNS pattern (after 14.55 minutes, i.e. 174 loading cycles,

with peak normal force 60 N and peak shear force 6 N).

Overall, the discomfort increased over time. Figure 7.4 shows the individual levels and group medians of discomfort over time for all force patterns. The multiple linear regression analyses for VAS over time per participant resulted in good fits (staircase: $R^2_{adj} = 0.94$, $F = 94860$; repN: $R^2_{adj} = 0.86$, $F = 282200$; repNS: $R^2_{adj} = 0.89$, $F = 374400$). The interaction effects for time and participant were significant for all participants except participants CT07, CT09 and CT13 in staircase, CT07 and CT12 in repN and CT07 and CT15 in repNS (all other $p < 0.01$). Those participants reported no or only very little discomfort in the respective trials.

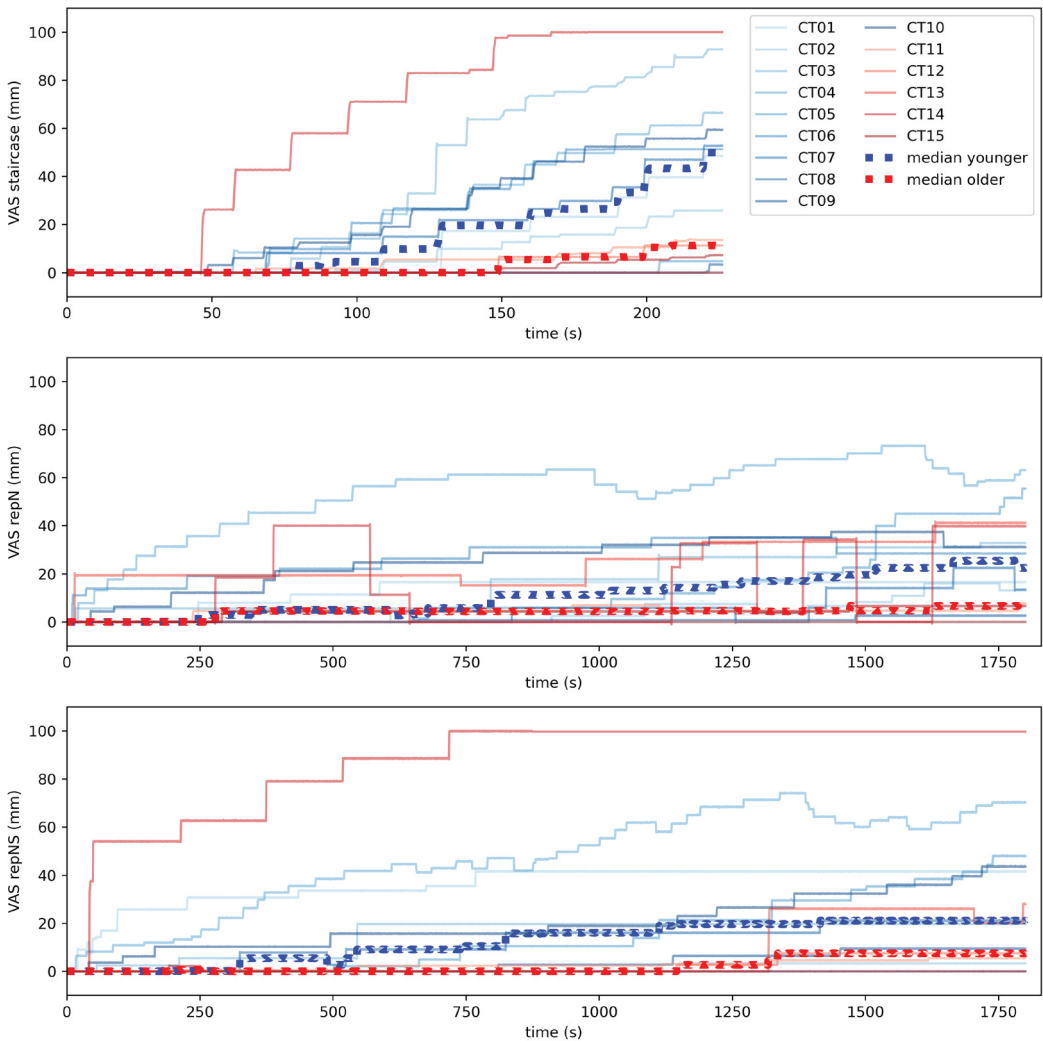


Figure 7.4| Discomfort over time per force pattern as individual results and group medians.

Table 7.3 shows the medians and IQR of the discomfort parameters and the results of the between-group analyses which included no significant differences between the two participant groups. There

were also no significant differences in the discomfort after 10, 20 and 30 minutes between the two different repetitive force patterns (Table 7.4).

Table 7.3 Medians and IQR of statistically analyzed parameters and the results of Kruskal-Wallis tests comparing participant groups.

	Median (IQR)			Kruskal-Wallis	
	Total	Younger	Older	Statistic	p-value
DDT (N)	100.0 (105.5)	90.0 (112.5)	160.0 (80.0)	0.14	0.71
endVAS _{staircase} (mm)	25.8 (50.1)	49.9 (47.7)	11.3 (6.3)	0.38	0.54
VASslope _{staircase} (mm/s)	0.08 (0.22)	0.15 (0.21)	0.03 (0.03)	0.38	0.54
VAS10 _{repN} (mm)	4.6 (18.0)	5.1 (22.7)	4.6 (6.9)	0.06	0.81
VAS20 _{repN} (mm)	12.0 (27.9)	14.3 (24.5)	4.6 (28.3)	0.38	0.54
endVAS _{repN} (mm)	16.6 (29.1)	22.5 (19.1)	7.6 (33.1)	0.38	0.54
VASslope _{repN} (mm/s)	0.01 (0.02)	0.02 (0.02)	0.004 (0.01)	0.96	0.33
tDDT _{repN} (s)	246.7 (324.5)	246.7 (628.5)	257.2 (101.2)	0.21	0.64
VAS10 _{repNS} (mm)	2.3 (18.7)	9.1 (19.6)	0.03 (2.3)	1.00	0.32
VAS20 _{repNS} (mm)	11.2 (19.8)	19.7 (16.6)	2.8 (3.1)	1.96	0.16
endVAS _{repNS} (mm)	20.4 (37.1)	21.1 (34.1)	7.5 (22.6)	0.22	0.64
VASslope _{repNS} (mm/s)	0.01 (0.02)	0.02 (0.02)	0.003 (0.01)	0.54	0.46
tDDT _{repNS} (s)	324.7 (767.5)	190.3 (543.1)	546.7 (953.6)	1.37	0.24

DDT: Discomfort Detection Threshold; PDT: Pain Detection Threshold; endVAS: Discomfort rating at termination of trial on the Visual Analog Scale (VAS); VAS10 and VAS20: Discomfort ratings after 10 and 20 minutes respectively of the repetitive force application; tDDT: Time to DDT.

We found moderate positive linear relationships between DDT and tDDT_{repNS} ($r = 0.59$), between endVAS_{staircase} and endVAS_{repNS} ($r = 0.66$) and between endVAS_{repN} and endVAS_{repNS} ($r = 0.76$). There were strong negative relationships between DDT and endVAS_{staircase} ($r = -0.790$) and between endVAS_{staircase} and tDDT_{repNS} ($r = -0.71$). None of the environmental conditions or anthropometrics recorded in this study were moderately or strongly correlated with any of the discomfort metrics.

Table 7.4 Results of Wilcoxon signed rank tests between repetitive normal force and repetitive normal and shear force patterns.

	Wilcoxon	
	Statistic	p-value
VAS10 (mm)	50.0	0.60
VAS20 (mm)	40.0	0.28
endVAS (mm)	44.0	0.39
tDDT (s)	38.0	0.23

VAS10 and VAS20: Discomfort ratings after 10 and 20 minutes respectively of the repetitive force application; endVAS: Discomfort rating at termination of trial; tDDT: Time to Discomfort Detection Threshold.

Tolerability and safety

There were no drop-outs and only two trials were ended due to reaching PDT. All participants experienced skin reddening at the cuff site in each of the trials, often especially around the cuff edges. All of those instances were mild and no participant experienced further skin injuries or pain at the cuff site. One participant (younger group) experienced mild muscle soreness at the thigh spreading distally in the leg to which the staircase pattern was applied during the following trial (repNS applied to contralateral leg). This experience was transient and the soreness was rated 3 on a pain scale from 0 to 10. Another participant (older group) experienced discomfort in the knee during repN which was also mild and transient and not experienced as painful. This was a known complaint for the participant. As to new negative signs reported during follow-up, there was one small circular bruise in a younger participant which was assumed to be unrelated to the study since it was proximal to the cuff site. Additionally, the feeling of heavy legs for approximately 3 hours on day 1 after study participation was reported by another younger participant. A participant from the older group reported slight feeling of pressure/soreness of the thigh when pressure was applied on day 1 after study participation. This was transient, mild, not painful and only experienced in the thigh to which the staircase and repNS patterns were applied.

DISCUSSION

The aim of this study was to gain new knowledge on safe and comfortable limit values for prolonged exertion of repetitive shear and normal forces through an exoskeleton cuff mimicking regular training use. To our knowledge, this study is the first investigating the development of discomfort over time in rehabilitation robots by mimicking prolonged repetitive force exertion through an exoskeleton cuff. We hypothesized that discomfort increases over time when cyclic loading is applied for a prolonged duration, and that discomfort increases faster when normal forces are combined with shear forces compared to normal force only. The relationship between discomfort and age group, BMI, temperature and humidity was investigated in order to inform safety considerations for exoskeleton use. We further explored the occurrence of negative signs in order to learn about the safety of the experiment and potential negative results of continuous and repetitive force application comparable to physical interaction with exoskeletons.

We found that discomfort increased over time when repetitive normal forces or a combination of repetitive normal and shear forces were applied, confirming our first hypothesis. Contrary to our second hypothesis, there was no difference between the two repetitive force patterns.

Discomfort and pain

Perception of discomfort and pain varied strongly between participants. Discomfort was detected at a median force of 100 N (i.e. 15 kPa) in the staircase force pattern, ranging from 40 N to not at all (set to 230 N for analysis). The median DDT found in this study was in the same order of magnitude as peak pressure during sitting [223], peak pressure during walking in the LOPES gait trainer [224] and DDT during ramp inflation of pneumatic cuffs [183]. Onset of pain was detected when the stop button was activated by a participant, which only occurred in one participant during the baseline trial and in one participant during the repetitive loading. The order of magnitude of the detected PDT in the baseline trial and the maximum applied force were comparable with reported DDT in pneumatic cuffs

with a staircase inflation pattern, PDT in ramp inflation pattern [183], and the average thigh pressure during walking in the REX exoskeleton [40]. Pain pressure thresholds for the thigh in literature and standardization [146], [177], [180] are between 30 and 16 times higher than the median DDT found in this study and 16 to 86 times higher than the lowest recorded PDT in this study. During the cyclic loading, discomfort (i.e. a change of the perceived comfort as indicated on a VAS as >0) was detected after a median of 247 s (4 min) when repetitive normal forces were applied and 325 s (5 min) when repetitive normal and shear forces were applied (corresponding to 49 and 65 loading cycles respectively). The times to discomfort detection ranged from 10 s to not at all and from 16 s to not at all respectively. DDT had a moderate positive correlation with $tDDT_{repNS}$ and no correlation with $tDDT_{repN}$ or the endVAS in the repetitive force patterns. This means that participants with a lower DDT and therefore lower magnitudes of forces applied during repN and repNS tended to experience discomfort earlier in the repNS trial and vice versa. This was not the case in the repN trial and DDT did not affect the discomfort after 30 minutes. This supports the observation of large interpersonal differences in perception of discomfort and tolerable force magnitudes. We also found negative correlations of $endVAS_{staircase}$ with DDT and $tDDT_{repNS}$ and positive relations of $endVAS_{staircase}$ with $endVAS_{repNS}$ as well as $endVAS_{repN}$ with $endVAS_{repNS}$. Participants who experienced strong discomfort in one force pattern were also likely to experience high discomfort in another force pattern. Also, lower forces applied due to lower DDT in the staircase trial did not necessarily lead to lower discomfort in the cyclic loading trials. This further stresses that people show a very individual reaction to cyclic loading.

Influence of environmental conditions and anthropometrics on discomfort

We found no statistical relationships between any of the investigated environmental conditions or participant characteristics and discomfort parameters. Although the group medians of discomfort over time were lower for the older group than for the younger group in each condition, statistical tests did not result in any significant differences since there were large variances. There was one outlier in the discomfort data of the older group, in the conditions staircase and repNS. This participant (CT14) is familiar with pain complaints. As stated in literature [181], chronic pain patients have lower DDT and PDT than persons without a history of pain complaints. It would therefore be interesting to repeat the experiments with different patient groups that might fall into the inclusion criteria of exoskeleton use and investigate how discomfort, pain and negative signs are affected by the conditions. The trend visible in the group medians might become more evident in larger participant groups, or it could be confirmed that interpersonal differences are larger than any group effects.

Safety and tolerability

The data on negative signs and PDT suggests that the procedure was safe and tolerable for the participant groups. We observed skin reddening at the cuff site after each trial. Frequent skin reddening was an expected negative sign since mild skin injuries have also been reported as the most frequent adverse effects in stationary robotic gait training and exoskeleton walking [44], [117]. The observation of more pronounced reddening around the cuff edges suggests that peak pressures and shear stresses occurred at those edges. Previous research has shown that peak pressures in the cuffs of exoskeletons can be considerably higher than the average pressure [40], [224]. Future studies could measure the distribution of interface pressure and shear to investigate how comfort relates to peak stresses. Although cuffs with different bending radii accommodated variations in thigh shape to some extent, peak stresses in relation to net forces might have differed between participants. An

investigation of shear and pressure distributions could give more insight in whether discomfort is more closely related to peak stresses than to net forces. The data on safety and tolerability suggests that the experiment can be repeated, potentially with higher force magnitudes or speeds and with patient populations, provided that any negative signs are closely monitored.

Implications for exoskeleton development and use

This study has shown that there are large interindividual differences in how discomfort caused by repetitive loading through a thigh cuff is experienced. The magnitude of acceptable yet uncomfortable force (onset of discomfort) varied strongly between participants. Although magnitudes of repetitive loading were based on individual DDT in this study, there was no correlation between the amount of applied load and the reported discomfort after 30 minutes of cyclic loading. The tolerance to the loads required to be applied by an exoskeleton should therefore be confirmed on an individual basis before exoskeleton training is started. 180 N of normal force (corresponding to 27 kPa) was considered acceptable (i.e. not painful) for all participants. Applying the individual DDT repetitively for 30 minutes caused discomfort in most participants but was not considered painful and did not lead to injuries beyond transient reddening of the skin. Only one participant experienced pain when 10% DDT shear force was added to the repetitive normal force, most other participants experienced discomfort. For exoskeleton training sessions longer than 30 minutes, participant's comfort should be monitored and breaks should be allowed. Furthermore, we found skin reddening in each trial and each participant. Specifically in the starting phase of exoskeleton training when the skin has not yet habituated to the stress [105], those signs should be closely monitored since non-blanchable skin redness can be considered the first stage of pressure injuries [127]. Exoskeleton developments should be aware of peak stresses at the cuff edges, causing reddening and indentation. Added compliance at the cuff edge could reduce this effect. Additional research should be performed to further increase the knowledge on acceptable force levels, specifically in potential user groups of exoskeletons.

Limitations

The generalizability of the results is limited by the small sample size, especially in the older group. While the present study provides a good starting point for identifying acceptable force levels exerted repetitively through an exoskeleton cuff, larger studies should be performed to further investigate personal or environmental risk factors. This should also include the microclimate, skin condition and cuff material, which have previously been mentioned as influencing factors for pressure injuries [99], [185]. We included healthy participants and showed that the procedure was safe and tolerable. We found a very large spread in the comfort thresholds between participants and set tDDT to the maximum trial duration of 30 minutes for statistical analysis. This underestimates tDDT for those participants and thereby underestimates the variance in onset of perceived discomfort. Patient groups that are eligible for exoskeleton training should be included in future studies to investigate how discomfort, pain and adverse reactions are affected by relevant medical conditions, such as stroke or spinal cord injury.

An obvious limitation to the study procedure and setup is that the participants were sitting. Force application during walking could alter the way the discomfort is perceived [182], but is not feasible with the current study design since the applied force would alter the gait pattern and potentially disturb participants' balance. Furthermore, the repetitive force patterns and especially the shear force application were rather slow due to limitations in the actuator speed. Applying shorter cycles and two

shear force peaks per cycle in repNS (i.e. one peak in each direction) might be more realistic and might result in larger differences between repN and repNS. Furthermore, the application of higher forces and longer durations of repetitive force application could extend the body of knowledge and would reduce the previously discussed limitations due to not reaching the DDT in some participants. A longitudinal study could investigate effects of summation of pain or habituation by applying repetitive forces several days in a row, and monitoring potential negative signs. When acceptable magnitudes and durations of force application are established, discomfort ratings could be combined with force measurements during exoskeleton walking to further investigate how the actually applied forces are perceived during use. Moreover, we measured net forces applied through the cuff but the relationship between applied force and contact stress is unclear. The stress distribution would be a valuable added measure to investigate relationships between peak stresses, discomfort and potential soft-tissue related injuries.

CONCLUSIONS AND FUTURE DIRECTIONS

We have shown that discomfort increases over time when cyclic loading is applied through a rigid thigh cuff for prolonged durations. This means that pain pressure thresholds obtained through one single quasi-static impact test are not acceptable thresholds for exoskeletons and other devices applying repetitive forces to human limbs, since they are 33 to 166 times higher than the median DDT in this study and do not consider increase in discomfort over time when cyclic loading is applied. Strong interpersonal variations lead to the conclusion that perception of discomfort is highly subjective. To further explore relationships between participant characteristics and discomfort and negative signs, larger groups should be tested. Next to participants of different age groups, this should include patient populations which are in the target population of exoskeletons.

Chapter 8

General discussion



OVERVIEW – WHAT HAVE WE LEARNED?

The general aim of this thesis was to gain more insight into safety challenges in rehabilitation robots and to take first steps towards addressing those challenges. This chapter summarizes the main findings and puts them into perspective, discussing the implications of what has already been achieved and providing an outlook on aspects that should be further investigated in future research as well as recommendations on how to improve rehabilitation robot safety in practice.

What are the most pressing risks and safety issues in rehabilitation robotics?

A systematic review of the literature (**Chapter 2**) revealed that in stationary robotic gait training studies, adverse events occur in about 8 to 13 % of the subjects. Soft tissue-related adverse events such as skin abrasions occur most frequently, followed by musculoskeletal adverse events which included muscle pain, joint pain and a bone fracture, among other things. When considering the severity of adverse events, the highest severity was found for physiological adverse events such as sudden blood pressure changes, since this requires cessation of training, followed by soft tissue-related adverse events. Similar types and frequency distributions of adverse events have been reported in overground exoskeleton training [44], [103]. After analyzing potential causes for these adverse events, excessive forces on the soft tissue level and on the musculoskeletal level were identified as the most relevant hazards in rehabilitation robotics when considering the physical human-robot interaction (**Chapter 3**). Soft tissue-related injuries are associated with normal forces and pressures as well as shear forces and friction applied to the patient's skin at the human-robot interface [105], [126], [127]. These can be influenced by many factors such as the design of the interface, materials present, surface topology and humidity [99], [101], [105], [115], [129], [130], [134], [135]. Excessive forces on the musculoskeletal structures can result from forces and torques applied to the musculoskeletal system by the robotic device to support the desired movements. Misalignments between the robot and anatomical joint axes as well as movements beyond the physiological range of motion can increase the risk for harmful joint forces and torques [44], [101], [104], [137]–[139].

How can those safety issues be avoided or managed?

During the development of a rehabilitation robot, standardized procedures for applying risk management to medical devices can be followed, as described in the standard ISO 14971 [119]. The typical workflow includes the identification of hazards, the assessment and evaluation of the resulting risk, and the identification of risk control measures. Contrary to machinery in industry where the risk has to be eliminated or reduced as far as possible [19], risk management in medical devices includes a benefit-risk analysis. If an unacceptable residual risk cannot be reduced any further, the manufacturer can analyze whether the benefits of using the device outweigh the risk which can make this residual risk acceptable. Patient-specific risk factors (e.g. bone mineral density, blood pressure fluctuations, body weight) as well as environmental factors (temperature, clothing worn at cuff site) might play a role in the risk analysis. The manufacturer can therefore choose to exclude certain patient groups or prohibit use in certain environmental conditions in the instructions for use.

To make sure that a risk has been successfully mitigated and is acceptable, a validation experiment can be performed. In such a validation experiment, the behavior of the device in a certain situation is assessed. If the device behaves in a safe manner staying within predefined safety ranges, this can be

used as proof that the implemented safety measures are working. Some test procedures relating to safety in physical human-robot interaction have been described in standards for industrial machinery. Although these do not come close to covering all relevant aspects yet [214], they might provide a starting point for validation experiments in not only industrial, but also rehabilitation robots. In the healthcare domain, guidelines for those procedures regarding validation of safe physical human-robot interaction are scarce. Especially smaller companies and startups struggle to find the relevant information in a myriad of standards and laws and need to invest a lot of time and resources into developing their own methods for safety validation tests since they are oftentimes not described in any of those documents. The COVR project has developed protocols to provide a guideline based on best practice, describing how to perform safety validation tests step by step [29]. Developing these procedures required knowledge on measurement techniques and devices to assess forces at the human-robot interface as well as on the musculoskeletal level of the robot user. Furthermore, manufacturers need to be informed about safe limit values in order to define pass/fail criteria for their validation experiments.

What are suitable methods to quantify metrics relevant for the identified safety issues?

To avoid injuries at the soft tissue level which were found to be the most frequent adverse events in robot-assisted gait training (**Chapter 2**) and other devices [44], [125], it is essential to have reliable measurement methods for assessing the forces and their distribution at the skin-robot interface. The stress distribution is especially relevant because forces at the robot-skin interface are usually not evenly spread and peak stresses play a major role in soft tissue injury development [99], [105], [115], [129], [132], [198]. From tests with a prototype measuring device (**Chapter 4**), it was concluded that while load cells can be used to measure the net forces and torques over the entire interface, different solutions are needed to assess the force interplay directly at the interface. Recent studies have used pressure mats [157]–[159], force sensitive resistors (FSRs) [40], [158], [160] and capacitive sensors (in non-robotic medical devices) [173] to achieve this. We found that the use of FSRs to map force distributions at the interface has a number of drawbacks, which were also supported by other literature. Hysteresis and sensor drift issues as well as sensitivity to surface curvature and temperature limit the reliability of the results [161], [162]. While the flexibility of arranging FSRs in grids of variable shapes and sizes is a great advantage, this also means that a portion of the force is applied in between the sensitive areas of the sensors and is therefore not picked up by the FSRs. Adding a layer of structures that push directly onto the sensitive areas can avoid this problem [38], [158], but also changes the nature of the contact area. The same problem arises when splitting the interface into several smaller surfaces which are each instrumented with a load cell or when using readily available pressure mats that are not tailored to the surface area and therefore do not cover the entire area or overlap partly. Flexible solutions which can be tailored to the interface area of interest and provide reliable data of contact pressure distributions are yet to be developed. The same holds true for solutions to measure shear stress and its distribution at the interface between human skin and a robot. While there is promising research into relatively thin and flexible sensing solutions [169]–[173], those sensors are not yet commercially available. With any sensor added to the interface, the characteristics of the interface will be changed. The challenge will always be to identify the actual forces present, as measurements can be influenced by the shape, size and behavior of the sensor itself, among other things.

Forces at the musculoskeletal level need to be kept within a safe range to avoid musculoskeletal adverse

events such as joint pain or bone fractures, which were found to be the second most frequent type of adverse events (**Chapter 2** and [103], [210]). Two challenges regarding assessment of the effects of forces on internal body structures are very present and often discussed: (1) How can the internal loads be assessed? (2) What role does the alignment play in hazards connected to internal loads? Both of those questions were assessed in **Chapter 5** and **Chapter 6**. Due to ethical considerations and practical feasibility, loads applied by rehabilitation robots onto the internal body structures cannot be measured *in vivo*. An instrumented dummy was therefore developed to measure the knee joint load in movements initiated through a manually flexed knee brace mimicking exoskeleton leg swing during walking. We concluded that it is feasible to measure changes in joint load through an instrumented dummy leg. The experiments showed that translational as well as rotational misalignments of an exoskeleton can increase internal joint forces during swing to a multiple of those experienced in a well-aligned situation. Investigations with different materials used as artificial soft tissue further revealed that the increase of joint loads with increasing misalignments is dependent on the softness of the surrounding tissue. When the limb is surrounded by harder (or less) soft tissue, the effect of misalignments on joint load are more pronounced than when softer tissues are present. This exploratory research helped gain a better understanding of how misalignments affect joint loads during exoskeleton use. The results provide a first step towards guidelines for how to approach risks connected to misalignments in exoskeleton development and for safety assessments, but should be complemented by further research. This can include the development of dummy limbs that better mimic the joint kinematics and tissue behavior of human limbs as well as testing under realistic loading (e.g. weight bearing in walking or sit-to-stand scenarios). Furthermore, once appropriate testing equipment and procedures are developed, the gap of acceptable limit values remains.

What are acceptable limit values to guarantee the safety of rehabilitation robot use?

There is very little knowledge on magnitudes and durations of forces that are acceptable for rehabilitation robot use. Previous research focused on pain pressure thresholds for incidental contacts [225], time-stress relationships for sliding contacts [116], and discomfort and pain thresholds in pneumatic circumferential pressure [182], [183]. The repetitive force application through a (semi-)rigid interface over long durations which is characteristic for rehabilitation robot use had not yet been investigated in terms of comfort thresholds. Such interaction was mimicked in **Chapter 7** by applying repetitive normal and shear forces to healthy participants' thighs through a cuff with straps. We found that, as expected, discomfort increases over time when a force that is perceived as slightly uncomfortable in short contacts is applied repetitively for 30 minutes. Adding a shear force to those repetitive loading cycles did not alter the perception of discomfort in our study. We found strong interindividual differences and no significant effects of participant characteristics (including age group, BMI) or environmental conditions (ambient temperature and humidity). Acceptable force magnitudes ranged from 40 to >230 N normal force (6 to >34.5 kPa average pressure) and the majority of participants did not experience pain but all participants developed skin reddening when repetitive forces were applied over prolonged durations. This research showed that pain pressure thresholds in literature are more than 30 times higher than the median discomfort detection threshold in this study and are therefore not an acceptable limit value for continuous interaction between rehabilitation robots and their users. While this study provides an indication of acceptable force magnitudes and changes of discomfort over time when prolonged repetitive loading is applied, more research is necessary to investigate

how the loading pattern, extended durations including multiple day use, and increased forces affect comfort and safety of the procedure. Moreover, literature states that patient populations can be more susceptible to injuries [99], [127] and have lower comfort thresholds [181]. Therefore, experiments with target populations of rehabilitation robots should be executed.

Acceptable limit values for loads on the musculoskeletal system, which can be affected by misalignments, are yet to be defined. Literature on bone fracture loads and ligament injury mechanisms [226], [227] can serve as a baseline for those limit values. However, one has to consider that pathologies can affect bone strength [228] and that the mechanics during rehabilitation robot use are different from those during injury scenarios in e.g. car crashes or sports accidents. Finding generally acceptable limit values for joint loads caused by misalignment or exceeding the anatomical range of motion is nearly impossible. Research that helps understand the mechanisms of human-robot interaction can however be a first step towards defining safety thresholds. Simulations such as the research in **Chapter 5** and **Chapter 6**, combined with knowledge about injury mechanisms, can provide insights into acceptable limit values for loads on the musculoskeletal system.

IMPLICATIONS FOR CLINICAL PRACTICE

Throughout this thesis, we learned that the load on the human body, created by physical interaction between rehabilitation robot and human, can be harmful, even though those loads are also necessary to fulfil the intended purpose of a rehabilitation robot. It is therefore very important that patients are closely monitored in studies as well as during clinical practice. Discomfort and early signs of injuries or other adverse events should be noted and followed up on. To get a better grip on risks of particular devices or device types as well as to better understand risk factors connected to the patient characteristics and environment, structured collection of safety-related information is pivotal. This information should follow unified guidelines to make sure all relevant aspects are covered (see the suggested guideline in **Chapter 2**) and should ideally be collected in a database where it is accessible for clinical and technical specialists. The EU reporting system EUDAMED (European database on medical devices, <https://ec.europa.eu/tools/eudamed>) can be a suitable tool for this. The database is still under development and is intended to contain information about registration of medical devices in the EU, notified bodies and certificates, clinical investigations and performance studies, and vigilance and market surveillance. It is not yet known whether this platform will collect data about serious adverse events only or whether adverse event data will also be available and which portion of the information will be available to the general public. A periodic analysis of safety-related data should be performed and disseminated to make appropriate use of the collected information and improve device safety over the years. The transition to the Medical Device Regulation (MDR), increasing the focus on safety and post-market surveillance, is an important step and will likely facilitate a better understanding of shortcomings in device safety.

An adequate training of therapists is of utmost importance. They should be able to pick up early signs of adverse events, know the potential negative effects of rehabilitation robot use, and be trained in managing (potentially) hazardous situations. Research has shown that discomfort and soft tissue injuries can often be resolved by making adjustments to the fitting or material at the interface

[74], [229], [230]. Furthermore, circumstances such as obesity, materials present at the interface, unexpected movements due to a (near-)fall incident, low bone mineral density or blood pressure fluctuations can increase the risk for injuries in some robotic devices [49], [82], [103], [210]. Therapists should be able to identify these factors and mitigate the risk or exclude patients from the training as to avoid harm. Literature reports that the use of technologies such as exoskeletons and the necessary training can be perceived as challenging or even overwhelming for physiotherapists [231]. Increasing the focus on safety during training might increase the mental load for the therapists even more. It is therefore important that sufficient time and support is available to ensure a successful training and that therapists use the devices regularly to gather more experience and avoid a loss of already acquired knowledge and skills over time. Using rehabilitation robots with patients demands a lot of responsibility. Regular meetings with groups of therapists working with robotic devices could encourage knowledge exchange regarding, among their individual experiences with the robot training, potential risk factors and mitigation strategies. Moreover, the technology could facilitate the process by including software and hardware to check whether a patient is suitable for inclusion and to monitor safety-relevant metrics during use.

IMPLICATIONS FOR REHABILITATION ROBOT DEVELOPERS

Safety needs to be considered early in the development phase. This is an advice that is often repeated at conferences, webinars and courses on medical device safety. While safety is an increasingly prominent topic on the agendas, device function is often still at the top of the priority list. Many developers tend to first focus on the design of a functional device and then try to find information on how to ensure and prove that the device is safe in order to achieve CE marking and enter the market. This will however cost a lot of extra time as the entire design might have to be changed to ensure safety. By considering safety as a part of the design process, safety by design features can be implemented which can make the need for some risk reduction measures obsolete [26]. The risk management can be prepared in parallel to the technical design which will decrease the workload towards the end of the development phase. The experience during this research effort has shown that developers are looking for low-threshold information to guide the way to knowledge on medical device safety. Especially smaller and younger companies often start the development of a product with a good idea but with little knowledge about the regulatory background and procedures that need to be followed. The applicability and status of standards is poorly understood, let alone the differences between different kinds of standardization documents such as harmonized standards, technical specifications and workshop agreements. The information published through the COVR Toolkit, partly informed by the research presented in this thesis, can provide an entrance point for robot developers. The concept of validating safety at a system level can be employed for all kinds of devices. Rehabilitation robot developers can implement the published test protocols as they are, or tailor them to their needs if the target behavior or environmental condition to be tested is not yet available in any of the protocols. Evaluations of the COVR protocols have shown that they are easily adaptable to the needs of the person in charge of the validation experiment [25]. Coinciding with, but also through the efforts of, the COVR project, a growing community of researchers, robot developers, manufacturers, and integrators focusing on safety in close human-robot interaction has formed over the past years. Rehabilitation robot developers can get involved with this community through the initiative of the COVR Hubs, to further shape the testing protocols and other safety-related

information by gaining new knowledge, sharing experiences and forming best practices.

Beyond these technical tools, the research presented in this thesis has uncovered some common safety issues and hazards related to rehabilitation robot use. The interface at which forces are applied to the rehabilitation robot user deserves special attention during the design process, to reduce the occurrence of soft tissue injuries and discomfort. Options for achieving optimal fit for all potential users need to be created. Moreover, manufacturers should provide guidelines on how to manage issues like pressure points. In certain scenarios, such as wearable robots that are used on a daily basis and for long durations, developers should consider a custom-made physical interface that is fit for each individual by an orthotist. Although soft tissue problems also occur in prosthetics and orthotics, they can be managed and resolved by the experienced specialists who are easily approachable by the device user [232]. Such direct contact can in most cases not be provided by the rehabilitation robot manufacturer. Where the manufacturer chooses a one-size-fits-all solution, the adjustment and fitting options need to be sufficient for the envisioned patient group and high-quality training material needs to be provided for the clinical specialists fitting the device. This research has further shown that misalignments can increase forces on the musculoskeletal level considerably. This is the case not only for translations of the exoskeleton joint axis with respect to the human joint axis, but also for rotations of the exoskeleton around the longitudinal axis of the limb. Conversations with therapists working with exoskeletons have shown, that they mostly consider proximal/distal misalignment as problematic and are often not aware of the potential risks connected to rotational misalignments. Exoskeleton developers should consider those misalignments as potential causes for hazardous force application and work on ways to mitigate this risk. Next to appropriate training for exoskeleton users to achieve optimal manual alignment, this should entail ways to compensate for misalignments, such as use of compliant elements or addition of kinematic redundancy [203].

HOW GUIDELINES CAN SUPPORT DEVICE DEVELOPERS

Many different levels of guidelines are available for topics related to rehabilitation robot safety. Although it can be difficult to navigate these different types of documents with various scopes and purposes, they all have their right to exist.

- **Law:** Regulations and directives are legislative acts that have to be followed. For mechanical rehabilitation robot safety, the most important ones are the MDR and the Machinery Directive. Regulations are laws that apply for all EU member states, while directives merely set out goals that all EU countries need to achieve, i.e. they act as a basis for national law.
- **Standards:** Standards are consensus-based, nationally or internationally recognized documents containing best practices or sets of requirements. The use of safety standards is voluntary. Standards that are harmonized with a law (such as the MDR or the Machinery Directive) grant the user the assumption of conformity to the essential health and safety requirements of that law. This means that having followed a harmonized standard, a manufacturer can assume that the outcomes comply with the respective law.
- **Other publications of standardization organizations:** Standardization organizations such as ISO (International Organization for Standardization), CEN (European Committee for Electrotechnical Standardization) and IEC (International Electrotechnical Commission) do

not only publish (inter-)national standards but also other documents, also referred to as pre-standards. Those documents are also based on consensus and best practice, but on a lower level than international standards. This includes guides, workshop agreements, specifications and technical reports. The advantage of these documents is that there is a lower threshold for publication which means that they can be published much faster than international standards and thus react faster to the developments on the market.

- **Scientific publications:** Scientific publications are a good way to share guidelines based on research or experiences in clinical practice. Those documents can also be consensus-based and the quality is guaranteed to some extent through peer-review. The reach of those publications is however somewhat limited to the scientific community.
- **Whitepapers:** Whitepapers and publication of information on the internet are easiest to access for a wide community. Although they are often helpful and easy to read, there is no real quality assurance.

The COVR project took some important steps towards creating a better overview of available (types of) guidelines and their applicability. In the COVR Toolkit, collaborative robot users and developers can find detailed information about the legal background, relevant literature, and a decision tree for finding the relevant legislation and standards for a particular device. Next to the limited knowledge of many robot developers regarding applicability of standards, some of the most important barriers to standardization are the cost of standards and the lack of information on testing procedures [22]. Both can be explained by the amount of time and effort it takes to reach industry-wide consensus that reaches the level required for an (international) standard. Harmonization of a standard even requires an extra step which has yet to be completed for most standards relevant for rehabilitation robotics, to which the MDR now applies. The route to an ISO international standard for example includes many steps with different deliverables which are voted upon by the national mirror committees [233], [234]. The committees consist of different stakeholders, such as device manufacturers and research institutes. Although there is no financial compensation for getting involved in standardization, it can be of advantage for companies as they are directly affected by the outcomes and can provide valuable insight as industry experts. The added workload might however not be desirable or achievable for some companies.

The standardization landscape is based on classifications. Domains, Technical Committees and Working Groups form its basic structure. In TC 299 for example, the technical committee for robotics, there are working groups in medical robot safety (JWG 5), service robot safety (WG 2) and industrial safety (WG 3), among others [235]. Those classifications are useful and necessary to ensure that each device that falls into a certain category is covered in a particular standard. On the other hand, these classifications can also create barriers and slow down developments. Trying to solve the same problem in two different communities is a waste of efforts. To take orthotics and exoskeletons as an example, both device classes bear similar safety issues relating to the contact between the orthosis or exoskeleton and the human, but they fall into different technical committees. The same applies to industrial exoskeletons falling under service robots and rehabilitation exoskeletons falling under medical robots. Instead of artificially building barriers, there should be an open discourse between groups with similar problems and an openness for a cross-domain approach. Within the course of this PhD work, COVR and Roessingh Research and Development were involved in two CEN Workshop Agreements (CWA) and one ISO Publicly Available Specification (PAS) [236]–[238]. During the two

COVR-initiated efforts [236], [238], we experienced strong resistance to the cross-domain approach employed within COVR. The critique regarding the cross-domain approach received through national mirror committees was based on the differences between legislation and risk management in medical devices compared to machinery. These differences should however not hamper a collaboration and an active flow of information between domains. Joint working groups spanning over several technical committees and covering safety aspects relevant for several domains could be a solution for this.

THE FUTURE OF SAFETY ASSESSMENTS IN PHYSICAL HUMAN-ROBOT INTERACTION

The research presented in this thesis revealed that loads on the soft tissue level and on the musculoskeletal level can be considered the most relevant safety-related aspects of physical human-robot interaction. We specifically focused on mechanical safety and therefore, aspects such as psychological safety (e.g. fear of falling) and (data) security are outside the scope of this work and should be addressed elsewhere. Currently, mechanical safety of rehabilitation robots is mainly assessed as part of performance tests or using qualitative measures, such as observations of users, questionnaires and interviews [239]. Rather than considering safety on the sideline of performance tests and relying on observations from pilot tests, experience from clinical practice with rehabilitation robots, and subjective measures, the safety of rehabilitation robots should be a focus point in the development phase. Safety tests should be performed early on, to evaluate the behavior of the device. To perform a safety assessment proving that the identified safety-relevant loads of the robot on the human are within safe ranges, a validation experiment can be done. The resulting information might also be useful for demonstrating conformity with the applicable regulation. Before rehabilitation robots are tested on humans, safety relevant metrics such as interaction forces should be quantified without a human in the loop, to avoid injuries to study participants. Test batteries mimicking the human-robot interaction, for example with the use of dummies or dummy segments, can be a viable and safe option for first validation experiments. Authors of regulatory and standardization documents should consider providing more guidance on those options to test without involving human subjects.

The findings in **Chapter 4** as well as other research [99], [105], [115], [129] have shown that the forces applied by the robot are not distributed evenly at the contact interfaces. Therefore, instead of only looking at the net forces and torques applied to the human body by the device under consideration, future safety assessments should consider the exact force interplay at the human-robot interface. Peak pressures and the combination of pressure and shear stress can cause soft tissue injuries [105], [132], [134], [198]. It is therefore important to investigate those stresses in a device so that the interface design can be altered in case large peak stresses occur. More research is required to reach a best practice for the measurement of shear stress and pressure distributions at the interface between human soft tissue and robot. Capacitive or piezoelectric sensors could be a viable solution to measure both pressure and shear in a thin and flexible sensor [31], [33], [46], [119], [136], [145], [149], [240]. A recent article [241] presents a capacitive sensor with mechanical properties similar to those of human skin. This is achieved by combining the sensing electrodes with different layers of silicone, including the Ecoflex silicone we used in **Chapter 6**. Its capabilities to measure shear in addition to pressure are yet to be investigated. There are no commercially available solutions yet which are able to measure

shear and pressure and are flexible enough to be fitted to the skin-robot interface. Further research and development of those solutions, providing reliable data of normal and shear force distribution and good adaptability to various cuff shapes and sizes, could enable an integration of such sensors into the padding of rehabilitation robot cuffs. This would allow a continuous monitoring of interaction forces without altering the composition of the interface. Finite element analysis is an alternative to measuring contact forces. In such a simulation, the stress and strain on the tissues is estimated based on the contact mechanics. Those estimations however depend on the modulus assigned to the soft tissues, which is not yet accurately defined in literature [99].

For assessing load applied to the human joints and other structures of the musculoskeletal system, the possibilities for measuring *in vivo* are limited. Metrics of physical human-robot interaction in the human joint, such as the effects of exoskeleton misalignment, could be measured directly in persons with instrumented total knee replacements [242], [243]. Such experiments however can only be acceptable if it can be confirmed beforehand that the prosthesis can withstand the resulting loads and that the safety of other body structures is also guaranteed. At this point in time, the knowledge about misalignment effects is not sufficient to make such a claim. Furthermore, one has to consider that the kinematics of an internal prosthesis differ from nonimplanted knee kinematics [244]. Cadaver studies can also be a means to assess effects of physical human-robot interaction on biological structures such as ligaments. Limitations of such an approach can be the limited muscle forces and different behavior of tissues compared to living human tissue [208].

The alternative for *in vivo* and *in vitro* measurements are simulations of the situation, either with a physical simulator of human structures (as was done in **Chapter 5** and **Chapter 6**) or with computational simulation. Physical simulators, or dummies, require additional research to improve how accurately human bodies can be mimicked. Dummy limbs should re-create the basic structure, dimensions, weight and kinematic behavior of human limbs. They should be instrumented so that the load on the joints and potentially bones can be measured. To accurately replicate human body behavior, dummy joints should be actuated [245]. This way, potentially hazardous situations can be assessed under realistic circumstances considering aspects like weight bearing, muscle stiffness and spasms. Furthermore, the soft tissue characteristics of humans need to be studied further to find appropriate material combinations for artificial soft tissues. The research presented in **Chapter 6** showed that the characteristics of soft tissue can significantly affect the load on the musculoskeletal system in potentially hazardous situations such as misalignments. Soft tissue compositions can vary strongly among potential rehabilitation robot users. Safety testing should consider this as a factor and perform tests in the most disadvantageous condition. Based on **Chapter 6**, we can assume that individuals with little soft tissue that allows only minimal compression are at higher risk to sustain musculoskeletal injuries. For soft-tissue related injuries, individuals with elevated adipose tissue levels might be at higher risk [49]. Therefore, dummies should allow for testing with wide ranges of body compositions. This does not only relate to the amount and properties of soft tissue but also to body height, weight and bone mass. While bone mineral density and previously sustained fractures might be difficult to mimic in a dummy, they should be considered in the safety thresholds for loads on the musculoskeletal system and potential exclusion criteria for the use of a device [44], [60], [210]. Defining those thresholds requires additional research. As technology in terms of sensing, materials and humanoid robots is progressing, future research should aim to develop more sophisticated dummies better replicating

the behavior of human rehabilitation robot users, including the possibility for mimicking situations involving weight bearing (e.g. for exoskeleton walking) and the human in co-control. Such dummies should be able to reliably measure the effects of rehabilitation robot use on soft tissue and skin stress as well as on musculoskeletal load. This is needed to truly understand the effects of misalignments and whether any increased load on the human body is actually harmful. Instrumented dummies could also be used to assess the success of misalignment compensation strategies and thereby help in their development. To accurately replicate human joint dynamics, the dummy joints should be actuated, enabling testing with varying joint stiffness and in load bearing situations. Instrumented outer layers which mimic human soft tissue and also measure force distributions (such as the one described in [241]) would be a great way to assess effects of physical human-robot interaction on the soft tissue level. In addition to those physical measurements, numerical simulation can help understand the physical interaction between humans and rehabilitation robots. Musculoskeletal modelling can be used to model the biomechanics of movements with rehabilitation robots such as exoskeletons. Using inverse dynamics, the joint loads can be calculated. By modeling the human-robot-system, the interactions can be simulated numerically, for example to assess effects of misalignments or optimize the exoskeleton mechanics [215], [246]–[248]. A major limitation to both musculoskeletal modeling and the use of instrumented dummies are the simplifications and assumptions that have to be made with regards to joint mechanics, tissue behavior, and musculotendon properties. This imposes uncertainties in the validity of the model behavior [104], [249]. Especially when considering safety of patient groups, generalized models are not a valid approximation of the situation.

In future research and safety testing, the two strategies of physical and numerical simulations can complement each other. Instrumented dummies with good biomimetic characteristics can close knowledge gaps regarding the contact behavior at the interface of soft tissue and cuff, misalignment effects, and the relation between net applied forces, force distributions at the interface, and loads on the musculoskeletal system. This information, together with knowledge from kinetic and kinematic movement analysis with humans using existing devices and knowledge about relationships between comfort, injury risk, device and patient characteristics, can feed into numerical simulation. Thereby, uncertainties of the numerical models can be reduced and eventually numerical simulation can be used to easily assess the effects of changes in the device design or control strategy or different robot user characteristics on safety in terms of joint loads, pressure points or comfort development over time.

Any safety validation experiment needs a pre-defined target behavior with limit values to use as a pass-fail criterion for the success of the validation. More research is needed to reach unified guidelines on those limit values. The experiments reported in **Chapter 7** should be repeated with larger sample sizes and also with several patient groups. According to literature, discomfort and pain thresholds can be different in patients than in healthy individuals [181] and so is the susceptibility to certain injuries [99], [105], [210]. Guidelines on safe limit values cannot replace the assessment of a specialist, deciding whether a certain patient can use or keep using a robotic device. They can however provide some guidance for target behaviors that can be employed during safety tests and inform rehabilitation robot developers about risk factors and differences between certain patient populations. This way, they can make informed decisions on exclusion criteria or special instructions for use for certain patient groups. More research into relationships between perceived discomfort or even development of injuries and

measures such as EMG, heart rate, deep tissue oxygenation or local skin temperature can help in defining objective warning signs, specifically for patients with impaired sensation [182], [250], [251].

In the future, rehabilitation robots could be equipped with sensing technology that does not affect their function and comfort but enables continuous measurement of safety-relevant metrics. In addition to load sensors in interfaces and joints, this could include measurements of heart rate, blood pressure, muscle activity and oxygenation, and humidity. Such a safety-related instrumentation of the device can be used during first tests in the development phase so that the results can help identify risks and possibilities for mitigation strategies. In the more distant future, devices could also be equipped with those features when they are already on the market. This way, risk factors or user discomfort during use of the rehabilitation robot could be automatically detected and subsequently mitigated, for example by suggesting a break. To achieve this, not only research on sensing technology that fits in seamlessly at the physical human-robot interface, but also research on relationships between quantifiable metrics and risk for injury is needed.

CONCLUSIONS

The work presented in this thesis aimed at gaining more insight into safety challenges in rehabilitation robots and taking first steps towards addressing those challenges. We found that there are remaining safety issues in rehabilitation robot use and that soft tissue injuries and musculoskeletal injuries can be considered the most frequent issues when focusing on mechanical safety and physical human-robot interaction. Those issues can be attributed to excessive forces exerted to the human body. The nature of interaction in rehabilitation robotics, characterized by continuous contacts, cyclic loading, vulnerable users, and sometimes uncontrolled environments, makes safety considerations complex. Even relatively small forces can lead to hazardous situations when they are e.g. applied for long durations, to impaired body structures, in interfaces with peak stresses or unfavorable microclimates. Safety validation experiments can be a useful approach to test physical human-robot interaction, preferably without a human in the loop, and develop mitigation strategies to reduce (peak) stresses and loads. We have discussed that additional research is required to accurately measure force distributions in all relevant directions at the contact interface between human and robot without affecting the force interplay. It has been established that misalignments are a prominent issue in exoskeleton use. While we have shown that misalignments can affect knee joint loads significantly in a dummy during swing, further research should investigate whether misalignment would lead to (potentially) harmful loads in weightbearing situations. Our research showed that discomfort increases over time when repetitive loads are applied through an exoskeleton cuff-like interface. Perception of comfort varies considerably between subjects. While it will be difficult to establish generally applicable guidelines for acceptable time-force relationships, future research can extend current knowledge by covering larger subject groups including patients, other force patterns, and multiple days experiments.

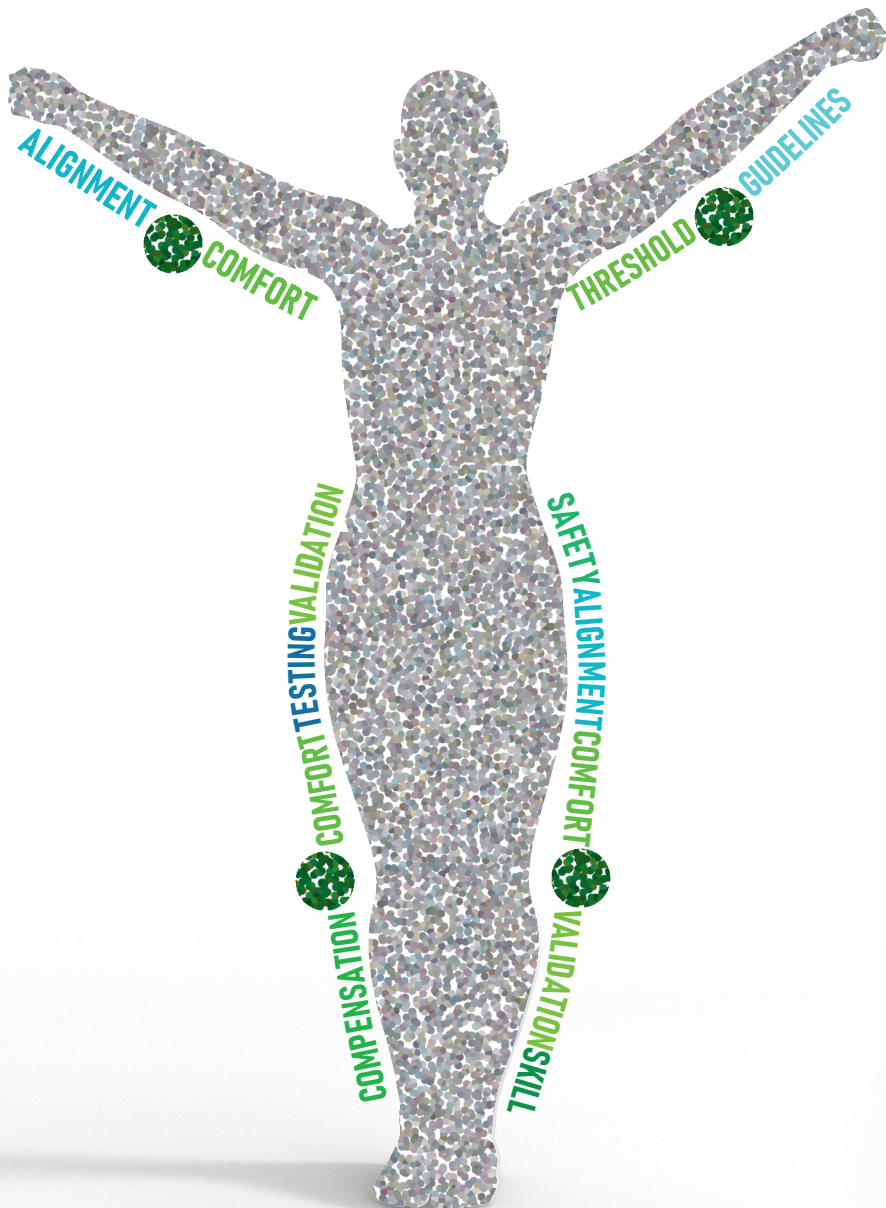
The ultimate aims of research and development efforts in rehabilitation robot safety should be to improve the safety of rehabilitation robots so that the occurrence of injuries is reduced (this is obvious), but also to gain knowledge and create guidelines which support rehabilitation robot developers in the safety certification process. Only if this is achieved, new developments can enter the market and

improve the life of patients. The list below can be seen as recommendations for a roadmap to achieve this.

- **Establish knowledge on safety gaps.** Monitor adverse events following unified guidelines on relevant aspects. Pool and analyze the information to generate better knowledge on risk factors and hazards.
- **Enable accurate assessments of interaction forces between rehabilitation robots and their users and find relationships between loads, use conditions and adverse events.** Develop pressure and shear stress sensors which are flexible, reliable, and adjustable to the cuff interface and use them in testing and potentially clinical practice. Relate metrics to occurrence of (soft tissue related) injuries / adverse events. Develop biomimetic instrumented dummies to test physical HRI without a human in the loop. Use the information gained from tests for numerical simulations such as musculoskeletal modelling.
- **Establish (diagnosis-specific) comfort and pain thresholds for rehabilitation robot use.** Perform research on discomfort and pain onset and development as well as occurrence of skin damage during repetitive prolonged force application through rehabilitation robot interfaces. Monitor objective measures such as muscle activity, heart rate and the microclimate at the interface to find relations between those measures and the self-reported comfort measures. Use findings to develop rules or software which can predict comfort or safety limits based on device properties, target population, and training duration.
- **Continue work on guidelines for safety assessments which are specific enough to be of added value but general enough to encompass all (future) device types.** Experience in this research and the COVR project has shown that step-by-step procedures which can be easily tailored to the specific use case are a viable option. Invest in cross-domain working groups for standards and guidelines to learn from each other and join forces to tackle shared safety issues.

&

References, List of abbreviations,
Summaries, Acknowledgements,
About the author, Progress range



REFERENCES

- [1] World Health Organization, "Disability and health," 2018. <https://www.who.int/news-room/fact-sheets/detail/disability-and-health> (accessed May 25, 2020).
- [2] World Health Organization, "Ageing and health," 2018. <https://www.who.int/news-room/fact-sheets/detail/ageing-and-health> (accessed May 25, 2020).
- [3] J. Mehrholz, M. Pohl, T. Platz, J. Kugler, and B. Elsner, "Electromechanical and robot-assisted arm training for improving activities of daily living, arm function, and arm muscle strength after stroke," *Cochrane Database Syst. Rev.*, vol. 2018, no. 9, Sep. 2018, doi: 10.1002/14651858.CD006876.pub5.
- [4] J. Mehrholz, S. Thomas, J. Kugler, M. Pohl, and B. Elsner, "Electromechanical-assisted training for walking after stroke," *Cochrane Database Syst. Rev.*, vol. 2020, no. 10, Oct. 2020, doi: 10.1002/14651858.CD006185.pub5.
- [5] H. S. Lo and S. Q. Xie, "Exoskeleton robots for upper-limb rehabilitation: State of the art and future prospects," *Med. Eng. Phys.*, vol. 34, no. 3, pp. 261–268, Apr. 2012, doi: 10.1016/j.medengphy.2011.10.004.
- [6] International Organization for Standardization, *Medical electrical equipment – Part 2-78: Particular requirements for basic safety and essential performance of medical robots for rehabilitation, assessment, compensation or alleviation*. IEC 80601-2-78:2019, 2019.
- [7] Exoskeleton Report, "Medical Exo Developer Archives - Exoskeleton Report," 2021. https://exoskeletonreport.com/exoskeleton-companies-and-organizations-directory/wpbdp_category/medical-exo-developer/ (accessed Mar. 07, 2022).
- [8] B. Marinov, "Updated Directory of Exoskeleton Companies and Industry Statistics Exoskeleton Report," 2021. <https://exoskeletonreport.com/2021/12/updated-directory-of-exoskeleton-companies-and-industry-statistics/> (accessed Mar. 07, 2022).
- [9] PubMed, "rehabilitation robotics - Search Results - PubMed," 2022. <https://pubmed.ncbi.nlm.nih.gov/?term=rehabilitation+robotics> (accessed Mar. 07, 2022).
- [10] Fortune Business Insights, "Rehabilitation Robots Market Size, Share | Global Analysis 2026," 2019. <https://www.fortunebusinessinsights.com/industry-reports/rehabilitation-robots-market-101013> (accessed Mar. 07, 2022).
- [11] M. Gandolfi *et al.*, "State of the art and challenges for the classification of studies on electromechanical and robotic devices in neurorehabilitation: a scoping review," *Eur. J. Phys. Rehabil. Med.*, vol. 57, no. 5, Nov. 2021, doi: 10.23736/S1973-9087.21.06922-7.
- [12] Exoskeleton Report, "Medical Archives - Exoskeleton Report," 2022. <https://exoskeletonreport.com/product-category/exoskeleton-catalog/medical/> (accessed Mar. 08, 2022).
- [13] G. Turchetti, N. Vitiello, L. Trieste, S. Romiti, E. Geisler, and S. Micera, "Why Effectiveness of Robot-Mediated Neurorehabilitation Does Not Necessarily Influence Its Adoption," *IEEE Rev. Biomed. Eng.*, vol. 7, pp. 143–153, 2014, doi: 10.1109/RBME.2014.2300234.
- [14] R. S. Calabrò *et al.*, "Who Will Pay for Robotic Rehabilitation? The Growing Need for a Cost-effectiveness Analysis," *Innov. Clin. Neurosci.*, vol. 17, no. 10–12, pp. 14–16, 2020, [Online]. Available: <http://www.ncbi.nlm.nih.gov/pubmed/33898096>.
- [15] H. Herr, "Exoskeletons and orthoses: classification, design challenges and future directions," *J. Neuroeng. Rehabil.*, vol. 6, no. 1, p. 21, Dec. 2009, doi: 10.1186/1743-0003-6-21.
- [16] R. S. Calabrò *et al.*, "Robotic gait rehabilitation and substitution devices in neurological disorders: where are we now?," *Neurological Sciences*, vol. 37, no. 4. Springer-Verlag Italia s.r.l., pp. 503–514, Apr. 01, 2016, doi: 10.1007/s10072-016-2474-4.
- [17] J. Babič *et al.*, "Challenges and solutions for application and wider adoption of wearable robots," *Wearable*

- of human-robot collisions," in *2014 IEEE International Conference on Robotics and Automation (ICRA)*, May 2014, pp. 3378–3383, doi: 10.1109/ICRA.2014.6907345.
- [33] S. Haddadin, A. Albu-Schaeffer, and G. Hirzinger, "Safety Evaluation of Physical Human-Robot Interaction via Crash-Testing," Jun. 2007, doi: 10.15607/RSS.2007.III.028.
- [34] N. Alavi, S. Zampierin, M. Komeili, S. Cocuzza, S. Debei, and C. Menon, "A preliminary investigation into the design of pressure cushions and their potential applications for forearm robotic orthoses," *Biomed. Eng. Online*, vol. 16, no. 1, p. 54, Dec. 2017, doi: 10.1186/s12938-017-0345-8.
- [35] T. Lenzi et al., "Mechatronics Measuring human – robot interaction on wearable robots: A distributed approach," *Mechatronics*, vol. 21, no. 6, pp. 1123–1131, 2011, doi: 10.1016/j.mechatronics.2011.04.003.
- [36] Y. Sugiura, M. Inami, and T. Igarashi, "A thin stretchable interface for tangential force measurement," in *Proceedings of the 25th annual ACM symposium on User interface software and technology - UIST '12*, 2012, p. 529, doi: 10.1145/2380116.2380182.
- [37] Y. Makino, Y. Sugiura, M. Ogata, and M. Inami, "Tangential force sensing system on forearm," in *Proceedings of the 4th Augmented Human International Conference on - AH '13*, 2013, pp. 29–34, doi: 10.1145/2459236.2459242.
- [38] C. Castellini and V. Ravindra, "A wearable low-cost device based upon Force-Sensing Resistors to detect single-finger forces," in *5th IEEE RAS/EMBS International Conference on Biomedical Robotics and Biomechatronics*, Aug. 2014, pp. 199–203, doi: 10.1109/BIOROB.2014.6913776.
- [39] Y. Ito, Y. Kim, and G. Obinata, "Acquisition of Contact Force and Slippage Using a Vision-Based Tactile Sensor with a Fluid-Type Touchpad for the Dexterous Handling of Robots," *Adv. Robot. Autom.*, vol. 03, no. 01, pp. 1–9, 2014, doi: 10.4172/2168-9695.1000116.
- [40] J. Tamez-Duque, R. Cobian-Ugalde, A. Kilicarslan, A. Venkatakrishnan, R. Soto, and J. Contreras-Vidal, "Real-Time Strap Pressure Sensor System for Powered Exoskeletons," *Sensors*, vol. 15, no. 2, pp. 4550–4563, Feb. 2015, doi: 10.3390/s150204550.
- [41] A. Wilkening, N. Puleva, and O. Ivlev, "Estimation of Physical Human-Robot Interaction Using Cost-Effective Pneumatic Padding," *Robotics*, vol. 5, no. 3, p. 17, Aug. 2016, doi: 10.3390/robotics5030017.
- [42] G. P. Sadarangani, X. Jiang, L. A. Simpson, J. J. Eng, and C. Menon, "Force Myography for Monitoring Grasping in Individuals with Stroke with Mild to Moderate Upper-Extremity Impairments: A Preliminary Investigation in a Controlled Environment," *Front. Bioeng. Biotechnol.*, vol. 5, no. 42, pp. 1–11, Jul. 2017, doi: 10.3389/fbioe.2017.00042.
- [43] P. D. Wettenschwiler, R. Stämpfli, S. Lorenzetti, S. J. Ferguson, R. M. Rossi, and S. Annaheim, "How reliable are pressure measurements with Tekscan sensors on the body surface of human subjects wearing load carriage systems?," *Int. J. Ind. Ergon.*, vol. 49, pp. 60–67, Sep. 2015, doi: 10.1016/j.ergon.2015.06.003.
- [44] Y. He, D. Eguren, T. P. Luu, and J. L. Contreras-Vidal, "Risk management and regulations for lower limb medical exoskeletons: a review," *Med. Devices Evid. Res.*, vol. Volume 10, pp. 89–107, May 2017, doi: 10.2147/MDER.S107134.
- [45] M. Ouzzani, H. Hammady, Z. Fedorowicz, and A. Elmagarmid, "Rayyan—a web and mobile app for systematic reviews," *Syst. Rev.*, vol. 5, no. 1, p. 210, Dec. 2016, doi: 10.1186/s13643-016-0384-4.
- [46] D. Moher, A. Liberati, J. Tetzlaff, and D. G. Altman, "Preferred Reporting Items for Systematic Reviews and Meta-Analyses: The PRISMA Statement," *PLoS Med.*, vol. 6, no. 7, p. e1000097, Jul. 2009, doi: 10.1371/journal.pmed.1000097.
- [47] A. Basteris, S. M. Nijenhuis, A. H. A. Stienen, J. H. Burke, G. B. Prange, and F. Amirabdollahian, "Training modalities in robot-mediated upper limb rehabilitation in stroke: A framework for classification based on a systematic review," *J. Neuroeng. Rehabil.*, vol. 11, no. 1, pp. 1–15, 2014, doi: 10.1186/1743-0003-11-111.

- [48] U.S. Department of Health and Human Services, "Common Terminology Criteria for Adverse Events (CTCAE) Version 5.0," 2017. https://ctep.cancer.gov/protocolDevelopment/electronic_applications/docs/CTCAE_v5_Quick_Reference_8.5x11.pdf (accessed Apr. 29, 2020).
- [49] I. Borggraeve *et al.*, "Safety of robotic-assisted treadmill therapy in children and adolescents with gait impairment: A bi-centre survey," *Dev. Neurorehabil.*, vol. 13, no. 2, pp. 114–119, Jan. 2010, doi: 10.3109/17518420903321767.
- [50] M. Aach *et al.*, "Voluntary driven exoskeleton as a new tool for rehabilitation in chronic spinal cord injury: a pilot study," *Spine J.*, vol. 14, no. 12, pp. 2847–2853, Dec. 2014, doi: 10.1016/j.spinee.2014.03.042.
- [51] A. T. Asbeck, S. M. M. De Rossi, K. G. Holt, and C. J. Walsh, "A biologically inspired soft exosuit for walking assistance," *Int. J. Rob. Res.*, vol. 34, no. 6, pp. 744–762, May 2015, doi: 10.1177/0278364914562476.
- [52] T. Aurich-Schuler, F. Grob, H. J. A. van Hedel, and R. Labruyère, "Can Lokomat therapy with children and adolescents be improved? An adaptive clinical pilot trial comparing Guidance force, Path control, and Freed," *J. Neuroeng. Rehabil.*, vol. 14, no. 1, p. 76, Dec. 2017, doi: 10.1186/s12984-017-0287-1.
- [53] Y.-H. Bae, S. M. Lee, and M. Ko, "Comparison of the effects on dynamic balance and aerobic capacity between objective and subjective methods of high-intensity robot-assisted gait training in chronic stroke patients: a randomized controlled trial," *Top. Stroke Rehabil.*, vol. 24, no. 4, pp. 309–313, May 2017, doi: 10.1080/10749357.2016.1275304.
- [54] J. Benito-Penalva *et al.*, "Gait Training in Human Spinal Cord Injury Using Electromechanical Systems: Effect of Device Type and Patient Characteristics," *Arch. Phys. Med. Rehabil.*, vol. 93, no. 3, pp. 404–412, Mar. 2012, doi: 10.1016/j.apmr.2011.08.028.
- [55] S. Carda, M. Invernizzi, A. Baricich, C. Comi, A. Croquelois, and C. Cisari, "Robotic Gait Training Is not Superior to Conventional Treadmill Training in Parkinson Disease: A Single-Blind Randomized Controlled Trial," *Neurorehabil. Neural Repair*, vol. 26, no. 9, pp. 1027–1034, Nov. 2012, doi: 10.1177/1545968312446753.
- [56] L. F. Chin, W. S. Lim, and K. H. Kong, "Evaluation of robotic-assisted locomotor training outcomes at a rehabilitation centre in Singapore.," *Singapore Med. J.*, vol. 51, no. 9, pp. 709–15, Sep. 2010, [Online]. Available: <http://www.ncbi.nlm.nih.gov/pubmed/20938611>.
- [57] A. E. Chisholm, R. A. Alamro, A. M. M. Williams, and T. Lam, "Overground vs. treadmill-based robotic gait training to improve seated balance in people with motor-complete spinal cord injury: a case report," *J. Neuroeng. Rehabil.*, vol. 14, no. 1, p. 27, Dec. 2017, doi: 10.1186/s12984-017-0236-z.
- [58] J. Chua, J. Culpán, and E. Menon, "Efficacy of an Electromechanical Gait Trainer Poststroke in Singapore: A Randomized Controlled Trial," *Arch. Phys. Med. Rehabil.*, vol. 97, no. 5, pp. 683–690, May 2016, doi: 10.1016/j.apmr.2015.12.025.
- [59] A. Esquenazi, S. Lee, A. Wikoff, A. Päckel, T. Toczyłowski, and J. Feeley, "A Comparison of Locomotor Therapy Interventions: Partial-Body Weight-Supported Treadmill, Lokomat, and G-EO Training in People With Traumatic Brain Injury," *PM&R*, vol. 9, no. 9, pp. 839–846, Sep. 2017, doi: 10.1016/j.pmrj.2016.12.010.
- [60] T. R. M. Filippo, M. C. L. De Carvalho, L. B. Carvalho, D. R. de Souza, M. Imamura, and L. R. Battistella, "Proximal tibia fracture in a patient with incomplete spinal cord injury associated with robotic treadmill training," *Spinal Cord*, vol. 53, no. 12, pp. 875–876, Dec. 2015, doi: 10.1038/sc.2015.27.
- [61] L. W. Forrester, A. Roy, C. Hafer-Macko, H. I. Krebs, and R. F. Macko, "Task-specific ankle robotics gait training after stroke: a randomized pilot study," *J. Neuroeng. Rehabil.*, vol. 13, no. 1, p. 51, Dec. 2016, doi: 10.1186/s12984-016-0158-1.
- [62] S. Freivogel, J. Mehrholz, T. Husak-Sotomayor, and D. Schmalohr, "Gait training with the newly developed 'LokoHelp'-system is feasible for non-ambulatory patients after stroke, spinal cord and brain injury. A feasibility study," *Brain Inj.*, vol. 22, no. 7–8, pp. 625–632, Jan. 2008, doi: 10.1080/02699050801941771.

- [63] S. Freivogel, D. Schmalohr, and J. Mehrholz, "Improved walking ability and reduced therapeutic stress with an electromechanical gait device," *J. Rehabil. Med.*, vol. 41, no. 9, pp. 734–739, 2009, doi: 10.2340/16501977-0422.
- [64] P. R. Geigle, S. K. Frye, J. Perreault, W. H. Scott, and P. H. Gorman, "Atypical autonomic dysreflexia during robotic-assisted body weight supported treadmill training in an individual with motor incomplete spinal cord injury," *J. Spinal Cord Med.*, vol. 36, no. 2, pp. 153–156, Mar. 2013, doi: 10.1179/2045772312Y.0000000033.
- [65] C. Geroin, A. Picelli, D. Munari, A. Waldner, C. Tomelleri, and N. Smania, "Combined transcranial direct current stimulation and robot-assisted gait training in patients with chronic stroke: a preliminary comparison," *Clin. Rehabil.*, vol. 25, no. 6, pp. 537–548, Jun. 2011, doi: 10.1177/02692155110389497.
- [66] L. Gizzi, J. Nielsen, F. Felici, J. C. Moreno, J. L. Pons, and D. Farina, "Motor modules in robot-aided walking," *J. Neuroeng. Rehabil.*, vol. 9, no. 1, p. 76, 2012, doi: 10.1186/1743-0003-9-76.
- [67] D. Grasmücke, O. Cruciger, R. C. Meindl, T. A. Schildhauer, and M. Aach, "Experiences in Four Years of HAL Exoskeleton SCI Rehabilitation," in *Converging Clinical and Engineering Research on Neurorehabilitation II*, vol. 15, J. Ibáñez, J. González-Vargas, J. M. Azorín, M. Akay, and J. L. Pons, Eds. Cham: Springer International Publishing, 2017, pp. 1235–1238.
- [68] S. Hesse and C. Werner, "Connecting research to the needs of patients and clinicians," *Brain Res. Bull.*, vol. 78, no. 1, pp. 26–34, Jan. 2009, doi: 10.1016/j.brainresbull.2008.06.004.
- [69] B. Husemann, F. Müller, C. Krewer, S. Heller, and E. Koenig, "Effects of Locomotion Training With Assistance of a Robot-Driven Gait Orthosis in Hemiparetic Patients After Stroke," *Stroke*, vol. 38, no. 2, pp. 349–354, Feb. 2007, doi: 10.1161/01.STR.0000254607.48765.cb.
- [70] A. Ikumi *et al.*, "Decrease of spasticity after hybrid assistive limb ® training for a patient with C4 quadriplegia due to chronic SCI," *J. Spinal Cord Med.*, vol. 40, no. 5, pp. 573–578, Sep. 2016, doi: 10.1080/10790268.2016.1225913.
- [71] O. Jansen *et al.*, "Hybrid Assistive Limb Exoskeleton HAL in the Rehabilitation of Chronic Spinal Cord Injury: Proof of Concept; the Results in 21 Patients," *World Neurosurg.*, vol. 110, pp. e73–e78, Feb. 2018, doi: 10.1016/j.wneu.2017.10.080.
- [72] O. Jansen *et al.*, "Functional Outcome of Neurologic-Controlled HAL-Exoskeletal Neurorehabilitation in Chronic Spinal Cord Injury: A Pilot With One Year Treatment and Variable Treatment Frequency," *Glob. Spine J.*, vol. 7, no. 8, pp. 735–743, Dec. 2017, doi: 10.1177/2192568217713754.
- [73] C. P. Kelley, J. Childress, C. Boake, and E. A. Noser, "Over-ground and robotic-assisted locomotor training in adults with chronic stroke: a blinded randomized clinical trial," *Disabil. Rehabil. Assist. Technol.*, vol. 8, no. 2, pp. 161–168, Mar. 2013, doi: 10.3109/17483107.2012.714052.
- [74] C. P. Kelley, J. Childress, and E. A. Noser, "Management of skin-related adverse events during locomotor training with robotic-assisted body weight supported treadmill: A case report," *Physiother. Theory Pract.*, vol. 29, no. 4, pp. 309–318, May 2013, doi: 10.3109/09593985.2012.731139.
- [75] J. Kim *et al.*, "Effects of robot-(Morning Walk®) assisted gait training for patients after stroke: a randomized controlled trial," *Clin. Rehabil.*, vol. 33, no. 3, pp. 516–523, Mar. 2019, doi: 10.1177/0269215518806563.
- [76] H. Kumru *et al.*, "Placebo-controlled study of rTMS combined with Lokomat® gait training for treatment in subjects with motor incomplete spinal cord injury," *Exp. Brain Res.*, vol. 234, no. 12, pp. 3447–3455, Dec. 2016, doi: 10.1007/s00221-016-4739-9.
- [77] H. Kumru, N. Murillo, J. Benito-Penalva, J. M. Tormos, and J. Vidal, "Transcranial direct current stimulation is not effective in the motor strength and gait recovery following motor incomplete spinal cord injury during Lokomat® gait training," *Neurosci. Lett.*, vol. 620, pp. 143–147, May 2016, doi: 10.1016/j.neulet.2016.03.056.

- [78] R. Labruyère and H. J. A. van Hedel, "Strength training versus robot-assisted gait training after incomplete spinal cord injury: a randomized pilot study in patients depending on walking assistance," *J. Neuroeng. Rehabil.*, vol. 11, no. 1, p. 4, 2014, doi: 10.1186/1743-0003-11-4.
- [79] A. C. Lo and E. W. Triche, "Improving Gait in Multiple Sclerosis Using Robot-Assisted, Body Weight Supported Treadmill Training," *Neurorehabil. Neural Repair*, vol. 22, no. 6, pp. 661–671, Nov. 2008, doi: 10.1177/1545968308318473.
- [80] A. C. Lo, V. C. Chang, M. A. Gianfrancesco, J. H. Friedman, T. S. Patterson, and D. F. Benedicto, "Reduction of freezing of gait in Parkinson's disease by repetitive robot-assisted treadmill training: a pilot study," *J. Neuroeng. Rehabil.*, vol. 7, no. 1, p. 51, 2010, doi: 10.1186/1743-0003-7-51.
- [81] A. Mayr, M. Kofler, E. Quirbach, H. Matzak, K. Fröhlich, and L. Saltuari, "Prospective, Blinded, Randomized Crossover Study of Gait Rehabilitation in Stroke Patients Using the Lokomat Gait Orthosis," *Neurorehabil. Neural Repair*, vol. 21, no. 4, pp. 307–314, Jul. 2007, doi: 10.1177/1545968307300697.
- [82] G. Morone *et al.*, "Who May Benefit From Robotic-Assisted Gait Training? A Randomized Clinical Trial in Patients With Subacute Stroke," *Neurorehabil. Neural Repair*, vol. 25, no. 7, pp. 636–644, Sep. 2011, doi: 10.1177/1545968311401034.
- [83] M. F. W. Ng, R. K. Y. Tong, and L. S. W. Li, "A Pilot Study of Randomized Clinical Controlled Trial of Gait Training in Subacute Stroke Patients With Partial Body-Weight Support Electromechanical Gait Trainer and Functional Electrical Stimulation," *Stroke*, vol. 39, no. 1, pp. 154–160, Jan. 2008, doi: 10.1161/STROKEAHA.107.495705.
- [84] A. Nilsson, K. Vreede, V. Häglund, H. Kawamoto, Y. Sankai, and J. Borg, "Gait training early after stroke with a new exoskeleton – the hybrid assistive limb: a study of safety and feasibility," *J. Neuroeng. Rehabil.*, vol. 11, no. 1, p. 92, 2014, doi: 10.1186/1743-0003-11-92.
- [85] M. Ochi, F. Wada, S. Saeki, and K. Hachisuka, "Gait training in subacute non-ambulatory stroke patients using a full weight-bearing gait-assistance robot: A prospective, randomized, open, blinded-endpoint trial," *J. Neurol. Sci.*, vol. 353, no. 1–2, pp. 130–136, Jun. 2015, doi: 10.1016/j.jns.2015.04.033.
- [86] A. Picelli *et al.*, "Robot-assisted gait training is not superior to balance training for improving postural instability in patients with mild to moderate Parkinson's disease: a single-blind randomized controlled trial," *Clin. Rehabil.*, vol. 29, no. 4, pp. 339–347, Apr. 2015, doi: 10.1177/0269215514544041.
- [87] A. Picelli *et al.*, "Robot-Assisted Gait Training in Patients With Parkinson Disease: A Randomized Controlled Trial," *Neurorehabil. Neural Repair*, vol. 26, no. 4, pp. 353–361, May 2012, doi: 10.1177/1545968311424417.
- [88] F. Schoenrath *et al.*, "Robot-Assisted Training Early After Cardiac Surgery," *J. Card. Surg.*, vol. 30, no. 7, pp. 574–580, Jul. 2015, doi: 10.1111/jocs.12576.
- [89] F. Schoenrath *et al.*, "Robot-assisted training for heart failure patients - a small pilot study," *Acta Cardiol.*, vol. 70, no. 6, pp. 665–671, Dec. 2015, doi: 10.1080/AC.70.6.3120178.
- [90] M. Sczesny-Kaiser *et al.*, "HAL@ exoskeleton training improves walking parameters and normalizes cortical excitability in primary somatosensory cortex in spinal cord injury patients," *J. Neuroeng. Rehabil.*, vol. 12, no. 1, p. 68, Dec. 2015, doi: 10.1186/s12984-015-0058-9.
- [91] M. Sczesny-Kaiser *et al.*, "Treadmill Training with HAL Exoskeleton—A Novel Approach for Symptomatic Therapy in Patients with Limb-Girdle Muscular Dystrophy—Preliminary Study," *Front. Neurosci.*, vol. 11, no. 449, pp. 1–9, Aug. 2017, doi: 10.3389/fnins.2017.00449.
- [92] O. Stoller, E. D. de Bruin, M. Schindelholz, C. Schuster-Amft, R. A. de Bie, and K. J. Hunt, "Efficacy of Feedback-Controlled Robotics-Assisted Treadmill Exercise to Improve Cardiovascular Fitness Early After Stroke: A Randomized Controlled Pilot Trial," *J. Neurol. Phys. Ther.*, vol. 39, no. 3, pp. 156–165, Jul. 2015, doi: 10.1097/NPT.0000000000000095.

- [93] O. Stoller, E. D. de Bruin, M. Schindelholz, C. Schuster-Amft, R. A. de Bie, and K. J. Hunt, "Cardiopulmonary exercise testing early after stroke using feedback-controlled robotics-assisted treadmill exercise: test-retest reliability and repeatability," *J. Neuroeng. Rehabil.*, vol. 11, no. 1, p. 145, 2014, doi: 10.1186/1743-0003-11-145.
- [94] S. Straudi, F. Manfredini, N. Lamberti, C. Martinuzzi, E. Maietti, and N. Basaglia, "Robot-assisted gait training is not superior to intensive overground walking in multiple sclerosis with severe disability (the RAGTIME study): A randomized controlled trial," *Mult. Scler. J.*, vol. 00, no. 0, pp. 1–9, Mar. 2019, doi: 10.1177/1352458519833901.
- [95] H. Tanaka *et al.*, "Spatiotemporal gait characteristic changes with gait training using the hybrid assistive limb for chronic stroke patients," *Gait Posture*, vol. 71, no. March, pp. 205–210, Jun. 2019, doi: 10.1016/j.gaitpost.2019.05.003.
- [96] M. Turiel *et al.*, "Robotic treadmill training improves cardiovascular function in spinal cord injury patients," *Int. J. Cardiol.*, vol. 149, no. 3, pp. 323–329, Jun. 2011, doi: 10.1016/j.ijcard.2010.02.010.
- [97] Q. Wu, X. Wang, F. Du, and X. Zhang, "Design and Control of a Powered Hip Exoskeleton for Walking Assistance," *Int. J. Adv. Robot. Syst.*, vol. 12, no. 3, p. 18, Mar. 2015, doi: 10.5772/59757.
- [98] C. Vaney *et al.*, "Robotic-Assisted Step Training (Lokomat) Not Superior to Equal Intensity of Over-Ground Rehabilitation in Patients With Multiple Sclerosis," *Neurorehabil. Neural Repair*, vol. 26, no. 3, pp. 212–221, Mar. 2012, doi: 10.1177/1545968311425923.
- [99] D. L. Bader, P. R. Worsley, and A. Gefen, "Bioengineering considerations in the prevention of medical device-related pressure ulcers," *Clin. Biomech.*, vol. 67, no. March, pp. 70–77, Jul. 2019, doi: 10.1016/j.clinbiomech.2019.04.018.
- [100] Y. Akiyama, Y. Yamada, and S. Okamoto, "Interaction forces beneath cuffs of physical assistant robots and their motion-based estimation," *Adv. Robot.*, vol. 29, no. 20, pp. 1315–1329, Oct. 2015, doi: 10.1080/01691864.2015.1055799.
- [101] E. Rocon *et al.*, "Human–Robot Physical Interaction," in *Wearable Robots: Biomechatronic Exoskeletons*, Chichester, UK: John Wiley and Sons, 2008, pp. 127–163.
- [102] X. Mao, Y. Yamada, Y. Akiyama, S. Okamoto, and K. Yoshida, "Development of a novel test method for skin safety verification of physical assistant robots," in *2015 IEEE International Conference on Rehabilitation Robotics (ICORR)*, Aug. 2015, pp. 319–324, doi: 10.1109/ICORR.2015.7281219.
- [103] F. H. M. van Herpen, R. B. van Dijksseldonk, H. Rijken, N. L. W. Keijsers, J. W. K. Louwerens, and I. J. W. van Nes, "Case Report: Description of two fractures during the use of a powered exoskeleton," *Spinal Cord Ser. Cases*, vol. 5, no. 1, p. 99, Dec. 2019, doi: 10.1038/s41394-019-0244-2.
- [104] Y. Akiyama, Y. Yamada, K. Ito, S. Oda, S. Okamoto, and S. Hara, "Test method for contact safety assessment of a wearable robot -analysis of load caused by a misalignment of the knee joint-," in *2012 IEEE RO-MAN: The 21st IEEE International Symposium on Robot and Human Interactive Communication*, Sep. 2012, pp. 539–544, doi: 10.1109/ROMAN.2012.6343807.
- [105] J. E. Sanders, B. S. Goldstein, and D. F. Leotta, "Skin response to mechanical stress: adaptation rather than breakdown - A review of the literature," *J. Rehabil. Res.*, vol. 32, no. 3, pp. 214–26, Oct. 1995, [Online]. Available: <http://www.ncbi.nlm.nih.gov/pubmed/8592293>.
- [106] M. B. Yandell, D. M. Ziemnicki, K. A. McDonald, and K. E. Zelik, "Characterizing the comfort limits of forces applied to the shoulders, thigh and shank to inform exosuit design," *PLoS One*, vol. 15, no. 2, pp. 1–12, Feb. 2020, doi: 10.1371/journal.pone.0228536.
- [107] T. G. Maak and J. D. Wylie, "Medical Device Regulation," *J. Am. Acad. Orthop. Surg.*, vol. 24, no. 8, pp. 537–543, Aug. 2016, doi: 10.5435/JAAOS-D-15-00403.

- [108] European Commission, "Draft Functional specifications for the European Database on Medical Devices (Eudamed) - First release to be audited." pp. 1–91, 2019, [Online]. Available: <https://ec.europa.eu/docsroom/documents/34304>.
- [109] K. F. Schulz, D. G. Altman, and D. Moher, "CONSORT 2010 Statement: updated guidelines for reporting parallel group randomised trials," *BMJ*, vol. 340, no. mar23 1, pp. c332–c332, Mar. 2010, doi: 10.1136/bmj.c332.
- [110] J. P. A. Ioannidis *et al.*, "Better Reporting of Harms in Randomized Trials: An Extension of the CONSORT Statement," *Ann. Intern. Med.*, vol. 141, no. 10, pp. 781–788, Nov. 2004, doi: 10.7326/0003-4819-141-10-200411160-00009.
- [111] B. Radder *et al.*, "Home rehabilitation supported by a wearable soft-robotic device for improving hand function in older adults: A pilot randomized controlled trial," *PLoS One*, vol. 14, no. 8, p. e0220544, Aug. 2019, doi: 10.1371/journal.pone.0220544.
- [112] C. Shirota *et al.*, "Robot-supported assessment of balance in standing and walking," *J. Neuroeng. Rehabil.*, vol. 14, no. 1, p. 80, Dec. 2017, doi: 10.1186/s12984-017-0273-7.
- [113] M. A. Gull, S. Bai, and T. Bak, "A Review on Design of Upper Limb Exoskeletons," *Robotics*, vol. 9, no. 1, p. 16, Mar. 2020, doi: 10.3390/robotics9010016.
- [114] M. D. C. Sanchez-Villamañan, J. Gonzalez-Vargas, D. Torricelli, J. C. Moreno, and J. L. Pons, "Compliant lower limb exoskeletons: A comprehensive review on mechanical design principles," *Journal of NeuroEngineering and Rehabilitation*, vol. 16, no. 1. BioMed Central Ltd., pp. 1–16, May 09, 2019, doi: 10.1186/s12984-019-0517-9.
- [115] M. Sposito, S. Toxiri, D. G. Caldwell, J. Ortiz, and E. De Momi, "Towards Design Guidelines for Physical Interfaces on Industrial Exoskeletons: Overview on Evaluation Metrics," in *Biosystems and Biorobotics*, vol. 22, Springer International Publishing, 2019, pp. 170–174.
- [116] X. Mao, Y. Yamada, Y. Akiyama, S. Okamoto, and K. Yoshida, "Safety verification method for preventing friction blisters during utilization of physical assistant robots," *Adv. Robot.*, vol. 31, no. 13, pp. 680–694, Jul. 2017, doi: 10.1080/01691864.2017.1318716.
- [117] J. Bessler, G. B. Prange-Lasonder, R. V. Schulte, L. Schaake, E. C. Prinsen, and J. H. Buurke, "Occurrence and Type of Adverse Events During the Use of Stationary Gait Robots—A Systematic Literature Review," *Front. Robot. AI*, vol. 7, Nov. 2020, doi: 10.3389/frobt.2020.557606.
- [118] International Organization for Standardization, *Safety of machinery – General principles for design – Risk assessment and risk reduction*. ISO 12100:2010, 2010.
- [119] International Organization for Standardization, *Medical devices – Application of risk management to medical devices*. ISO 14971:2019, 2019.
- [120] European Parliament and Council of the European Union, "REGULATION (EU) 2020/561 OF THE EUROPEAN PARLIAMENT AND OF THE COUNCIL of 23 April 2020 amending Regulation (EU) 2017/745 on medical devices, as regards the dates of application of certain of its provisions," *Off. J. Eur. Union*, 2020, Accessed: Aug. 17, 2020. [Online]. Available: [moz-extension://172fba97-b9e5-4c8e-8a4f-5513e4f53242/enhanced-reader.html?openApp&pdf=https%3A%2F%2Feur-lex.europa.eu%2Flegal-content%2FEN%2FTXT%2FPDF%2F%3Furi%3DCELEX%3A32020R0561%26from%3DEN](https://eur-lex.europa.eu/legal-content/EN/TXT/PDF/?uri=CELEX:3A32020R0561%26from%3DEN).
- [121] International Organization for Standardization, *Clinical investigation of medical devices for human subjects – Good clinical practice*. ISO 14155:2020, 2020.
- [122] European Commission, "Draft standardisation request as regards medical devices in support of Regulation (EU) 2017/745 and in vitro diagnostic medical devices in support of Regulation (EU) 2017/746." Brussels, pp. 1–25, 2019, [Online]. Available: <https://ec.europa.eu/docsroom/documents/36104>.

- [123] H. Rodgers *et al.*, "Robot assisted training for the upper limb after stroke (RATULS): a multicentre randomised controlled trial," *Lancet*, vol. 394, no. 10192, pp. 51–62, Jul. 2019, doi: 10.1016/S0140-6736(19)31055-4.
- [124] T. Nef, M. Mihelj, and R. Riener, "ARMin: a robot for patient-cooperative arm therapy," *Med. Biol. Eng. Comput.*, vol. 45, no. 9, pp. 887–900, Sep. 2007, doi: 10.1007/s11517-007-0226-6.
- [125] D. Schwartz, Y. K. Magen, A. Levy, and A. Gefen, "Effects of humidity on skin friction against medical textiles as related to prevention of pressure injuries," *Int. Wound J.*, vol. 15, no. 6, pp. 866–874, Dec. 2018, doi: 10.1111/iwj.12937.
- [126] I. Hoogendoorn, J. Reenalda, B. F. J. M. Koopman, and J. S. Rietman, "The effect of pressure and shear on tissue viability of human skin in relation to the development of pressure ulcers: a systematic review," *J. Tissue Viability*, vol. 26, no. 3, pp. 157–171, Aug. 2017, doi: 10.1016/j.jtv.2017.04.003.
- [127] National Pressure Ulcer Advisory Panel, European Pressure Ulcer Advisory Panel, and Pan Pacific Pressure Injury Alliance, "Prevention and Treatment of Pressure Ulcers: Quick Reference Guide," *Clinical Practice Guideline*. pp. 1–75, 2014, [Online]. Available: <https://www.epuap.org/wp-content/uploads/2016/10/quick-reference-guide-digital-npuap-epuap-pppia-jan2016.pdf>.
- [128] T. Kermavnar, V. Power, A. De Eyto, and L. W. O'Sullivan, "Computerized Cuff Pressure Algometry as Guidance for Circumferential Tissue Compression for Wearable Soft Robotic Applications: A Systematic Review," *Soft Robot.*, vol. 5, no. 1, pp. 1–16, 2018, doi: 10.1089/soro.2017.0046.
- [129] J. T. Meyer, S. O. Schrade, O. Lambercy, and R. Gassert, "User-centered Design and Evaluation of Physical Interfaces for an Exoskeleton for Paraplegic Users," in *2019 IEEE 16th International Conference on Rehabilitation Robotics (ICORR)*, Jun. 2019, pp. 1159–1166, doi: 10.1109/ICORR.2019.8779527.
- [130] R. J. Varghese, G. Mukherjee, R. King, S. Keller, and A. D. Deshpande, "Designing Variable Stiffness Profiles to Optimize the Physical Human Robot Interface of Hand Exoskeletons," in *2018 7th IEEE International Conference on Biomedical Robotics and Biomechanics (Biorob)*, Aug. 2018, pp. 1101–1108, doi: 10.1109/BIOROB.2018.8487862.
- [131] D. Zanutto, Y. Akiyama, P. Stegall, and S. K. Agrawal, "Knee Joint Misalignment in Exoskeletons for the Lower Extremities: Effects on User's Gait," *IEEE Trans. Robot.*, vol. 31, no. 4, pp. 978–987, Aug. 2015, doi: 10.1109/TRO.2015.2450414.
- [132] N. Jarrassé and G. Morel, "Connecting a Human Limb to an Exoskeleton," *IEEE Trans. Robot.*, vol. 28, no. 3, pp. 697–709, Jun. 2012, doi: 10.1109/TRO.2011.2178151.
- [133] Y. Akiyama, S. Okamoto, Y. Yamada, and K. Ishiguro, "Measurement of Contact Behavior Including Slippage of Cuff When Using Wearable Physical Assistant Robot," *IEEE Trans. Neural Syst. Rehabil. Eng.*, vol. 24, no. 7, pp. 784–793, Jul. 2016, doi: 10.1109/TNSRE.2015.2464719.
- [134] N. Bergstrom *et al.*, *Treatment of Pressure Ulcers. Clinical Practice Guideline*, No. 15. AH. Rockville, MD: DIANE Publishing, 1994.
- [135] F. Motamen Salehi, A. Neville, and M. Bryant, "Bio-tribology of incontinence management products: additional complexities at the skin–pad interface," *Tribol. - Mater. Surfaces Interfaces*, vol. 12, no. 4, pp. 193–199, Oct. 2018, doi: 10.1080/17515831.2018.1512784.
- [136] P. F. D. Naylor, "EXPERIMENTAL FRICTION BLISTERS.," *Br. J. Dermatol.*, vol. 67, no. 10, pp. 327–342, Oct. 1955, doi: 10.1111/j.1365-2133.1955.tb12657.x.
- [137] R. Mallat, M. Khalil, G. Venture, V. Bonnet, and S. Mohammed, "Human-Exoskeleton Joint Misalignment: A Systematic Review," in *2019 Fifth International Conference on Advances in Biomedical Engineering (ICABME)*, Oct. 2019, vol. 2019-October, pp. 1–4, doi: 10.1109/ICABME47164.2019.8940321.
- [138] D. L. Hettinga, "III. Normal Joint Structures and their Reactions to Injury," *J. Orthop. Sport. Phys. Ther.*, vol. 1, no. 3, pp. 178–185, Jan. 1980, doi: 10.2519/jospt.1980.1.3.178.

- [139] E. A. L. M. Verhagen, A. J. van der Beek, and W. van Mechelen, "The Effect of Tape, Braces and Shoes on Ankle Range of Motion," *Sport. Med.*, vol. 31, no. 9, pp. 667–677, 2001, doi: 10.2165/00007256-200131090-00003.
- [140] H. van der Kooij, E. H. F. van Asseldonk, J. Geelen, J. P. P. van Vugt, and B. R. Bloem, "Detecting asymmetries in balance control with system identification: first experimental results from Parkinson patients," *J. Neural Transm.*, vol. 114, no. 10, pp. 1333–1337, Oct. 2007, doi: 10.1007/s00702-007-0801-x.
- [141] J. A. M. Haarman *et al.*, "Paretic versus non-paretic stepping responses following pelvis perturbations in walking chronic-stage stroke survivors," *J. Neuroeng. Rehabil.*, vol. 14, no. 1, p. 106, Oct. 2017, doi: 10.1186/s12984-017-0317-z.
- [142] COVR, "8 reasons why you shouldn't carry our collision tests with your collaborative robot on your employees," 2019. <https://safearoundrobots.com/stories/8-reasons-why-you-shouldn-t-carry-out-collision-tests-with-your-collaborative-robot-on-your-employees/> (accessed Jul. 06, 2020).
- [143] International Organization for Standardization, *Robots and robotic devices – Safety requirements for personal care robots*. ISO 13482:2014, 2014.
- [144] Giannakopoulos, Suresh, and Chenut, "Similarities of stress concentrations in contact at round punches and fatigue at notches: implications to fretting fatigue crack initiation," *Fatigue Fract. Eng. Mater. Struct.*, vol. 23, no. 7, pp. 561–571, Jul. 2001, doi: 10.1046/j.1460-2695.2000.00306.x.
- [145] M. Huelke and H. J. Ottersbach, "How to approve collaborating robots - the IFA force pressure measurement system," in *7th International Conference on Safety of Industrial Automation Systems—SIAS*, 2012, pp. 11–12.
- [146] International Organization for Standardization, *Robots and robotic devices – Collaborative robots*. ISO/TS 15066:2016, 2016.
- [147] International Organization for Standardization, *Robotics – Application of ISO 13482 – Part 1: Safety-related test methods*. ISO/TR 23482-1:2020, 2020.
- [148] P. D. Wettenschwiler *et al.*, "Validation of an instrumented dummy to assess mechanical aspects of discomfort during load carriage," *PLoS One*, vol. 12, no. 6, p. e0180069, Jun. 2017, doi: 10.1371/journal.pone.0180069.
- [149] L. Pipkin, "Effect of model design, cushion construction, and interface pressure mats on interface pressure and immersion," *J. Rehabil. Res. Dev.*, vol. 45, no. 6, pp. 875–882, Dec. 2008, doi: 10.1682/JRRD.2007.06.0089.
- [150] E. W. Tam, A. F. Mak, W. N. Lam, J. H. Evans, and Y. Y. Chow, "Pelvic movement and interface pressure distribution during manual wheelchair propulsion," *Arch. Phys. Med. Rehabil.*, vol. 84, no. 10, pp. 1466–1472, Oct. 2003, doi: 10.1016/S0003-9993(03)00269-7.
- [151] D. P. Apatsidis, S. E. Solomonidis, and S. M. Michael, "Pressure distribution at the seating interface of custom-molded wheelchair seats: Effect of various materials," *Arch. Phys. Med. Rehabil.*, vol. 83, no. 8, pp. 1151–1156, Aug. 2002, doi: 10.1053/apmr.2002.33987.
- [152] T. Defloor, "The effect of position and mattress on interface pressure," *Appl. Nurs. Res.*, vol. 13, no. 1, pp. 2–11, Feb. 2000, doi: 10.1016/S0897-1897(00)80013-0.
- [153] T. Moysidis *et al.*, "Prevention of pressure ulcer: interaction of body characteristics and different mattresses," *Int. Wound J.*, vol. 8, no. 6, pp. 578–584, Dec. 2011, doi: 10.1111/j.1742-481X.2011.00814.x.
- [154] B. Hemmes, L. A. de Wert, P. R. G. Brink, C. W. J. Oomens, D. L. Bader, and M. Poeze, "Cytokine IL1 α and lactate as markers for tissue damage in spineboard immobilisation. A prospective, randomised open-label crossover trial," *J. Mech. Behav. Biomed. Mater.*, vol. 75, pp. 82–88, Nov. 2017, doi: 10.1016/j.jmbm.2017.06.026.

- [155] E. Al-Fakih, N. Abu Osman, and F. Mahmad Adikan, "Techniques for Interface Stress Measurements within Prosthetic Sockets of Transtibial Amputees: A Review of the Past 50 Years of Research," *Sensors*, vol. 16, no. 7, p. 1119, Jul. 2016, doi: 10.3390/s16071119.
- [156] V. Rajtukova, R. Hudak, J. Zivcak, P. Halfarova, and R. Kudrikova, "Pressure distribution in transtibial prostheses socket and the stump interface," in *Procedia Engineering*, Jan. 2014, vol. 96, pp. 374–381, doi: 10.1016/j.proeng.2014.12.106.
- [157] K. Huysamen, M. de Looze, T. Bosch, J. Ortiz, S. Toxiri, and L. W. O'Sullivan, "Assessment of an active industrial exoskeleton to aid dynamic lifting and lowering manual handling tasks," *Appl. Ergon.*, vol. 68, no. 4, pp. 125–131, Apr. 2018, doi: 10.1016/j.apergo.2017.11.004.
- [158] L. Levesque, S. Pardoel, Z. Lovrenovic, and M. Doumit, "Experimental comfort assessment of an active exoskeleton interface," in *2017 IEEE International Symposium on Robotics and Intelligent Sensors (IRIS)*, Oct. 2017, pp. 38–43, doi: 10.1109/IRIS.2017.8250095.
- [159] M. Xiloyannis, D. Chiaradia, A. Frisoli, and L. Masia, "Characterisation of pressure distribution at the interface of a soft exosuit: Towards a more comfortable wear," in *Biosystems and Biorobotics*, vol. 22, Springer International Publishing, 2019, pp. 35–38.
- [160] A. Rathore, M. Wilcox, D. Z. Morgado Ramirez, R. Loureiro, and T. Carlson, "Quantifying the human-robot interaction forces between a lower limb exoskeleton and healthy users," in *2016 38th Annual International Conference of the IEEE Engineering in Medicine and Biology Society (EMBC)*, Aug. 2016, pp. 586–589, doi: 10.1109/EMBC.2016.7590770.
- [161] J. G. Dabling, A. Filatov, and J. W. Wheeler, "Static and cyclic performance evaluation of sensors for human interface pressure measurement," in *2012 Annual International Conference of the IEEE Engineering in Medicine and Biology Society*, Aug. 2012, pp. 162–165, doi: 10.1109/EMBC.2012.6345896.
- [162] J. S. Schofield, K. R. Evans, J. S. Hebert, P. D. Marasco, and J. P. Carey, "The effect of biomechanical variables on force sensitive resistor error: Implications for calibration and improved accuracy," *J. Biomech.*, vol. 49, no. 5, pp. 786–792, Mar. 2016, doi: 10.1016/j.jbiomech.2016.01.022.
- [163] J. Bessler, L. Schaake, R. Kelder, J. H. Buurke, and G. B. Prange-Lasonder, "Prototype measuring device for assessing interaction forces between human limbs and rehabilitation robots - A proof of concept study," in *IEEE International Conference on Rehabilitation Robotics*, Jun. 2019, vol. 2019-June, pp. 1109–1114, doi: 10.1109/ICORR.2019.8779536.
- [164] M. Klaassen, E. G. de Vries, and M. A. Masen, "Friction in the contact between skin and a soft counter material: Effects of hardness and surface finish," *J. Mech. Behav. Biomed. Mater.*, vol. 92, no. September 2018, pp. 137–143, Apr. 2019, doi: 10.1016/j.jmbbm.2019.01.006.
- [165] L. A. de Wert, D. L. Bader, C. W. J. Oomens, L. Schoonhoven, M. Poeze, and N. D. Bouvy, "A new method to evaluate the effects of shear on the skin," *Wound Repair Regen.*, vol. 23, no. 6, pp. 885–890, Nov. 2015, doi: 10.1111/wrr.12368.
- [166] P. A. Lazzarini *et al.*, "Measuring Plantar Tissue Stress in People With Diabetic Peripheral Neuropathy: A Critical Concept in Diabetic Foot Management," *J. Diabetes Sci. Technol.*, vol. 13, no. 5, pp. 869–880, Sep. 2019, doi: 10.1177/1932296819849092.
- [167] M. Y. Cheng, C. L. Lin, Y. T. Lai, and Y. J. Yang, "A polymer-based capacitive sensing array for normal and shear force measurement," *Sensors (Switzerland)*, vol. 10, no. 11, pp. 10211–10225, 2010, doi: 10.3390/s101110211.
- [168] H. K. Lee, J. Chung, S. Il Chang, and E. Yoon, "Normal and shear force measurement using a flexible polymer tactile sensor with embedded multiple capacitors," *J. Microelectromechanical Syst.*, vol. 17, no. 4, pp. 934–942, 2008, doi: 10.1109/JMEMS.2008.921727.

- [169] P. Laszczak, L. Jiang, D. L. Bader, D. Moser, and S. Zahedi, "Development and validation of a 3D-printed interfacial stress sensor for prosthetic applications," *Med. Eng. Phys.*, vol. 37, no. 1, pp. 132–137, Jan. 2015, doi: 10.1016/j.medengphy.2014.10.002.
- [170] G. Liang, Y. Wang, D. Mei, K. Xi, and Z. Chen, "Flexible Capacitive Tactile Sensor Array with Truncated Pyramids as Dielectric Layer for Three-Axis Force Measurement," *J. Microelectromechanical Syst.*, vol. 24, no. 5, pp. 1510–1519, 2015, doi: 10.1109/JMEMS.2015.2418095.
- [171] J. Tang *et al.*, "A combined kinematic and kinetic analysis at the residuum/socket interface of a knee-disarticulation amputee," *Med. Eng. Phys.*, vol. 49, pp. 131–139, 2017, doi: 10.1016/j.medengphy.2017.08.014.
- [172] M. Valero *et al.*, "Interfacial pressure and shear sensor system for fingertip contact applications," *Healthc. Technol. Lett.*, vol. 3, no. 4, pp. 280–283, 2016, doi: 10.1049/htl.2016.0062.
- [173] P. Laszczak *et al.*, "A pressure and shear sensor system for stress measurement at lower limb residuum/socket interface," *Med. Eng. Phys.*, vol. 38, no. 7, pp. 695–700, 2016, doi: 10.1016/j.medengphy.2016.04.007.
- [174] A.-M. Georgarakis, R. Stampfli, P. Wolf, R. Riener, and J. E. Duarte, "A Method for Quantifying Interaction Forces in Wearable Robots," in *2018 7th IEEE International Conference on Biomedical Robotics and Biomechatronics (Biorob)*, Aug. 2018, pp. 789–794, doi: 10.1109/BIOROB.2018.8487701.
- [175] M. Aso, Y. Yamada, K. Yoshida, Y. Akiyama, and Y. Ito, "Evaluation of the mechanical characteristics of human thighs for developing complex dummy tissues," in *2013 IEEE International Conference on Robotics and Biomimetics (ROBIO)*, Dec. 2013, pp. 1450–1455, doi: 10.1109/ROBIO.2013.6739670.
- [176] X. Mao, Y. Yamada, Y. Akiyama, and S. Okamoto, "Characteristics of Dummy Skin Contact Mechanics During Developing Process of Skin Abrasion Trauma," *Tribol. Lett.*, vol. 65, no. 4, p. 133, Dec. 2017, doi: 10.1007/s11249-017-0916-7.
- [177] R. Behrens and G. Pliske, "Final Report Human-Robot Collaboration: Partial Supplementary Examination [of Pain Thresholds] for Their Suitability for Inclusion in Publications of the DGUV and Standardization," 2019. Accessed: Jul. 14, 2020. [Online]. Available: https://www.dguv.de/projekt Datenbank/0430/ab_18.12.2019_fp430_englisch.pdf.
- [178] M. Melia *et al.*, "Pressure pain thresholds: Subject factors and the meaning of peak pressures," *Eur. J. Pain*, vol. 23, no. 1, pp. 167–182, Jan. 2019, doi: 10.1002/ejp.1298.
- [179] A. Muttray, M. Melia, B. Geissler, J. König, and S. Letzel, "Wissenschaftlicher Schlussbericht zum Vorhaben FP-0317: 'Kollaborierende Roboter-Ermittlung der Schmerzempfindlichkeit an der Mensch-Maschine-Schnittstelle,'" Mainz, 2014. Accessed: Jul. 14, 2020. [Online]. Available: https://www.dguv.de/projekt Datenbank/0317/wissenschaftlicher_schlussbericht_final_18.12.2014.pdf.
- [180] J. Belda-Lois, R. Poveda, and M. J. Vivas, "Case study: Analysis of pressure distribution and tolerance areas for wearable robots," in *Wearable Robots: Biomechatronic Exoskeletons*, Chichester, UK: John Wiley and Sons, 2008, pp. 154–156.
- [181] T. Kermavnar, V. Power, A. de Eyto, and L. O'Sullivan, "Cuff Pressure Algometry in Patients with Chronic Pain as Guidance for Circumferential Tissue Compression for Wearable Soft Exoskeletons: A Systematic Review," *Soft Robot.*, vol. 5, no. 5, pp. 497–511, Oct. 2018, doi: 10.1089/soro.2017.0088.
- [182] T. Kermavnar, K. J. O'Sullivan, V. Casey, A. de Eyto, and L. W. O'Sullivan, "Circumferential tissue compression at the lower limb during walking, and its effect on discomfort, pain and tissue oxygenation: Application to soft exoskeleton design," *Appl. Ergon.*, vol. 86, no. March, 2020, doi: 10.1016/j.apergo.2020.103093.
- [183] T. Kermavnar, K. J. O'Sullivan, A. de Eyto, and L. W. O'Sullivan, "Discomfort/Pain and Tissue Oxygenation at the Lower Limb During Circumferential Compression: Application to Soft Exoskeleton Design," *Hum. Factors J. Hum. Factors Ergon. Soc.*, vol. 62, no. 3, pp. 475–488, May 2020, doi: 10.1177/0018720819892098.

- [184] P. F. D. Naylor, "THE SKIN SURFACE AND FRICTION.," *Br. J. Dermatol.*, vol. 67, no. 7, pp. 239–248, Jul. 1955, doi: 10.1111/j.1365-2133.1955.tb12729.x.
- [185] S. Derler and L.-C. Gerhardt, "Tribology of Skin: Review and Analysis of Experimental Results for the Friction Coefficient of Human Skin," *Tribol. Lett.*, vol. 45, no. 1, pp. 1–27, Jan. 2012, doi: 10.1007/s11249-011-9854-y.
- [186] E. Shaked and A. Gefen, "Modeling the Effects of Moisture-Related Skin-Support Friction on the Risk for Superficial Pressure Ulcers during Patient Repositioning in Bed," *Front. Bioeng. Biotechnol.*, vol. 1, p. 9, Oct. 2013, doi: 10.3389/fbioe.2013.00009.
- [187] J. M. Soucie *et al.*, "Range of motion measurements: reference values and a database for comparison studies," *Haemophilia*, vol. 17, no. 3, pp. 500–507, May 2011, doi: 10.1111/j.1365-2516.2010.02399.x.
- [188] D. Hahn, M. Olvermann, J. Richtberg, W. Seiberl, and A. Schwirtz, "Knee and ankle joint torque–angle relationships of multi-joint leg extension," *J. Biomech.*, vol. 44, no. 11, pp. 2059–2065, Jul. 2011, doi: 10.1016/j.jbiomech.2011.05.011.
- [189] D. E. Anderson, M. L. Madigan, and M. A. Nussbaum, "Maximum voluntary joint torque as a function of joint angle and angular velocity: Model development and application to the lower limb," *J. Biomech.*, vol. 40, no. 14, pp. 3105–3113, Jan. 2007, doi: 10.1016/j.jbiomech.2007.03.022.
- [190] J. A. Galvez *et al.*, "Measuring Human Trainers' Skill for the Design of Better Robot Control Algorithms for Gait Training after Spinal Cord Injury," in *9th International Conference on Rehabilitation Robotics, 2005. ICORR 2005.*, 2005, vol. 2005, pp. 231–234, doi: 10.1109/ICORR.2005.1501092.
- [191] J. F. Veneman, R. Kruidhof, E. E. G. Hekman, R. Ekkelenkamp, E. H. F. Van Asseldonk, and H. van der Kooij, "Design and Evaluation of the LOPES Exoskeleton Robot for Interactive Gait Rehabilitation," *IEEE Trans. Neural Syst. Rehabil. Eng.*, vol. 15, no. 3, pp. 379–386, Sep. 2007, doi: 10.1109/TNSRE.2007.903919.
- [192] Y. Takahashi, F. Matsuoka, H. Okuyama, and I. Imaizumi, "Development of Injury Probability Functions for the Flexible Pedestrian Legform Impactor," *SAE Int. J. Passeng. Cars - Mech. Syst.*, vol. 5, no. 1, pp. 2012-01–0277, Apr. 2012, doi: 10.4271/2012-01-0277.
- [193] T. Fujikawa, Y. Asano, T. Nishimoto, and R. Nishikata, "Static fracture tolerance of human metatarsal in being run over by robot," in *2017 IEEE/RSJ International Conference on Intelligent Robots and Systems (IROS)*, Sep. 2017, pp. 6935–6942, doi: 10.1109/IROS.2017.8206618.
- [194] A. Soni, A. Chawla, and S. Mukherjee, "Effect of muscle contraction on knee loading for a standing pedestrian in lateral impacts," 2007.
- [195] P. Eser, A. Frotzler, Y. Zehnder, and J. Denoth, "Fracture threshold in the femur and tibia of people with spinal cord injury as determined by peripheral quantitative computed tomography," *Arch. Phys. Med. Rehabil.*, vol. 86, no. 3, pp. 498–504, Mar. 2005, doi: 10.1016/j.apmr.2004.09.006.
- [196] A. H. A. Stienen, E. E. G. Hekman, F. C. T. van der Helm, and H. van der Kooij, "Self-Aligning Exoskeleton Axes Through Decoupling of Joint Rotations and Translations," *IEEE Trans. Robot.*, vol. 25, no. 3, pp. 628–633, Jun. 2009, doi: 10.1109/TRO.2009.2019147.
- [197] R. Rupp *et al.*, "Safety and Efficacy of At-Home Robotic Locomotion Therapy in Individuals with Chronic Incomplete Spinal Cord Injury: A Prospective, Pre-Post Intervention, Proof-of-Concept Study," *PLoS One*, vol. 10, no. 3, p. e0119167, Mar. 2015, doi: 10.1371/journal.pone.0119167.
- [198] M. Klaassen, "The static friction behaviour of skin with relevance to pressure ulcer prevalence," University of Twente, Enschede, The Netherlands, 2018.
- [199] H. Choi, K. Seo, S. Hyung, Y. Shim, and S.-C. Lim, "Compact Hip-Force Sensor for a Gait-Assistance Exoskeleton System," *Sensors*, vol. 18, no. 2, p. 566, Feb. 2018, doi: 10.3390/s18020566.
- [200] A. Manorama, R. Meyer, R. Wiseman, and T. R. Bush, "Quantifying the effects of external shear loads on

- arterial and venous blood flow: Implications for pressure ulcer development," *Clin. Biomech.*, vol. 28, no. 5, pp. 574–578, Jun. 2013, doi: 10.1016/j.clinbiomech.2013.04.001.
- [201] M. Shisheghar, D. Kerr, and J. Blake, "A systematic review of research into how robotic technology can help older people," *Smart Heal.*, vol. 7–8, pp. 1–18, Jun. 2018, doi: 10.1016/j.smhl.2018.03.002.
- [202] J. Bessler *et al.*, "Safety assessment of rehabilitation robots: A review identifying safety skills and current knowledge gaps," *Front. Robot. AI*, vol. 8, p. 33, 2021, doi: 10.3389/frobt.2021.602878.
- [203] M. B. Näf, K. Junius, M. Rossini, C. Rodriguez-Guerrero, B. Vanderborght, and D. Lefeber, "Misalignment Compensation for Full Human-Exoskeleton Kinematic Compatibility: State of the Art and Evaluation," *Appl. Mech. Rev.*, vol. 70, no. 5, pp. 1–19, Sep. 2018, doi: 10.1115/1.4042523.
- [204] S. V. Sarkisian, M. K. Ishmael, and T. Lenzi, "Self-Aligning Mechanism Improves Comfort and Performance With a Powered Knee Exoskeleton," *IEEE Trans. Neural Syst. Rehabil. Eng.*, vol. 29, pp. 629–640, 2021, doi: 10.1109/TNSRE.2021.3064463.
- [205] J. Li *et al.*, "Influence of a Compatible Design on Physical Human-Robot Interaction Force: a Case Study of a Self-Adapting Lower-Limb Exoskeleton Mechanism," *J. Intell. Robot. Syst.*, vol. 98, no. 2, pp. 525–538, May 2020, doi: 10.1007/s10846-019-01063-5.
- [206] M. A. Regalbuto, J. S. Rovick, and P. S. Walker, "The forces in a knee brace as a function of hinge design and placement," *Am. J. Sports Med.*, vol. 17, no. 4, pp. 535–543, Jul. 1989, doi: 10.1177/036354658901700415.
- [207] J. C. Singer and M. Lamontagne, "The effect of functional knee brace design and hinge misalignment on lower limb joint mechanics," *Clin. Biomech.*, vol. 23, no. 1, pp. 52–59, Jan. 2008, doi: 10.1016/j.clinbiomech.2007.08.013.
- [208] S. P. Hacker, F. Schall, A. Ignatius, and L. Dürselen, "The effect of knee brace misalignment on the anterior cruciate ligament," *Prosthetics Orthot. Int.*, vol. 43, no. 3, pp. 309–315, Jun. 2019, doi: 10.1177/0309364618824443.
- [209] W. T. Dempster and G. R. L. Gaughran, "Properties of body segments based on size and weight," *Am. J. Anat.*, vol. 120, no. 1, pp. 33–54, Jan. 1967, doi: 10.1002/aja.1001200104.
- [210] A. M. Spungen *et al.*, "Indications and Contraindications for Exoskeletal-Assisted Walking in Persons with Spinal Cord Injury," in *Proceedings of the 5th International Symposium on Wearable Robotics, WeRob2020*, J. C. Moreno, J. Masood, U. Schneider, C. Maufroy, and J. L. Pons, Eds. Online: Springer, 2021, pp. 227–231.
- [211] W. Yu, Y. Li, Y. P. Zheng, N. Y. Lim, M. H. Lu, and J. Fan, "Softness measurements for open-cell foam materials and human soft tissue," *Meas. Sci. Technol.*, vol. 17, no. 7, pp. 1785–1791, Jul. 2006, doi: 10.1088/0957-0233/17/7/017.
- [212] P. Jöhal, A. Williams, P. Wragg, D. Hunt, and W. Gedroyc, "Tibio-femoral movement in the living knee. A study of weight bearing and non-weight bearing knee kinematics using 'interventional' MRI," *J. Biomech.*, vol. 38, no. 2, pp. 269–276, Feb. 2005, doi: 10.1016/j.jbiomech.2004.02.008.
- [213] J. Bessler *et al.*, "COVR – Towards Simplified Evaluation and Validation of Collaborative Robotics Applications Across a Wide Range of Domains Based on Robot Safety Skills," in *Wearable Robotics: Challenges and Trends Proceedings of the 4th International Symposium on Wearable Robotics, WeRob2018, October 16-20, 2018, Pisa, Italy*, 2019, pp. 123–126, doi: 10.1007/978-3-030-01887-0_24.
- [214] M. Valori *et al.*, "Validating Safety in Human–Robot Collaboration: Standards and New Perspectives," *Robotics*, vol. 10, no. 2, p. 65, Apr. 2021, doi: 10.3390/robotics10020065.
- [215] P. Agarwal, M. S. Narayanan, L.-F. Lee, F. Mendel, and V. N. Krovci, "Simulation-Based Design of Exoskeletons Using Musculoskeletal Analysis," in *Volume 3: 30th Computers and Information in Engineering Conference, Parts A and B*, Jan. 2010, pp. 1357–1364, doi: 10.1115/DETC2010-28572.
- [216] B. Kim and A. D. Deshpande, "An upper-body rehabilitation exoskeleton Harmony with an anatomical

- shoulder mechanism: Design, modeling, control, and performance evaluation," *Int. J. Rob. Res.*, vol. 36, no. 4, pp. 414–435, Apr. 2017, doi: 10.1177/0278364917706743.
- [217] Y. Shiraishi, S. Okamoto, N. Yamada, K. Inoue, Y. Akiyama, and Y. Yamada, "Effective position of the rotation axis of an ankle stretching machine and the effect of misalignment," *J. Biomech. Sci. Eng.*, vol. 15, no. 4, pp. 20-00202-20–00202, 2020, doi: 10.1299/jbse.20-00202.
- [218] J. Bessler-Etten, L. Schaake, G. B. Prange-Lasonder, and J. H. Buurke, "Assessing effects of exoskeleton misalignment on knee joint load during swing using an instrumented leg simulator," *J. Neuroeng. Rehabil.*, vol. 19, no. 1, p. 13, Dec. 2022, doi: 10.1186/s12984-022-00990-z.
- [219] K. Jayawardana, N. C. Ovenden, and A. Cottenden, "Quantifying the Frictional Forces between Skin and Nonwoven Fabrics," *Front. Physiol.*, vol. 8, no. MAR, p. 107, Mar. 2017, doi: 10.3389/fphys.2017.00107.
- [220] R. Shimizu and Y. Nonomura, "Preparation of Artificial Skin that Mimics Human Skin Surface and Mechanical Properties," *J. Oleo Sci.*, vol. 67, no. 1, pp. 47–54, 2018, doi: 10.5650/jos.ess17152.
- [221] J. L. Sparkset al., "Use of Silicone Materials to Simulate Tissue Biomechanics as Related to Deep Tissue Injury," *Adv. Skin Wound Care*, vol. 28, no. 2, pp. 59–68, Feb. 2015, doi: 10.1097/01.ASW.0000460127.47415.6e.
- [222] J. C. Cool, "Biomechanics of orthoses for the subluxed shoulder," *Prosthet. Orthot. Int.*, vol. 13, no. 2, pp. 90–96, Jan. 1989, doi: 10.3109/03093648909078219.
- [223] C.-T. Li, C.-H. Chen, Y.-N. Chen, C.-H. Chang, and K.-H. Tsai, "Biomechanical evaluation of a novel wheelchair backrest for elderly people," *Biomed. Eng. Online*, vol. 14, no. 1, p. 14, Dec. 2015, doi: 10.1186/s12938-015-0008-6.
- [224] S. M. M. De Rossi et al., "Sensing Pressure Distribution on a Lower-Limb Exoskeleton Physical Human-Machine Interface," *Sensors*, vol. 11, no. 1, pp. 207–227, Dec. 2010, doi: 10.3390/s110100207.
- [225] R. Behrens, G. Pliske, M. Umbreit, S. Piatek, F. Walcher, and N. Elkmann, "A Statistical Model to Determine Biomechanical Limits for Physically Safe Interactions With Collaborative Robots," *Front. Robot. AI*, vol. 8, Feb. 2022, doi: 10.3389/frobt.2021.667818.
- [226] B. P. Boden, F. T. Sheehan, J. S. Torg, and T. E. Hewett, "Noncontact Anterior Cruciate Ligament Injuries: Mechanisms and Risk Factors," *Am. Acad. Orthop. Surg.*, vol. 18, no. 9, pp. 520–527, Sep. 2010, doi: 10.5435/00124635-201009000-00003.
- [227] P. Bhattacharya and G. H. Van Lenthe, "Experimental quantification of bone mechanics," in *Bone Substitute Biomaterials*, Elsevier, 2014, pp. 30–71.
- [228] A. Unnanuntana, B. J. Rebolledo, M. M. Khair, E. F. DiCarlo, and J. M. Lane, "Diseases Affecting Bone Quality: Beyond Osteoporosis," *Clin. Orthop. Relat. Res.*, vol. 469, no. 8, pp. 2194–2206, Aug. 2011, doi: 10.1007/s11999-010-1694-9.
- [229] L. N. Awad, A. Esquenazi, G. E. Francisco, K. J. Nolan, and A. Jayaraman, "The ReWalk ReStore™ soft robotic exosuit: a multi-site clinical trial of the safety, reliability, and feasibility of exosuit-augmented post-stroke gait rehabilitation," *J. Neuroeng. Rehabil.*, vol. 17, no. 1, p. 80, Dec. 2020, doi: 10.1186/s12984-020-00702-5.
- [230] A. Megía-García, A. J. Del-Ama, V. Lozano-Berrio, I. Sinovas-Alonso, N. Comino-Suárez, and A. Gil-Agudo, "Safety, Feasibility and Acceptance with HANK Ambulatory Robotic Exoskeleton in Incomplete Spinal Cord Injury Patients," 2022, pp. 935–939.
- [231] E. Read, C. Woolsey, C. A. McGibbon, and C. O'Connell, "Physiotherapists' Experiences Using the Ekso Bionic Exoskeleton with Patients in a Neurological Rehabilitation Hospital: A Qualitative Study," *Rehabil. Res. Pract.*, vol. 2020, pp. 1–8, Jan. 2020, doi: 10.1155/2020/2939573.
- [232] M. J. Highsmith et al., "Interventions to Manage Residual Limb Ulceration Due To Prosthetic Use in Individuals with Lower Extremity Amputation: A Systematic Review of the Literature," *Technol. Innov.*, vol.

- 18, no. 2, pp. 115–123, Sep. 2016, doi: 10.21300/18.2-3.2016.115.
- [233] International Organization for Standardization, “Guidance for ISO national standards bodies Engaging stakeholders and building consensus,” 2019.
- [234] International Organization for Standardization, “ISO - Deliverables,” 2022. <https://www.iso.org/deliverables-all.html> (accessed Apr. 12, 2022).
- [235] International Organization for Standardization, “ISO - ISO/TC 299 - Robotics,” 2022. <https://www.iso.org/committee/5915511.html> (accessed Apr. 12, 2022).
- [236] National Research Council of Italy *et al.*, *Guidelines for the development and use of safety testing procedures in human-robot collaboration*. CWA 17835: CEN Workshop Agreement, 2022.
- [237] Spanish National Research Council *et al.*, *Lower-limb wearable devices - Performance test method for walking on uneven terrain*. CWA 17664, 2021.
- [238] International Organization for Standardization, “ISO - ISO/AWI PAS 5672 - Robotics – Collaborative applications – Test methods for measuring forces and pressures in quasi-static and transient contacts between robots and human,” 2021. <https://www.iso.org/standard/82488.html> (accessed Apr. 12, 2022).
- [239] J. T. Meyer, R. Gassert, and O. Lamberg, “An analysis of usability evaluation practices and contexts of use in wearable robotics,” *J. Neuroeng. Rehabil.*, vol. 18, no. 1, p. 170, Dec. 2021, doi: 10.1186/s12984-021-00963-8.
- [240] K. Langlois *et al.*, “Integration of 3D Printed Flexible Pressure Sensors into Physical Interfaces for Wearable Robots,” *Sensors*, vol. 21, no. 6, p. 2157, Mar. 2021, doi: 10.3390/s21062157.
- [241] M. Teyssier, B. Parilusyan, A. Roudaut, and J. Steimle, “Human-Like Artificial Skin Sensor for Physical Human-Robot Interaction,” in *2021 IEEE International Conference on Robotics and Automation (ICRA)*, May 2021, pp. 3626–3633, doi: 10.1109/ICRA48506.2021.9561152.
- [242] A. Mündermann, C. O. Dyrby, D. D. D’Lima, C. W. Colwell, and T. P. Andriacchi, “In vivo knee loading characteristics during activities of daily living as measured by an instrumented total knee replacement,” *J. Orthop. Res.*, vol. 26, no. 9, pp. 1167–1172, Sep. 2008, doi: 10.1002/jor.20655.
- [243] J. N. Torrão, M. P. S. dos Santos, and J. A. Ferreira, “Instrumented knee joint implants: innovations and promising concepts,” *Expert Rev. Med. Devices*, vol. 12, no. 5, pp. 571–584, Sep. 2015, doi: 10.1586/17434440.2015.1068114.
- [244] M. R. Angerame, D. C. Holst, J. M. Jennings, R. D. Komistek, and D. A. Dennis, “Total Knee Arthroplasty Kinematics,” *J. Arthroplasty*, vol. 34, no. 10, pp. 2502–2510, Oct. 2019, doi: 10.1016/j.arth.2019.05.037.
- [245] A. Melendez-Calderon and S. Maggioni, “Challenges in Adaptive Robot-Assisted Gait Training: The Balancing Act of Minimizing Assistance While Preserving Safety,” in *Converging Clinical and Engineering Research on Neurorehabilitation IV*, D. Torricelli, M. Akay, and J. L. Pons, Eds. Springer, 2022, pp. 39–43.
- [246] L. Zhou *et al.*, “Lower limb exoskeleton parasitic force modeling and minimizing with an adaptive trajectory controller,” *Mech. Mach. Theory*, vol. 170, p. 104731, Apr. 2022, doi: 10.1016/j.mechmachtheory.2022.104731.
- [247] L. Zhou, Y. Li, and S. Bai, “A human-centered design optimization approach for robotic exoskeletons through biomechanical simulation,” *Rob. Auton. Syst.*, vol. 91, pp. 337–347, May 2017, doi: 10.1016/j.robot.2016.12.012.
- [248] M. Tröster, U. Schneider, T. Bauernhansl, J. Rasmussen, and M. S. Andersen, “Simulation Framework for Active Upper Limb Exoskeleton Design Optimization Based on Musculoskeletal Modeling Simulation Framework for Active Upper Limb Exoskeleton Design Optimization Based on Musculoskeletal Modeling,” in *Technische Unterstützungssysteme, die die Menschen wirklich wollen*, 2018, pp. 345–353.
- [249] E. P. Grabke, K. Masani, and J. Andrysek, “Lower Limb Assistive Device Design Optimization Using Musculoskeletal Modeling: A Review,” *J. Med. Device.*, vol. 13, no. 4, Dec. 2019, doi: 10.1115/1.4044739.

&

- [250] M. Cifrek, V. Medved, S. Tonković, and S. Ostojić, "Surface EMG based muscle fatigue evaluation in biomechanics," *Clin. Biomech.*, vol. 24, no. 4, pp. 327–340, May 2009, doi:10.1016/j.clinbiomech.2009.01.010.
- [251] F. Hashmi, B. S. Richards, S. Forghany, A. L. Hatton, and C. J. Nester, "The formation of friction blisters on the foot: the development of a laboratory-based blister creation model," *Ski. Res. Technol.*, vol. 19, no. 1, pp. e479–e489, Feb. 2013, doi: 10.1111/j.1600-0846.2012.00669.x.



LIST OF ABBREVIATIONS

AE	Adverse event
AIMDD	Active Implantable Medical Devices Directive
ASIA	American Spinal Injury Association
BMI	Body mass index
BWS	Body-weight support
CE	Conformité Européenne
CEN	European Committee for Electrotechnical Standardization
Cobot	Collaborative robot
CP	Cerebral palsy
CWA	CEN Workshop Agreement
DDT	Discomfort detection threshold
DOF	Degrees of freedom
endVAS	VAS at end of trial
EU	European Union
EUDAMED	European database on medical devices
FAC	Functional ambulation category
FDA	Food and Drug Administration of the United States
FSRs	Force Sensitive Resistors
FT	Force and torque
GCP	Good Clinical Practice
HRI	Human-robot interaction
IEC	International Electrotechnical Commission
ILS	Instrumented leg simulator
IQR	Interquartile ranges
ISO	International Organisation for Standardisation
M	Mean
MA	Misalignment
MAUDE	Manufacturer and User Facility Device Experience
MDD	Medical Device Directive
MDR	Medical Device Regulation
MS	Multiple sclerosis
PAS	Publicly Available Specification
PD	Parkinson's disease
PDT	Pain detection threshold
PFL	Power and Force Limiting
pHRI	Physical human-robot interaction
PMCF	Post market clinical follow-up
RACA robot	rehabilitation, assessment, compensation and alleviation robot
RAGT	Robot-assisted gait training
RCT	Randomized controlled trial
repN	Repetitive normal force pattern
repNS	Repetitive normal and shear force pattern

SAE	Serious adverse event
SCI	Spinal cord injury
SD	Standard deviation
SG	Specific gravity
SRMS	Safety-Rated Monitored Stop
SSM	Speed and Separation Monitoring
TBI	Traumatic brain injury
tDDT	Time to DDT
VAS	Visual analog scale
VAS10	VAS after 10 minutes
VAS20	VAS after 20 minutes
VASslope	Slope of VAS development over time



SUMMARY

In recent years, various robotic devices have been developed to be used in rehabilitation, assist patients, compensate for or alleviate disabilities. Those rehabilitation robots interact very closely with humans and transfer energy to their body to fulfil their purpose. This naturally introduces risks which have to be assessed carefully as rehabilitation robot use should be safe for patients and healthcare professionals. How can the safety of rehabilitation robots be ensured? This question needs to be answered for each device under development before it can go to market and be implemented in clinical practice. Safety certification is perceived as difficult for many rehabilitation robot developers. To shed light on safety challenges in rehabilitation robotics and take first steps towards addressing those challenges, the research presented in this thesis focused on the following research questions (**Chapter 1**):

1. **What are the most pressing risks and safety issues in rehabilitation robotics?**
2. **How can those safety issues be avoided or managed?**
3. **What are suitable methods to quantify metrics relevant for the identified safety issues?**
4. **What are acceptable limit values to guarantee the safety of rehabilitation robot use?**

In **Chapter 2**, the question on the most pressing safety issues was approached by means of a systematic literature review. We analyzed the occurrence and type of adverse events during the use of stationary robotic gait trainers to cover one common type of rehabilitation robots. The review included 50 studies involving 985 subjects. We noticed that information about adverse events is often incomplete or lacking completely. We found that soft tissue-related injuries and musculoskeletal complaints were the most commonly reported adverse events. Further analyses (**Chapter 3**) revealed that those are also the most frequently reported issues in other devices and that injuries in rehabilitation robot use can often be attributed to excessive forces applied to the human body by the device. More specifically, excessive loads on the soft tissue level and on the musculoskeletal level were identified as the most relevant hazards in physical interaction between humans and rehabilitation robots. We further identified important factors which can potentially lead to excessive force application, such as exceeding the anatomical range of motion and misalignments between the device and the anatomical structures of the user.

There can be many technical approaches to manage or avoid a certain safety issue and the solutions are often very individual and dependent on the device. Nevertheless, we joined forces with four other research and technology organizations within the EU-funded COVR project to approach safety on a system level and develop guidelines which are universally applicable across various domains dealing with robots that closely interact with humans. The approach is described in detail in **Chapter 3**. Next to following the applicable directives and regulations (for rehabilitation robotics, the Medical Device Regulation applies) and implementing procedures for risk management laid down in standards, (rehabilitation) robot developers can perform validation experiments. Instead of focusing on the exact technical implementation of a risk reduction measure, those validation experiments can be designed in such a way that a certain behavior is tested on the system level. We combined the knowledge about adverse event occurrence and risk factors with experience regarding safety validation experiments in other domains to develop step-by-step procedures for testing the safety of rehabilitation robots. During this process, it became apparent, that there is a lack of knowledge on measurement techniques and

devices to assess the forces of interest and on safe limit values for those forces.

To fill some of the knowledge gaps regarding testing procedures, a prototype measuring device was developed to assess the force interplay between a human arm and a splint. The proof of concept study presented in **Chapter 4** describes the measuring device based on force sensitive resistors and a force/torque sensor and discusses some drawbacks and potential improvement options. Force sensitive resistors are fairly cheap and easy to use but issues such as hysteresis and the loss of information when forces are transmitted between the sensing areas of the sensors limit their reliability when used at the contact interface of rehabilitation robots. Load cells are reliable and can measure forces in all directions, but are not slim enough to be used at the skin-robot interface. To accurately investigate the safety-relevant force interplay at the human-robot interface on the soft tissue level, thin and flexible sensors are needed. Those sensors should be able to record normal and shear stresses and should not alter the interface.

A direct assessment of loads on the musculoskeletal system *in vivo* is almost impossible. **Chapter 5 and Chapter 6** therefore focused on ways to assess these loads with an instrumented leg simulator (dummy), specifically focusing on the risk factor misalignment. The leg simulator developed for this study was equipped with a 6 degrees of freedom force and torque sensor to assess the loads on its knee joint. We attached a passive knee brace to the leg simulator and imposed misalignments (internal/external rotation, proximal/distal translation, anteroposterior translation) to assess their effects on joint load during swing. In **Chapter 5**, those experiments were performed with the original leg simulator, equipped with a polyurethane foam to mimic soft tissue. In **Chapter 6**, we repeated the experiments (excluding anteroposterior translational misalignment) with 3 additional materials to mimic soft tissue, namely one softer foam and two silicone/gel materials which were harder than the original foam and had been suggested as suitable materials to mimic soft tissue behavior in literature. We found that misalignments of a leg exoskeleton in each of the investigated directions can increase internal knee forces and torques during swing to a multiple of those experienced in a well-aligned situation. The investigations further showed that those changes in joint loads induced by misalignments are significantly affected by the characteristics of (artificial) soft tissue. There was a tendency for stronger increases of peak joint loads in harder materials. This research showed that dummies can be a suitable tool to measure joint loads. Future research should work towards improving the accuracy with which dummies simulate the physical human-robot interaction.

The study presented in **Chapter 7** focused on investigating how loads applied by rehabilitation robotics affect comfort and safety. More specifically, we investigated how discomfort develops and changes over time when forces are exerted repetitively and for extended durations through a rigid cuff. The experimental cuff and the exerted force patterns were based on what is known about the interaction with gait exoskeletons. Three force patterns were applied to healthy participants (n=15) of two age groups, who continuously indicated their perceived (dis-)comfort on a visual analog scale during each force pattern. A baseline trial was used to detect each participant's individual discomfort detection threshold. The two other trials consisted of repetitive forces applied for 30 minutes (normal force only and normal and shear force combined) and the magnitudes were based on the individual discomfort detection threshold. The discomfort detection thresholds (median 100 N; range 40 N to >230 N) and times to discomfort detection in repetitive force trials (median 4.1 minutes in repetitive normal force and 5.4 minutes in repetitive normal and shear force) varied strongly between participants. The force

applications resulted in skin reddening but usually no pain. No relationships between discomfort and age group, force pattern, environmental conditions or other participant characteristics were found. There were no significant differences between the two repetitive force patterns. We saw that discomfort increases over time when a force that is perceived as slightly uncomfortable in one single contact is applied repetitively.

Finally, in **Chapter 8**, the main findings of this thesis are discussed, giving rise to recommendations for future research and development concerning mechanical safety of rehabilitation robots. In addition, implications for clinical practice and (guidelines for) safety assessments are presented. While this research has taken steps in several directions to close knowledge gaps and simplify safety assessments in rehabilitation robots, a number of issues remain. We found that excessive loads on the soft tissue and musculoskeletal tissue can be considered the most relevant hazards in physical interaction between rehabilitation robots and their users. The nature of interaction in rehabilitation robotics, characterized by continuous contacts, cyclic loading, vulnerable users, and sometimes uncontrolled environments, makes safety considerations complex. Even relatively small forces can lead to hazardous situations when they are e.g. applied for long durations, to impaired body structures, in interfaces with peak stresses or unfavorable microclimates. Safety validation experiments can be a useful approach to test physical human-robot interaction, preferably without a human in the loop, and develop mitigation strategies to reduce (peak) stresses and loads. We have discussed that additional research is required to accurately measure force distributions in all relevant directions at the contact interface between human and robot without affecting the force interplay. It has been established that misalignments are a prominent issue in exoskeleton use. While we have shown that misalignments can affect knee joint loads significantly in a dummy during swing, further research should investigate whether misalignment would lead to (potentially) harmful loads in weightbearing situations. Our research showed that discomfort increases over time when repetitive loads are applied through an exoskeleton cuff-like interface. Perception of comfort varies considerably between subjects. While it will be difficult to establish generally applicable guidelines for acceptable time-force relationships, future research can extend current knowledge by covering larger subject groups including patients, and other force patterns.

The research in this thesis provided valuable insights into current safety issues and research gaps regarding rehabilitation robot safety. It is a first step towards building a knowledge base which can support the development and market entrance of safer rehabilitation robots through comprehensive guidelines.

SAMENVATTING

In de afgelopen jaren zijn verschillende robotische systemen ontwikkeld voor gebruik tijdens revalidatie, om patiënten te helpen, om beperkingen te compenseren, of te verlichten. Deze revalidatiebots werken in zeer nauwe samenspraak met mensen en brengen energie over op het lichaam van de patiënt om hun doel te bereiken. Dit brengt uiteraard risico's met zich mee die zorgvuldig moeten worden beoordeeld, aangezien het gebruik van revalidatiebots veilig moet zijn voor patiënten en zorgprofessionals. Hoe kan de veiligheid van revalidatiebots worden gewaarborgd? Deze vraag moet voor elk apparaat in ontwikkeling worden beantwoord voordat het op de markt kan worden gebracht en in de klinische praktijk kan worden toegepast. Veiligheids certificering wordt door veel ontwikkelaars van revalidatiebots als moeilijk ervaren. Om licht te werpen op de uitdagingen m.b.t. veiligheid van revalidatiebots en om de eerste stappen te zetten om deze uitdagingen aan te pakken, richtte het onderzoek in dit proefschrift zich op de volgende onderzoeksvragen (**Hoofdstuk 1**):

1. **Wat zijn de meest urgente risico's en veiligheidsproblemen bij revalidatiebots?**
2. **Hoe kunnen deze veiligheidsproblemen worden vermeden of beheerd?**
3. **Wat zijn geschikte methoden om uitkomstmaten te kwantificeren die relevant zijn voor de geïdentificeerde veiligheidsproblemen?**
4. **Wat zijn aanvaardbare grenswaarden om de veiligheid van het gebruik van revalidatiebots te garanderen?**

In **Hoofdstuk 2** werd de vraag naar de meest urgente veiligheidsproblemen benaderd door middel van een systematisch literatuuronderzoek. We analyseerden het vóórkomen en de aard van ongewenste voorvallen tijdens het gebruik van stationaire looprobots, aangezien dat een veelvoorkomend type revalidatiebot is. Het onderzoek omvatte 50 studies waarbij 985 proefpersonen betrokken waren. Het viel ons op dat informatie over ongewenste voorvallen vaak onvolledig is of geheel ontbreekt. Het bleek dat letsels aan weke delen en klachten van het spierskeletstelsel de vaakst gemelde ongewenste voorvallen waren. Uit verdere analyses (**Hoofdstuk 3**) bleek dat dit ook de meest gerapporteerde problemen zijn bij andere hulpmiddelen en dat letsel bij het gebruik van revalidatiebots vaak kan worden toegeschreven aan excessieve krachten die door het apparaat op het menselijk lichaam worden uitgeoefend. Meer specifiek werd excessieve belasting van de weke delen en van het bewegingsapparaat geïdentificeerd als de meest relevante gevaren in de fysieke interactie tussen mensen en revalidatiebots. Verder hebben we relevante factoren geïdentificeerd die kunnen leiden tot excessieve interactiekrachten, zoals het overschrijden van het anatomische bewegingsbereik en verkeerde uitlijning tussen het apparaat en de anatomische structuren van de gebruiker.

Er kunnen vele technische benaderingen zijn om een bepaald veiligheidsprobleem te beheersen of te vermijden en de oplossingen zijn vaak zeer individueel en afhankelijk van het hulpmiddel. Niettemin hebben wij binnen het door de EU gefinancierde COVR-project onze krachten gebundeld met vier andere onderzoeks- en technologieorganisaties, om veiligheid op systeemniveau te benaderen en richtsnoeren te ontwikkelen die universeel toepasbaar zijn in verschillende domeinen die te maken hebben met robots die nauw samenwerken met mensen (collaboratieve robots, of cobots). De aanpak wordt in detail beschreven in **Hoofdstuk 3**. Naast het volgen van de geldende richtlijnen en verordeningen (voor revalidatiebots is de Medical Device Regulation van toepassing) en het toepassen van procedures

voor risicobeheer die in normen zijn vastgelegd, kunnen (revalidatie)robotontwikkelaars validatietesten uitvoeren. In plaats van zich te richten op de exacte technische implementatie van een risicobeperkende maatregel, kunnen die validatietesten zo worden opgezet dat een bepaald gedrag op systeemniveau wordt getest. Wij hebben de kennis over het optreden van ongewenste voorvallen en risicofactoren gecombineerd met ervaring in veiligheidstesten in andere domeinen om stapsgewijze procedures te ontwikkelen voor het testen van de veiligheid van revalidatierobots. Tijdens dit proces werd duidelijk dat er een gebrek is aan kennis over meettechnieken en apparatuur om de betreffende krachten te beoordelen en over veilige grenswaarden voor die krachten.

Om enkele hiaten in de kennis over testprocedures op te vullen, werd een prototype meetinstrument ontwikkeld om de interactiekrachten tussen een menselijke arm en een spalk te onderzoeken. De in **Hoofdstuk 4** gepresenteerde proof-of-concept studie beschrijft het meetapparaat op basis van dunne druksensoren (force sensitive resistors, FSRs) en een kracht/momentsensor. Enkele nadelen en mogelijke verbeteringen worden daarbij besproken. FSRs zijn vrij goedkoop en gemakkelijk te gebruiken, maar problemen zoals hysteresis en het verlies van informatie wanneer krachten worden overgedragen tussen de meetgebieden van de sensoren beperken hun betrouwbaarheid bij gebruik op de interface tussen mens en revalidatierobot. Load cells zijn betrouwbaar en kunnen krachten in alle richtingen meten, maar zijn niet slank genoeg voor gebruik op de huid-robot interface. Om nauwkeurig te kunnen onderzoeken hoe interactiekrachten tussen mens en robot het risico op beschadiging van weke delen beïnvloeden, zijn dunne en flexibele sensoren nodig. Die sensoren moeten normaal- en schuifkrachten kunnen registreren en mogen de interface niet veranderen.

Het direct meten van de belasting op het bewegingsapparaat *in vivo* is vrijwel onmogelijk. **Hoofdstuk 5** en **Hoofdstuk 6** waren daarom gericht op manieren om deze belasting te meten met een geïnstrumenteerde beensimulator (dummy), waarbij specifiek aandacht werd besteed aan het risico van een onjuiste uitlijning van de robot ten opzicht van de menselijke anatomie. De beensimulator was uitgerust met een kracht- en momentsensor met 6 vrijheidsgraden om de belasting in het kniegewricht te kwantificeren. We bevestigden een passieve kniebrace om de beensimulator met verschillende richting en mate van (onjuiste) uitlijning (interne/externe rotatie, proximale/distale translatie, antero-posterieure translatie) om de effecten daarvan op de gewrichtsbelasting tijdens de zwaafase te beoordelen. In **Hoofdstuk 5** zijn deze experimenten uitgevoerd met de eerste versie van de beensimulator, voorzien van polyurethaanschuim om zacht weefsel (huid, spieren, etc.) na te bootsen. In **Hoofdstuk 6** herhaalden we de experimenten (exclusief verschillende mate van antero-posterieure uitlijning) met drie extra materialen om zacht weefsel na te bootsen, namelijk een zachter schuim en twee silicone/gelmaterialen. De gelmaterialen waren harder dan het oorspronkelijke schuim en zijn in de literatuur voorgesteld als geschikte materialen om menselijk zacht weefsel na te bootsen. Uit deze experimenten bleek dat een verkeerde uitlijning van een beenexoskelet in elk van de onderzochte richtingen de interne kniekrachten en -momenten tijdens de zwaafase kan vervelvoudigen in vergelijking met een goed uitgelijnde situatie. Uit het onderzoek bleek verder dat die veranderingen in gewrichtsbelasting als gevolg van verkeerde uitlijning sterk worden beïnvloed door de eigenschappen van (kunstmatige) weke delen. Er was een tendens tot sterkere toename van de piekbelasting in de knie bij hardere materialen. Uit dit onderzoek bleek verder dat dummy's een geschikt instrument kunnen zijn om belasting op het spier-skeletstelsel te meten. Toekomstig onderzoek is nodig om de nauwkeurigheid waarmee dummy's de fysieke mens-robot interactie simuleren te kunnen verbeteren.

De in **Hoofdstuk 7** gepresenteerde studie richtte zich op het onderzoeken van de invloed van belasting door revalidatierobots op comfort en veiligheid. Meer specifiek onderzochten we hoe ervaren ongemak verandert in de tijd wanneer herhaaldelijk en langdurig krachten worden uitgeoefend via een stijve manchet. Het gekozen manchet en de ingestelde krachtpatronen waren gebaseerd op wat bekend is over de interactie met loopexoskeletten. Drie krachtpatronen werden toegepast bij gezonde deelnemers (n=15) van twee leeftijdsgroepen (ouder en jonger), die tijdens elk krachtpatroon continu hun ervaren ongemak aangaven op een visuele analoge schaal. Tijdens een basistest werd de individuele waarde waarop iemand ongemak gaat ervaren (discomfort detection threshold, DDT) bepaald. De twee andere testen bestonden uit herhaalde krachtoefening gedurende 30 minuten (alleen normaalkracht en normaal- en schuifkracht gecombineerd) met krachtniveaus gebaseerd op de individuele DDT. De kracht ten tijde van de DDT (mediaan 100 N; range 40 N tot >230 N) en de tijd tot DDT (mediaan 4,1 minuten bij repetitieve normaalkracht en 5,4 minuten bij repetitieve normaal- en schuifkracht) varieerden sterk tussen de deelnemers. De toegepaste interactiekrachten leidden tot een rode huid, maar meestal niet tot pijn. Er werd geen verband gevonden tussen ervaren ongemak en leeftijdsgroep, krachtpatroon, omgevingsomstandigheden of andere kenmerken van de deelnemers. Er waren geen significante verschillen tussen de twee herhaalde krachtpatronen. We zagen dat het ervaren ongemak in de tijd toeneemt wanneer een kracht, die bij één enkel contact als licht ongemakkelijk wordt ervaren, herhaaldelijk wordt uitgeoefend.

Tot slot worden in **Hoofdstuk 8** de belangrijkste bevindingen van dit proefschrift besproken, die aanleiding geven tot aanbevelingen voor toekomstig onderzoek en ontwikkeling met betrekking tot mechanische veiligheid van revalidatierobots. Daarnaast worden implicaties voor de klinische praktijk en (richtlijnen voor) veiligheidsbeoordelingen gepresenteerd. Hoewel dit onderzoek stappen heeft gezet in verschillende richtingen om leemtes in de kennis op te vullen en het testen van veiligheid van revalidatierobots te vereenvoudigen, blijven er een aantal uitdagingen bestaan. Wij hebben gevonden dat overmatige belasting van het zachte weefsel en het spier-skeletstelsel als de meest relevante gevaren kunnen worden beschouwd bij fysieke interactie tussen revalidatierobots en hun gebruikers. De aard van de interactie bij revalidatierobots, gekenmerkt door langdurig contact, cyclische belasting, kwetsbare gebruikers en soms ongecontroleerde omgevingen, maakt veiligheidsoverwegingen complex. Zelfs relatief kleine krachten kunnen tot gevaarlijke situaties leiden wanneer zij bijvoorbeeld gedurende lange tijd worden uitgeoefend op beschadigde lichaamsstructuren, in interfaces met piekbelastingen of ongunstige microklimaten. Veiligheid beoordelen door validatietesten kan een nuttige aanpak zijn om de fysieke mens-robot-interactie te meten, bij voorkeur zonder directe betrokkenheid van de mens. Hiermee kunnen vervolgens mitigatiestrategieën ontwikkeld worden om (piek)belasting op het lichaam te verminderen.

Aanvullend onderzoek is nodig om de krachtverdeling in alle relevante richtingen op het raakvlak tussen mens en robot nauwkeurig te meten zonder de interactiekrachten te beïnvloeden. Uit ons onderzoek blijkt dat onjuiste uitlijning een belangrijk probleem is bij het gebruik van exoskeletten. Hoewel wij hebben aangetoond dat verkeerde uitlijning de belasting van het kniegewricht in een dummy tijdens de zwaai aanzienlijk kan beïnvloeden, moet verder onderzoek uitwijzen of verkeerde uitlijning leidt tot (potentieel) schadelijke belasting in situaties waarbij gewicht wordt gedragen op het (dummy) been. Ons onderzoek toonde verder aan dat ervaren ongemak over tijd toeneemt wanneer herhaalde belasting wordt uitgeoefend op het been via een exoskelet-achtige interface. De perceptie van comfort verschilt

aanzienlijk tussen proefpersonen. Hoewel het moeilijk zal zijn algemeen geldende richtlijnen vast te stellen voor aanvaardbare tijd-krachtrelaties, kan toekomstig onderzoek de huidige kennis uitbreiden door grotere groepen proefpersonen te betrekken, waaronder patiënten, en andere krachtpatronen toe te passen.

Het onderzoek in dit proefschrift heeft waardevolle inzichten opgeleverd in de huidige veiligheidsproblemen en kennishiaten met betrekking tot de veiligheid van revalidatierobots. Het is een eerste stap naar het bouwen van een kennisbasis die de ontwikkeling en marktintroductie van veiligere revalidatierobots kan ondersteunen door middel van uitgebreide richtlijnen.

ZUSAMMENFASSUNG

In den letzten Jahren wurden verschiedene Rehabilitationsroboter entwickelt, die eingesetzt werden, um Patienten zu unterstützen, Behinderungen zu kompensieren oder deren Auswirkungen zu lindern. Diese interagieren sehr eng mit dem Menschen und übertragen mechanische Energie auf seinen Körper, um ihren Zweck erfüllen zu können. Dies bringt Risiken mit sich, die sorgfältig bewertet werden müssen, da der Einsatz von Rehabilitationsrobotern für Patienten und medizinisches Fachpersonal sicher sein sollte. Es muss für jedes in der Entwicklung befindliche Gerät vor Marktreife und Einsatz in der klinischen Praxis beantwortet werden, wie diese Sicherheit gewährleistet werden kann. Die Sicherheitszertifizierung wird von vielen Entwicklern von Rehabilitationsrobotern als schwierig empfunden. Um die Sicherheits Herausforderungen in der Rehabilitationsrobotik zu beleuchten und erste Schritte zur Bewältigung dieser Herausforderungen zu unternehmen, konzentrierte sich die in dieser Arbeit vorgestellte Forschung auf die folgenden Forschungsfragen (**Kapitel 1**):

- 1. Was sind die relevantesten Risiken und Sicherheitslücken in der Rehabilitationsrobotik?**
- 2. Wie können diese Sicherheitsprobleme vermieden oder bewältigt werden?**
- 3. Was sind geeignete Methoden zur Quantifizierung von Messgrößen, die für die identifizierten Sicherheitslücken relevant sind?**
- 4. Was sind akzeptable Grenzwerte, um die Sicherheit des Einsatzes von Rehabilitationsrobotern zu gewährleisten?**

In **Kapitel 2** wurde die Frage nach den relevantesten Sicherheitsproblemen mit Hilfe einer systematischen Literaturanalyse angegangen. Wir analysierten das Auftreten und die Art von unerwünschten Ereignissen bei der Verwendung von stationären robotergestützten Gangtrainern, die einen gängigen Typ von Rehabilitationsrobotern darstellen. In die Literaturstudie wurden 50 Studien mit 985 Probanden einbezogen. Wir stellten fest, dass die Informationen über unerwünschte Ereignisse oft unvollständig sind oder sogar ganz fehlen. Die am häufigsten beschriebenen unerwünschten Ereignisse waren Weichteilverletzungen und Beschwerden des Bewegungsapparats. Weitere Analysen (**Kapitel 3**) ergaben, dass dies auch die am häufigsten gemeldeten Probleme bei anderen Arten von robotergestützten Therapiegeräten sind und dass Verletzungen beim Einsatz von Rehabilitationsrobotern häufig auf übermäßige Kräfte zurückzuführen sind, die vom Gerät auf den menschlichen Körper ausgeübt werden. Auf Basis davon wurden übermäßige Belastungen auf der Weichteilebene und auf der Ebene des Bewegungsapparats als die wichtigsten Gefahren bei der physischen Interaktion zwischen Menschen und Rehabilitationsrobotern identifiziert. Darüber hinaus haben wir wichtige Faktoren identifiziert, die zu einer übermäßigen Krafteinwirkung führen können, wie z. B. die Überschreitung des anatomischen Bewegungsausmaßes und Fehlausrichtungen zwischen dem Gerät und den anatomischen Strukturen des Benutzers.

Es kann viele technische Ansätze geben, um ein bestimmtes Sicherheitsproblem zu bewältigen oder zu vermeiden. Die Lösungen sind oft sehr individuell und vom jeweiligen Gerät abhängig. Dennoch haben wir uns im Rahmen des von der EU finanzierten COVR-Projekts mit vier anderen Forschungs- und Technologieorganisationen zusammengetan, um die Sicherheit auf der Systemebene zu betrachten und Richtlinien zu entwickeln, die in verschiedenen Bereichen, in denen Roboter eng mit Menschen interagieren (kollaborative Roboter), universell anwendbar sind. Dieser Ansatz wird in **Kapitel 3**

ausführlich beschrieben. Neben der Einhaltung der geltenden Richtlinien und Verordnungen (für die Rehabilitationsrobotik gilt die Medizinprodukteverordnung, MDR) und der Umsetzung von in Normen festgelegten Verfahren für das Risikomanagement, können Entwickler von (Rehabilitations-)Robotern Prüfungen zur Validierung durchführen. Anstatt sich auf die genaue technische Umsetzung einer Risikominderungsmaßnahme zu konzentrieren, können diese Prüfungen so gestaltet werden, dass ein bestimmtes Verhalten auf Systemebene getestet wird. Wir haben das Wissen über das Auftreten von unerwünschten Ereignissen und Risikofaktoren im Rehabilitationsbereich mit den Erfahrungen aus Sicherheitsprüfungen in anderen Bereichen kombiniert, um Schritt-für-Schritt Protokolle für die Sicherheitsprüfung von Rehabilitationsrobotern zu entwickeln. Während dieses Prozesses wurde deutlich, dass es an Wissen über Messtechniken und -geräte zur Bewertung der relevanten Kräfte und über sichere Grenzwerte für diese Kräfte mangelt.

Um erste Wissenslücken in Bezug auf die Testverfahren zu schließen, wurde der Prototyp eines Messgeräts entwickelt, mit dem das Zusammenspiel der Kräfte zwischen einem menschlichen Arm und einer Schiene beurteilt werden kann. Die in **Kapitel 4** vorgestellte Proof-of-Concept-Studie beschreibt das Messgerät, das auf dünnen Drucksensoren (force sensitive resistors, FSRs) und einem Kraft-/Drehmomentsensor basiert. Einige Nachteile des Prototyps und mögliche Verbesserungsoptionen werden in diesem Kapitel erörtert. FSRs sind relativ kostengünstig und einfach zu verwenden. Allerdings schänken Probleme wie Hysterese und der Verlust von Informationen bei der Übertragung von Kräften zwischen den Messbereichen der Sensoren ihre Zuverlässigkeit bei der Verwendung an der Mensch-Roboter-Schnittstelle ein. Kraftsensoren sind zuverlässig und können Kräfte in alle Richtungen messen, sind aber nicht dünn genug, um an der Haut-Roboter-Schnittstelle eingesetzt zu werden. Um das sicherheitsrelevante Zusammenspiel von Kräften an der Mensch-Roboter-Schnittstelle auf der Weichteilebene genau zu untersuchen, werden dünne und flexible Sensoren benötigt. Diese Sensoren sollten in der Lage sein, Normal- und Scherkräfte zu erfassen und das Zusammenspiel der Kräfte an der Schnittstelle nicht verändern.

Eine direkte Auswertung der Belastungen auf den Bewegungsapparat *in vivo* ist nahezu unmöglich. In **Kapitel 5** und **Kapitel 6** wurden daher Möglichkeiten zur Bewertung dieser Belastungen mit einem instrumentierten Beinsimulator (Dummy) untersucht, wobei der Schwerpunkt auf dem Risikofaktor der Fehlausrichtung zwischen Mensch und Roboter lag. Der für diese Studie entwickelte Beinsimulator war mit einem Kraft- und Drehmomentsensor mit 6 Freiheitsgraden ausgestattet, um die Belastungen des Kniegelenks zu messen. Wir befestigten eine passive Knieorthese am Beinsimulator und führten Fehlausrichtungen (Innen-/Außenrotation, proximale/distale Translation, anteroposteriore Translation) durch, um deren Auswirkungen auf die Gelenkbelastung während der Schwungphase zu ermitteln. Zunächst wurden diese Experimente mit der ersten Version des Beinsimulators durchgeführt, die mit einem Polyurethanschaum ausgestattet war, um Weichgewebe zu imitieren (**Kapitel 5**). Für **Kapitel 6** wiederholten wir die Experimente (mit Ausnahme der anteroposterioren Translationsfehlausrichtung) mit drei zusätzlichen Materialien zur Nachahmung von Weichgewebe, nämlich einem weicheren Schaumstoff und zwei Silikon/Gel-Materialien. Die Silikon/Gel-Materialien waren härter als der ursprüngliche Schaumstoff und werden in der Literatur als geeignete Materialien zur Nachahmung von Weichgewebe vorgeschlagen. Wir fanden heraus, dass Fehlausrichtungen eines Exoskeletts für die untere Extremität in jeder der untersuchten Richtungen die Kräfte und Drehmomente im Knie während der Schwungphase im Vergleich zur perfekten Ausrichtung auf ein Vielfaches erhöhen können. Die

Untersuchungen zeigten weiter, dass diese durch Fehlansrichtungen induzierten Veränderungen der Gelenkbelastungen wesentlich von den Eigenschaften des (künstlichen) Weichgewebes beeinflusst werden. Bei härteren Materialien war die Tendenz zu einem stärkeren Anstieg der Spitzengelenkbelastungen zu beobachten. Diese Studie hat gezeigt, dass Dummys ein geeignetes Instrument zur Messung von Gelenkbelastungen sein können. Künftige Forschungsarbeiten sollten darauf abzielen, die Genauigkeit zu verbessern, mit der Dummys die physische Mensch-Roboter-Interaktion simulieren.

In der in **Kapitel 7** vorgestellten Studie wurde untersucht, wie sich die von Rehabilitationsrobotern ausgeübten Belastungen auf Komfort und Sicherheit auswirken. Genauer gesagt haben wir untersucht, wie sich Beschwerden entwickeln und im Laufe der Zeit verändern, wenn durch eine starre Manschette wiederholt und über längere Zeiträume Kräfte ausgeübt werden. Die Versuchsmanschette und die ausgeübten Kraftmuster basierten auf dem, was über die Interaktion mit Gang-Exoskeletten bekannt ist. Drei Kraftmuster wurden auf gesunde Teilnehmer (n=15) aus zwei Altersgruppen angewandt, die während jedes Kraftmusters kontinuierlich ihr empfundenen Unbehagen auf einer visuellen Analogskala angaben. In einer Basismessung wurde die individuelle Unbehaglichkeitsschwelle eines jeden Teilnehmers ermittelt. Die beiden anderen Versuche bestanden aus sich wiederholenden Kräfteinwirkungen, die 30 Minuten lang ausgeübt wurden (nur Normalkraft und Normal- und Scherkraft in Kombination), wobei die Stärke der Kräfte auf der individuellen Unbehaglichkeitsschwelle beruhte. Die Schwellenwerte für die Erkennung von Unbehagen (Median 100 N; Bereich 40 N bis >230 N) und die Zeit bis zum ersten Empfinden von Unbehagen bei den Versuchen mit repetitiver Kraft (Median 4,1 Minuten bei repetitiver Normalkraft und 5,4 Minuten bei repetitiver Normal- und Scherkraft) variierten stark zwischen den Teilnehmern. Die Kräfteinwirkungen führten zu einer Hautrötung, aber in der Regel nicht zu Schmerzen. Es wurden keine Zusammenhänge zwischen dem Unbehagen und der Altersgruppe, dem Kraftmuster, den Umgebungsbedingungen oder anderen Teilnehmermerkmalen festgestellt. Es gab keine signifikanten Unterschiede zwischen den beiden sich wiederholenden Kraftmustern. Wir konnten feststellen, dass das Unbehagen mit der Zeit zunimmt, wenn eine Kraft, die bei einem einzigen Kontakt als leicht unangenehm empfunden wird, wiederholt ausgeübt wird.

In **Kapitel 8** werden schließlich die wichtigsten Ergebnisse dieser Arbeit diskutiert und Empfehlungen für die zukünftige Forschung und Entwicklung im Bereich der mechanischen Sicherheit von Rehabilitationsrobotern gegeben. Darüber hinaus werden Implikationen für die klinische Praxis und für (Leitlinien für) Sicherheitsbewertungen vorgestellt. Obwohl diese Forschungsarbeit Schritte in verschiedene Richtungen unternommen hat, um Wissenslücken zu schließen und die Sicherheitsbewertung von Rehabilitationsrobotern zu vereinfachen, gibt es noch eine Reihe von ungelösten Problemen. Wir haben festgestellt, dass übermäßige Belastungen der Weichteile und des Bewegungsapparats als die wichtigsten Gefahren bei der physischen Interaktion zwischen Rehabilitationsrobotern und ihren Benutzern angesehen werden können. Die Art der Interaktion in der Rehabilitationsrobotik, die durch ständige Kontakte, zyklische Belastungen, verletzte Benutzer und manchmal unkontrollierte Umgebungen gekennzeichnet ist, macht Sicherheitsüberlegungen komplex. Selbst relativ kleine Kräfte können zu gefährlichen Situationen führen, wenn sie z. B. über einen längeren Zeitraum, auf beeinträchtigte Körperstrukturen, an Schnittstellen mit Belastungsspitzen oder in ungünstigen Mikroklimata einwirken. Sicherheitsvalidierungsexperimente können ein sinnvoller Ansatz sein, um die physische Mensch-Roboter-Interaktion zu prüfen, vorzugsweise ohne einen Menschen zu

involvieren, und Strategien zur Verringerung von (Spitzen-)Belastungen zu entwickeln. Wir haben erörtert, dass zusätzliche Forschung erforderlich ist, um die Kraftverteilungen in allen relevanten Richtungen an der Mensch-Roboter-Schnittstelle genau zu messen, ohne das Kräftezusammenspiel zu beeinflussen. Es wurde festgestellt, dass Fehlausrichtungen ein wichtiges Problem bei der Verwendung von Exoskeletten darstellen. Wir haben zwar gezeigt, dass Fehlausrichtungen die Kniegelenksbelastungen bei einem Dummy während der Schwungphase erheblich beeinflussen können, aber weitere Studien sollten untersuchen, ob Fehlausrichtungen zu (potenziell) schädlichen Belastungen in Situationen mit Gewichtsbelastung führen würden. Unsere Forschung hat gezeigt, dass das Unbehagen mit der Zeit zunimmt, wenn wiederholte Belastungen durch eine Exoskelett-Manschette auf die Haut ausgeübt werden. Die Wahrnehmung des Unbehagens variiert erheblich zwischen den Probanden. Es wird zwar schwierig sein, allgemein gültige Richtlinien für akzeptable Zeit-Kraft-Verhältnisse aufzustellen, aber künftige Forschungen können das derzeitige Wissen erweitern, indem sie größere Probandengruppen, einschließlich Patienten, sowie andere Kraftmuster berücksichtigen.

Die für diese Arbeit durchgeführten Untersuchungen lieferten wertvolle Einblicke in aktuelle Sicherheitsfragen und Forschungslücken in Bezug auf die Sicherheit von Rehabilitationsrobotern. Die Arbeit ist ein erster Schritt zum Aufbau einer Wissensbasis, die die Entwicklung und Markteinführung von sichereren Rehabilitationsrobotern durch umfassende Leitfäden unterstützen kann.

ACKNOWLEDGEMENTS | DANKWOORD | DANKSAGUNG

This is it. The very last bits of my PhD thesis. It wouldn't have come together if it weren't for all the people who have supported me personally and in my professional development for the past years.

8 Chapters, 150 pages

First of all, I would like to express my gratitude to my graduation committee. Thank you for agreeing to read and evaluate my thesis and for your willingness to take part in my defence.

12 trips to 8 countries, 6 first author publications and 100+ PhD meetings

Jaap. Thank you for giving me the chance to take on this challenge and do my PhD research at RRD. Thank you for trusting in my abilities even though my CV didn't show a very straight path leading up to this job. Thank you for giving me the opportunity to travel a lot for work, especially in the first years of my PhD where traveling to conferences and plenary meetings was still a thing. Also thank you for going through with the slightly crazy idea of taking me to the ERF in Tampere, Finland on my first day of work. You had just been appointed professor at BSS when I started – I found out on said trip – and I am very proud and grateful to have you as my promotor. Your experience and insights from the clinical standpoint added a very valuable perspective to my work and I want to thank you for all the things you taught me.

Gerdienke. I couldn't have wished for a better fit for my daily supervisor. Even though the start wasn't as easy with COVR being a very special project for a PhD project and you being on maternity leave, I quickly realized that I am very lucky to have you as my supervisor, my colleague, my mentor, my conversation partner and my most critical reviewer (sometimes with a super strong magnifying glass...). I really enjoyed our trips together (the one to Toronto and the Niagara falls together with Erik won't be soon forgotten) and am thankful that I had the opportunity to learn firsthand from you what being a researcher means. Not only did I learn a whole lot from you, I also really value your genuine interest in everything that I had going on, whether it was work-related or not. Our sometimes less efficient meetings (totally against my German mindset) were extra good for the soul, especially in lonely Covid-times. Thank you for that and for your feedback that, although sometimes slightly frustrating (the standard e-mail was 'Looks really good already! I only have a few minor remarks.' and those few minor remarks sometimes managed to turn each page red), always made the output so much better!

Leendert. We've spent lots of time together on trains, planes, in meetings, in the lab and standing in each other's office to quickly discuss something. Thank you for helping me navigate through consortium meetings and small talk at conferences, especially in the first months. I think you know that RRD would be lost without you and so would I have been so many times when it came to test setups, regulatory questions and sensor output. I really appreciated having you as a bonus-supervisor. Thanks for all the technical input you gave for this thesis!

Erik. Somehow it makes sense to mention you at this point as well. You transformed from my travel buddy to my boss. On our first trip to Tampere you made it really easy for me to feel at ease with the pretty strange situation of leaving for a conference before even getting an office space assigned. And that was not predominantly due to your slipping and sliding on the icy Finnish roads, but due to your

openness and good sense of humor. Travelling with you always meant good food and wine and nice conversations. So thank you for that and also for providing valuable input by sharing your view on things at the coffee corner, at cluster meetings and feedback meetings.

1 project

I can't end this thesis without a big shoutout to Team COVR! The biggest learning of many of my fellow PhD students is how difficult and frustrating the work and communication in an international project consortium is. I am extremely grateful that I had a very different experience. Thank you for the very pleasant meetings online and offline and for the fruitful collaboration.

3 roomies in 4 years and 3 months at RRD

Marijke, Eline en Cindy. Dank jullie wel voor de leuke tijd in kamer 19! Marijke, jij had altijd ruzie met je laptop en gaf me daardoor wat afleiding van de soms wat lastige begintijd met veel lezen en veel vraagtekens over mijn PhD project. Bedankt voor de gezelligheid bij de koffiehoek en ook buiten RRD, bijvoorbeeld bij het cycling dinner (nogmaals sorry voor de rode wijn op je mooie houten vloer!).

Eline, wij zijn bijna tegelijk begonnen bij RRD en ik weet nog heel goed dat jij op mijn eerste dag in het kantoor langskwam en vroeg of we samen een lunchwandeling wilden doen. Er volgden waarschijnlijk honderden gezamenlijke lunches met jou en de rest van de junioren club. Dankjewel voor je luisterend oor en voor je inspirerende manier van je eigen ding doen!

Cindy. Toen wij kamergenootjes werden was mijn tijd bij RRD al bijna afgelopen. Alsnog heb ik er erg van genoten om met jou bij te kletsen over alles en nog wat. En wat ben ik blij dat je op 19 januari naast mij gaat staan en mij wilt ondersteunen als paranimf. Dankjewel!

Robert. Wij hadden misschien wel de meeste overlap in onze tijd bij RRD. Dankjewel voor je top humor die ervoor zorgde dat een dag die niet heel goed begon, vaak na de eerste kleine pauze bij de koffiehoek al een stuk beter was. Ook heel erg bedankt dat je altijd klaar stond bij python problemen en bij vragen hoe het nou precies moet als je over een paar weken gaat promoveren. Wat fijn dat ook jij naast mij wilt staan tijdens de verdediging!

En natuurlijk zal ik niet de rest van de (oud-)junioren vergeten. Het is echt niet vanzelfsprekend om zo'n leuke club mensen op je werk te hebben. Jullie maakten de leuke dagen nog leuker en de frustrerende dagen draaglijk. Bedankt voor alle koffiepauzes, lunchwandelingen, spelletjesavonden, uitjes en etentjes. Ook al vond ik het in het begin erg vermoeiend omdat mijn Nederlands nog niet zo goed was, door jullie is niet alleen dat beter geworden maar heb ik ook ontzettend veel lol gehad. Dankjulliewel! Anne – je bent allang geen junior meer bij RRD, maar ik wil je alsnog bedanken voor de leuke tijd bij RRD en dat ik bij jou promotie al mocht beleven wat het betekend, een PhD af te ronden. Ik ben ontzettend blij dat we nog contact hebben.

Ook wil ik graag alle andere collega's bij RRD bedanken. De werksfeer bij RRD is ontzettend fijn en dat komt vooral door jullie! Bedankt voor de gezelligheid en de leuke gesprekken op de gang. Inger en Brigitte, dank voor jullie oprechte interesse en dat jullie altijd voor iedereen klaar staan. Jos, ook jou wil ik heel erg bedanken! Dankjewel voor de gezelligheid bij RRD en dat je het design voor de voorkant

&

van dit boekje voor mij wilde maken. Bedankt voor je geduld en het omgaan met mijn perfectionisme!

6 students and 15 study participants

Roy, Nicole, Palash, Charlotte, Hylke and Martijn. Thank you for giving me the opportunity to learn from you with your various backgrounds and thank you for the work you put into the research that led to this thesis.

I would also like to thank everyone who participated in my study. Without your time and effort, an essential part of this thesis would not have been possible.

5 years to the day from the job interview to the public defence

This thesis wouldn't have come together if it weren't for the people outside of work who believed in me but also distracted me in the right moments. So here's a big thank you to my family and friends! Lena, Lena, und Dina. Danke, dass ihr mich seit so vielen Jahren begleitet und immer für mich da seid. Lena R. (eigentlich für mich ja für immer A.), Danke für die mittlerweile fast 20-jährige Freundschaft und dass du so viel Liebe ausstrahlst. Lena U., wir können uns nicht nur fachlich austauschen und uns gemeinsam beklagen über die frustrierenden Momente in einem PhD-Projekt, sondern können auch Arbeit einfach Arbeit sein lassen und bei unseren gemeinsamen Wochenenden einfach Spaß haben. Danke! Dina. Deine Abenteuerlust und Freude ist einfach ansteckend und ich bin dir so dankbar für jedes Abenteuer, was wir zusammen erleben. Und wer weiß, vielleicht wäre ich ohne unser Neuseeland-Abenteuer gar nicht da gelandet wo ich jetzt bin.

Jetzt noch ein Riesendankeschön an meine ganze Familie. Ihr seid ein wilder Haufen und genauso gehört ihr zu mir. Danke für alles! Daarbij hoort natuurlijk ook mijn schoonfamilie. Bedankt voor jullie betrokkenheid en steun!

Mama und Papa. Danke für euer uneingeschränktes Vertrauen in uns, unsere Fähigkeiten und die Entscheidungen, die wir auf unserem Weg treffen. Papa, unsere gemeinsamen Spaziergänge in der Coronazeit haben mir immer gut getan. Danke für alle gemeinsamen Ausflüge, die aus meiner kindlichen Neugierde eine wissenschaftliche Neugierde haben werden lassen. Mama, danke dass du immer die richtigen Worte findest, wenn ich nicht weiter weiß und mit mir über Gelenkwinkel und Artikelfeedback fachsimpelst. Danke für alle nötigen Schubser und jedes Auffangen, wenn es mal nicht so lief wie geplant. Lena. Einfach danke, dass du die beste Schwester bist, die man sich vorstellen kann. Wenn ich mal eine Pause brauche, bist du immer für einen Kaffee, einen Stadtbummel oder einen Spaziergang zu haben und das ist verdammt viel wert. Ich bin stolz auf dich, wie du alles mit so viel Herz und Empathie anpackst und darauf, dass ich für immer deine kleine Schwester sein kann.

And (I told you I'm keeping the best for last) – Robin. When I started at RRD, we had just moved in together. Your first home and job in Germany and my first work experiences in the Netherlands. In the meantime, we bought our first car (and home on wheels) together, you've made me your wife, our own home is being built and now we're expecting our first child. I can't tell you how happy you make me. Thank you for listening to my stories and complaints, even though you had no idea what I'm talking about most of the time. Thank you for always having my back. Thank you for taking me to the sea whenever I needed a change of scenery. Thank you for being you.



ABOUT THE AUTHOR

Jule Bessler was born in Ibbenbüren, Germany, on June 11, 1992. In 2014, she obtained her BSc in Environmental Science from the Carl von Ossietzky University in Oldenburg, Germany. After taking some time off for traveling, she went on to study Human Technology in Sports and Medicine at the German Sports University Cologne, Germany and obtained her Master in 2018. During the studies for her master's degree, Jule specialized in rehabilitation technology and human movement sciences. This reflected in an internship with a short research project at a prosthetic leg component manufacturer and in her master's thesis which focused on the optimizing potential of variable-stiffness joints for ankle foot orthoses.

In 2018, Jule started as a junior researcher and PhD candidate at Roessingh Research and Development (RRD) and the University of Twente in Enschede, the Netherlands. She was mostly working for the European project COVR (Horizon 2020), but also had the opportunity to contribute to other projects such as FutureGlove (Eurostars). In connection to the COVR project, Jule researched gaps and needs in safety of rehabilitation robots and explored experimental options to fill those gaps. Parts of that work are presented in this thesis.

Currently, Jule is working at pediatric assistive device manufacturer Schuchmann GmbH & Co. KG in Bissendorf, Germany. In her position as regulatory affairs and quality manager, she can take her research experiences to practice and contribute to the safety of medical devices.

Journal publications

- J. Bessler**, G. B. Prange-Lasonder, R. V. Schulte, L. Schaake, E. C. Prinsen, and J. H. Buurke, "Occurrence and Type of Adverse Events During the Use of Stationary Gait Robots—A Systematic Literature Review," *Front. Robot. AI*, vol. 7, 2020, doi: 10.3389/frobt.2020.557606.
- J. Bessler**, G. B. Prange-Lasonder, L. Schaake, J. Saenz, C. Bidard, I. Fassi, M. Valori, A. B. Lassen, J. Buurke, "Safety assessment of rehabilitation robots: A review identifying safety skills and current knowledge gaps," *Front. Robot. AI*, vol. 8, p. 33, 2021, doi: 10.3389/frobt.2021.602878.
- M. Valori, A. Scibilia, I. Fassi, J. Saenz, R. Behrens, S. Herbster, C. Bidard, E. Lucet, A. Magisson, L. Schaake, **J. Bessler**, G. B. Prange-Lasonder, M. Kühnrich, A. B. Lassen, K. Nielsen, "Validating Safety in Human–Robot Collaboration: Standards and New Perspectives," *Robotics*, vol. 10, no. 2, p. 65, 2021, doi: 10.3390/robotics10020065.
- J. Bessler-Etten**, L. Schaake, G. B. Prange-Lasonder, and J. H. Buurke, "Assessing effects of exoskeleton misalignment on knee joint load during swing using an instrumented leg simulator," *J. Neuroeng. Rehabil.*, vol. 19, no. 1, p. 13, 2022, doi: 10.1186/s12984-022-00990-z.
- J. Saenz, **J. Bessler-Etten**, M. Valori, G. B. Prange-Lasonder, I. Fassi, C. Bidard, A. B. Lassen, I. Paniti, A. Toth, T. Stuke, S. Wrede, K. Nielsen, "An Online Toolkit for Applications Featuring Collaborative Robots Across Different Domains," *IEEE Trans. Human-Machine Syst.*, pp. 1–11, 2022, doi: 10.1109/THMS.2022.3213416.

Conference contributions

- J. Bessler**, E. C. Prinsen, G. B. Prange-Lasonder, L. Schaake, and J. H. Buurke, "Assessing Safety and Performance Indicators in Rehabilitation Robotics," in *School and symposium on advanced neurorehabilitation SSNR2018*, 2018, pp. 28–29.
- J. Bessler**, L. Schaake, C. Bidard, J. H. Buurke, A. E. B. Lassen, K. Nielsen, J. Saenz, F. Vicentini, "COVR – Towards Simplified Evaluation and Validation of Collaborative Robotics Applications Across a Wide Range of Domains Based on Robot Safety Skills," in *Wearable Robotics: Challenges and Trends Proceedings of the 4th International Symposium on Wearable Robotics, WeRob2018, October 16-20, 2018, Pisa, Italy*, 2019, pp. 123–126, doi: 10.1007/978-3-030-01887-0_24.
- J. Bessler**, L. Schaake, R. Kelder, J. H. Buurke, and G. B. Prange-Lasonder, "Prototype measuring device for assessing interaction forces between human limbs and rehabilitation robots - A proof of concept study," in *IEEE International Conference on Rehabilitation Robotics*, Jun. 2019, vol. 2019-June, pp. 1109–1114, doi: 10.1109/ICORR.2019.8779536.
- J. Saenz, **J. Bessler**, S. Herbster, A. Lassen, C. Bidard, G. B. Prange-Lasonder, L. Schaake, A. Scibilia, M. Valori, I. Fassi, R. Behrens, K. Nielsen, "COVR - Using Robotics Users' Feedback to update the Toolkit and Validation Protocols for Cross-domain Safety of Collaborative Robotics," 2021.
- J. Saenz, I. Fassi, G. B. Prange-Lasonder, M. Valori, C. Bidard, A. B. Lassen, **J. Bessler-Etten**, "COVR Toolkit – Supporting safety of interactive robotics applications," in *2021 IEEE 2nd International Conference on Human-Machine Systems (ICHMS)*, Sep. 2021, pp. 1–6, doi: 10.1109/ICHMS53169.2021.9582659.

Regulatory publications

- Spanish National Research Council, IUVO S.r.l, Automotive Technology Centre of Galicia, Axiles Bionics, Dong-Eui University, euRobotics aisbl, Hocoma AG, Intespring B.V., Karlstad University, Laboratoire national de métrologie et d'essais, Össur hf, Otto Bock SE & Co. KGaA, **Roessingh Research and Development**, Sejong University, SNCF Voyageurs, Technaid S.L., Tecnalia Research and Innovation, Te Dalle Molle Institute for Artificial Intelligence, *Lower-limb wearable devices - Performance test method for walking on uneven terrain*. CWA 17664, 2021.
- National Research Council of Italy, CEA LIST, **Roessingh Research and Development**, Italian National Institute for Insurance against Accidents at Work, Leiden University, Datalogic s.r.l., Danish Technological Institute, University of Brescia, ABLE Human Motion S.L., Spanish National Research Council, Swedish Work Environment Authority, Joanneum Research Robotics, University of Bologna, *Guidelines for the development and use of safety testing procedures in human-robot collaboration*. CWA 17835: CEN Workshop Agreement, 2022.

Submitted for publication

- J. Bessler-Etten**, L. Schaake, S. Massardi, D. Torricelli, J. H. Buurke, and G. B. Prange-Lasonder, "Soft tissue characteristics affect the relation between leg-exoskeleton misalignments and knee joint loads in a dummy leg," *Submitted for publication*.
- J. Bessler-Etten**, L. Schaake, J. H. Buurke, and G. B. Prange-Lasonder, "Investigating change of discomfort during repetitive force exertion through an exoskeleton cuff," *Submitted for publication*.

PROGRESS RANGE

The following publications have been published in the Progress range by Roessingh Research and Development, Enschede, the Netherlands. Copies can be ordered, when available, via info@rrd.nl.

1. J.W.G.A. Pot, H. Boer, W.H. van Harten, H.J. Hermens, E.R. Seydel. Comprehensive Need-Assessment. Ontwikkeling van een meetinstrument voor zorgbehoeften en kwaliteitsbeoordeling door patiënten. September 1994, ISBN: 90-25452-01-2
2. N.G.A. van Leerdam, H.J. Hermens. Revalidatietechnologie in Euregio. July 1995, ISBN: 90-75452-02-0
3. L. Duda, L.O. van Noort, S. Röseler, B.O.L. Greitemann, W.H. van Harten, N.S. Klazinga. Rehabilitation in Germany and The Netherlands, A comparison of two rehabilitation-systems. August 1995, ISBN: 90-75452-03-9
4. H.J. Hermens, A.V. Nene, G. Zilvold. Electrophysiological Kinesiology, Proceedings of the 11th congress of the International Society of Electrophysiology and Kinesiology in Enschede, The Netherlands 1996. October 1996, ISBN: 90-75452-04-7
5. W.H. van Harten. Bouwen aan een kwaliteitssysteem in de revalidatiezorg. Een poging tot constructieve technology assessment van een kwaliteitssysteem in een gezondheidszorginstelling. December 1997, ISBN: 90-75452-07-1
6. G. Baardman, M.J. IJzerman. Design and evaluation of a hybrid orthosis for people with paraplegia. November 1997, ISBN: 90-75452-08-X
7. M.M.R. Hutten. Lumbar Dynamometry: A useful method for assessment of patients with chronic low back pain? November 1999, ISBN: 90-75452-13-6
8. van der Salm, W.H. van Harten, C.G.B. Maathuis. Ketenkwaliteit Cerebrale Parese Zorg. Een beschrijving van de cerebrale parese zorg en mogelijke verbeteringen hierin. April 2001, ISBN: 90-75452-19-5
9. M.J. Nederhand. Muscle activation patterns in post traumatic neck pain. March 2003, ISBN: 90-75452-27-6
10. M.J.A. Jannink. Usability of custom-made orthopaedic shoes in patients with degenerative disorders of the foot. September 2004, ISBN: 90-75452-28-4
11. M.G.B.G. Blokhorst. State-dependent factors and attention in whiplash associated disorder. January 2005, ISBN: 90-365-2111-4
12. J.H. Buurke. Walking after stroke co-ordination patterns & functional recovery. February 2005, ISBN: 90-365-2140-8
13. van der Salm. Spasticity reduction using electrical stimulation in the lower limb of spinal cord injury patients. October 2005, ISBN: 90-365-2253-6
14. G.J. Snoek. Patient preferences for reconstructive interventions of the upper limb in tetraplegia. December 2005, ISBN: 90-365-2255-2
15. J.R. de Kroon. Therapeutic electrical stimulation of the upper extremity in stroke. December 2005, ISBN: 90-365-2269-2
16. H. van Dijk. Motor skill learning, age and augmented feedback. March 2006, ISBN: 90-365-2302-9
17. C.A.J. Mes. Improving non-optimal results in chronic pain treatment. January 2007, ISBN: 90-365-2435-0

18. G.E. Voerman. Musculoskeletal neck-shoulder pain: a new ambulant myofeedback intervention approach. March 2007, ISBN: 90-365-2460-1
19. L.A.C. Kallenberg. Multi-channel array EMG in chronic neck-shoulder pain. March 2007, ISBN: 90-365- 2459-8
20. M.H.A. Huis in 't Veld. Work-related neck-shoulder pain: The role of cognitive-behavioural factors and remotely supervised treatment. December 2007, ISBN: 978-90-365-2584-8
21. J.F.M. Fleuren. Assessment of Spasticity: From EMG to patients' perception. October 2009, ISBN: 978- 90-365-2869-6
22. J. Reenalda. Dynamic sitting to prevent pressure ulcers in spinal cord injured. October 2009, ISBN: 978- 90-365-2884-9
23. G.B. Prange. Rehabilitation Robotics: Stimulating restoration of arm function after stroke. October 2009, ISBN: 978-90-365-2901-3
24. M. Vos-van der Hulst. Prognostic factors and underlying mechanisms in chronic low back pain. November 2009, ISBN: 978-90-365-2881-8
25. A.I.R. Kottink-Hutten. Assessment of a two-channel implantable peroneal nerve stimulator post-stroke. February 2010, ISBN: 978-90-365-2959-4
26. M.G.H. van Weering. Towards a new treatment for chronic low back pain patients. May 2011, ISBN: 978-90-365-3180-1
27. J. Gulmans. Crossing Boundaries: Improving Communication in cerebral palsy care. February 2012, ISBN: 978-90-365-3305-8
28. B.I. Molier. Influence of augmented feedback on learning upper extremity tasks after stroke. March 2012, ISBN: 978-90-365-3296-9
29. R. Dubbeldam. Towards a better understanding of foot and ankle kinematics in rheumatoid arthritis. October 2012, ISBN: 978-90-365-3407-9
30. R.M.H. Evering. Ambulatory feedback at daily physical activity patterns. April 2013, ISBN: 978-90-365- 3512-0
31. S. Malhotra. Does spasticity interfere with functional recovery after stroke? November 2013, ISBN: 978-90-365-3567-0
32. M. Tabak. Telemedicine for patients with COPD. New treatment approaches to improve daily activity behaviour. February 2014, ISBN: 978-94-6108-590-0
33. H.R. Trompetter. ACT with pain. Measurement, efficacy and mechanisms of Acceptance and Commitment Therapy. September 2014, ISBN: 978-90-365-3708-7
34. H. op den Akker. Smart Tailoring of Real-Time Physical Activity Coaching Systems. October 2014, ISBN: 978-90-365-3762-9
35. S.M. Jansen-Kosterink. The added value of telemedicine for physical rehabilitation. December 2014, ISBN: 978-90-823196-0-6
36. I.M. Velstra. Advanced insights in upper limb function of individuals with cervical spinal cord injury. December 2015, ISBN: 978-90-365-3929-6
37. M.G.M. Kloosterman. Keep on Rolling. Functional evaluation of power-assisted wheel-chair use. June 2016, ISBN: 978-90-365-4120-6
38. E.C. Prinsen. Adapting to Change. Influence of a microprocessor-controlled prosthetic knee on gait adaptations. December 2016, ISBN: 978-90-365-4206-7
39. M.D.J. Wolvers. A coach in your pocket. On chronic cancer-related fatigue and physical behavior. March 2017, ISBN: 978-90-365-4299-9



40. M. Cabrita. Active and pleasant ageing supported by technology. November 2017, ISBN: 978-90-365-4390-3
41. J.A.M. Haarman. TIBAR - Therapist Inspired Balance Assisting Robot. November 2017, ISBN: 978-90-365-4407-8
42. S.M. Nijenhuis. Roll up your sleeves! Technology-supported arm and hand training at home after stroke. April 2018, ISBN: 978-90-365-4510-5
43. K. Cranen. Acceptance of telerehabilitation in chronic pain: the patients' perspective. June 2018, ISBN: 978-90-365-4555-6
44. S.T. Boerema. Sensing human activity to improve sedentary lifestyle. September 2018, ISBN: 978-90-365-4604-1
45. B. Radder. The wearable hand robot - Supporting impaired hand function in activities of daily living and rehabilitation. November 2018, ISBN: 978-90-365-4658-4
46. T. Krabben. A reaching hand - towards an active therapeutic device for the upper extremity following stroke. December 2018, ISBN: 978-90-365-4660-7
47. J.G. Timmerman. Cancer rehabilitation at home - The potential of telehealthcare to support functional recovery of lung cancer survivors. January 2019, ISBN: 978-90-365-4701-7
48. C.D.M. Nikamp-Simons. The sooner the better?! - Providing ankle-foot orthoses in the rehabilitation after stroke. May 2019, ISBN: 978-90-365-4747-5
49. R. Achterkamp. Towards a balanced and active lifestyle. June 2019, ISBN: 978-94-6323-656-0
50. C. Engbers. Keep Cycling. How Technology can Support Safe and Comfortable Cycling for Older Adults. September 2019, ISBN: 978-90-365-4848-9
51. A.L. van Ommeren. Offering a helping hand. Getting a grip on needs and preferences of stroke patients regarding soft-robotic technology supporting hand function. October 2019, ISBN: 978-90-365-4835-9
52. S. ter Stal. Look Who's Talking. Appearance of Embodied Conversational Agents in eHealth. March 2021, ISBN: 978-90-365-5126-7
53. T.C. Beinema. Tailoring coaching conversations with virtual health coaches. December 2021, ISBN: 978-90-365-5260-8
54. M.Z.M. Hurmuz. eHealth – In or out of our daily lives? Measuring the (non-)use of eHealth in summative evaluations. June 2022, ISBN: 978-90-365-5360-5
55. M.C. Broekhuis. Meet my HUBBI: he's an expert on ehealth usability. September 2022, ISBN: 978-90-365-5443-5
56. R.V. Schulte. Up to one's knees in data, data-driven intent recognition using electromyography for the lower limb. December 2022, ISBN: 978-90-365-5486-2
57. J. Bessler-Etten. Safety first in rehabilitation robots! Investigating how safety-related physical human-robot interaction can be assessed. January 2023, ISBN: 978-90-365-5503-6



Roessingh
Research and Development

57

Progress in rehabilitation science

ISBN 978-90-365-5503-6